University of Reading

Identification and characterisation of a potential adrenocortical stem cell population

A THESIS SUBMITTED FOR THE DEGREE OF DOCTOR OF PHILOSOPHY

Mohammed Al-Bedhawi

April 2018

School of Biological Sciences

Declaration

I confirm that this is my own work and the use of all material from other sources has been properly and fully acknowledged.

Signed:

Abstract

The adrenal gland is a small endocrine organ with inherent regenerative capacity. Numerous studies proposed a stem cell niche located in the capsule of adrenal cortex. This project investigated mRNA and protein spatial expression of potential stem cell markers in the adrenal cortex. One of these markers (Thy-1) was used to isolate potential stem cells from dispersed primary adrenal cortex cells using magnetic-activated cell sorting (MACS). Thy-1 positive cells were monitored while they survived in vitro for over one year. Thy-1 cells were demonstrated to be undifferentiated fibroblastic-like cells with characteristics similar to those of mesenchymal stem cells in vitro such as plastic adherent, can form colonies, the confluent cells have a whirlpool-like formation and the significant ($P< 0.05$) increase of Thy-1 expression during cultivation in vitro. Thy-1 positive cells showed the expression of other stem cell markers such as Wt1, Etv5 and ID4. The monitoring of Thy-1 positive cells behavioural changes in vitro showed slow division rate, slow cell migration and the coexistence of senescent cells in their early months of cultivation. In comparison, in the late months of cultivation, the cells showed a significant ($P< 0.05$) increase in cell division rate and cell migration similar to cancer cell behaviour in vitro. As these cells were generally undifferentiated and they have characteristics of mesenchymal stem cells, differentiation attempts were first conducted using external differentiation factors (forskolin, ACTH and AT20 cell line media). However, the results showed non-significant responses to these treatments. The second differentiation experiments were conducted by forcing expression of Sf1 protein in Thy-1 positive cells using a cloning vector. Transfection with Sf1caused a significant ($P< 0.05$) reduction in ID4 mRNA expression and significantly ($P< 0.05$) elevated the expression of the progenitor marker Gli1 and the expression of steroidogenic enzyme genes (Cyp11A1 and 3βHSD) consistent with previous reports for several mesenchymal stem cell types.

Acknowledgment

I would like to express my sincere gratitude to my supervisor Andrew Bicknell for his guidance and continuous support of my PhD study and related research. His support and guidance were the best help I get at all the times of my study during and after the lab experiments and during writing this thesis. I would like to thank him also for his patience, and motivation.

I would like to thank the rest of my reports committee: Phil Dash, Ketan Patel and Keith Foster, for their comments, suggestions and encouragement.

My sincere thanks also go to Dr Elisabeth Lander for her advice in the lab, correcting English and enriching my lexicon with new British terms and idioms.

I would also thank my lab mates: Mhairi, Rob, Moufaq, Mahmmod, Maha, Khatab, Salem, Bandar, Darean, Clementino and Dhurgham for the good times we spent conducting experiments even during long nights.

I deeply would like to thank my family for their patient and prayers: My parents, children (Mohammed Bqer, Fatimah and Mohammed Taqi) and especially my faithful wife.

Last but not least my sincere gratitude to my sponsor ministry of higher education and scientific research of Iraq who has provided for me to live, to study and to travel to United Kingdom.

Table of content

List of figures

List of tables

Abbreviations

3βHSD	3β-Hydroxysteroid dehydrogenase
ACTH	Adrenocorticotropic hormone
Ad4BP	Adrenal 4 binding protein
AGP	Adreno-gonadal primordium
ARMC5	Armadillo repeat-containing 5
AtT-20 cells	Mouse pituitary tumor *cell* line
BCP	bromochloropropane
BM	Bone marrow
BSA	bovine serum albumin
CLIP	Corticotropin-like intermediate peptide
Ct	threshold cycle value
CXCR4	C-X-C chemokine receptor type 4
CYP11A1	cytochrome P450, family 11, subfamily A, polypeptide 1
CyP11B1	cytochrome P450 family 11 subfamily B member 1
Cyp11B2	cytochrome P450 family 11 subfamily B member 2
Cyp21a1	cytochrome P450 family 21 subfamily A member 1
DAPI	4',6-diamidino-2-phenylindole
DAX1	Dosage sensitive sex reversal, Adrenal hypoplasia congenita, on the .X chromosome, number 1
DDW	double distilled water
DHAS	Dehydroepiandrosterone sulphate
Dhh	Desert hedgehog signalling pathway
DMEM	Dulbeccos Modified Eagle's Medium
DMSO	Dimethyl sulfoxide
E.coli	*Escherichia coli*
ELISA	Enzyme Linked Immune Sorbent Assay
EMT	epithelial-mesenchymal transition
ER	endoplasmic reticulum

ESCs	Embryonic stem cells
EST	expressed sequence tag
Etv5	E-twenty-six (Ets) variant gene 5
FBS	foetal bovine serum
FCS	Foetal Calf Serum
FGF-2	Fibroblast growth factor 2
FISH	Fluorescent *In situ* hybridisation
GAPDH	glyceraldehyde-3-phosphate dehydrogenase
GPB	gelatine phosphate buffer (0.25% w/v gelatin in PBS
GSK3β	Glycogen synthase kinase 3
HCN4	Potassium/sodium hyperpolarization-activated cyclic nucleotide-gated channel 4
Hh	Hedgehog signalling pathway
HIF-1α	hypoxia-induced transcription factor 1α
HLA-DR	Human leukocytes antigen-antigen D related
HPA	Hypothalamic–pituitary–adrenal
HRP	horseradish peroxidase
ID4	Inhibitor of DNA Binding 4
Ihh	Indian hedgehog signalling pathway
iPSCs	Induced pluripotent stem cells
IRES 1, 2	internal ribosomal entry site 1 and 2
ISH	*In situ* hybridisation
Itgb2	integrin subunit beta 2
JP	joining peptide
kDa	kilo Dalton
KLF5	Krüppel-like factor 5
LB	Luria-Bertani broth
LCM	Laser capture microdissection
MACS	Magnetic activated cell sorting

MCP-1	monocyte chemoattractant protein-1
MCS	Multi cloning site
MEM	Minimum Essential Media
MET	mesenchymal-epithelial transition
MSCs	Mesenchymal stem cells
NPR	N-terminal-POMC-Receptor
NR5a1	Nuclear Receptor Subfamily 5 Group A Member 1
OD	optical density
PBS	phosphate buffer saline
PBT	phosphate-buffered saline containing Triton
PCNA	proliferating cell nuclear antigen
PFA	Paraformaldehyde
PKA	Protein kinase cAMP-dependent
POMC	Proopiomelanocortin
PVDF	polyvinylidene difluoride
qPCR	quantitative PCR
RPMI medium	Roswell Park Memorial Institute medium
RQ	relative quantitation
RT-PCR	Reverse transcription-polymerase chain reaction
Scc	cholesterol side-chain cleavage enzyme
SDF-1	stromal cell-derived factor 1
SDS-PAGE	Sodium Dodecyl Sulfate-Polyacrylamide Gel Electrophoresis
SF1	Steroidogenic factor 1
SFM	serum-free media
Shh	Sonic hedgehog signalling pathway
ssRNA	single-stranded RNA
StAR	steroidogenic acute regulatory protein
TAE	Tris Acetate EDTA

TBST	Tris-Buffered Saline Tween
TERT	Telomerase reverse transcriptase
TGF-β1	Transforming growth factor beta 1
Thy-1	Thy-1 cell surface antigen
TMB	tetra methyl benzidine
Tmem121	Transmembrane protein121
WT1	Wilms tumour 1
zF	zona Fasciculata
zG	zona Glomerulosa
zI	zona Intermedia
zR	zona Reticularis
β-END	β-endorphin
β-LPH	β -lipotropin
β-MSH	β-melanocyte-stimulating hormone
γ-LPH	γ-lipotropin
γ-MSH	γ-melanocyte-stimulating hormone

Chapter one

Introduction

1.1 Adrenal cortex structure and function

The adrenal glands are two small endocrine organs; one located upon each kidney. They consist of two distinct tissues the adrenal medulla and the adrenal cortex which are different in function and origin. Generally, the adrenal cortex, which is the subject of this study is described as a small thin endocrine gland, which is composed of three different layers or zones (Figure 1.1) and each of these zones has specific morphological and functional aspects (Wang and Rainey, 2012).

The cortex is surrounded by a capsule inside which is the zona Glomerulosa (zG), this is responsible for producing and releasing mineralocorticoids, the hormones that control sodium reabsorption in the blood. Aldosterone is the typical mineralocorticoid in mammals, and it regulates the amount of potassium and sodium passed into the urine through the renin angiotensin aldosterone system (Norris and Carr, 2013).

The next layer is the zona Fasciculata (zF), which produces glucocorticoids. These hormones regulate the metabolism of carbohydrates, fats and proteins. Glucocorticoids such as cortisol stimulate the liver to convert glucose to glycogen and release lipids and fatty acids into the blood from adipose tissue. However, cortisol increases blood glocouse because it has insulin-antagonistic effects (Lager, 1991). Furthermore, glucocorticoids can affect skeletal muscle and stimulate it to release proteins or amino acids into the bloodstream. In addition, glucocorticoids participate in the inflammatory response (Stachenko and Giroud, 1964). Since the main model in this study is the rat, it is important to take into consideration that the major glucocorticoid in rat and other rodents is corticosterone, due to lack of 17α-

hydroxylase in the adrenal cortex of the rodents. In comparison, cortisol is the main glucocorticoid in humans (Mitani, 2014).

The final, inner, layer is called the zona Reticularis (zR) which is responsible for releasing dehydroepiandrosterone (DHEA) and the sulphated dehydroepiandrosterone (DHEAS) in humans and other primates, which is also known as adrenal androgen. DHEA is similar to other male sex hormones, which also allow the development of male characteristics during early embryonic growth and puberty. In steroidogenesis, DHEA is considered the precursor of sex hormones. It is found to be reduced with aging and is similar to cortisol in several functions such as having insulin-antagonistic effects and its association with obesity. However, the release of adrenal androgen from the zR is not exhibited in rodents such as mice and rats (Mitani, 2014), due to lack of cyp17α-hydroxylase (van Weerden et al., 1992). Furthermore, studies based on histological assays on rats revealed a cell zone located between the innermost portion of the zG and the outermost portion of the zF which is called the zona Intermedia (zI) and does not show any hormonal releasing activity when tested by immunohistochemical staining methods. These cells have a high proliferative activity and work as a pool to provide progenitor cells to both zones (zG and zF) (Mitani, 2014).

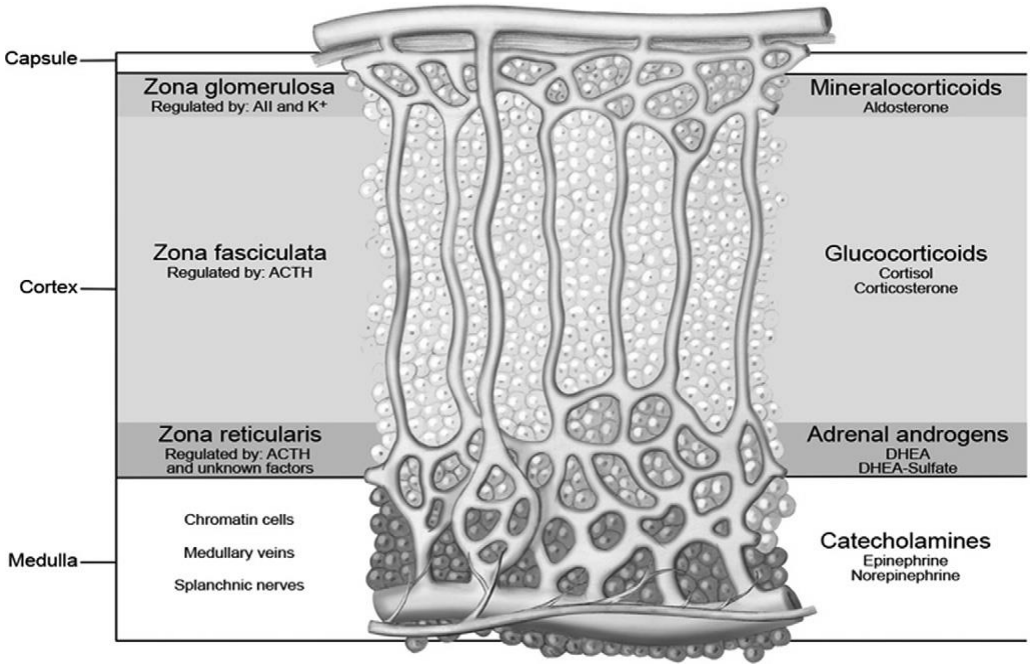

Figure 1.1 Diagrammatic representation of the adrenal cortex showing the three distinct zones of the cortex: the zona Glomerulosa (zG) the source of mineralocorticoids; the zona Fasciculata (zF) synthesises cortisol and the zona Reticularis (zR), which produces adrenal androgens (Wang and Rainey, 2012).

1.2 Steroidogenesis in adrenal cortex

Steroidogenesis is the process by which steroid hormones are synthesised. In mammals, it takes place mainly in the ovary, testis and adrenal cortex. Generally, cytochrome P450 proteins and steroid oxidoreductases are the main enzymes responsible for steroidogenesis, using cholesterol as the starting material. In addition to its role in the stress axis, ACTH is the main hormone that stimulates the biosynthesis of steroid hormones in the adrenals. ACTH triggers a series of molecular events that lead to the conversion of cholesterol to pregnenolone by cholesterol side-chain cleavage enzyme (P450 Scc) (Jefcoate et al., 1992).

Subsequently, each of the zones of the adrenal cortex expresses enzymes that convert pregnenolone to different hormones via a set of oxidoreductase reactions. For example, androgen in the form of dehydroepiandrosterone (DHEA) is the final product of the zR, while the zF converts pregnenolone to glucocorticoids such as corticosterone in rodents or cortisol in humans (Conley and Bird, 1997). In response to angiotensin II, the zG converts pregnenolone to the mineralocorticoid, aldosterone (figure 1.2). Both zF and zG have same group of catalytic enzymes that synthesiseing steroids from cholesterol with a zG specific final step enzyme (Cyp11B2) that is also called aldosterone synthase and zF specific expression of the final step enzyme (Cyp11B1) (King et al., 2009). Since the three active zones of the adrenal cortex have major roles in controlling a variety of physiological functions, a genetic disorder or mutation of protein within this gland often results in lethal or incurable diseases. Histologically, zF represents the major zone of the adrenal cortex in most organisms like humans and rodents and it has an important role in hypothalamic–pituitary–adrenal (HPA) axis or also known as stress axis.

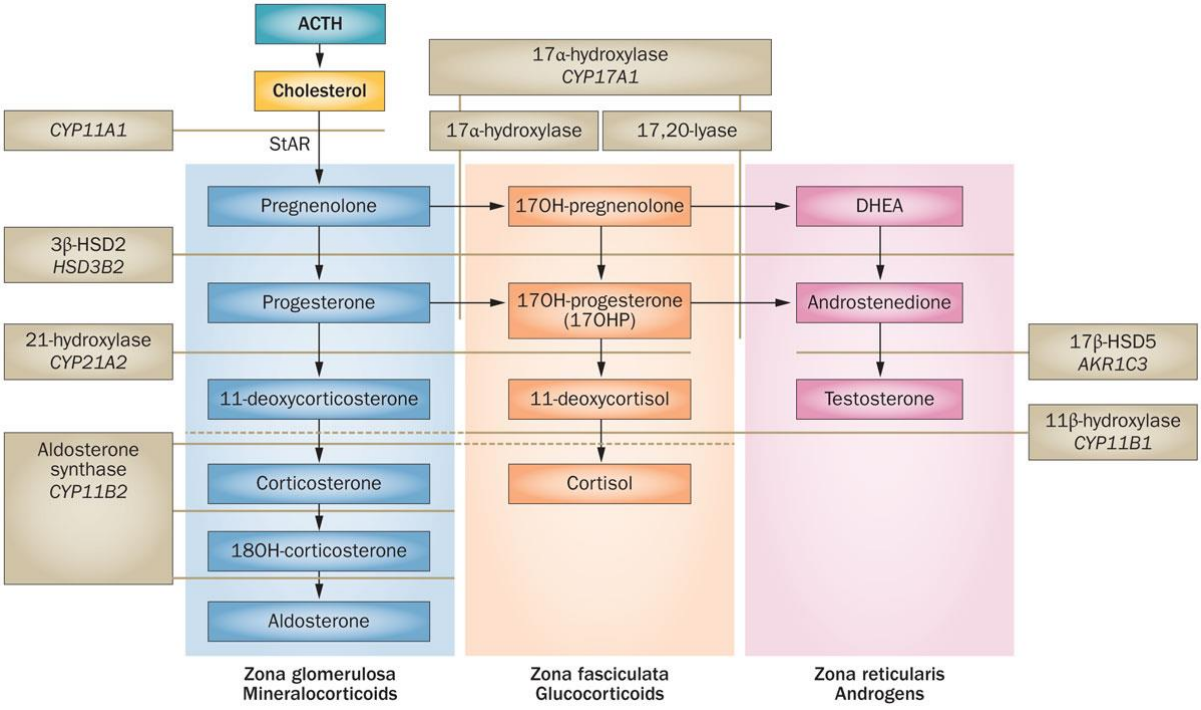

Figure 1.2 The steroidogenic pathway in the adrenal cortex, ACTH stimulates molecular events which result in the production of steroid hormones initiated by the conversion of cholesterol to pregnenolone, this process requires StAR, which allows cholesterol to enter mitochondria where the cholesterol side-chain cleavage enzyme P450 Scc (encoded by the cytochrome P450, family 11, subfamily A, polypeptide 1 (CYP11A1)), converts the cholesterol to pregnenolone in all three zones of the cortex. 3β-hydroxysteroid dehydrogenase (3β-HSDs) converts the pregnenolone to progesterone, 17OH-pregnenolone to 17OH-progesterone and DHEA to androstenedione in the zG, zF and zR respectively. The enzyme 21-hydroxylase (CYP21) converts progesterone to 11-deoxycorticosterone, 17OH-progesterone to 11-deoxycortisol in the zG and the zF. While the 17a-hydroxlyse (CYP17) is absent in the zG, both zF and zR use the hydroxylase activity of CYP17 to produce17-OH pregnenolone from pregnenolone in the zF, and 17-OH progesterone from progesterone in zR. CYP17 also catalyses 17α-OH progesterone to produce (DHEA) in the zR. The enzyme (3βHSDs) in the zR, converts DHEA to androstenedione, which in turn is converted to adrenal testosterone by 17β-hydroxysteroid dehydrogenase (Han et al., 2014).

1.3 Adrenal cortex and the stress axis

Stress stimuli usually cause disruption to the physiological homeostasis of the body and the body has a neuroendocrine system designed to respond to these stimuli and restore homeostasis. The stress signal is received by both the central and peripheral nervous system. The stress processing system includes a number of hormones such as corticotrophin releasing hormone, arginine vasopressin, hormones and peptides derived from proopiomelanocortin, glucocorticoids, adrenaline and nor-adrenaline. All these factors are included within the stress or HPA axis system (Charmandari et al., 2005). This HPA axis system is tightly regulated to adapt to environmental stresses by releasing glucocorticoids from the zF also known as stress hormones. This end-products (glucocorticoids) of this neuroendocrine system, play the main role in the physiological adaptation of the organism against the stress factors (Nicolaides et al., 2015). The HPA axis system activates when the stress signal reaches the nuclei of the corticotropin-releasing hormone (CRH)-secreting parvocellular neurons of the hypothalamus, which respond by stimulating release of the proopiomelanocortin (POMC) from the pituitary gland into blood stream (Goncharova, 2013). POMC undergoes enzymatic cleavage by the prohormone convertases, which result in a number of hormones and peptides in addition to adrenocorticotropic hormone (ACTH). ACTH induces the zF to produce and release the glucocorticoids. Glucocorticoids such as cortisol have multi targets as a stress hormone preparing the organism to react toward the stressors by stimulating the immune system (Castro et al., 2011) and glycogen synthesis in the liver (Mersmann and Segal, 1969). Glucocorticoids also elevate blood pressure, counter-act insulin effects, increase catabolism of protein and raise plasma glucose (Macfarlane et al., 2008). Although all these changes are associated with preparing the body to adapt to maintain homeostasis during stress, any dysregulation of this response due to increasing the level or the period of stress will result in deterioration of homeostasis and might end with several acute and chronic diseases (Nicolaides et al., 2015).

1.4 POMC-derived peptides and receptors

The exsistance of POMC as a precursor of multiple hormones and biologically active peptides was not known until the late seventies of the last century. The early studies of Ascoli & Legnani in 1912 revealed the basic relationship between the pituitary gland and the adrenal gland when scientists recorded adrenal atrophy in dogs after hypophysectomy (Lowry, 1984). This finding was later confirmed by studying the effect of re-implanting the pituitary in hypophysectomised rats, which restored the adrenal cortex from atrophy and it was subsequently proposed that an adrenal controlling factor was released from the pituitary (Smith, 1930). Over time bioassays were developed to identify ACTH as the hormone that influence the growth of adrenal gland (Howard et al., 1955, Bell, 1954). However, the ACTH precursor (POMC) was not recognised until 1977 when two different experiments were conducted to investigate the relationship between ACTH and β-lipotrophin (as they were sharing similarities that led to the hypothesis that both might derive from the same precursor). The first group showed that both ACTH and β-lipotrophin (β-LPH) have the same precursor molecule, when they immunoprecipitated the same 31 kiloDalton (kD) molecule from AtT-20 (mouse pituitary tumour cells) media after using antisera to endorphins (END) or ACTH (Mains et al., 1977). The second group used a cell-free translation system under the direction of mRNA isolated from AtT-20 cells. They identified a 28 kD protein (represents POMC without glycosylation) with both antisera to β-lipotrophin and ACTH (Roberts and Herbert, 1977). Cloning of the gene encoding the precursor was reported two years later (Nakanishi et al. 1979), later research followed to reveal the structure of the POMC gene (which includes three exons) and all the peptides (figure 1.3). The ACTH peptide sequence is located in the centre of POMC, the β-LPH that is cleaved to generate γ-LPH, β-endorphin and β-MSH was

at the C-terminal of the ACTH. While γ-MSH, the 16 kD fragment and the secretory signal sequence were at the N-terminal of the ACTH (Pritchard et al., 2002).

Further research followed to reveal the structure and the functions of POMC-derived peptides and their receptors. The application of molecular cloning technologies in the 1990s revealed a group of melanocortin receptors, which were cloned and subtyped into five receptors (Mountjoy et al., 1992). The melanocortin receptors: MC1R, MC2R, MC3R, MC4R and MC5R are all G protein-coupled receptors and they share 7 membrane domains. However, they have different sequences at the N-terminus and the C-terminus (Cone, 2006). Each of these receptors is mainly associated with a different function such as pigmentation, glucocorticoid biosynthesis, energy homeostasis, and the regulation of food intake and exocrine glands (Dores et al., 2014).

Although each of these receptors has a specific ligand, ACTH can bind and activate all of these subtypes. However, MC2R is specific for ACTH. The other POMC-melano peptides (α-MSH, β-MSH and γ-MSH) can activate MC1R, MC3R, MC4R and MC5R but they have different affinity to each of these receptors (Brzoska et al., 2008, Caruso et al., 2014). The functional capacity of each POMC-derived-peptide is primarily due to their effects on a specific MCR. For example, α-MSH has an immune-modulating capacity because its receptor (MC1R) is localised on macrophages, monocytes and dendritic cells (Luger et al., 2003).

The system of POMC-peptides and the melanocortin receptors is one of the most important systems regulating mammalian energy homeostasis and food intake. The result of applying the advanced technologies such as Cre-LoxP transgenic animals and optogenetics facilitated the understanding of the nature of these receptors in the plasma membrane, which have various active and inactive forms (Mountjoy, 2015). The advances of these new technologies facilitated new findings on POMC-peptide-receptor-systems and their potential of protecting the immune system and CNS and to develop MCR targeted therapies (Lisak and Benjamins,

2017). For example, MC4R deficiency is now a well-documented cause of obesity and the most recent research aims to design MC4R agonists as obesity controlling drugs (Ju et al., 2018).

Figure 1.3 Diagram showing the POMC three exon gene and the translated protein in humans, mice and rats, which represents the precursor hormone of over 30 kilodaltons. The precursor hormone (POMC) contains three main regions or groups of peptides that are eventually cleaved into smaller and more functional peptides. The N-terminal of POMC (1-76) comes after the secretory signal peptide and contains γ1-MSH and γ3-MSH. The central region (ACTH region) comes after the joining peptide (JP) and contains α-MSH and corticotropin-like intermediate peptide (CLIP). The C-terminal region contains beta-lipotrophin (β-LPH), which is cleaved into β-endorphin and γ-LPH. The γ-LPH is cleaved to generate N-LPH and β-MSH. The MSH core peptide sequences are shown in red. The information in the figure was adapted from (Mountjoy, 2010, Millington, 2007, Bicknell, 1997).

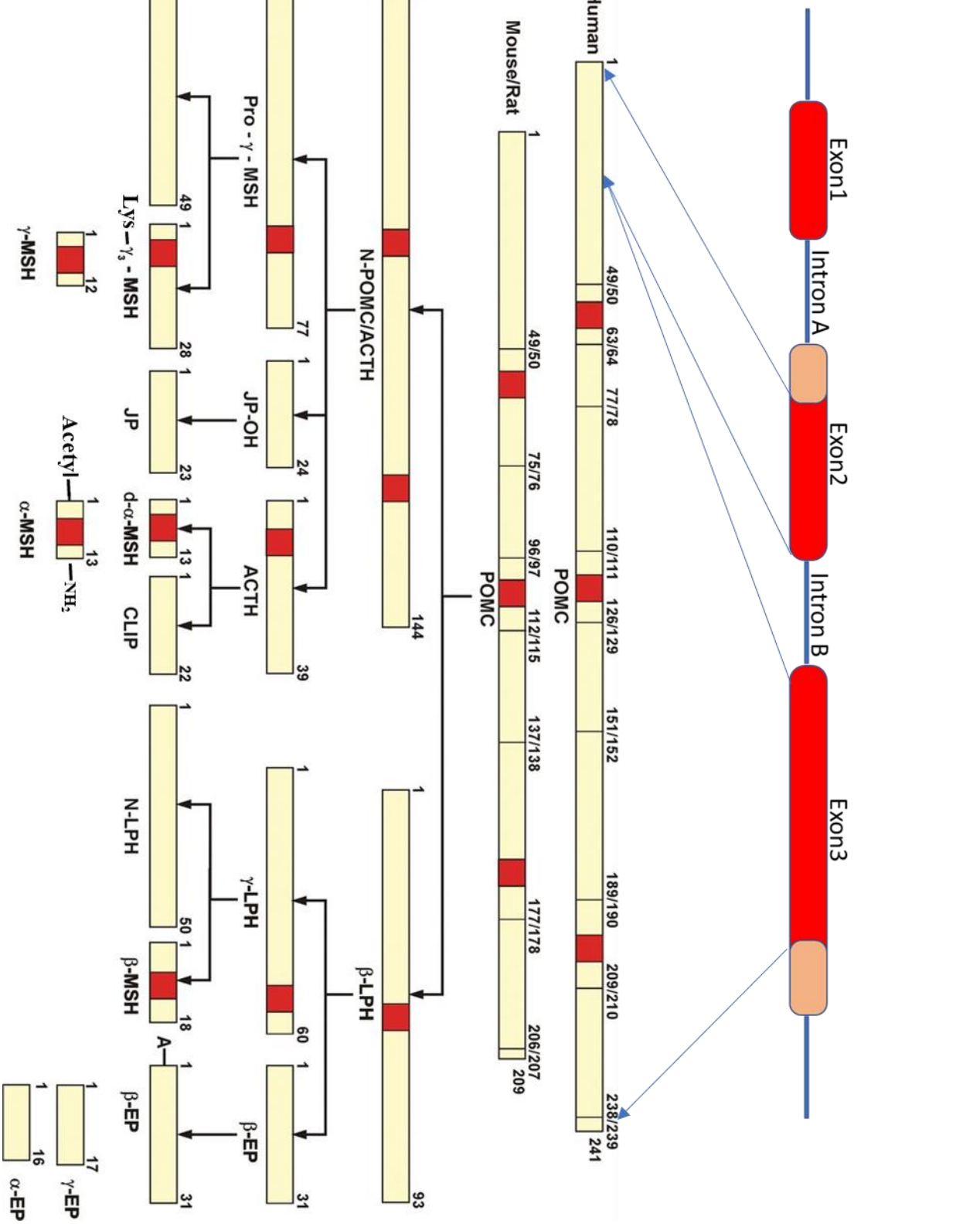
Exon1
Intron A
Exon2
Intron B
Exon3
Human
Mouse/Rat
POMC
N-POMC/ACTH
Pro - γ - MSH
Lys–γ3 - MSH
γ-MSH
JP-OH
JP
ACTH
d-α-MSH
CLIP
α-MSH
Acetyl—
—NH2
β-LPH
γ-LPH
N-LPH
β-MSH
β-EP
γ-EP
α-EP

1.3 POMC and adrenal growth

The early findings of Ascoli & Legnani in 1912 sparked the investigation to identify a factor that was released from the pituitary and affected the growth of adrenal gland. Even before identifying POMC, the 1970s scientific observations suggested ACTH was the main factor maintaining adrenal growth and steroid production (Mulrow, 1972). However, later research showed the opposite of that where ACTH treatment caused inhibition of primary adrenal cell proliferation *in vitro* (Ohare and Neville, 1973) and the quantitative evaluation of the rat adrenal gland did not change after treating the rats with anti-ACTH antiserum (Rao et al., 1978). These findings suggested specific mitogenic peptide or peptides different from ACTH were stimulating adrenal cortex growth and cell proliferation. Promising findings were recorded after Estivariz and Coworkers isolated pro-γ-MSH from the frozen human pituitary (Estivariz et al., 1980). The N-terminal derivatives of pro-γ-MSH were proposed to be responsible for adrenal growth because the post-secretion cleavages of pro-γ-MSH at the lysine sites (at N-terminal see figure 1.1) suggested to induce adrenal growth and mitogenesis (Estivariz et al., 1982). However, the processing of N-terminal POMC was not clearly understood at that time and it was assumed that the cleavage occurred after the lysine site that forms the (1–48) of the N-POMC and (51–76) of the γ3-MSH, while the cleavage occurs after the arginine site that forms (1–49) of the N-POMC and (50–76) Lys-γ3-MSH as reviewed in (Bicknell, 2016). However, it was not recognised by Estivariz and his group in 1982, which of these peptides or their derivatives stimulate the adrenal growth and mitogenesis. Several experiments were carried out to investigate the role of pro-γ-MSH derivatives in compensatory adrenal growth. The most interesting findings were recorded from a series of experiments, one of which included administration of an antibody against N-POMC (1–28) two hours before removing one adrenal gland that resulted in stopping

compensatory adrenal growth, which was recognised by the elimination of increase in the remaining adrenal weight and DNA content after 24 hours as it was suggested as indicator of an inhibition of hyperplasia (Lowry et al., 1983). Further studies were carried out investigating the growth factor during compensatory growth, one of which used an antibody against γ3-MSH that significantly inhibited the increase in DNA content (Al-Dujaili et al., 1982). Al-Dujaili and his co-workers proposed that this antibody might inhibit the proteolytic cleavage that is required to produce the γ3-MSH derivative that induces adrenal growth. Although a few investigations supported this hypothesis, non-have provided proof until a study demonstrated the cloning and characterisation of a serine protease that cleaved the γ3-MSH, which was essential during the adrenal compensatory growth response (Bicknell et al., 2001).

The regenerative capacity of the adrenal gland following enucleation (pressing out the adrenal medulla and most of the inner cortex after incision in the adrenal capsule) provides another model to test POMC derivatives and their effect on adrenal growth. For example, Estivariz et al (1988) tested the administration of either ACTH or purified human 1–28 of N-POMC on the mitotic index of the female rat adrenal after adrenal enucleation and removing the pituitaries, the results showed that N-POMC(1–28) compensates by preventing the atrophy of regenerating adrenal glands in comparison with saline controls (Estivariz et al., 1988a). The follow-up study from the same group calculated the mitotic index on adrenal sections after the administration of anti-N-POMC(1–28) antiserum and anti-ACTH antiserum followed by injecting the rats with colchicine on the next day. The results showed that anti-N-POMC (1–28) antibody produced a significant decrease in mitotic counts, while the ACTH antibody only decreased the production of corticosterone (Estivariz et al., 1988b). Although the purified human 1–28 of N-POMC showed promising findings regarding adrenal growth,

the cost and difficulties that accompany the purification process of the human 1–28 of N-POMC restrict conducting more experiments, which called for using a synthetic one.

However, the effect of synthetic N-terminal 1–28 POMC recorded significantly less mitotic activity in comparison with purified 1–28 of N-POMC (Estivariz et al., 1988a). Researchers imputed that the reduction in activity of the synthetic N-POMC was most likely due to the differences of disulfide bridge arrangements (Bennett, 1984). Even in POMC gene null mice, the administration with synthetic 1–28 N-POMC did not affect adrenal growth, but reduced food intake and weight (Coll et al., 2006). Torres and co-workers emphasise the importance of disulphide bridges on proliferation when the modified synthetic 1-28 of N-POMC (disulphide bridges were changed and cysteines were replaced with methionines) increased the DNA synthesis in the zG and zF of the rat adrenal (Torres et al., 2010). These findings provoked more investigations concerning the effect of ACTH and N-POMC (1-28) on the proteins associated with the cell cycle of the adrenal cortex such as cyclin D and one of the cyclin-dependent kinase (Cdk) inhibitor proteins (P27) in the zG. Both ACTH and N-POMC inhibited the expression of P27 and upregulated the D2 and D3 cyclins (de Mendonca et al., 2013). Others studied the effects of the treatments with POMC-derived peptides on the expression of other cell cycle key genes such as Ccnb2, Camk2a and Nek2 in the rat zG and zF after the inhibition of the HPA axis. The treatments with N-POMC peptides compensated the decreased expression of Nek2 and Notch2 that result from the inhibition of the HPA axis (de Mendonca et al., 2014).

1.4 Centripetal migration of adrenocortical cells

The centripetal migration of cells from the sub-capsular area toward the adrenal cortex /medulla boundary can be proposed on the basis of cell proliferation level in the region of the adrenal sub-capsule and the predominant level of apoptosis in the border between the zR and medulla. The centripetal migration phenomenon provides the adrenal cortex with

regenerative capacity and it was shown that the capsule is necessary for the regeneration of the adrenal cortex in earlier studies (Ingle and Higgins, 1938). Later, several attempts were conducted to trace these proliferating and migrating cells. The earliest cell tracing studies showed that the proliferative cells reach the region between the zona Fasciculata and the zona Reticularis one month after tritiated thymidine injection, and the zona reticularis was enriched with these cells two months after injection in rats (Diderholm and Hellman, 1960). Other researchers (Zajicek et al., 1986) estimated most of the labelled cells were localised in the capsule one day after injection of the rats with thymidine, these cells then crossed the cortex zones, reaching the medulla surface after 104 days. During the journey, 50% of the proliferative cells die, while the rest are eliminated at the boundary of the zR with the medulla. Proliferating cells were detected by other methods such as the analysis of the expression of proliferating cell nuclear antigen (PCNA) (Mitani et al., 1994). In rats, most of the labelled cells were localised in the zI and the capsule, suggesting these areas to be the regions where proliferative activity is highest Mitani et al.,(2003). Adrenal enucleation experiments revealed the role of the remaining capsular and sub-capsular cells, after enucleation and these cells were found to be responsible for regenerating the adrenal cortex (Bland et al., 2003). The regenerative capacity of the adrenal cortex has also been observed in allowing continuous adrenal cortex replenishment after injury (Yates et al., 2013).

1.5 Embryonic development of the adrenal cortex

The embryonic origin of the adrenal gland has been intensively studied in mammals such as humans and rodents and has revealed similar characteristics in such mammals. The adrenal cortex shares a common developmental origin with the gonads and kidneys originating from the urogenital ridge and/or intermediate mesoderm of the mesothelium. The development begins with a single layer of the mesothelium (coelomic epithelium) enlarging in thickness at the urogenital ridge at around E9.5 in mice (Bandiera et al., 2013, Hatano et al., 1996) and around the fourth week of gestation in humans (Norris and Carr, 2013). The thick cellular area of the coelomic epithelium forms the adreno-gonadal primordium (AGP), which is the precursor of the adrenal cortex and gonads. The cells that are meant to become the adrenal cortex (adrenal primordium) of the AGP start to appear distinct from surrounding structures by differentiating into acidophilic and slightly larger cells (Hanley et al., 1999).

These cells partially penetrate or attach to the basic mesenchyme, which forms the primitive or foetal adrenal cortex. These foetal cortex cells are infiltrated by the medullary primordium cells that migrate from the embryonic neural crest to the innermost part of the foetal cortex, which will form the adrenal medulla. Around the sixth week of gestation, the mesothelium provides more cells to surround the original foetal acidophilic cortex cells, but these incoming cells are basophilic smaller cells, which densely pack at the exterior of the foetal zone. At the 8^{th} week of gestation, the developing foetal cortex acquires two simple zones: the inner foetal zone, which comprises large eosinophilic cells, and the outer definitive zone that contains small packed basophilic cells (Goto et al., 2006, Hanley et al., 2001). The mesenchymal capsule starts to surround the developing foetal cortex and around the 9^{th} week of gestation, the foetal cortex becomes fully encapsulated (Ishimoto and Jaffe, 2011).

The morphology of the prenatal cortex preserves a relatively constant structure: the narrow outer layer of small cells underneath the capsule, which represent the definitive zone that exhibit characteristics of proliferative cells and the inner foetal zone that is composed of columns-like cells that reach the outer border of the medulla. During the meddle of gestation the cells of the definitive zone contain a low level of lipids. However, after that, as the embryo developing these cells gradually accumulate lipid and become steroidogenically active. While, the large columns-like cells (foetal zone) have typical characteristics of steroidogenic cells (Sucheston and Cannon, 1968, Mesiano et al., 1993).

The foetal cortex undergoes rapid regression after birth and the definitive cortex expands on top of the degraded foetal cortex. However, not all the foetal cells undergo degradation, a Cre recombinase experiment examining the lineage of foetal adrenal cells, suggested that there are a population of cells belonging to the foetal adrenal buried among adult cortical cells, which form a third zone between the definitive zone and foetal zone called the transitional zone (Ishimoto and Jaffe, 2011). Cells in the transitional zone show characteristics of both zones (definitive and foetal zone) and they are capable of synthesising cortisol (McNutt and Jones, 1970). These infringing foetal cortical cells are potentially involved in the pathway of the adult cortex cell development till mouse embryonic day 14.5 (Zubair et al., 2008). As gestation advances to around the 30^{th} week, the human foetal adrenal cortex starts to exhibit the fundamental form of the adult zG and zF of definitive zone and transitional zone respectively (Sucheston and Cannon, 1968). Furthermore, in primate mammals such as humans, the outer layer of the foetal zone differentiates to form the zR (Brugger and Prayer, 2006, Xing et al., 2015, Malendowicz, 2010).

1.5.1 **Factors associated with adrenal cortex development**

Several essential influences have been described as crucial for the development of the adrenal cortex such as blood supply, hormonal factors and paracrine adrenocortical factors (Willenberg and Bornstein, 2000). Several pathways and factors have been revealed to be important for adrenal development.

1.5.1.1 **Wingless-type MMtv (Wnt) signalling pathway**

The Wnt signalling pathway has been recorded as an evolutionarily conserved pathway, which regulates several characteristics of the mammalian cell such as cell migration, cell polarity and organogenesis during development. The large family of Wnt glycoproteins involved in signalling pathways are activated after the Wnt ligand binds to its respective Frizzled receptor. This pathway has been categorized into canonical (Wnt/β-catenin dependent) pathway and the non-canonical (β-catenin-independent) pathway, which can include planar cell polarity or the Wnt/Ca^{2+} pathways (Komiya and Habas, 2008). Several of the Wnt pathways have been recorded to play an important role in the homeostasis and the development of adrenal cortex. For instance, Wnt4 is been involved in the growth and development of several organs such as the gonads, kidney, adrenal, mammary gland and pituitary (Bernard and Harley, 2007). A defect of Wnt4 (noncanonical Wnt) caused a disturbance in the cell migration during the development of the mammalian gonad and adrenal cortex (Jeays-Ward et al., 2003). In the adult tissue, the inhibition of Wnt signalling by protein kinase cAMP-dependent (PKA) in adrenal cortex suppresses malignancy (Drelon et al., 2016).

1.5.1.2 **Hedgehog signalling pathway**

Hedgehog (Hh) was first identified during genetic screening aimed to understand the body segmentation of the *Drosophila melanogaster* embryo (Nusslein-Volhard and Wieschaus, 1980). The hedgehog (Hh) pathways are important for embryonic development and mammalian cell proliferation and differentiation (Ingham and McMahon, 2001). The Hh signalling pathways have been associated with the regulation of vertebrate stem cell fate (Blank et al., 2008). These developmental and well-conserved signalling pathway molecules have been recorded in the development of limbs, lungs, skin and the neural tube (Xie and Abbruzzese, 2003, Blank et al., 2008). The Hh pathways are activated by molecules called ligands/morphogens such as Indian hedgehog, Desert hedgehog and Sonic hedgehog (Shh). These ligands are formed, modified and then secreted from the cells (Burke et al., 1999). Each of these ligands interacts and moves through the extracellular matrix to locate their receiving cells where they bind to a Patched-1 receptor, which cause the endocytosis and degradation of Hh. The endocytosis of Shh promotes the translocation of Smoothened (Class Frizzled G protein-coupled receptor) from plasma to the cell membrane. The promotion of Smoothened is critical to activate a family of transcription factors called the glioma-associated oncogenes (Glis) (Ching and Vilain, 2009). The pathway activated by the sonic hedgehog (Shh) ligand has been suggested as important for adrenal cortex development in mice (Bitgood and McMahon, 1995, Guasti et al., 2011). As Shh is essential for adrenal cortex organogenesis, its transcriptional factor (Gli1) is found to be expressed in the mouse adrenal capsule (Ching and Vilain, 2009). The expression of Shh is also detected in the sub-capsular area in mice (Guasti et al., 2011, King et al., 2009). The important role of Wilms tumour 1(WT1) and Shh in adrenal cortex development and are also involved in stem cell

maintanance (Walczak and Hammer, 2015). Recent findings showed that the activation of Wnt signalling (that support the regeneration of the adrenal cortex after long-term treatment with glucocorticoid) was related to shh signalling (Finco et al., 2018).

1.5.1.3 **Steroidogenic factor 1 (SF1) and Wilms tumour 1 (WT1)**

The key fate inducer of adrenocortical cells is the steroidogenic factor 1 (Sf1) or also called Adrenal 4 binding protein (Ad4bp), which is a transcription factor that initiates a differentiation programme, transforming the embryonic mesenchymal cells into differentiated steroidogenic cells (Luo et al., 1994). The role of Sf1 is to continue to regulate the transcription of steroidogenic genes for both the adrenal cortex and the gonads because it has binding sites up-stream of the promoter or the enhancer regions of several steroidogenic genes (Schimmer and White, 2010).

In addition to Sf1, there are other transcription factors associated with adrenal cortex development such as Wilms tumour 1 (WT1), which is a protein that comprises four zinc-finger motifs at the C-terminus and a DNA-binding domain enriched with glutamine and proline at the N-terminus. WT1 plays an essential role in the normal development of the urogenital system (Berry et al., 2015) and regulates the development of interstitial progenitor cells during the embryonic development of the mouse testis (Wen et al., 2016). Additionally, it is thought to be involved in the stem/progenitor adrenocortical cell state (Bandiera *et al*., 2013). Furthermore, WT1 assists with the regulation of SF1 transcription during gonadal and adrenal development (Wilhelm and Englert, 2002, Val et al., 2007). The important role of WT1 and Shh in adrenal cortex development has been proposed to be involved in the maintenance of the stem cells of the adrenal cortex (Walczak and Hammer, 2015).

More factors were found to be involved in adrenal cortex development such as transcription factor called co-factor Cited2, which has been described to be associated with the adrenal cortex development because of its expression in the urogenital ridge and it was found to be required to specify a group of AGP cells into adrenal cortex cells when it interacts with WT1. This interaction promotes the expression of Sf1 in the AGP prior the splitting of gonad and adrenal cortex (Val et al., 2007). Factors such as homeodomain protein Pbx1 (homebox protein family of transcriptional factors) are suggested to induce adrenal cortex differentiation because the deficiency of Pbx1 reduces the outgrowth of urogenital ridge and in Pbx1 mutants showed minimum Sf1 expression levels in adrenal (Schnabel et al., 2003).

Other factors like the nuclear receptor transcription factor called Dosage-sensitive sex reversal, Adrenal hypoplasia congenita, on the X chromosome, number 1 (DAX1), a protein encoded by NR0B1 was found to be important for the adrenal cortex development because of the consequences associated with its mutation that cause developmentally relevant adrenal dis-function conditions such as congenital adrenal hypoplasia or adrenal regression (El-Khairi et al., 2011, Xing et al., 2017).

Additional factors and pathways have been studied *in vitro* or in lineage tracing genetic studies have been found to be associated with the regulation of adrenal cortex development. Armadillo repeat-containing 5 (ARMC5) is one such factor identified in these studies and found to be associated with the Wnt/β-catenin signalling pathway in a subset of zona Fasciculata cells. Inactivating mutations of this gene have been found to be associated with a adrenal cortex disorder called primary macronodular adrenal hyperplasia (this disorder can be diagnosed by several small hormone-producing nodules in the adrenal glands) (Berthon et al., 2017).

1.6 Diseases and disorders of the adrenal cortex

The hormones derived from the adrenal cortex are involved in different metabolic activities. When the adrenal cortex is unable to produce its steroids, described as adrenal insufficiency, death results in most cases if not treated. Adrenal insufficiency might result indirectly from various causes such as autoimmune diseases and genetic disorders. Epidemiological studies relate adrenal insufficiency to adrenal crisis. However, recent studies showed that factors related to the adrenal crisis were more complicated than primary and central adrenal insufficiency (Iwasaku et al., 2017). Such adrenal crisis usually requires lifelong treatment via hormone replacement which is not adequate or always available for most cases. Furthermore, the physiological need for adrenal cortex hormones is notably variable and related to patient stress levels and the time of the day, which reduce the efficiency of the common treatments (Dunn et al., 2004).

1.7 Stem cells

Every cell in an organ or tissue has specific functions that make it capable of a special role within these tissues until it dies, whereas stem cells are more concerned with regeneration. These cells such as embryonic stem cells have the ability of self-renewal and differentiation making them able to regenerate different types of body cells (Lu and Zhang, 2015). This remarkable potential of stem cells allows them to develop into almost all cell types providing the tissue that they reside in with a repair system that can be used in case of injury or normal regeneration. These cells specialise in repletion cells of a tissue by asymmetric divisions as well as replenishing themselves by symmetric divisions. These two functions are balanced in the tissue of organs (Morrison and Kimble, 2006). These two special features of stem cells are the main targets for researchers because they play a crucial role in regenerative medicine, which allows in principle researchers to regenerate tissues or organs from these cells, and

then use them as spare parts for humans or animals. Over the last few years, stem cell therapy has received much attention, because of the potential medical revolution being made possible by tissue reprogramming and regenerative medicine (Liu et al., 2017, Lim et al., 2017, Henderson et al., 2017). Stem cells are classified into three types based on their ability to differentiate to other cell types, the first type of stem cells are called totipotent; these are cells that can differentiate into all cell types which represent the blastomeres of the embryonic cells of early stages, which quickly transit from totipotent to pluripotent (Morgani et al., 2013). The second type is called pluripotent; these cells are capable of forming all somatic cells with the exception of forming the embryonic trophoblast (Mitalipov and Wolf, 2009). The final type is called multipotent; these cells can differentiate into a few cell types. Although it is difficult to identify stem cell type due to differences in isolation methods and approaches to characterising these cells, the International Society for Cellular Therapy has taken the responsibility to address human stem cells by proposing criteria to describe these cells (Dominici et al., 2006). However, these standards have proven to be changeable and depend on the new findings regarding stem cell markers (Samsonraj et al., 2015).

1.7.1 Stem cells types

Stem cells can be characterised by several criteria such as their differentiation potentials as described before in section (1.7); these include the number of cell divisions that a stem cell can undergo and remain undifferentiated (self-renewal capacity) or can be characterised by their tissue source. There are different sources of stem cells, which can generally be divided into several classes:

1.7.1.1 Embryonic stem cells (ESCs)

Embryonic stem cells are the most potent normal stem cells that derive from the embryo and have a natural capacity to generate all cell classes in the normal body. Manipulating these cells to become a specific cell type for use in a tissue transplant is practically difficult (Turinetto and Giachino, 2015). These stem cells need to be directed into an adult cell type rather than being transformed into cancer cells, which is a possible dangerous unwanted effect after transplantation. Although ESCs are the most potent stem cells, isolation and cultivation of these cells is quite challenging. ESCs are usually generated from an *in vitro* fertilised ovum and the embryo must be maintained *in vitro* until the formation of the blastocyst, or isolation of the blastocyst from the pregnant female before it reaches the implantation stage into the uterus. Then the ESCs can be isolated from the inner cell mass of the cavity of the blastocyst (Fischbach and Fischbach, 2004). Further to the technical challenges, the medical community raises ethical problems related to the origin of this type of stem cell, since it might be involved in eliminating embryos, especially if ESCs are isolated from humans. These ethical issues have led the medical community to establish policies to limit these treatments (de Wert and Mummery, 2003). Even with approved isolation, the cultivation of ESCs is quite demanding. The normal (non- embryonic) or cancer cell culture requires transferring cells from their natural environment into a plastic culture dish in the laboratory, where the cells are growing over the surface of the dish in the culture medium. In addition to that usual requirement for *in vitro* cultivation, ESCs require special culture medium to maintain their undifferentiated state otherwise they will normally differentiate (Tsuji et al., 2008). Furthermore, the surface of the plastic culture dish, which faces the cells should be coated with a feeder layer. This feeder layer of human or mouse embryonic fibroblast cells is adopted to improve the attachment of ESCs to the culture dish and provide them with factors to support their stemness state (Eiselleova et al., 2008). The wide range of

differentiation capacity that ESCs have allow scientists to analyse different features of several diseases and study the opportunities of using them in medical treatment for incurable diseases such as cardiac disorders (Hausburg et al., 2017).

1.7.1.2 Adult stem cells or somatic stem cells

Adult stem cells are a kind of undifferentiated cell within adult tissues or organs that have self-renewing and multi-differentiation abilities. However, they have less differentiation potential than embryonic stem cells. Since embryonic stem cells are derived from embryos, they have a potential capacity to differentiate into almost all cell classes in the body (Turinetto and Giachino, 2015). Adult stem cells however work as providers of new cells within a tissue or the organ by replacing the dead or damaged cells in order to maintain the viability of the tissue. Their existence in different types of organs has been well established, for instance in the skin, intestine, muscle and other organs (Pittenger et al., 1999). The most widely studied adult stem cell type is bone marrow stem cells which are the progenitors to the various different types of blood cell (Lebouvier et al., 2015). The heart was thought not to have self-renewal capacity, but there have been studies which suggest the presence of stem cells that have a role in the healing process after heart injury (Finan and Richard, 2015). It has also been suggested that the neural stem cells in the central nervous system have the ability to differentiate into astrocytes and neurones (Chu et al., 2015). Generally, most of the clinical research in this area focuses on methods to control the differentiation ability of adult stem cells in order to use them in transplantation therapies. Furthermore, recent studies emphasise that adult stem cells can be used to manage rheumatic diseases such as rheumatoid arthritis and osteoarthritis (Franceschetti and De Bari, 2017).

The limited differentiation ability of adult stem cells (multipotent) is not the only challenge that faces the researchers but also that adult stem cells usually remain quiescent unless they have been activated. For instance, the olfactory epithelium stem cells (sensory neurones

precursor cells) are quiescent in aged mice. However, after induction by a surgical or chemical lesion, these cells shifted functionally and morphologically from quiescent, flattened, horizontal basal cells to proliferative and pyramidal cells (Brann et al., 2015). The importance and the usage of adult stem cells have been well established in different types of adult organs. For instance, the epidermal stem cells of the skin are responsible for skin epithelium homeostasis, wound healing and hair renew cycle processes (Lacina et al., 2015). Another example is the stem cells in the dental pulp that have the ability to generate expanded colonies that can be used to form fibroblast colony units on plastic (Yasui et al., 2015).

The variety of stem cells has been detected in several adult tissues or organs derived from the main three embryonic primary germ layers. For example, endodermic stem cells which are detected in the thyroid gland (Thomas et al., 2006). Ectodermic stem cells such as dopaminergic neurones can give rise to neurones and support (glial) cells (Vermilyea et al., 2017). Mesenchymal stem cells that are derived from the mesoderm, which are well studied as they are present in almost all vascularised organs of the body (Crisan et al., 2008), the adrenal cortex is also derived from the mesoderm, which might possess mesenchymal stem cells.

1.7.1.3 Mesenchymal stem cells (MSCs)

MSCs have been considered as the most potent adult stem cells with the most potential for clinical therapy because of their high capacity for regeneration and differentiation into various cell types. Furthermore, simple isolation and conventional *in vitro* cultivation methods can be used with MSCs, this facilitates the study of these cells and their use in research and in the clinic, especially in regenerative medicine. Unlike human embryonic stem cells, the growth and maintenance of MSCs do not necessitate the use of a feeder layer. On

the other hand, MSCs are usually isolated from adult tissues and the isolated stem cells will experience a new *in vitro* environment after a long term period in their *in vivo* microenvironment, which might alter the cell function and structure. This environmental alteration after transfer of the cells from *in vivo* to *in vitro* might result in losing the required information for development of these cells in particular (Higuita-Castro et al., 2017). These limitations necessitate quality controlled isolation methods for MSCs, which are based on the capacity of these cells to adhere to plastic and express appropriate surface stem cells markers (Harichandan et al., 2013).

One of the natural therapeutic potentials of MSCs is their capacity to migrate toward special targets within the tissue they are raised in. The migration properties of MSCs make these cells capable of transporting to the damaged sites in animal tissue, but the molecular mechanism of MSCs migration within damaged tissue remains unclear (Tang et al., 2017, Xu et al., 2017). However, a few studies have suggested that chemokine receptors, ligands and adhesion molecules are involved in facilitating the migration for tissue repair *in vivo* (Chamberlain et al., 2007). Examples of these facilitating mediators include: platelet-derived growth factor receptor (Nakamizo et al., 2005, Fiedler et al., 2002), integrin α4β1)/vascular cell adhesion molecule-1 (Cui et al., 2017), stem cell factors such as cytokines that bind to receptors like c-kit, HGF/c-Met (Forte et al., 2006), stromal cell-derived factor 1 (SDF-1)/C-X-C chemokine receptor type 4 (CXCR4) (Son et al., 2006, Nakamizo et al., 2005), high mobility group box 1/receptor for advanced glycation end-products (Palumbo and Bianchi, 2004, Palumbo et al., 2007), vascular endothelial growth factor receptor (Ball et al., 2007), monocyte chemoattractant protein-1 (MCP-1)/C-C chemokine receptor type 2 (Dwyer et al., 2007) and other cell adhesion molecules (Ip et al., 2007, Son et al., 2006).

These chemokine receptors and cytokines also regulate the response of white blood cells (leukocytes) to inflammation, injury or tumour microenvironment. MSCs are therefore

thought to respond in a similar manner to leukocytes (Balkwill, 2004). The inflammatory and tumour signalling might induce MSC migration. For example, the chemokine receptor pairs, SDF-1 and CXCR4 are important mediators for the recruitment of the MSCs to tumours (Nakamizo et al., 2005). The cellular hypoxia that results from the expression of proangiogenic molecules which are expressed in several tumour microenvironments induces transcription factors such as hypoxia-induced transcription factor (HIF-1α) that up regulates genes like vascular endothelial growth factor, tumour necrosis factors, macrophage migration inhibitor factor, and other cytokines (Winner et al., 2007). The cellular hypoxia also generates chemokines such as monocyte chemoattractant protein-1, which has a role in the migration of MSCs to tumours (Dwyer et al., 2007). However, other chemokine-receptor interactions are required to induce MSC migration toward inflammatory and tumour sites for therapeutic purposes.

Additional therapeutic action of MSCs includes their ability to secrete soluble factors that can induce an immunomodulatory environment *in vitro* (Ye et al., 2008) and *in vivo* (Joo et al., 2010).

MSCs have been isolated from a number of human and animal tissues such as dental pulp, heart, spleen, liver, adipose tissue, testes, hair follicles, dermis and bone marrow (Augello and De Bari, 2010). Additionally, their clinical regenerative potentials have shown applicable results. For example, in spite of several MSC cultures being shown to have heterogeneous populations of cells, MSCs have been used for various pre-clinical and clinical experiments to treat several conditions like cartilage injury (Borakati et al., 2017), infarction of myocardium, liver diseases, graft-versus-host disease (transplant rejection) and defective osteogenesis (Kim and Cho, 2013, Joo et al., 2010, Killington et al., 2017). Furthermore, managing the use of MSCs from amniotic in trans-amniotic stem cell therapy to treat new-borne illness has shown significant improvement in the abdominal wall defects caused by

gastroschisis (Fauza, 2017). The sources of MSC cultures isolated from different tissues and cultured *in vitro* with different conditions raises complications in MSC identity. Even though there are intensive studies regarding the identification MSCs markers, there is no definite consensus as to what markers specific for identifying MSCs.

1.7.1.5 Induced pluripotent stem cells (iPSCs)

In 2006, scientists developed a genetic reprogramming method that induces changes in typical cells in the laboratory to become potentially like embryonic stem cells. Skin cells have been transformed into pluripotent cells through this technique. Controlling cell behaviour by specific genetic modification in this way therefore results in the generation of embryonic like stem cells (Turinetto and Giachino, 2015). The process of generating iPSCs involves transfecting the target cells in a two stage process with Yamanaka factors; the first transfection is with c-Myc and Klf4 and the second transfection with Oct4, Sox2 and Klf4. This process mainly aims to establish bivalent chromatin domains (an area where the DNA has epigenetic modifications to increase or decrease its accessibility to RNA polymerase) by the first wave, and DNA methylation by the second wave for obtaining pluripotency (Polo et al., 2012). More recent cell reprogramming methods involve using viral vectors such as Sendai viruses to transduce the Yamanaka factors to the target cells (Fusaki et al., 2009). The recombinant single-stranded RNA (ssRNA) viruses undergo cytoplasmic replication in the host cell and do not enter the nucleus or need to form a DNA intermediate to integrate with the host cell DNA. In addition, they are neither pathogenic nor tumorigenic to humans (Nakanishi and Otsu, 2012, Chichagova et al., 2015). Such promising techniques might replace older methods of harvesting stem cells from human embryos and thus release stem cell therapy from ethical issues to some degree. However, several mutations in signalling pathways that lead to cancer are similar to those induced during pluripotency, which reveals

the notable resemblances of cellular reprogramming with tumorigenesis (Stadtfeld and Hochedlinger, 2010).

1.7.1.4 Foetal trophoblast derived stem cells.

ESCs are usually isolated from the inner cell mass of the cavity of the blastocyst (Fischbach and Fischbach, 2004). The remaining trophoblastic portion gives rise to organs and tissues such as placenta, amniotic fluid and umbilical cord, which also possess stem cells. The trophoblastic foetal tissues have stem cells that enhance and activate the growth and development of all foetal organs from their location inside their tissues. In comparison to adult tissues, foetal tissues contain relatively large numbers of stem cells, which are also accessible to appropriate isolation methods making them an important source of stem cells (Pop et al., 2015). One of the advantages of these stem cells, in addition to their young age, is their relative lack of ethical conflicts because all of the trophoblast system (placenta, amniotic fluid and umbilical cord) is normally discarded post-partum. The use of these stem cells in regenerative medicine is suggested to be more amenable than stem cells derived from the bone marrow for myocardial regenerative therapy (Makhoul et al., 2013). Furthermore, regarding the fact that different stem cells have different potentials and differentiation tendencies based on their different sources, the two sides of the human placenta (foetal and maternal origins) have two different therapeutic potentials (Zhu et al., 2014). Recent studies identify a subset of placental stem cells, which have a higher migration rate to wound injury and a highly effective wound healing capacity (Wang et al., 2017).

Additionally, stem/progenitor cells also exist in the amniotic fluid, which is described as multipotent. Several recent studies suggest their ability to be differentiated into myocardial cells (Jiang and Zhang, 2017) and distal lung phenotype cells (Jensen et al., 2017, Lesage et al., 2017).

Furthermore, the umbilical cord stem cells and the blood stem cells within the umbilical cord are tissue-specific. Similar to the stem cells in the adult bone marrow, these are thought to be multipotent and may differentiate into all the cells in the normal bone marrow. Various studies have used blood stem cells isolated from umbilical cords therapeutically to treat diseases. For example, umbilical cord stem cells were used to treat blood diseases and repair serious cardiac injuries that frequently cause heart failure (Hollweck et al., 2012). These stem cells have also been used for the treatment of children with perinatal brain injury (McDonald et al., 2017) and the treatment of acute ocular burns in children (Sharma et al., 2017). Scientists are also working to manipulate these stem cells by preserving the discarded placenta and umbilical cord blood from newborn babies for potential future use because these tissues showed potential pluripotency (Beeravolu et al., 2017).

1.7.2 Stem cells markers

Specific proteins or genes that can be used for identifying and isolating stem cells are known as stem cells markers. Using these markers can allow efficient stem cell isolation using a method such as flow cytometry or magnetic cell sorting. Considering the functions of stem cells markers is important for characterising and understanding the mechanisms by which stem cells maintain their pluripotency/multipotency and self-renewal (Zhao et al., 2012). For instance, markers such as Sox2, Klf4 contribute to maintaining stem cell stability and inhibit the transcriptional activity that might result in differentiation (Liebau et al., 2014). Nanog and Oct4 were the first proteins identified as being required for maintaining the pluripotent state in ES cells (Loh et al., 2006, Hayashi et al., 2015). Since then, several other stem cell markers for pluripotency have been discovered. Furthermore, Liebau et al. (2014) address the intrinsic role of stem cell markers not only as proteins that can be used for identifying or isolating the

stem cells but also can be used for reprogramming adult cells to act as pluripotent stem cells such as Oct4, Sox2, Klf4 and c-Myc.

There is no agreement on a unique surface molecule to identify MSCs from various sources because identifying a specific set of unique characteristics facilitating reliable identification of these multipotent stem cells has been challenging (Lee et al., 2014).

However, a few criteria were suggested to be the minimum for the identification of human MSCs, such as their capacity to remain adherent to plastic under the standard *in vitro* culture conditions. Along with their capacity to express CD105, CD73 and CD90 and lack of expression of CD45, CD34, CD14 or CD11b, CD79a or CD19 and human leukocyte antigen – antigen D related (HLA-DR) and that they are potentially capable of differentiating into chondrocytes, osteoblasts and adipocytes (Dominici et al., 2006). As the bone marrow (BM) is the most studied source of MSCs, other surface antigens were recognised to expressed by this type of MSCs including CD29, CD13, CD10 and CD44 (Buhring et al., 2007). There are two types of markers proposed for identifying MSCs: first is the sole marker, which represents a core characteristic of MSCs such as the plastic adherence capacity of MSC that is appropriate for identification or isolation of MSCs from their natural tissues or a sole marker that can substitute the presence or absence of the other defined markers for MSCs such as CD271 (Flores-Torales et al., 2010). Second markers are called the stemness markers, which can identify the population of MSCs with multipotency and high colony forming units or markers that can specify an ESC-like population within the isolated MSCs. Therefore, the sole marker is required to be highly expressed while the stemness markers can be less expressed but at a detectable level.

The most recognised finding regarding identifying and isolating MSCs using stem cell markers is the heterogeneity of the isolated cells. The heterogeneity of isolated MSCs

populations is now widely accepted and criteria that characterise MSCs represent a proportion of the isolated cells, and such heterogeneity may be reflected by some markers like CD200 (Pontikoglou et al., 2016). The tissue source that MSCs are originated from, might influence the potential capacity of the cells. For example, in addition to BM, several alternative tissues were recognised to be sources for MSCs and they are expected to have the capacity for clonogenicity and multipotency. However, only a fraction of the isolated plastic adherent MSCs and colony-forming units showed multipotency, which indicates a heterogeneous cell population with differential protein expression and cytokine profiles. This heterogenicity may relate back to their different niches *in vivo,* which result in a different commitment from their lineage *in vitro* (Russell et al., 2010). The multipotency and the tendency for differentiation of the isolated MSCs from different sources are also different. For instance, the potency of MSCs of BM to differentiate into osteocytes was higher than their potency to differentiate into adipocytes (Muraglia et al., 2000). While the dental follicle stem cells have a spontaneous tendency to differentiate into osteocytes (Lucaciu et al., 2015). In a differentiation comparison study, the ectopic transplantation of MSCs originating from BM resulted in differentiation into heterotopic bone tissue, while dental pulp-derived MSCs differentiated into reparative dentin-like tissue (Batouli et al., 2003). Furthermore, MSCs might possess an immature cell population, which present embryonic stem cell criteria by expressing markers like Oct-4 and Sox2 (Kuroda et al., 2010).

1.7.3. Stem cells niches

The stem cell microenvironment or so-called “niche” has been reported to have a crucial role in the regulation and maintenance of stem cells. Different niches promote different activities. For example, osteoblastic niches support a quiescent state where the hematopoietic stem cells maintain slow cycling or stay in the G0 state due to the hypoxic environment, the oxygenic vascular niche stimulates the proliferating activity of these stem cells (Yin et al., 2006).

Although several tissue stem cells types have been proven to be quiescent in their niches, they have the potential to be able to differentiate, proliferate and self-renew (Li and Clevers, 2010, Wilkinson and Gottgens, 2013). The interaction between the stem cells and their niches provides a state that allows lifelong maintenance of the tissue and safeguards the stem cells from various stressful conditions, as well as stimulating these cells to proliferate and support the tissues with progenitor and differentiated cells (Arai and Suda, 2008).

1.7.4. Stem cells in the adrenal cortex

The adrenal cortex is an active endocrine organ that contains a number of different cell types that are replenished continuously. The existence of stem cells is required for cortical homeostasis where centripetal migration of the adrenocortical cells from the capsular and sub-capsular areas move cells towards the border between cortex and medulla where the differentiated cells undergo apoptosis (Pihlajoki et al., 2015). Several studies on adrenal cortical stem cells have investigated the capsule, not only as a simple layer that supports the cortex to integrate the gland structure as most histological studies describe but also as a niche for adrenocortical stem cells that serve as originator cells for other cells in the cortex (Walczak and Hammer, 2015). The proposed existence of stem and progenitor cells within the adrenal cortex date back to early studies of the 1930s. These studies revealed the capacity of the capsule and sub-capsular layers to restore the adrenal cortex 6 weeks after adrenal enucleation (Ingle and Higgins, 1938). A few years later, lineage tracing experiments were conducted to reveal a genetic clonal relationship between the adrenocortical capsule cells and the differentiated cells beneath it, which showed that inner differentiated cortex cells are derived from the mesenchymal Sf1-negative capsule (Salmon and Zwemer, 1941).

The adrenal cortex of several mammalian species have been suggested to have a mix of clusters of undifferentiated cells in the sub-capsular layer along with cells expressing Cyp11B2 within the zona glomerulosa which are known to have limited steroidogenic

capacity in mice (Heikkila et al., 2002) and humans (Nishimoto et al., 2010). These findings suggest the presence of a stem/progenitors cells population in the adrenal cortex.

Microarray data (donated by Dominic Cavlan, William Harvey Research Institute, Barts and The London School of Medicine) from a whole rat genome array was used to compare the expression in the zF, capsule and zI. This data highlighted a range of potential stem or progenitor cell markers that have been over-expressed in one or both the capsule and the zI in comparison to their expression level in the zF.

1.3 Aims of study

1- Firstly, this project aims to confirm these microarray data by nominating and examining a number of these markers and detecting their locations of expression and segregation in the adrenal cortex.

2- Identify the best potential marker to be used for isolating potential stem cells and isolate the target cells.

3- Study the isolated cells *in vitro* to investigate their gene expression including other stem cells markers.

3- Study the capacity of these cells for self-renewal, viability and stability after long-term *in vitro* cultivation.

4- Then investigate their differentiation response after a number of differentiation methods.

Chapter two

Detection of potential stem cell marker mRNAs and protein in the adrenal cortex

2.1 Introduction

The aim of this chapter is to characterise a number of potential adrenocortical stem cell markers. Although, several studies have proposed the existence of adrenocortical stem cells (Heikkila et al., 2002, Nishimoto et al., 2010, Mitani, 1994, Walczak and Hammer, 2015), to our knowledge specific adult stem cell markers for adrenal cortex have not been established. Most of the research refers to the capsule of the adrenal gland as the niche for these stem cells. However, Mitani, 1994 refers to the potential of the zI in rat adrenal cortex to possess stem/progenitor cells as it did not show corticosteroid enzymatic activity.

Finding stem cell markers in the adrenal cortex during this project started with bioinformatic analysis of microarray data (donated by Dominic Cavlan, William Harvey Research Institute, Barts and The London School of Medicine) from a rat whole genome array, which was used to compare the expression of all genes in the zF, capsule and zI. This data highlighted a range of potential stem or progenitor cell markers that were over-expressed in one or both the capsule and the zI in comparison to their expression level in the zF. This array analysis resulted in the identification of a wide range of potential markers. These nominated markers underwent further investigation in the previous studies regarding their role in stem cells characteristics. This combined information resulted in few nominated markers. The gene expression of these potential stem cell markers was examined to confirm the array data. So Reverse transcription polymerase

chain reaction (RT-PCRs) were conducted using specific primers (table 2.1) to confirm the gene expression of these potential stem cell markers. Further investigations were then conducted to reveal details of where the mRNA and protein of these potential markers were along with the spatial expression in the adrenal cortex. These investigations included molecular cloning, labeled-RNA probe generation, *in situ* hybridisation, immunohistofluorescent, microscopy and imaging analysis. Three proteins were identified as potential adrenocortical stem cell markers. Transmembrane protein121 (Tmem121), Thy-1 cell surface antigen (Thy-1) and Krüppel-like factor 5 (KLF5). They were selected from the microarray data (table 2.2) based on their expression patterns in the adrenal cortex. All of these investigations obtained primary information on these markers in the adrenal cortex and aided specification of the best marker for the next steps of this project.

2.2 Material and methods

The work within this project started with the analysis of microarray data donated by Dominic Cavlan, (William Harvey Research Institute, Barts and The London School of Medicine) to identify stem cell markers. Laser capture microdissection (Figure 2.1) of a rat adrenal gland section was conducted and whole genome array analysis was used to compare expression in the zF, capsule and zI. The analysis of these data included sort the data in Microsoft Excel to show the fold ratios of gene expression of over 30,000 genes based on their expression in the adrenal capsule divided by their expression in zF and zI. Then the fold ratios of gene expression in the adrenal zI were sorted in the same way, by dividing their expression in the zI by their expression in capsule and zF. The resulting ratios were then sorted from high-low to present clear data of sorted genes that were highly expressed in the capsule and zI, but have low expression in zF. A number of these genes were then disregarded as they represented an unknown expressed sequence tag (EST). The rest of the analysis was conducted by reviewing the related articles regarding over 60 nominated genes that show the highest expression in the capsule in comparison with zF and/or zI in comparison with zF. These genes or markers might identify important MSCs characteristics, such as the ones that have a role in self-renewal of stem cells. The potential stem cell markers were then practically tested in order to confirm the array data.

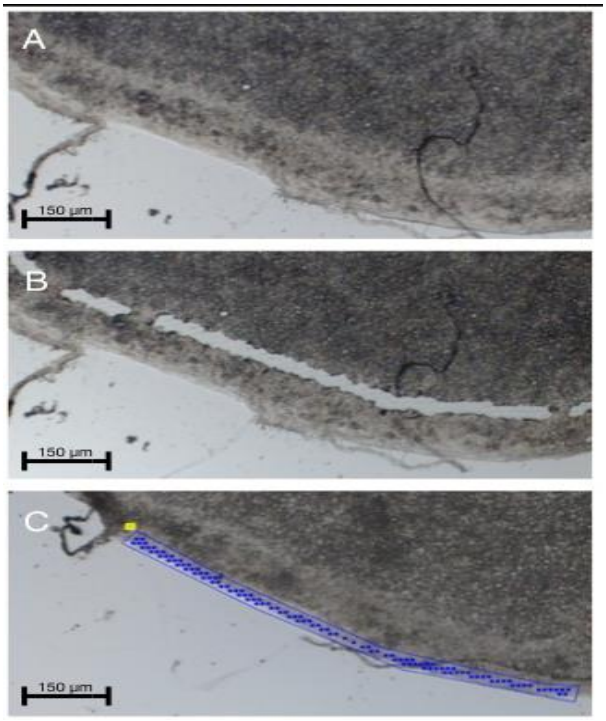

Figure 2.1 Laser capture microdissection (LCM) of the rat adrenal cortex, targeting the nominated stem cell zones (capsule and zI). A: Intact rat adrenal cortex slide. B: Adrenal cortex slide after removing zI. C: Adrenal cortex slide with the laser system targeting the capsule before capture (Dominic Cavlan, William Harvey Research Institute Barts and The London School of Medicine).

All materials for experiments were sourced from Thermo-Fisher Scientific unless stated otherwise.

2.2.1. Adrenal tissue

To test the array data regarding the gene expression of the potential stem cell markers their expression was examined in rat adrenal tissues. All the adrenal tissues used in this study were freshly isolated from adult Wistar-rats (weight 250-350g) from Harlan Envigo UK were housed in rooms where the ambient temperature and light were under automatic control. The rats were

treated under the United Kingdom Home Office Animals Act 1986. Rats were euthanised by CO_2 asphyxiation.

2.2.1.1 RNA isolation from rat adrenal tissue (TRIzol Reagent method)

TRIzol reagent (Ambion) was used for the isolation of RNA from rat adrenals. TRIzol Reagent is a mixture of phenol, guanidine isothiocyanate, red dye and other proprietary components which is ready to use reagent for the isolation of total RNA. One ml of TRIzol reagent was added to a single adrenal gland in a 1.5ml microcentrifuge tube for homogenization. After homogenization, samples could be stored at -70°C for up to 1 year. To remove insoluble particles after homogenization the mixture was centrifuged at 12,000 g for 10 min at 4°C before the addition of 0.1 ml (10% v/v of TRIzol reagent used) of bromochloropropane (BCP), and the supernatant was then transferred to a clean tube. The sample was then mixed by inversion for 15 seconds and incubated at room temperature for 15 min. Three phases were then observed upon addition of BCP: a colourless upper phase which contained RNA, a white cloudy interface which contained DNA and a red organic phase which contained proteins. Samples were then centrifuged for 15 min at 12,000 g at 4°C. The microcentrifuge tubes were removed from the centrifuge and placed directly into a cooled rack. The colourless top layer that contained the RNA was carefully transferred into a clean 1.5ml microcentrifuge tubes before the addition of 0.5 ml of isopropanol (50% v/v of TRIzol reagent used). Tubes were mixed by inversion and left to stand at room temperature for 15 min before centrifugation at 12,000 g for 25 min at 4°C (the precipitated RNA formed a pellet on the bottom of the tube), the supernatant was discarded and 0.5 ml of 75% (v/v) ethanol was added and mixed to wash the RNA. Next samples were centrifuged at 7,500 x g for 5 min at 4°C. The ethanol was discarded and the pellet was suspended in 50µl of double distilled water (DDW).

To eliminate genomic DNA contamination, DNase treatment was conducted, 6µl of 10x DNase I reaction buffer (Appendix A.1) and 5µl DNase I RNase-free enzyme (1unit/µl) was added to 49µl RNA and mixed which was then followed by incubation at 37°C (water bath) for 15 min. The RNA was then purified by the addition of 300µl of TRIzol reagent per microcentrifuge tube and the RNA was re-purified using the above procedure using proportionally less of each reagent based on the addition of 300µl of TRIzol reagent instead of 1ml. The final RNA pellet was dissolved in 50µl of DDW. Analysis by spectrophotometry using a Nanodrop (2000) was carried out to measure the concentration and the purity of isolated RNA using 1µl of the isolated RNA. The 260/230 and 260/280 ratio were used to estimate the RNA purity. The 260 nm wavelength represents the peak absorbance of the nucleic acid bases in DNA and RNA, this varies due to different ratios and types of bases that construct the nucleic acids. These differences alter depending on the concentration. RNA absorbance is doubled at 260nm to 280nm, whereas DNA absorbance at 260nm is 1.8 of its absorbance at 280nm. Therefore a 260/280 ratio of ~1.8 is generally accepted as "pure" for DNA and a ratio of ~2.0 is generally accepted as "pure" for RNA. If this ratio was lower than expected it might indicate the presence of contaminants such as protein or phenol that absorb at or near 280nm, any other contaminants that absorb at or near 280nm may cause the same low ratio.

2.2.1.2 RNA electrophoresis

The isolated RNA was analysed by agarose gel electrophoresis to test its integrity. The RNA was mixed with loading buffer (6X DNA loading dye). The gel was prepared by melting agarose at a concentration of 1.2% w/v in 1X Tris Acetate EDTA (TAE) buffer (Severn Biotech) in a microwave for 1 min, the solution was cooled to ~65°C. Ethidium bromide was then added to a final concentration of 0.1µg/ml, the solution was then mixed thoroughly and poured into gel tray.

The agarose gel underwent electrophoresis for 1 hour, at 7 volts/centimetre (v/cm). Lastly, the gel was visualised by a transilluminator to identify the ribosomal RNA 28 subunit (28s) and 18 subunits (18s) RNA bands, to confirm RNA integrity.

2.2.2 cDNA synthesis (RT-PCR)

For synthesis of total cDNA, a RevertAid First Strand cDNA synthesis kit was used. After thawing the components of the kit, they were mixed, briefly centrifuged and stored on ice. An aliquot of 1-5µg of isolated RNA was mixed with 1µl (100µM) oligo (dT)18 primer, or a mix of 0.5µl (100µM) oligo (dT)18 primer and 0.5µl (100µM) random primers depending on the targeted gene. The volume was made up to 12 µl by the addition of nuclease-free water. Subsequently, the reaction volume was made up to 20µl by adding 4µl of 5X reaction buffer (Appendix A.2), 1µl of (20u/µl) of RiboLock RNase Inhibitor, 2µl (10 mM) deoxydNTP Mix and finally 1µl of (200u/µl) RevertAid reverse transcriptase. The reaction was incubated at 42°C for 1 hour, before termination at 70°C for 5 minutes.

Table 2.1 List of primers (Invitrogen) used in the RT-PCR, their reference number, position in the mRNA sequence and their product size.

Gene symbol	**Forward primer 5`-3` (position in the sequence)**	**Reverse primer5`-3` (position in the sequence)**	**Segment Size(bp)**	**Gene code**
GAPDH	CAAGGTCATCCATGACAACTTTG (540-562)	GTCCACCACCCTGTTGCTGTAG (1035-1014)	496	XM_017593963.1
Klf5	CACAGCGCCAGAGGTGAACAATATC (507-531)	ATGGATGCGTCGCTTCTCCAGATC (1020-997)	514	XM_006252403.3
Thy-1	CCTCCAAGCCACGGACTTCATTTC (865-888)	AAGGCTCAGCAGCGCTCTCCTATC (1377-1354)	513	XM_017595476.1
Tmem121	TTGGTAGGCGATGTGTGCTTCCTG (393-416)	ATCATCTTCTGCGGTGCGATGTGC (901-878)	509	XM_006240674.3
M13	CGCCAGGGTTTTCCCAGTCAGC	TCACACAGGAAACAGCTATGAC		
NR5a1	AATTCTCCTTCCGTTCAGCGGACG (113-136)	GTTCTCCTGCTTCAAGGCCCG (471-451)	359	NM_001191099.1

2.2.3 Generating amplicons of target genes by PCR

PCR was used to detect the expression of the genes of interest, as well as amplifying the desired amplicons that can be used later for generating RNA probes. A 25µl PCR reaction was prepared in 0.2 ml microcentrifuge tube by mixing 12.5µl pre-aliquoted Extensor Hi-Fidelity PCR master mix, 1µl of each primer (10µM), 1µl cDNA (20ng/µl) and 9.5µl of nuclease-free water to make the total volume 25µl. The components of the reaction were then mixed. The PCR conditions used were as follows: 94°C for 1 min for initial denaturation and activation of Taq polymerase, followed by 29 cycles of 94°C for 20 sec for denaturation, 58°C for 20 sec for primer annealing, finally the extension was performed at 72°C for 1 min which was carried out to ensure the completion of full length DNA product. The same preparations were conducted for each PCR with slight changes depending on the annealing temperature. After the reaction was complete the PCR products were then profiled by electrophoresis on a 1.2% (w/v) agarose gel with a 1Kb plus ladder (Generuler).

2.2.4 Purification of DNA from agarose gel slices

The QIAquick Gel Extraction Kit (Qiagen) was used to purify DNA from agarose gel slices. The band of interest was excised from the gel using a clean scalpel blade, placed in a 1.5ml microcentrifuge tube and weighed to estimate the needed volumes (assuming a density of 1g/ml). Three volumes of Buffer QG (Appendix A.3) were added to each 1 volume of the gel. The gel slices were incubated at 50°C, mixing every 2-3 minutes until the gel slice had completely dissolved. After the gel slice had dissolved, 1 gel volume of isopropanol was added to the sample and mixed. Then the mixture was transferred to a QIAquick spin column in the provided 2 ml

collection tube. The sample was centrifuged at 17,900 x g for 1 min to bind DNA, and the flow-through was discarded. If the DNA was to be used for *in vitro* transcription, 0.5 ml Buffer QG was added to the QIA quick column and it was centrifuged for 1 min. The flow-through was then discarded and the QIAquick column placed back into the same tube.

In order to wash the DNA, 0.75 ml of Buffer PE (Appendix A.4) was added to the QIAquick column, which was centrifuged for 1 min, the flow-through was discarded and the QIAquick column placed back into the same tube. The QIAquick column was then centrifuged for 1 min at 17,900 x g to remove residual wash buffer. Finally, to elute the DNA, the QIAquick column was placed into a clean 1.5 ml microcentrifuge tube, and 50 µl of nuclease-free water was added to the centre of the QIAquick membrane. In order to increase the yield of purified DNA the column was left to stand for 1-5 min before centrifugation for 1 min. The purified DNA was analysed by agarose gel electrophoresis (section 2.2.1.2).

2.2.5. Ligation

The cloning of inserts into the pGEM-T Easy vector (Promega) was conducted by TA ligation. Ligation reactions were carried out using T4 ligase (Promega) to ligate the genes of interest into the pGEM-T Easy plasmid vector. The reaction mixture was 10µl in total, and contained 1µl of 10x ligation buffer (Appendix A.5). Then the vector and the insert were added. The addition of the DNA insert and the vector was conducted using a 3:1 (insert: vector DNA) molar ratio. Lastly, T4 ligase (1-3 Weiss units) was added. The reactions were mixed by pipetting and incubated overnight at 4°C.

2.2.6 Competent *E. coli* preparation and transformation

The Inoue method for "Ultra Competent" cell preparation and transformation (Inoue *et al*., 1990) was used to prepare Mach1™ *Escherichia coli (E. coli)*.

2.2.6.1 Preparation of competent cells

A frozen *E coli* culture at -80ºC was thawed and used to seed 25ml of Luria-Bertani broth (LB) (Appendix A.6) in a 50ml falcon tube. The tubes were incubated for 6-8 hours at 37ºC with vigorous shaking (250-300 rpm). After incubation, the starter culture was used to inoculate three 1litre flasks, each containing 250 ml of LB. The first flask received 2ml of starter culture, the second received 1 ml and the third received 0.5 ml. All three flasks were incubated overnight at 18-22ºC with moderate shaking (190 rpm).

The following morning, the optical density at 600 nm (OD600) of all three cultures was monitored every 45 minutes. When the OD600 of one of the cultures reached 0.55, the culture vessel was transferred to an ice-water bath for 10 minutes and the two other cultures were discarded. The cells were harvested by centrifugation at 2,500g for 10 minutes at 4ºC. The medium was removed by vacuum aspiration ensuring that any drops of remaining media adhered to walls of the centrifuge bottle or trapped in its neck were removed. Next, the cells were suspended by swirling in 80 ml of ice-cold Inoue transformation buffer (Appendix A.7), before centrifugation at 2,500g for 10 minutes at 4ºC to remove the buffer.

The cells were re-suspended in 20 ml of ice-cold Inoue transformation buffer, before the addition of 1.5 ml of dimethyl sulfoxide (DMSO) which was followed by mixing. Working quickly, 0.25ml aliquots of the suspension were dispensed into chilled, sterile microcentrifuge tubes. The competent cells were snap-frozen immediately by immersion in a bath of liquid nitrogen. The microcentrifuge tubes were then transferred to a dry ice before finally being stored at -80 ºC until needed. Before each use, a tube of competent cells was removed from the -80ºC freezer and thawed slowly in an ice bath.

2.2.6.2 Transformation

Aliquots of 50µl of competent cells were thawed on ice before the addition of the ligation reaction mix (10µl). The tubes were mixed gently and two control tubes for each transformation experiment were prepared. This included a tube of competent bacteria that received the same quantity of a standard ligation preparation but with empty plasmid DNA and a tube of cells that received just water. The tubes were incubated on ice for 30 minutes before a heat shocking step at 42ºC in a water bath for 50 seconds without shaking. This heat shock step was a critical step because this step efficiently closes pores in the bacterial cell membrane. The tubes were quickly transferred to an ice bath allowing them to cool for 1-2 minutes. Subsequently, 400 µl of LB medium was added to each tube. To maximise the efficiency of transformation the cultures were incubated at 37ºC for 1 hour at 200 rpm before 200 µl of cells were transferred onto LB agar plates containing the appropriate antibiotic (Appendix A.6). The plates were then inverted and incubated overnight at 37ºC.

2.2.7 Purification of plasmid

The blue-white screening was conducted for identifying recombinant bacteria that contained the plasmid of interest. Plasmid DNA was isolated using either the Qiagen Miniprep or the Midiprep purification kit. The buffers of each kit were prepared and stored according to the provider's recommendations before their use. The RNase A solution was centrifuged briefly before being added to the Buffer P1 bottle. The Buffers P2 and N3 were checked for SDS precipitation due to the low storage temperatures. LyseBlue was added to Buffer P1 in a ratio of (1:1000 v/v) and absolute ethanol was added to Buffer PE before use according to the provider's recommendations.

2.2.7.1 Miniprep

This kit is designed to purify up to 20µg of plasmid from 1-5ml of *E. coli* cultures. The white colonies from the agar plate were picked using a sterilised tip (one colony for each insert) and used to inoculate 10 ml of (LB broth) containing ampicillin (50µg/ml) to maintain the propagation of the targeted bacteria. The culture was incubated overnight at 37ºC and shaken at 200 rpm. Cells (3ml) were pelleted by centrifugation before being suspended in 250µl Buffer P1 (Appendix A.8). After the suspension, 250µl of Buffer P2 (Appendix A.9) was added and mixed thoroughly by inverting the tube 4–6 times until the solution became viscous. Buffer N3 (350 µl) (Appendix A.10) was added and immediately mixed thoroughly by inverting the tube. The solution became cloudy and was centrifuged for 10 minutes at 13,000 rpm. The supernatant was then transferred to a QIAprep spin column, centrifuged for 1 minute and the flow-through discarded. The QIAprep spin column was subsequently washed by adding 0.75 ml Buffer PE (Appendix A.11) and centrifuged for 1 minute. The flow-through was discarded and an additional centrifugation step was conducted for 1 minute to remove residual wash buffer. The QIAprep columns were then placed in a clean 1.5ml microcentrifuge tube and the plasmid DNA was eluted by adding 50 µl of nuclease-free water to the centre of the QIAprep spin column, which was left to stand for 5 minutes to increase the DNA yield before being centrifuged for another 1 minute. The concentrations of the purified plasmids were analysed spectrophotometrically with a Nanodrop spectrophotometer.

2.2.8 Plasmid sequencing

The plasmids in this project were sequenced in order to verify the targeted nucleotide sequences and to determine the orientation of the inserts in the p-GEM®-T easy vector (Promega) (Appendix B.1). Ten microliter of each plasmid (100ng/µl) were submitted to Source BioScience

for sequencing in both directions using the appropriate primer sites located in each vector.

2.2.9 Digestion of plasmids with restriction enzymes

Digestion of the plasmid DNA was carried out using type II endonucleases such as EcoRI and their specific buffers from Promega in a total volume of 20µl. The components were assembled in a sterile tube. The deionized water was added first, then 2µl of 10x the appropriate digestion buffer, which was mostly the 10X MULTI-CORE™ Buffer (Appendix A.17). After this, 0.2µl of acetylated BSA (10µg/µl) and then 200ng of the DNA was added and then mixed by gentle pipetting. Restriction enzymes were finally added (5 units). The reactions were mixed by gentle pipetting, spinning and then incubated for 2-4 hours at 37ºC in a water bath. The digested DNA was mixed with 6x the loading buffer then profiled by agarose gel electrophoresis.

2.2.10 *In vitro* transcription

2.2.10.1 Generating the RNA-probes

The synthesis of the RNA probes was conducted after the isolation of RNA from rat adrenals using a TRIzol reagent. This was followed by cDNA synthesis and then the presence of genes of interest was confirmed by PCR using forward and reverse primers (Table 1). The amplified band was then cloned into the pGEM®-T Easy vector. Subsequently, competent *E. Coli* cells were transformed (Inoue *et al*., 1990) using the recombinant vector and the insertion and orientation of genes of interest were detected by sequencing.

The orientation of the clone in the pGEM®-T Easy vector was important to generate the right probe. Consequently, PCR experiments were set using M13 primers together with primers specific for the inserts for two purposes: firstly, to detect in which direction each insert was ligated to the vector. Secondly, to add the transcription sequence for T7 or SP6 promoters to the inserts, in order to use them later for *in vitro* transcription reaction (figure 3a).

M13 primers (F or R) were used with both forward and reverse primers for each gene to add the promoter sequence to the inserts using PCR. Mixing the primers in all four possibilities for each insert (M13 R primer with other genes F primers / M13 F primer with other genes R primers and M13 F primer with other genes F primers / M13 R primer with other genes R primers) would reveal in what direction the inserts were ligated with the vector. If the PCR of different primers (F primers with R primers) result in distinct DNA bands, that means the insert is bound to the vector where the M13 forward primer and the T7 promoter sequences are in the vector upstream the forward primer of the insert. This alignment will be referred to as (correct orientation), but if the PCR of similar primers (F primers with F primers or R primers with R primers) resulted in

distinct DNA bands, that means the insert bound to the vector where the M13 reverse primer and the SP6 promoter sequences in the vector is upstream the forward primer sequence of the insert and we will refer to that alignment as (opposite orientation)

(figure 2.1). The PCR products were analysed by agarose gel electrophoresis and the resulted bands were extracted and used for *in vitro* transcription.

The +1G of the start codon (ATG) of the RNA polymerase promoter sequence in the DNA template is the first base incorporated into the transcription product (figure 2.2). To make sense RNA, the 5' end of the coding strand (the target strand) must be +1 G of the promoter. For antisense RNA to be transcribed the 5' end of the noncoding strand must be downstream of the +1 G.

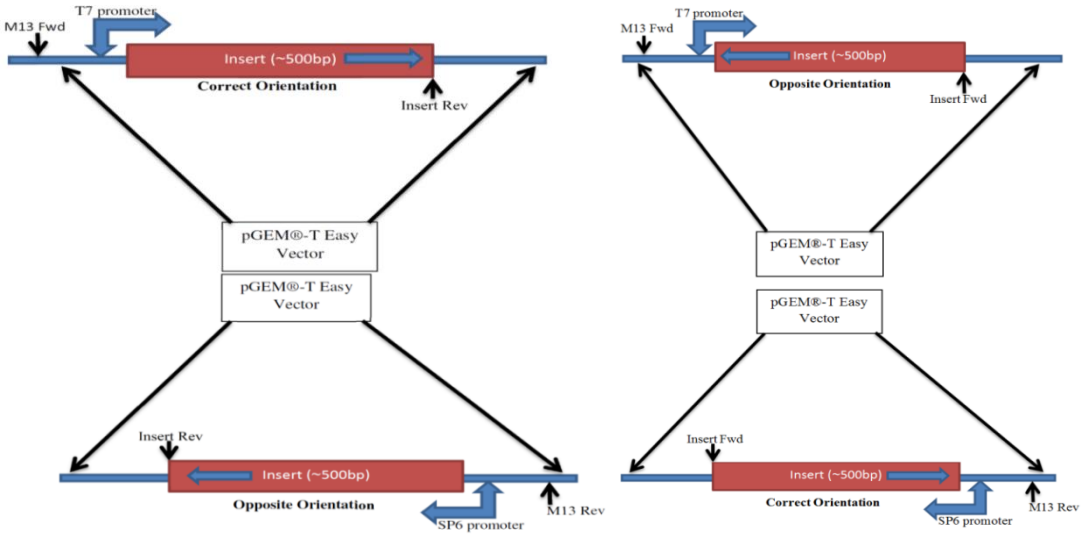

Figure 2.2 The possible orientations of the inserts in the pGEM®-T Easy Vector. This was revealed by one of the M13 primers with one of the insert primers showing which of the RNA Polymerase promoters (T7 or Sp6) can be used for *in vitro* transcription to produce **antisense ribprobes** (on the **right**) , or **sense riboprobes** (on the **left**).

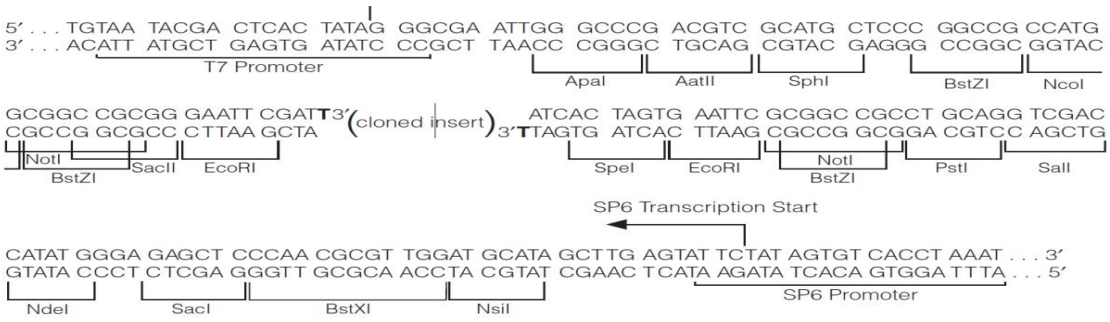

Figure 2.3 The location of the RNA polymerase promoters (T7 and Sp6) and the transcription initiation site (+1G) in the pGEM®-T Easy Vector.

2.2.10.2 *In vitro* transcription reaction

Labelled-RNA probes were synthesised to produce two types of Digoxigenin labelled-RNA. The first synthesis, of coding RNA strands (sense probes) were used as a control. The second, of non-coding RNA strands (antisense probe), were used to detect their mRNA targets in the tissues. These RNA strands were generated using Digoxigenin RNA labelling NTPs mix, which made them detectable probes through an *in vitro* transcription reaction

In order to prepare the antisense probe for the inserts, an *in vitro* transcription reaction was setup in a 1.5ml microcentrifuge tube with a total reaction volume of 20µl. The mix contained DNA template (200ng), 2µl of 10x Digoxigenin RNA labelling NTPs mix (Roche) and 4µl of the 5x Transcription buffer (Appendix A.18). Finally, 1µl of (20u/µl) RNase inhibitor and 2µl of (20u/µl T7 or SP6) RNA polymerase was added according to the insert orientation in the vector. The total volume of the reaction was made up to 20µl with RNase-free water.

Each reaction was mixed and briefly spun before incubating at 37°C for 2 hours. Finally, 2µl of DNase I RNase-free (1unit/µl) was added and the reaction was incubated for a further 15 minutes. Following transcription, 2µl of the reaction was run on an agarose gel to detect the formation of RNA. The probe concentration was measured by spectrophotometry. Three positive control probes of Sf1 were also prepared to be used for the *in situ* hybridisation experiments.

2.2.10.3 Ribo-probe cleaning

The Qiagen's RNeasy Mini Kit was used to clean up the RNA by removing all the enzymes and similar entities'. All steps of this procedure were carried out quickly at room temperature. To achieve this, the necessary solutions were prepared before starting the procedure. The volume of the reaction was adjusted to 100µl with RNase-free water, to which 350 µl of buffer RLT was

added, and mixed. Then 250µl of ethanol (96–100%) was also added, and mixed well by pipetting. The sample (700µl) was then transferred to an RNeasy Mini spin column and placed in a 2 ml tube. The tubes were centrifuged for 15 seconds at 9,000 x g and then the flow-through was discarded. The collection tubes in the previous step were reused, 500 µl of Buffer RPE was added to the RNeasy spin column, and centrifuged for 15 seconds at 9,000 x g to wash the spin column membrane, as before, the flow-through was then discarded.

The second wash for the spin column membrane was conducted using 500µl of buffer RPE, centrifuged for 2 minutes and the flow-through discarded. After each centrifugation step, the RNeasy spin columns were carefully removed from the collection tubes to prevent any contact with the flow-through in order to avoid carryover of ethanol.

Finally, the RNeasy spin column was placed in a new 1.5 ml collection tube, then 35µl of RNase-free water was added directly to the centre of the column membrane, followed by centrifugation at 9,000 x g for 1 minute to elute the RNA, after which the RNA concentration was measured using the Nanodrop device.

2.2.11 Fluorescent *In situ* hybridisation (FISH)

2.2.11.1 Preparing of adrenal cryosections

Adrenal glands from adult Wistar-rat described in (2.1) were used. Adrenal glands were collected as fast as possible, cleaned and placed on a tissue base mould with shallow embedding media to position the samples. They were covered with cryosection mounting media OCT (Cell path), with special attention paid to prevent air bubbles formation. The moulds were then placed into dry ice before being stored at -80°C overnight.

The tissue sections were prepared using a cryostat (Bright 5040) to a thickness of 25µm and were placed onto new Superfrost plus or Polysine slides which are suitable for *in situ* hybridisation and immunohistochemistry. Each of these steps was carried out in RNAse-free conditions.

2.2.11.2 FISH

The sections were thawed and dried for 20 minutes at 55°C, then fixed with 4% (w/v) paraformaldehyde (PFA) in phosphate buffer saline (PBS) (Appendix A.19) for 20-25 minutes, after which the slides were moved to a sterile and RNase-Zap treated humid chamber. The sections were then washed with PBS, dehydrated using a series of ethanol solutions (70%- 80%- 95%-100% v/v) for 3 minutes each and rehydrated using the opposite ethanol concentrations; between the dehydration and rehydration process, the samples were di-lipidated in chloroform for 5 minutes. The slides were washed three times with PBS for 3 minutes before being treated with proteinase K (Roche) 100µg/ml in RNase free water for 30 minutes at 37°C in order to increase the permeability.

The pre-hybridisation step was conducted with a hybridisation buffer (Appendix A.20) for 4 hours at 60°C to block non-specific binding. The sections were surrounded with rubber cement glue (Elmers) with an open side; this formed a U shape border around all sections. Then a coverslip was placed on each slide to form a cavity space between it and the slide sufficient for around 500µl, which was subsequently filled with the hybridisation buffer containing the labeled probe (500ng/ml) of interest. The edges of the slides were dried with microscope tissue (Kimberly-Clark Medical Wipes) before applying the glue, but the sections were kept untouched and moisturised with the hybridisation buffer during the glue bordering process. Then the open side was sealed with the glue to eliminate the evaporation of the hybridisation buffer during

hybridisation and to protect it from any possible effects of RNase. The probes were diluted with RNase free water to concentrations of 100ng/µl and 5µl of each diluted probe was added to 1ml of the hybridisation buffer (500ng/ml) before being hybridised with the probe-hybridisation buffer for around 30 hours at 60°C in a sterilised and RNase-Zap treated humidified chamber.

After hybridisation, the glue and coverslips were carefully removed using a new and sterilised scalpel blade. The slides were washed twice in 5xSSC (Appendix A.21) and treated with a RNA wash buffer (Appendix A.22) for 30 minutes. Then the sections were washed twice with 5XSSC, the first wash at room temperature and the second wash at 55 ºC for 30 minutes each. Subsequently, slides were washed with 0.1X SSC at 55 ºC. The hybridisation signals were detected using the ELF 97 mRNA *in situ* hybridisation signal detection kit (Molecular Probes). After performing the post-hybridisation, the slides were transferred to a jar containing 1X wash buffer for 5 minutes at room temperature. Slides were kept undried (wet) during the ELF signal detection protocol. When the slides were removed from the wash buffer jar and placed in a humid chamber, the blocking buffer was applied to the tissue sections (250µL for each slide) and they were incubated for one hour at room temperature. A polyclonal sheep anti-digoxigenin (Fab-segments), conjugated to alkaline phosphatase (750 U/ml) (Roche,) was diluted 1:5000 (150 mU/ml) in a blocking buffer. 250µL of the solution was added to each slide and they were again incubated for 30 minutes at room temperature.

The amount of ELF 97 phosphatase substrate needed was prepared for the day's experiments by a 10-fold dilution into the developing buffer (Component C) according to the manufacturer's instructions. This was filtered into a sterile vial using a 0.2µm pore-size filter (Minisart), and centrifuged for 10 seconds in a 1.5 microcentrifuge tube. These filters allow a very small volume to be filtered without significant loss of sample. The substrate additive 1 (Component E) and the

substrate additive 2 (Component F) were both diluted each 1:500 into the substrate working solution. The resulting solution was vortexed and used immediately.

After the incubation with the anti-digoxigenin-AP, the slides were washed three times, for 5 minutes each time, with 1x wash buffer. A substrate working solution was applied to the slides (400µL per slide) and the samples were incubated for 15 minutes up to a maximum of 1 hour, depending on the abundance of the signal. To monitor this, the fluorescence microscope was prepared before adding the substrate working solution to be ready to check the signal every 10 minutes. Once the signal developed sufficiently, the excess solution was removed and the slides washed immediately with 1x wash buffer. In order to maintain long-term signal preservation, the sections were treated with a post-fixation solution (Appendix A.23) for 15–30 minutes at room temperature. The sections were mounted by applying 3–5 drops of mounting medium (ELF 97) to each slide and placing a coverslip on top and these slides were examined using a fluorescent microscope with the 546nm filter on 5x and 20x objective.

2.2.12 Immunohistofluorescence

Adrenal cryosections were prepared as described in section (2.2.11.1) with the exception of the thickness of the sections, which was 10µm rather than 25µm. The slides were dried for 20-30 minutes at room temperature and then were fixed by immersion in a jar full of pre-cooled acetone for 20 minutes. After which they were removed and allowed to dry for 20-30 minutes at room temperature.

Slides were washed twice with phosphate-buffered saline containing Triton (PBT) (Appendix A.24) for 5 minutes each and blocked with blocking buffer (10% v/v goat serum in PBS for 1 hour; the serum being derived from the species in which the secondary antibody was raised, usually goat serum).

The blocking buffer was then drained off from the section and the primary antibody working solution was prepared by mixing the suitable amount of primary antibody with an antibody dilution buffer (0.5% v/v of the same serum in PBS). A drop (100-200µl) of the primary antibody working solution was applied to each section and they were incubated in a humidified chamber overnight at 4°C.

The sections were each washed twice with PBT for 5 minutes before the addition of a drop (100-200µl) of diluted (1:200) secondary antibody in the antibody dilution buffer. Then they were incubated in the dark, in a humidified chamber, at room temperature for 30 minutes before being washed twice in PBS for 5 minutes each. The sections were then mounted in mounting medium for fluorescence with DAPI (Vectashield) to stain the nucleus and covered with coverslips. The control sections were treated with the appropriate IgG protein instead of the primary antibody. In the dual immunohistofluorescence both primary and secondary antibodies (mouse and rabbit) were mixed together in the primary and secondary incubation steps, respectively.

2.2.13 Microscopy

The immunofluorescent imaging for *in situ* hybridisation and immunohistofluorescence experiments was carried out using a Zeiss-Axio Imager A1 fluorescent microscope with four filters: Blue/cyan filter for (4',6-diamidino-2-phenylindole (DAPI)), Alexa Fluor (AF) 488 green, AF 546 yellow and AF 660 red. The magnification powers of the objective lenses used in these experiments were 5x, 10x, 20x and 40x. The fluorescent microscope was fitted with a camera (Axio cam MRm) linked to a computer and controlled by AxioVison software (Rel.4.8). This software was used to adjust the colours, measures, and quality of the images. The quality of the images was adjusted using the microscope fine adjustment.

2.3 Results

Several potential stem cell markers were selected after a bioinformatics analysis of a whole rat adrenal transcriptome microarray data set. This data showed the expression of potential stem or progenitor cell markers based on their high expression in the capsule, or capsule and zI, in comparison with zF. The expression values in the microarray data were manipulated to be displayed in fold differences between the capsule, or capsule and zI, in comparison with zF. Further analysis was required for the potential stem cell markers that displayed a 50-800 fold increase in their expression in the capsule or capsule and zI in comparison with zF. Over 60 potential stem/progenitor cells markers of the rat whole transcriptome were observed and research was conducted to collect further information about their roles in the literature. The selection of the potential markers was mainly based on a combination of the array data and the information in the literature that implied potential roles in stem/progenitor cells characteristics, cell proliferation and migration. In addition to the proteins that were rarely studied but they have a potential role in the stem cell characteristics. However, not all of the nominated stem cell markers met all the criteria of selection. Three potential markers were selected because they showed high expression in the capsule and zI in comparison with zF (table 2.2): Transmembrane protein121 (Tmem121), Thy-1 cell surface antigen (Thy-1) and Krüppel-like factor 5 (KLF5).

The next steps were conducted to confirm the microarray data and to reveal the expression pattern of these potential markers in the adrenal cortex. Several molecular experiments were conducted in order to examine the expression of these markers followed by cloning a fragment of these genes into the p-GEM®-T easy vector. This was followed by *in vitro* transcription to produce probes to detect the mRNA expression patterns of these markers in the rat adrenal cortex

by FISH. Immunohistofluorescence experiments also followed to detect the localisation of the proteins of interest in adrenal sections.

Table 2.2 Microarray data of the genes of interest showing the levels of gene expression in the capsule, zF and zI. The genes have higher expression in the capsule and zI (the potential stem/progenitor cell layers) in comparison with zF.

Gene title	Gene symbol	Capsule	zF	zI
Kruppel-like factor 5	Klf5	149.9184	2.547829	78.12353
Thy-1 cell Surface antigen	Thy-1	334.6493	5.828303	51.53768
Transmembrane protein121	Tmem121	138.4809	2.175656	68.63601

2.3.1 Extraction of RNA from adrenal tissue

RNA was extracted from adrenal glands using TRI reagent. The RNA was analysed using agarose gel electrophoresis (figure 2.4) and spectrophotometry. The first extracted RNA from one frozen adrenal was 125.3ng/µl and the A260/230 ratio was 2.19, which indicated low contamination with either polyphenol or polysaccharide. The A260/280 ratio was 1.8 which indicated very low protein or phenol contamination. As opposed to frozen adrenal glands that stored in -80 ºC for over six months, RNA extraction from freshly isolated adrenal gland showed high quality RNA (as it measured using a spectrophotometric method) and the concentration of RNA was 400-1200 ng/µl per one adrenal gland.

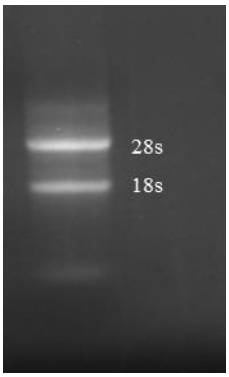

Figure 2.4 Agarose gel electrophoresis of 10µl of 125.3 ng/µl RNA after isolation from whole rat adrenal using Trizol method. The appearance of 28S and 18S ribosomal RNA subunits bands indicate the RNA was obtained with minimum degradation.

2.3.2 First strand cDNA synthesis

cDNA synthesis resulted in the generation of single stranded cDNA from the isolated RNA. Analysis by spectrophotometry showed that it had a concentration of 77ng/µl.

2.3.3 Gene detection by PCR and agarose gel electrophoresis

Polymerase chain reaction (PCR) was carried out to detect the expression of the three potential stem cell marker genes (figure 2.5) (Klf5, Thy-1, and Tmem121) in the adrenals and to provide template fragmetns suitable for riboprobe generation. The bands were excised from the gel and purified using the Qiagen QIAquick Gel Extraction Kit. The concentrations of these segments after purification were measured by spectrophotometry and showed to be 32ng/µl, 30ng/µl and 28ng/µl, respectively.

2.3.4 Transformation of *E.coli* with the cloned segments

The DNA segments were ligated into the p-GEM®-T Easy plasmid and subsequently transformed into competent *E. Coli* cells. The transformed colonies were grown on LB agar plates; the numbers of transformed colonies were different among the three types of inserts, while the control group showed no growth.

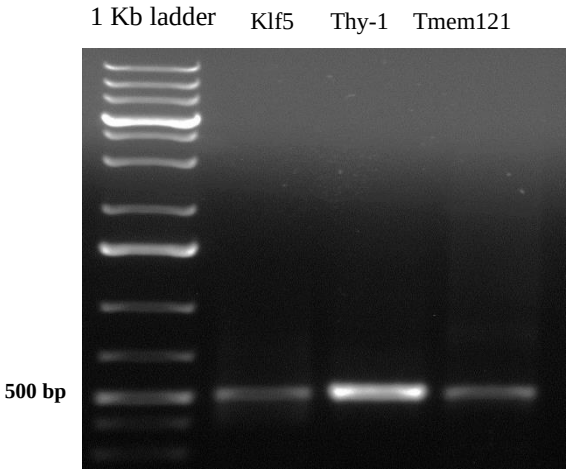

Figure 2.5 Agarose gel electrophoresis of 10µl of the PCR products that represent an approximatly 500bp segment of each of the three genes Klf5, Thy-1 and Tmem121. The PCR was conducted using specific primers to detect these genes from rat whole adrenal cDNA. This picture reveals the presence of the three bands of all three gene segments.

.

2.3.5 Plasmid isolation and restriction enzyme digestion

In order to confirm the ligation of an insert into the vector, one colony was picked from each plate and grown in 10ml of LB broth. Plasmids were then isolated using a Qiagen miniprep kit and then subsequently digested with *EcoR1* in a total volume of 10µl. Since the restriction sites

of *EcoR1* in the p-GEM®-T easy plasmid were adjacent to the two ends of the insert (Appendix B.1), the isolated plasmids from the colonies were digested with *EcoR1* to confirm that the segments were successfully cloned. After digestion, the products were separated by agarose gel electrophoresis (Figure 2.6). The bands of each digested plasmid were observed, where the upper band represented the plasmid backbone (approximately 3000bp), and the lower bands were the inserts of approximately 500bp. The successful cloning was also confirmed by sequencing.

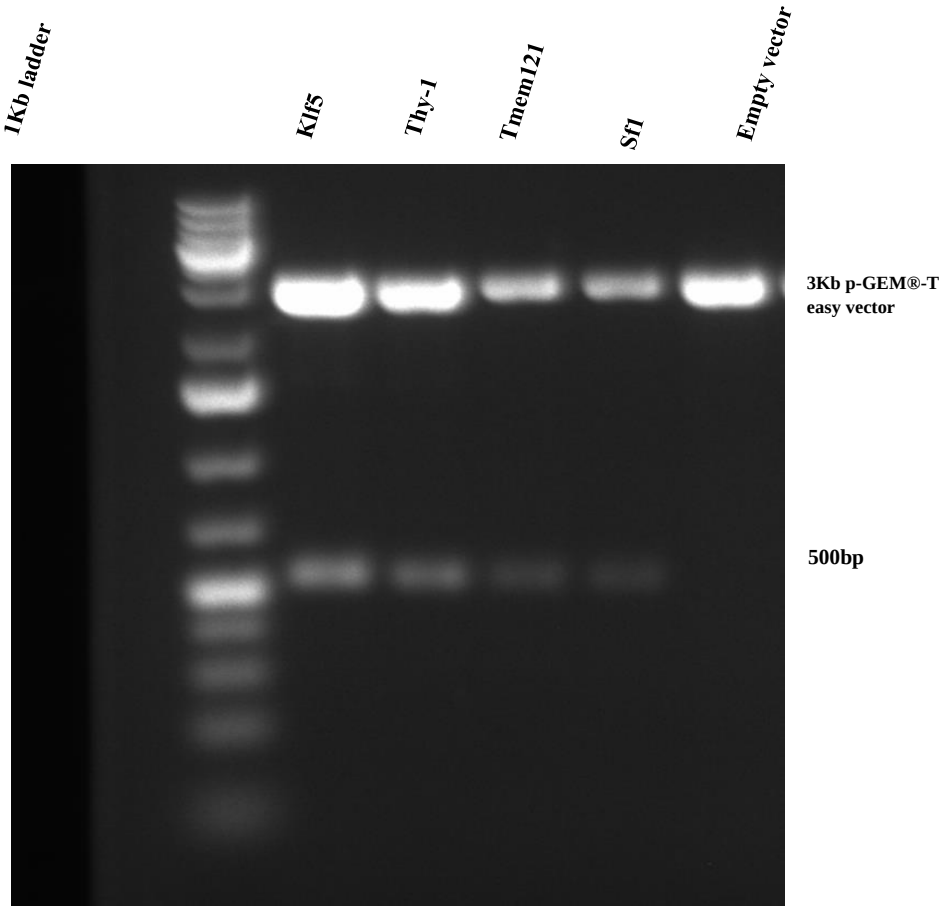

Figure 2.6 Agarose gel electrophoresis of the three cloned inserts of the genes of interest Klf5, Thy-1 and Tmem121 with Sf1 insert as control and the mere-vector (p-GEM®-T easy), after digestion with *EcoR1*. The digestion releases the inserts from the vector, which were then separated by their size allowing profiling on an agarose gel. This analysis showed the appearance of digested DNA of the inserts at around 500bp, where the larger bands (3,000bp) represent the vector backbone.

2.3.6 Generation of templates suitable for *in vitro* transcription

The RNA-probes were not generated from the insert in the p-GEM®-T Easy vector by digestion with an appropriate restriction enzyme and then using either the T7 or SP6 RNA promoters to initiate transcription. However, amplification of the desired segment by PCR was preferable as

this added either T7 or SP6 promoter to the insert and the DNA product of the PCR were much more than the DNA product from the digestion. To achieve this, PCR was used with one primer specific for the insert together with either an M13 forward or reverse primer. This revealed the orientation of the insert in the vector at the same time as adding either T7 or SP6 RNA polymerase promoter sequences to the insert. If the PCR of different primers (F primers with R primers) resulted in distinct DNA bands, that meant the insert bound to the vector where the M13 forward primer and the T7 promotor sequences in the vector were upstream of the forward primer of the insert (correct orientation), However, if the PCR of similar primers (F primers with F primers or R primers with R primers) resulted in distinct DNA bands, that meant the insert bound to the vector where the M13 reverse primer and the SP6 promotor sequences in the vector were upstream of the forward primer sequence of the insert (opposite orientation). The results revealed that both Thy-1 and Tmem121 inserts were ligated into the vector in the correct orientation such that the T7 promoter sequence of the plasmid could be used to generate the sense RNA of the insert. In contrast, the Klf5 insert as well as the control insert (Sf1) were in the opposite orientation such the SP6 promoter sequence could be used to generate sense RNA of the insert (Figure 2.7).

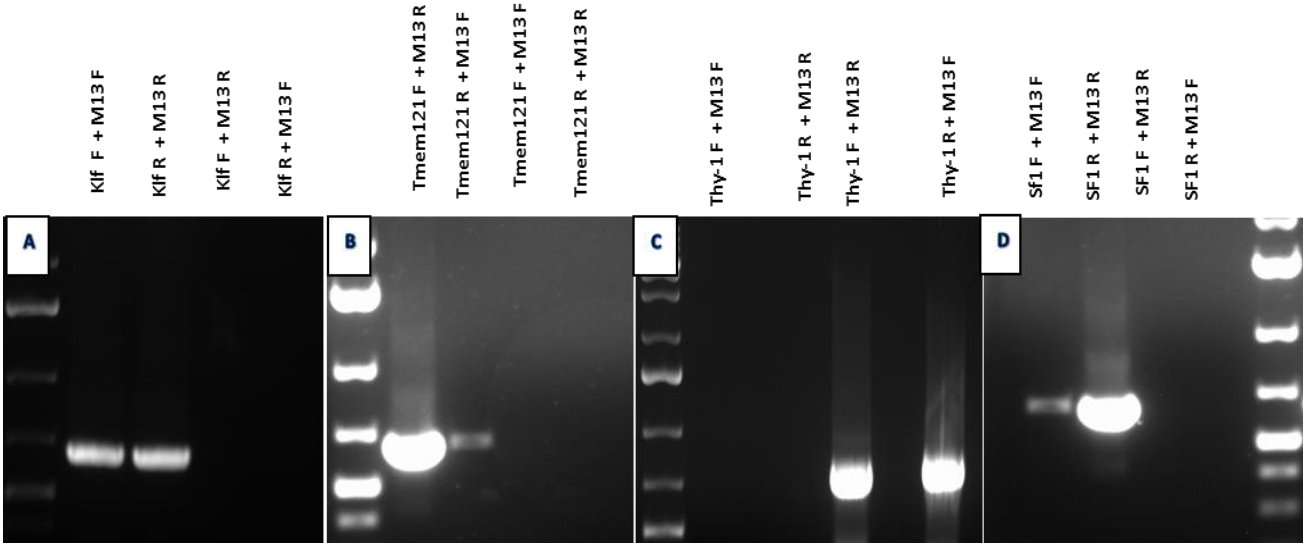

Figure 2.7 Agarose gel electrophoresis of the PCR products of the three genes Klf5, Thy-1, Tmem 121 and the control (Sf1) with a segment of the T7 or SP6 promoters that were added by using M13 primers in all possible combinations. This in turn referred to the direction in which the inserts had ligated to the vector. A and D showed the products of all similar primer combinations (insert F primers with M13F primers and insert R primers with M13 R primers). This showed the Klf5 and Sf1 bands, revealing their opposite orientation in the vector. B and C showed the products of all different primer combinations (insert F primers with M13R primers and insert R primers with M13F primers). This showed the bands of Thy-1 and Tmem121 revealing their correct orientation in the vector.

2.3.7 *In vitro* transcription and RNA purification

DIG labelled RNA probes were synthesised by *in vitro* transcription using the DNA segments described in section 3.7 along with the appropriate RNA polymerase. The RNA probes were purified using the RNeasy Mini Kit (Qiagen) and analysed using agarose electrophoresis (figure 2.8) to check that the synthesis was successful. The concentration of the Klf5, Thy-1, Tmem121

and SF1 probes was determined by spectrophotometry to be 1780ng/µl, 1903ng/µl, 1650ng/µl and 1245ng/µl, respectively. The concentration of the probes decreased dramatically after purification.

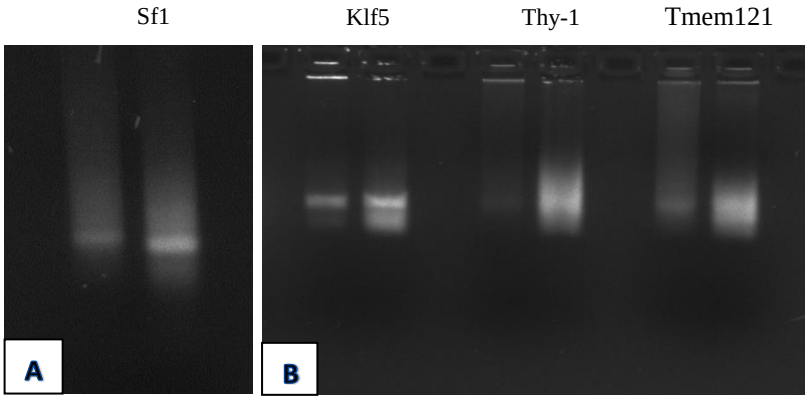

Figure 2.8 Agarose gel electrophoresis of the RNA probe bands of Klf5, Thy-1, Tmem121 and Sf1 after *in vitro* transcription. (A) The antisense RNA probe bands of Sf1. (B) The three antisense RNA probes bands of Klf5, Thy-1, Tmem121 and Sf1. The right-hand bands shown in A and B are the probes before purification, while the left-hand bands are after purification.

2.3.8 Fluorescent *in situ* hybridisation (FISH)

Spatial expression of the three genes in the rat adrenal was determined using fluorescent *in situ* hybridisation. The mRNA of Klf5, Thy-1 and Tmem121 was detected in normal adult rat adrenal glands. Expression of all three genes was detected within the adrenal cortical zones with expression being found mainly in the capsule and sub-capsular areas (Figure 2.9). Amongst the tested genes, Klf5 mRNA expression was mainly localised to the capsule (Figure 2.9), but Klf5 was also expressed in the zG and zF (definitive zones). The expression of Klf5 was intense in the capsule, but its expression expanded into both definitive zones of the adrenal cortex (zG and zF) and reached the adrenal medulla. Tmem121 expression was low in the definitive zones and was

mainly restricted to the capsule and sub-capsular areas with slight expansion toward the zG zone (Figure 2.9).

Thy-1 mRNA expression was mostly confined to the capsule and sub-capsular area (Figure 2.9) with high expression intensity in the capsular area. Thy-1 had the lowest expansion toward the definitive zones after the negative control (no probe).

In the adrenal cortex definitive zones, the Sf1 antisense probe showed high expression in comparison with its expression in the capsule (Figure 2.9), and also in comparison with all of the other genes in the definitive zones.

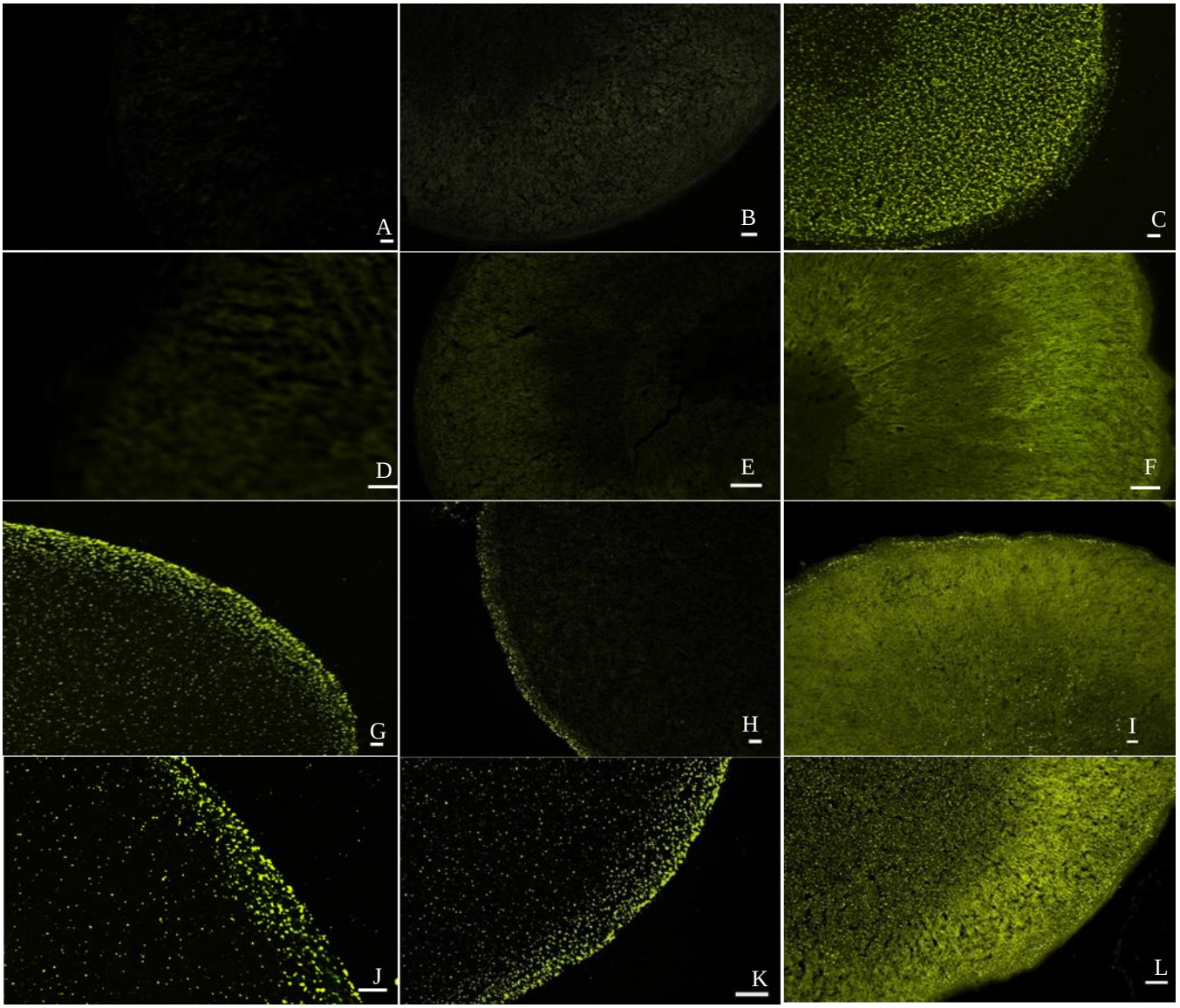

Figure 2.9 *In situ* hybridisation of the genes of interest on rat adrenal cryosections. A-F are the control group. A and D show the adrenal section where no probe was applied (negative control), B and E show the binding of the Sf1 sense RNA probe (sense probe control). C and F show the expression of the Sf1 antisense RNA probe (positive control). The upper row (A, B and C) is at low magnification and the second row (D, E and F) is at high magnification. G-L are the genes of interest group. G and J show the expression of the Tmem121 antisense RNA probe. H and K show the expression of the Thy-1 antisense RNA probe. I and L show the expression of the Klf5 antisense RNA probe. The third row (G, H and I) is at low magnification and the forth row (J, K and L) is at high magnification). Scale bars: 50µm.

2.3.9 Immunohistofluorescence

The detection of the mRNA of the genes of interest using FISH, was followed by detection of the protein expression of the same targets using immunohistofluorescence because it was necessary to confirm that these transcripts were being translated.

The Klf5, Thy-1 and Tmem121 proteins were detected in normal adult rat adrenal glands. Using primary antibodies for the three proteins and IgG protein as a control. In agreement with the *in situ* hybridisation results, the Klf5, Thy-1 and Tmem121 protein expression results were mainly observed in the capsular and the subcapsular area (Figure 2.10-2.12). Tmem121 proteins expression was highly observed in the sub-capsular area. The pattern of Tmem121 protein expression was ranging from a few cells in the sub-capsular area to a long line of cells along the capsule with slight expansion toward the zG (Figure 2.10). As with the Tmem121 protein expression the Klf5 protein expression was highly prominent in the capsule and sub-capsular area. However, the pattern of Klf5 protein expression was high in the capsule and reduced gradually in the zG and zF (Figure 2.11). Thy-1 protein expression was mostly confined to the capsule when compared to the other proteins of interest (Figure 2.12).

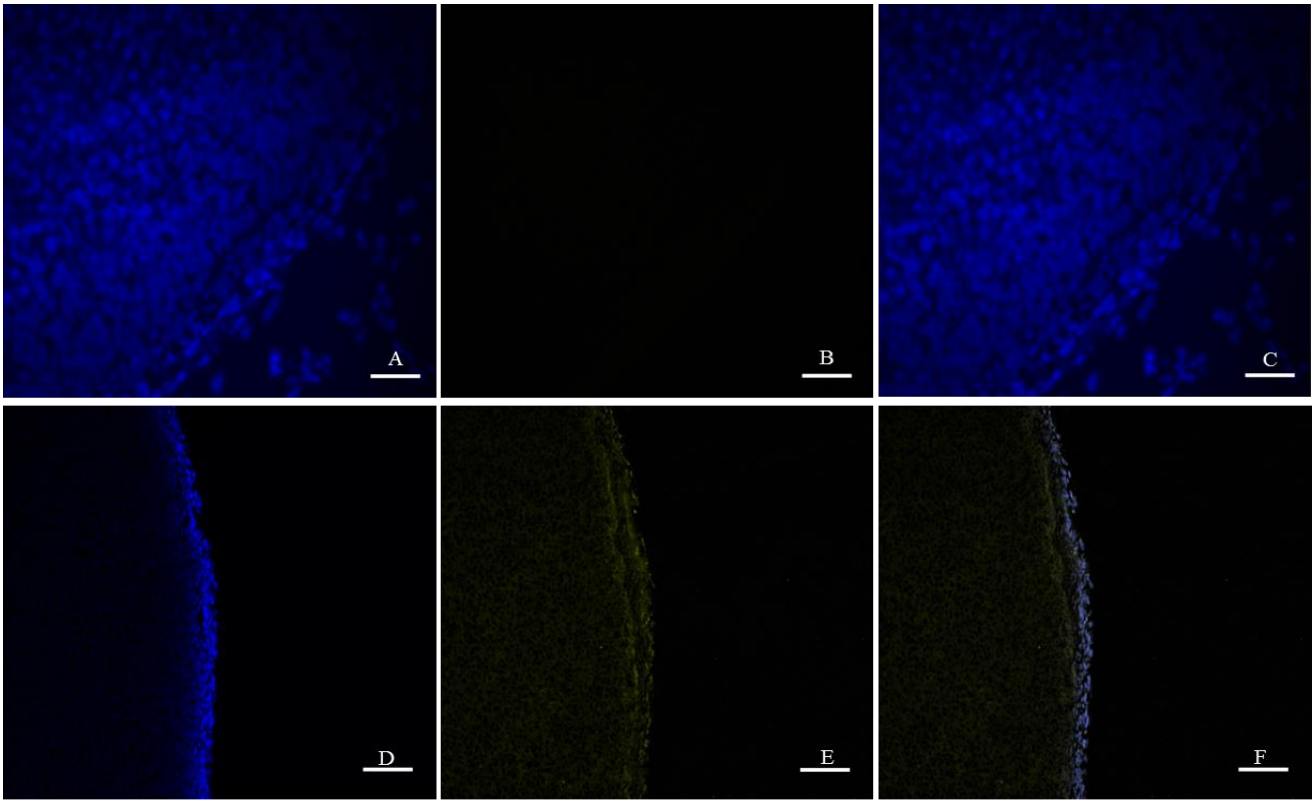

Figure 2.10 Immunohistofluorescence of Tmem121 protein on rat adrenal cryosections. (A and D) Immunofluorescence of nuclei stained with DAPI. (B and E) Immunofluorescence of Tmem121 positive cells incubated with primary rabbit anti-Tmem121 antibody (ab151077) before detection with secondary anti-rabbit Alexa 546 in B and E. Merged images of (A) and (B) are shown in (C) and of (D) and (E) in (F). Scale bars: 50µm.

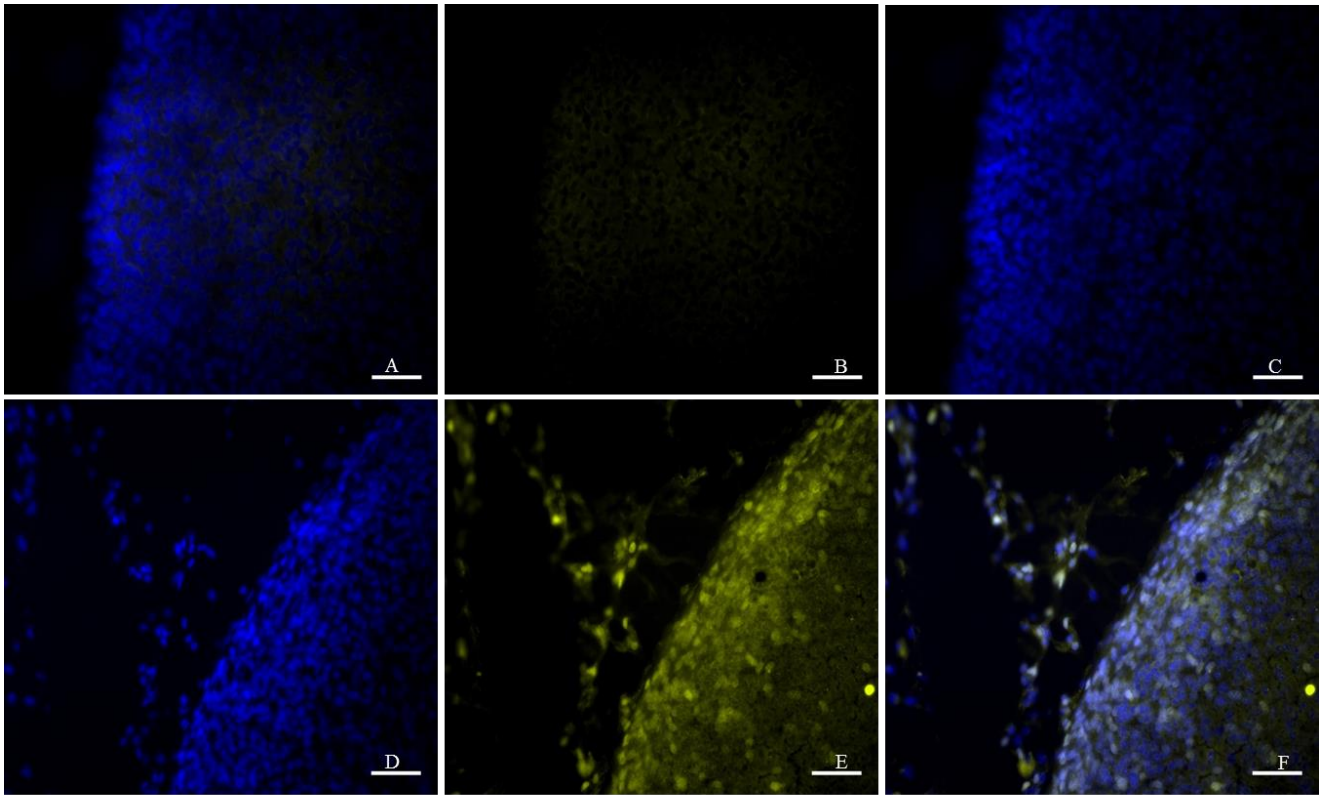

Figure 2.11 Immunohistofluorescence of Klf5 protein on the rat adrenal cryosections. (A and D) Immunofluorescence of nuclei stained with DAPI. (B and E) Immunofluorescence of Klf5 positive cells incubated with primary rabbit anti-Klf5 antibody (ab137676) before detection with secondary anti-rabbit Alexa 546 in B and E. Merged images of (A) and (B) are shown in (C) and of (D) and (E) in (F). Scale bars: 50µm.

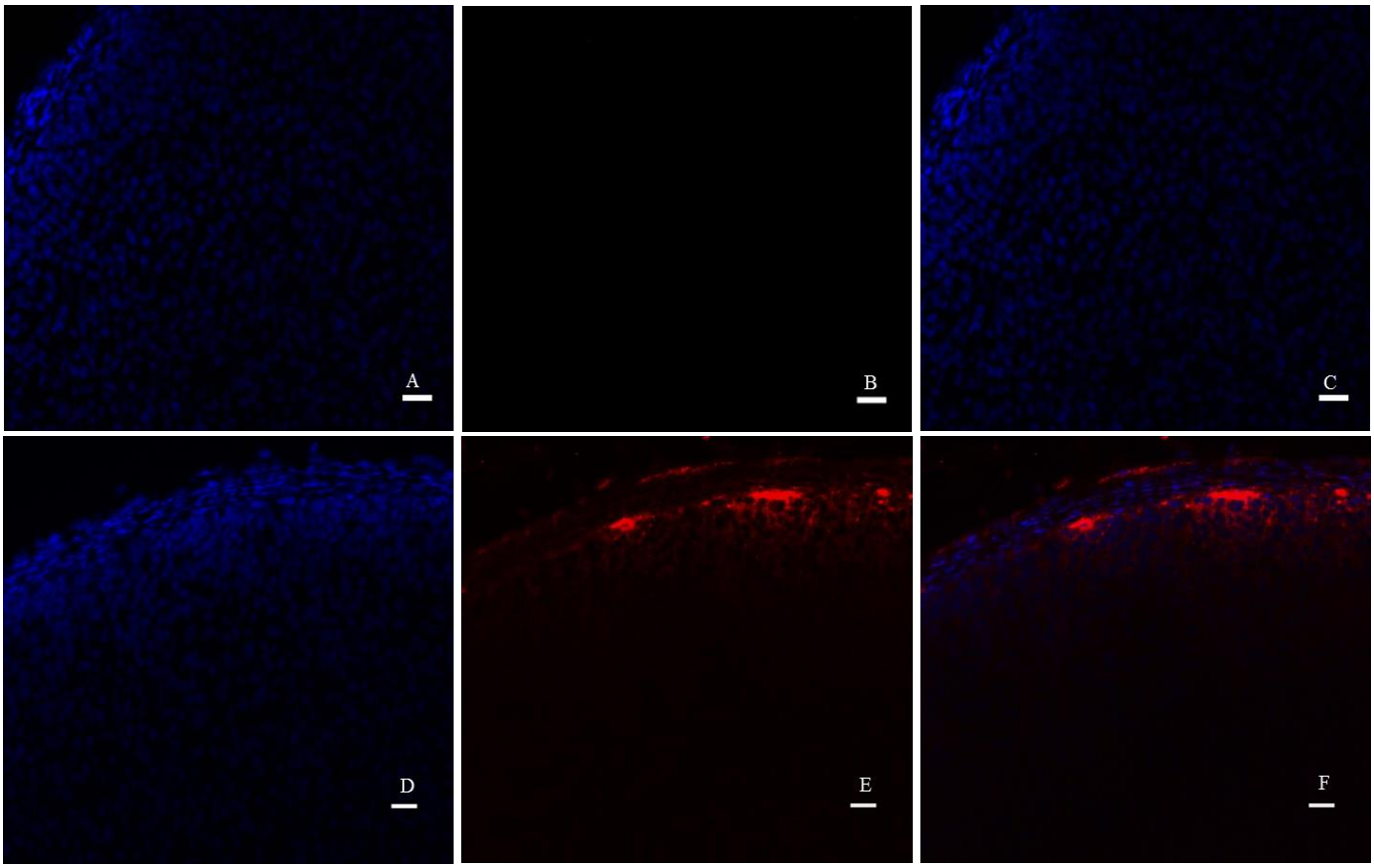

Figure 2.12 Immunohistofluorescence of Thy-1 protein on rat adrenal cryosections. (A and D) Immunofluorescence of nuclei stained with DAPI. (B and E) Immunofluorescence of Thy-1 positive cells incubated with primary mouse anti-Thy-1 antibody (BD Pharmingen 554895) before detection with secondary anti-mouse Alexa 546 in B and Alexa 647 in E. Merged images of (A) and (B) are shown in (C) and of (D) and (E) in (F). The upper row (A-C) low magnification, the lower row (D-F) high magnification. Scale bars: 20µm.

Due to the lack of information regarding Tmem121 and the pattern of its area of expression in the adrenal cortex, dual antibody detection experiments were conducted to assay the co-expression of Tmem121 with the proliferation marker Ki67 (Figure 2.13). The result of co-expression between the two proteins was 0.74 (according to Spearman's rank correlation value, which was calculated using Image J 1.49 software). This represents high (74%) but not complete co-expression of the Tmem121 with the proliferation marker Ki67.

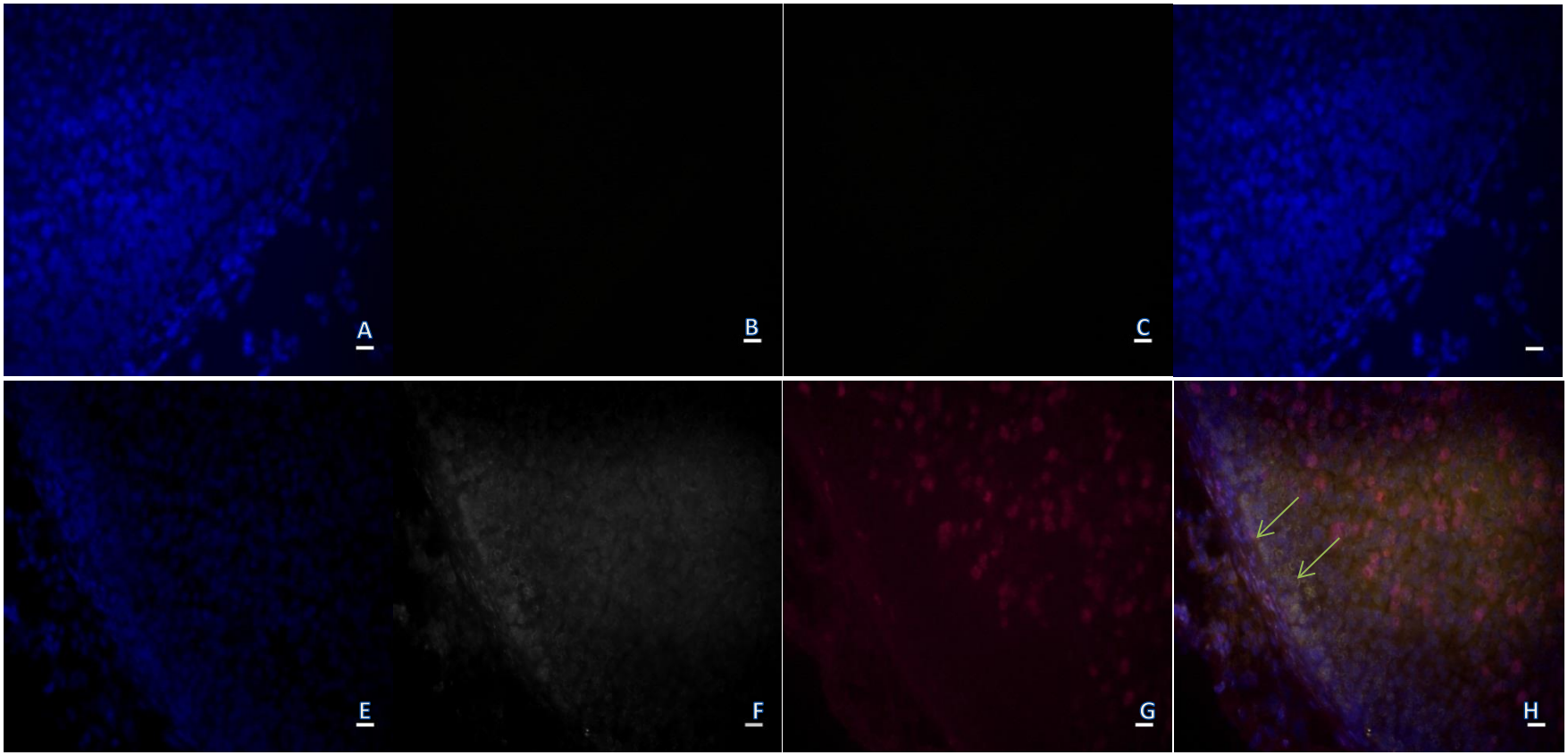

Figure 2.13 Dual Immunohistofluorescence of rat adrenal cryosections showing the co-expression of Tmem121 protein with the proliferation marker Ki67 using rabbit anti-TMEM121 antibody (ab151077) with mouse anti-Ki67 antibody (BD Pharmingen550609). (A and E) Immunofluorescence of nuclei stained with DAPI. (B) Adrenal gland sections were incubated with control rabbit IgG. (C) Adrenal gland sections were incubated with control mouse IgG. (F) sections were incubated with primary rabbit anti-Tmem121 antibody before detection with secondary anti-rabbit Alexa546 in (B and F). (G) Adrenal gland sections were incubated with primary mouse anti-Ki67 antibody before detection with secondary anti-mouse Alexa 647 in (C) and (G). Merged images of (A), (B) and (C) are shown in (D) and of (E), (F) and (G) in (H). Scale bars: 20µm.

The major results of this chapter can be summarized in (table 2.3).

Table 2.3 The major results of mRNA and protein expression of the stem cell nominated markers in the adrenal cortex after *in situ* hybridisation and immunohistofluorescence assays. The results showed the detection of the Klf5 mRNA and protein expression in the capsule, zG and zF. Tmem121 mRNA and protein expression were detected in the capsule and zG. Thy-1 mRNA expression was detected in the capsule and zG. While Thy-1 protein expression was confined to the capsule.

The gene/protein of interest	mRNA expression			Protein expression		
	Capsule	zG	zF	capsule	zG	zF
Klf5	yes	yes	yes	yes	yes	yes
Tmem121	yes	yes	no	yes	yes	no
Thy-1	yes	yes	no	yes	no	no

2.3 Discussion

The rat adrenal microarray data showed expression of more than 60 potential stem/progenitor cell markers in the rat whole genome. However, not all of them met the selection criteria. The selection of the potential markers considered the capsule (Walczak and Hammer, 2015) and zI (Mitani, 2014) as potential niches for adrenocortical stem/progenitor cells but the expression pattern of the nominated markers was mainly either out or beyond the capsule and/or zI. The combination of the array data analysis and the information in the literature regarding these markers implied potential roles in stem/progenitor cell characteristics and facilitated the nomination of three markers: Tmem121, Klf5 and Thy-1.

Tmem121

Although the array data showed an interesting expression pattern in the capsule with low expression in the zF, Tmem121 is a poorly studied protein. However, Tmem family members are highly conserved between species and are highly expressed in most embryonic tissues (Zhou et al., 2005), which might involve in the characteristic of stem cells. A human wound healing study showed that Tmem121 is one of the genes that contribute to cell proliferation and migration in human endothelial cells and its expression was co-expressed with the endothelial marker, CD31. Therefore, these results suggested that it might have a potential role in skin wound healing (Bronneke et al., 2015).

Krüppel-like factor 5 (KLF5)

KLF5 is a member of the zinc finger protein family called Krüppel-like factors. They have a crucial role for the initiation and preservation of stem cell pluripotency in the embryo and regulate several biological processes. KLF5 participates in the formation of the trophectoderm and inner cell mass, and also has a role in suppressing the development of the primitive endoderm (Lin et al., 2010). All these interesting data therefore referred to it having a proposed role in the characteristics of stem cells.

KLF5 has a role in maintaining proliferation of several tissues. For instance, in intestinal epithelium tissue where cells undergo constant self-renewal activities (Kuruvilla et al., 2015), and has indirect effects on vascular smooth muscle proliferation (Gao et al., 2015). Klf5 also has an essential role in regulating the differentiation of the skeletal muscle (Hayashi et al., 2016).

However, KLF5 expression in embryonic stem cells might imply its role in tumorigenesis and cancer cells but its exact role is unclear since it shows both tumour promoting and suppressing activities. Although several studies favour the role of KLF5 as a tumour suppressor (Xing et al., 2014). Recent studies suggest KLF5 targeting in the PKA_Glycogen synthase kinase 3 (GSK3β)_KLF5 pathway induces degradation in breast cancer stem cells (Shi, Liu et al. 2017). However the proliferation of carcinoma cells was not influenced by KLF5. Over expression of KLF5 also inhibits differentiation of oral carcinoma (Shibata et al., 2015).

Thy-1(CD 90)

Thy-1 is a highly conserved cell surface protein of 25–37kDa. It is expressed in various cell types of several mammalian species including humans and rodents (Petersen et al., 1998). The expression of Thy-1 is one of the minimal criteria for human MSC (Dominici et al., 2006a). The

use of Thy-1 as a marker to isolate stem cells has been recorded in several foetal and adult tissues cells types such as bone marrow (Dennis et al., 2007) and human liver (Herrera et al., 2006). It has a role in regulating the cell matrix and cell to cell interaction, in addition to its role in cellular migration and adhesion (Rege and Hagood, 2006).

The first laboratory experiment conducted to confirm the microarray data regarding the three genes of interest was RT-PCR to detect and amplify a segment of approximately 500bp of each of the genes of interest in the adrenal gland cDNA. These experiments were successful and the expression of these genes was detected in the adrenal gland (Figure 2.5). After ascertaining that these potential markers were being expressed in the rat adrenal, it was important to investigate the localisation of this expression. Therefore, the PCR product of each was inserted into a vector with SP6/T7 promoters to allow *in situ* hybridisation probe generation.

The next steps aimed to produce RNA probes by *in vitro* transcription using the cloned segments as templates. The RNA probes were generated and several *in situ* methods were attempted to achieve *in situ* hybridisation, these included the whole mount *in situ* hybridisation procedure described by Nieto *et al*. (1996), wax and cryosection *in situ* hybridisation protocols. Although the valid working protocol with the adrenal sections that showed gene most consistent replicates was found to be the one described by Lomthaisong (2001), several modifications were required to reduce RNA degradation and increase the stringency.

The *in situ* hybridisation results confirmed the microarray data showing expression in the capsular and the subcapsular areas of the adrenal cortex (Figure 2.9).

Klf5 mRNA had a high narrow and intense expression in the capsule with weak and expanded expression in the zG and zF (Figure 2.9). The Klf5 protein expression pattern was in agreement with *in situ* hybridisation with a lower expansion in the zG and Zf, meaning that not all the

mRNA were translated into protein. Although the Klf5 protein is considered to be one of the pluripotency markers in certain embryonic stages (Hou et al., 2016), the expansion of expression in the two main differentiated zones (zG and zF) might not be related to the pluripotent stem cells within the adult adrenal cortex. This result suggested that Klf5 is not a stem cell marker in the adrenal cortex.

Tmem121 mRNA expression was the highest in the capsule with a slight expansion in zG, this pattern of expression represents most of the capsular area and a small fraction of the zG. The Tmem121 protein expression agreed with the *in situ* hybridisation result. The long expanded line of Tmem121 protein expression mainly slight the Tmem121 from being a stem cell marker because the presence of stem cell populations within the adult tissue have a limited existence, as seen in adipose tissue (Zaman et al., 2014), heart (Navarro-Betancourt and Hernandez, 2015) and bone-marrow (Guerin et al., 2015), which represent less than 0.1% of the main cell populations. However, this interesting expression pattern of Tmem121 might suggest a role for Tmem121 in the adrenal cortex cell proliferation and migration, because the adrenal cortex undergoes centripetal migration that starts from the subcapsular area towards the adrenal cortex medulla border. The detection of Tmem121 protein expression co-expressing with the Ki67 proliferation marker (Figure 2.13), primarily revealed a high co-expression between the two proteins (0.74 according to Spearman's rank correlation value). This value may refer to the existence of Tmem121 protein during cell proliferation (based on the Ki67) and that it might participate or have a role in cell proliferation, but it is not essential to this process since not all the proliferative cells were expressing it.

This result marks the beginning of further investigation regarding the role of Tmem121 protein in adrenal cortex cell proliferation and migration. The high expression of Thy-1 mRNA in the capsule, in comparison with other marker mRNAs, combined with a restricted expression pattern and the molecular structure of the Thy-1 protein in the cells as a cell surface antigen, nominated Thy-1 as a marker for isolating the potential stem cells and to conduct further investigations.

Furthermore, Thy-1 has the lowest expression level in the zG and zF, these zones represent the most differentiated part of the adrenal cortex. The low and intense expression in just a few parts of the capsule with a slight expansion to the sub-capsular area suggested Thy-1 to be the most potential target for the isolation of stem cells because of the presence of stem cell populations within the adult tissue having a limited existence and mainly representing less than 0.1% of the main cells populations.

The results of *in situ* hybridisation and immunohistofluorescence experiments aimed to establish the capsule and sub-capsular area as the stem cells niche. However, Mitani et al.,(2003) suggested that the zI might be a stem cell niche. This result might be down to strain differences in the rats used in the experiments but it has also been suggested that the adrenal cortical stem cells are Sf1 negative but the progenitor cells are Sf1 positive as they start to express Sf1 before differentiation and commencing steroidogenesis (Kim et al., 2009). The expression of Sf1 was detected in the adrenal cortex including the zI (Figure 2.9).

Mitani et al.,(2003) suggested the zI as a stem/progenitor cell zone, because cell proliferation activity was observed in the zI after BrdU rat injection, but Mitani et al.,(2003) also observed that these cells migrated into the zI from the outer portion of the zG reaching the inner potion of the zF and the number of these migrating labelled cells increased 3-fold. However, several studies have come to conclusions regarding adrenal cortical stem cells, describing them as

quiescent and self-renewing cells (Kim et al., 2009). A decade after the Mitani et al.,(2003) study, a simlar study was conducted and showed that the cells were retained within the capsular and sub-capsular cortex 23 weeks after administrating BrdU (Chang et al., 2013). Furthermore, MSCs might transport only toward the damaged sites in animals tissue, but the molecular mechanisms of MSCs migration within damaged tissue remain unclear (Tang et al., 2017, Xu et al., 2017). So, the description of the cells in the zI as migrating and proliferating cells by Mitani et al.,(2003) might reduce the possibility of the zI being a stem cell niche in the rat.

These findings suggest that the stem cells of the adrenal cortex are quiescent or have a slow cycling feature within the capsule. Furthermore, the rat whole genome microarray data showed over-expression of the Sf1 gene in zI, which means the zI might possess progenitor or steroidogenic cells but not stem cells. These results generally showed that a few cells within the capsule express a high level of the Thy-1 protein, which represents a specific cell type within the capsule, that might be stem cells according to the most recent adrenal cortex stem cells hypothesis (Walczak and Hammer, 2015). Furthermore, Thy-1 as a cell surface antigen is considered one of the mesenchymal multi-potent stem cell markers according to a statement from the “International Society for Cellular Therapy” (Dominici et al., 2006b).

Chapter three

Isolation and characterisation of the Thy-1 positive cells

4.1. Introduction

This chapter is dedicated to the isolation of potential stem cells, their culture *in vitro*, the study of the expression of other stem cell markers in the isolated cells and the monitoring of their cellular and molecular changes for over one year of *in vitro* cultivation.

Stem cells represent the regenerative capacity of a tissue or organ from which the next generation of progenitors will arise. Hence, the symmetric divisions of stem cells sustain self-renewal in balance with asymmetric division to produce progenitor cells and this is essential for determining the age and continuity of the tissue of interest. Stem cell activity is associated with the presence of certain factors known as markers, which can be found as genes or proteins and have been widely used to identify several stem cell populations. Since the final recommendation of the previous chapter was to use the cell surface antigen (Thy-1) as a marker for the isolation of the potential stem cells it will be the main factor of this study and further information regarding the characteristics and the roles of this marker is presented.

Thy-1 is a small (25–37kD) heavily N-glycosylated, glycophosphatidylinositol protein. The DNA of the Thy-1 maps to chromosome 11 in humans, 8 in rats and 9 in mice. It is considered one of the first glycophosphatidylinositol anchored proteins to be purified and sequenced. Early

investigations recognised the 110 amino acids that represent the core of the human Thy-1 protein. While in rodent, the core protein of Thy-1 contains 111 or 112 amino acids (Pont, 1987). The post translational modifications of protein such as glycosylation (Reinders and Sickmann, 2007) and the addition of carbohydrate molecules contributes to 30% of Thy-1's total mass (Barclay et al., 1976).

Thy-1 glycophosphatidylinositol group is anchored to the outer layer of the plasma membrane bilayer by the di-acyl group, while the glycoprotein faces the extracellular matrix (Low and Kincade, 1985). The glycoprotein that faces the matrix might be responsible for regulating its role in cell to cell communication and cell to matrix interaction (Rege and Hagood, 2006). Thy-1 protein efficiency as a cell surface antigen with its anchored glycophosphatidylinositol facilitates its use as a marker for identifying and isolating specific cells types, such as human foetal hepatic progenitor cells (Masson et al., 2006), epithelial like cells from eutopic endometrium with a stem cell differentiation capacity (Henriquez et al., 2011) and thyro-trophic cells from the pituitary (Horiguchi et al., 2016). In general, it is considered to be one of the embryonic and MSCs markers (Oltulu et al., 2015).

Thy-1 contributes to the interpretation of several cellular mechanisms, such as understanding retinal neuron recruitment of ion channel protein in complexes with Thy-1, and the role of anchored glycophosphatidylinositol in connection with the Potassium-sodium hyperpolarization/activated cyclic nucleotide-gated channel 4 (HCN4) subunits (Partida et al., 2012). Others suggest this cell surface molecule enhances the adhesive capacity of cells (He et al., 1991), and is necessary for focal adhesion formation in astrocyte adhesion (Henriquez et al., 2011).

Although Thy-1 has been used for a number of applications, Thy-1 protein expression is quite sensitive to the changes of its microenvironment. Early studies showed that cytotoxic materials were found to reduce Thy-1 expression *in vitro* (Herberman et al., 1978). Others showed a significant decrease during thyrotoxicosis *in vivo* (Oltulu et al., 2015). Thy-1 distribution in adipose-derived stem cells decreased when the foetal bovine serum (FBS) in the culture media was replaced with alternatives such as Bovine Serum Lipids.

So to use Thy-1 as marker for the isolation process, a production process of anti-Thy-1 antibody started in large scale, because a large amount was required for isolating the targeted cells and several later experiments. Primary cell cultures from whole rat adrenal gland were prepared and assessed for their normal response to ACTH, which induced the production of corticosterone. This experiment was required to show the capacity of the primary cells to show normal response *in vitro* as *in vivo*. The next primary cultures were carried out after enucleation of the adrenal gland to exclude the medulla and most of the zF because the target cells were located in the capsule and sub capsular areas.

Magnetic activated cell sorting (MACS) was carried out using the anti-Thy-1 antibody to enrich the Thy-1 positive cells of the adrenocortical primary cultures. MACS is a well-documented method used for isolating target cells such as stem cells (Amiri et al., 2015, Zhong et al., 2015).

The novelty of this chapter is not only the isolation of the Thy-1 positive cells from the adrenal cortex but also the interesting findings after culturing these cells and the changes that these cells underwent after cultivation for a long-term period.

More information regarding stem cell relating markers, molecular and morphological changes are presented in the next sections.

4.1.2. Wilms Tumour 1(WT1)

This WT1 protein is a transcription factor that encloses four zinc-finger motifs at the C-terminus and DNA-binding domain enriched with glutamine and proline at the N-terminus. It plays an essential role in the normal development of the urogenital system; the loss of the WT1 gene expression causes disruption to the kidney's normal development resulting in Wilms' tumours (Berry et al., 2015). The WT1 mRNA in humans and rats undergoes RNA editing in specific tissues such as testis and kidney and is associated with proliferation and differentiation (Sharma et al., 1994).

Stress factors for the urogenital system, such as hypertension, are associated with the down-regulation of WT1 expression (Mazzei et al., 2016). It is thought to be a coordinator of the embryonic developmental reversible processes, known as mesenchymal-epithelial transition (MET) and epithelial-mesenchymal transition (EMT) these processes are available in the development of the organs such as the kidney and the heart (Sampson et al., 2014). Although it was identified as a tumour suppressor, it has an important role in mesenchymal to epithelial transition in several malignancies, such as mesothelioma, which led to the suggestion that it could be used as a target in mesothelioma therapy (Plones et al., 2017). It also induces the hybrid transition of epithelial-mesenchymal and mesenchymal-epithelial in which malignant cells maintain both EMT and MET characteristics that might induce cell plasticity and progression of a tumour (Sampson et al., 2014).

As a stem cell marker, the expression of WT1 contributes to the mesenchymal progenitors of pulmonary smooth muscle cells during the early stages of lung development (Moiseenko et al., 2017). It regulates the development of interstitial progenitor cells during the embryonic

development of the mouse testis (Wen et al., 2016) and it is thought to be involved in the stem/progenitor adrenocortical cell state (Bandiera *et al*., 2013).

4.1.3. E-twenty-six (Ets) variant gene 5 (Etv5)

Etv5 belongs to a group of 26 transcription factors, that contribute to several cellular processes such as embryonic development, growth and apoptosis (Sharrocks, 2001). It has been found to be a transcriptional regulator in several cell types, such as controlling the self-renewal process of the spermatogonial stem cell population (Wu et al., 2011). The up-regulation of the Etv5 gene *in vitro* indirectly maintain the spermatogonial stem cell self-renewal process (Ishii et al., 2012) and it plays an important role in spermatogonial stem cell activity by regulating male fertility (Alankarage et al., 2016). A high expression of the Etv5 protein has been recorded in the primary salivary stem cells of humans (Srinivasan et al., 2017) and was not only involved in the proliferation of somatic stem cells but also in embryonic stem cells (Akagi et al., 2015).

4.1.4. Inhibitor of DNA Binding 4 (ID4)

ID4 is one of several highly conserved genes (ID1-4) encoding transcription factor proteins. These genes are expressed during several cellular activities, such as the proliferation and embryonic development. Although ID4 is a member of this family, it has different molecular pathways, expressions and functions. Several studies identify the roles of ID4 in different types of stem cells, for example, the regulation of stem cell proliferation and differentiation of neurones (Yun et al., 2004) and a regulatory role in the mammary stem cell (Junankar et al., 2015). The expression of ID4 maintains the stemness state of spermatogonial stem cells (Oatley et al., 2011) and is essential for spermatogenesis in mice (Sun et al., 2015). Recent findings show

the expression levels of ID4 are indicators of the regenerative capacity of spermatogonial stem cells (Helsel et al., 2017).

4.1.5. Senescence of the primary cells *in vitro*

Cell senescence is identified when the doubling time of cell division in culture increased and then proceeds to cell death. This cellular phenomenon usually associated with morphological changes. The phenomenon was first described in human fibroblasts in culture, which undergo senescence after approximately 50 cell divisions, so-called the Hayflick limit (Hayflick and Moorhead, 1961). Although this phenomenon was observed in the primary cells *in vitro*, it might be related to the age of the organism (Yegorov and Zelenin, 2003). The senescence of MSCs was recorded in several publications which manifested in three main characteristics: morphological changes, reduction in proliferation and differentiation potential (Zhu et al., 2015). The senescence of cells has been recorded even with the most pluripotent stem cells such as human embryonic cells (Munoz-Espin et al., 2013) and mouse embryonic cells, which is not only consider as a defect but also as mechanism that contributes to embryonic development, growth and cell patterning (Storer et al., 2013). Certain studies refer to the interior molecular factors that are involved in the induction of the cell senescence. These factors include specific mRNAs and micro RNAs, which are considered as the main factors contributing to the senescence of the MSCs such as miR-199b-5p which was suggested as an indirect regulator of bone marrow MSC senescence (Yoo et al., 2014). While the micro RNAs 543 and 590-3p directly regulate MSCs senescence (Lee et al., 2014). Others found the expression level of the miR-29c-3p was increased significantly when the MSC undergo senescence (Shang et al., 2016). On the other side, exterior factors are involved in MSCs senescence such as high glucose in the culture media (Xu et al., 2015). Later studies ceased the MSCs senescence and rejuvenated the old cells by down

regulation of the MicroRNA-195 and reactivating Telomerase reverse transcriptase (TERT). These findings referred to the senescence of MSCs as it might result from internal and external factors. So the senescence of MSCs can be stopped or reversed.

4.1.6 Immortalisation of primary cells *in vitro*

Transformation of normal primary cells to immortal cells *in vitro* with characteristics similar to that of tumour cells has been recorded (Gordon et al., 2014) and also the transformation of MSCs to immortal cells *in vitro* has been recorded (Urraca et al., 2015). The differences between normal cells and tumour cell lines from the same tissue have been widely studied and revealed epigenetic changes in the gene expression and DNA methylation (Baylin and Jones, 2011, Ehrlich, 2009). The loss of DNA methylation in the tumour cells was the main sign that this epigenomic alteration from normal cells to cancer cells resulted in down regulation of tumour suppressor genes (Jones and Baylin, 2002, Lubecka-Pietruszewska et al., 2015). The abnormal methylation of the tumour cells can be caused by several factors such as mutations, removing or altering certain genomic DNA sequences (Parsons et al., 2012). In spite of the variety of literature suggesting these changes are associated with this abnormal transformation of cells from normal to tumour cells, how and when the cells initiate this transformation is unclear. Although the mutations take place and change few primary cells in the beginning, it was hard to detect or separate the tumour cells from the normal ones in that time and it can impute the presence of the cancer stem cells (Visvader and Lindeman, 2008). However, later publications recorded the isolation of several cancer stem cells (Lucarelli et al., 2015, Xie et al., 2014, Yang and Lai, 2013). Although the transforming of primary cells to immortal cells is not in favour, certain studies suggest the capacity of immortalised MSCs such as dental pulp stem cells to differentiate into functional neurons (Urraca et al., 2015). Therefore, certain studies attempted to immortalise

MSCs for gaining more of these pluripotent cells because the immortalisation of MSCs will provides more cells than the mortal cells. Immortalisation attempts were applied to the amniotic mesenchymal cells (Teng et al., 2013) and dental pulp stem cells (Gao et al., 2015). However, this immortalisation should be under control to avoid oncogenic transformation, which required knockdown of p53 and up-regulation of TERT (Liu et al., 2013). In short the immortalisation of the MSCs is more promising than the immortalisation of the primary cells *in vivo* or *in vitro* which more likely to consider as tumour or cancer cells.

The aim of this chapter is to isolate Thy-1 positive cells and culture them *in vitro*. The cells in culture were then used for monitoring and observing their morphological aspects, and also for studying their molecular and cellular characteristics. Their stability in culture and their capacity to survive *in vitro* for the long-term period was also investigated, as it is one of the characteristics of MSCs. The cell behaviour and the ongoing molecular and cellular changes were also noted. Finally, this investigation also included the detection of expression of other stem cells markers in Thy-1 positive cells.

3.2 Material and methods

3.2.1 Primary culture of adrenal cells

Primary cultures of adrenal cells were prepared from freshly isolated adrenal glands using mechanical and enzymatic digestion. Adrenal cells were isolated using a modified version of the procedures described by (Poolman and Brooks, 1998), (Bestervelt et al., 1993) and (Caroccia et al., 2010). Although the following description is the isolation of the cells of interest from the adrenal cortex, which includes the capsule, zG, zI and zF, the isolation of the cells from the whole adrenal gland was conducted for general examination and ACTH treatment.

Adrenal glands were cleaned of fat tissue and blood and a small incision was made on the side of the adrenal gland. A micro- scissor was inserted into the opening and pointed forceps were used to conduct adrenal enucleation (a process of removing most of the inner core of adrenal gland medulla and most of the zF, leaving the adrenal capsule intact). The outermost part of each adrenal gland (containing the capsule and zG) was divided into several slices and the cells were dispersed by serial mechanical and enzymatic digestions (3 digests of 15 minutes each) in Minimum Essential Media (MEM) (Gibco) containing 1mg/ml Collagenase type I (Worthington) and Pancreatin (Sigma) 0.5 mg/ml using a shaking water bath at 37°C.

After each digestion, the isolated adrenal cells were harvested and enzymatic activity was inhibited by the addition of 10% v/v Foetal Calf Serum (FCS) (Invitrogen) in MEM. The digests were pooled, the cells pelleted by centrifugation (800g for 5 minutes) and suspended in Dulbeccos Modified Eagle's Medium (DMEM) (Gibco) containing penicillin (100 U/ml), streptomycin (100 µg/ml) (Invitrogen), L-glutamine (2µM) (Invitrogen) and 10 %v/v foetal calf serum. Cell viability was assessed using trypan blue exclusion staining and the number of cells was determined using a haemocytometer. The isolated cells were maintained for 24 hours in

DMEM at 37°C in a humidified atmosphere of 5% CO_2 in an air incubator. They were incubated for 1-2 days before any further investigation or treatment.

3.2.2 Trypan blue dye-exclusion

The viability of the cells was assessed using trypan blue dye-exclusion; an equal quantity (50µl) of cell suspension and 0.4% (w/v) trypan blue in PBS was mixed thoroughly. The mixture was left to stand at room temperature for 2-3 minutes. The viable cells were round in shape and clear, while the dead cells were blue. The cells were counted using a haemocytometer under the microscope. The number of viable cells was calculated as follows:

[1.00 – (Number of blue cells ÷ Number of total cells)] × 100.

3.2.3 Treatment of primary cells with adrenocorticotropic hormone (ACTH)

This treatment was conducted for the general assessment of the viability and hormonal response activity of the isolated cells. The cells were divided into five groups with each group having three wells of a 96 well cell culture plate (Cellstar) containing $1x10^5$ cells in a volume of 200µl of DMEM media. They were incubated at 37°C in a humidified atmosphere of 5% CO_2 in an air incubator before being treated with various doses of ACTH (Bachem), between 1nM and 1pM. The media of the treated cells was collected after four hours of treatment and the corticosterone concentrations were determined by an Enzyme Linked Immune Sorbent Assay (ELISA).

3.2.4 Corticosterone detection using ELISA

A competitive ELISA was applied to detect and quantify corticosterone. Maxisorp microtitre 96 well plates (Nunc) were coated with 50µl (5ng) corticosterone-BSA (Sigma) diluted in 0.1 M sodium bicarbonate and incubated overnight at room temperature. The coated plates were washed four times with 0.1% Tween v/v in PBS before the addition of a 250µl gelatine

phosphate buffer (0.25% w/v gelatin in PBS (GPB)). They were stored for a minimum of 4 hours before use and for a maximum of three weeks in a moist box at 4°C.

The coated plates were washed four times with 0.1% Tween v/v in PBS before use. Standards and samples were pipetted into appropriate wells (100µl/well). For this assay a series of 10 doubling dilutions of corticosterone standard were prepared in GPB (standard range 0.5 – 250ng/ml). A corticosterone antibody diluted 1:20000 in GPB (Biogenesis) was added to each well (100µl) with the exception of the blank zero tracer wells. The plates were incubated overnight at room temperature in a moist box before washing four times with 0.1% Tween v/v in PBS.

The secondary antibody, 200µl of goat anti-rabbit IgG-horseradish peroxidase (Cell signalling) diluted 1:2000 in GPB was added to each well and incubated for at least 1 hour in a humidified box. The plates were washed four times with 0.1% Tween v/v in PBS before the addition of tetra methyl benzidine (TMB) substrate (Appendix A.25) The reaction was allowed to proceed until a blue colour developed and the reaction was stopped by adding 100µl of 0.5 M HCl. The absorbance of each well was measured at 450nm (600nm ref) using an ELISA plate reader (Molecular Devices).

3.2.5 Trypsinisation

The cultured cells were trypsinised using TrypLE (Gibco) when they reached confluence. The cells were washed with PBS and then TrypLE was applied to detach them. Media was then added to deactivate the TrypLE and the cells were pelleted by centrifugation at 800g at 4^{o}C for 5 minutes. After this, the supernatant was discarded and the cells were re-suspended in the desired

media. Then the cells were either split into more flasks or frozen in the complete medium containing 10% dimethyl sulfoxide (DMSO).

3.2.6 Thy-1 monoclonal antibody production from hybridoma

Thy-1 antibody was produced in-house from the OX-7 hybridoma cell line. Thy-1 monoclonal antibody production was necessary in this project because a large amount was required for the experiments carried out. The OX-7 Hybridoma cells Catalogue No.: 84112008 (Sigma) produce mouse anti-Thy-1.1 IgG (Biochem J 1980;187:1). Hybridoma cells were received in a box of dry-ice containing the frozen vial. The vial was transferred to liquid nitrogen until all requirements for culturing the suspension cell line had been prepared.

The culture medium was prepared for the suspension cell line using [Roswell Park Memorial Institute (RPMI) 1640 Medium containing penicillin (100 U/ml), streptomycin (100µg/ml), L-glutamine (2µM) and 10% v/v foetal calf serum]. Before thawing the cells, 20ml of the medium was pipetted in a 25cm^2 flask and kept at 37°C in a humidified atmosphere of 5% CO_2 in the air. In a laminar flow cabinet, a piece of tissue paper sprayed with 70% alcohol was wiped around the cap of the frozen vial and the cap was turned a quarter turn to release any residual liquid nitrogen that may be trapped. The cap was then retightened and warmed by hand for a few seconds. Finally, the ampoule was transferred to a 37^{o}C water bath for 1-2 minutes until only small ice crystals remained. This process was key, because any delay in the thawing process may have caused damage to the cells membranes.

3.2.6.1 Growing hybridoma cells

The cells were seeded at 50,000 viable cells/ml into T75cm^2 flask (20ml) and incubated for two days where they reached 90% confluency. They were sub-cultured into three T175 cm^2 flasks,

with each flask receiving 5ml of the culture with 60ml of the media, 65 ml in total in each flask. The cells were cultivated and split into four T175 cm^2 flasks.

3.2.6.2 Monoclonal antibody production

The cell culture content of four T175 cm^2 flasks was split into five 50ml tubes, spun at 800g at 40°C for 5 minutes and re-suspended gently in 7ml sterile PBS for each tube in order to wash the serum from the cells. The tubes were spun again and this time the pellets were re-suspended with the Hybridoma-serum-free media (SFM), before being transferred to 175cm flasks and incubated at 37°C in a humidified atmosphere of 5% CO_2 in the air. Hybridoma-SFM is a serum-free product optimised for the growth of hybridomas and monoclonal antibody production. It contains a low protein concentration (<20 μg/mL) and has no polypeptide growth or attachment factors. These characteristics reduce the number of factors that might interfere with Thy-1 monoclonal antibody purification.

3.2.6.3 Binding Thy-1 monoclonal antibody to the protein G bind column

Hodgkinson and Lowry's (1982) protein affinity binding and recovery method was used to purify Thy-1 monoclonal antibody because the Hybridoma cells were releasing the antibody into the media. The media were centrifuged at 1000g at 4°C for 5 minutes to remove the cells. The supernatant was then filtered with a 0.22μm filter. Since this Thy-1 monoclonal antibody is a mouse lgG1, it has a higher affinity to bind to Protein G in comparison with protein A of the immunoglobulin-binding proteins.

The protein G bind column (HiTrap Protein G HP column) was prepared for binding the Thy-1 monoclonal antibody. The column was washed with 10ml saline (0.15M NaCL) and the filtered media were passed through the column for around 15 hours using a slow MINIPULS machine

(Gilson). The time required to pass all the media was pre–adjusted by adjusting the speed of the flow, which was necessary to avoid drying the column during the process. The saline was re-attached just before the end of media to avoid drying the column.

3.2.6.4 Elution of the Thy-1 monoclonal antibody from the protein G column

The binding capacity of the column is affected by the pH, so it forms the basis of the releasing process. First, 5ml of saturated sodium bicarbonate was prepared; 150µl of sodium bicarbonate solution was aliquoted into the 1.5 ml collection tubes.

The first column wash was with saline followed by 0.5M sodium acetate, it was then washed with 50mM sodium acetate with 20% acetonitrile pH 6 (pH adjusted with acetic acid) and approximately 1 ml of buffer was collected into each of the first 4 tubes.

Then the elution was started with 50mM sodium acetate with 20% acetonitrile pH 4 (formic acid was used to adjust the pH), around 1 ml of buffer was collected into each one of the second group of 4 tubes and they were mixed. Then further elution was conducted with a lower pH solution of 50mM sodium acetate with 20% acetonitrile pH 3.5 (formic acid was used to adjust the pH again). Around 1 ml of buffer was collected into each of the third group of 4 tubes and the protein presence was examined by Coomassie Blue. A NUNC 96 well plate was used for this test with 50µl of each tube being pipetted into one well of the plate. Then 100µl of Coomassie Blue was added. The wells in which a blue colour developed, meaning they contain the targeted protein and tubes are the targeted tubes, which were mixed together with the ones before and after the tubes that contain the protein. The acetonitrile was evaporated from the purified antibody using a centrifuge evaporator (1ss110bbSpeedVac system), on medium speed for 80 minutes to reduce the total volume. The protein concentration was measured using a

spectrophotometer in which the UV wavelength was set to 280nm. The appropriate volume of PBS (300µl) was used as a blank solution, then 300µl of the antibody solution was measured to determine the antibody concentration. This was adjusted to less than 500 µg/µl, then the solution was divided into 300µl aliquots, snap-frozen in liquid nitrogen, and moved to a -80°C freezer.

3.2.7 Western blotting

Western blotting was conducted to separate and visualise proteins, these images were employed to confirm the size and the presence of the proteins of interest. Proteins released in the culture media were detected directly by profiling a sample of the media, while the proteins inside the cell were detected after preparation of cell lysate.

3.2.7.1 Preparation of cell lysates

The cells were processed after removing the media by centrifuging at 1500 g for 15 minutes at 4^{o} C. The cells were then washed with ice-cold PBS using the same previous centrifugation step. Then the chilled lysis buffer (a protein inhibitor cocktail and RIPA buffer mixture (1:100)) was added to the pellets. The cells were added in a concentration of $1x10^{7}$/ml of lysis buffer and mixed well.

The lysates were passed through 21 gauge blunt needles a minimum of ten times and then incubated at 4^{o}C for 30 minutes. Finally, the lysates were transferred to 1.5 ml microcentrifuge tubes and centrifuged at 13,000 g for 15 minutes in 4^{o}C and the supernatant was collected and stored at -20^{o}C.

3.2.7.2 Sodium Dodecyl Sulfate-Polyacrylamide Gel Electrophoresis (SDS-PAGE)

Glass plates were assembled according to the vertical electrophoresis tank instructions (BioRad), the concentration and volume of the separating gel (resolving gel) was determined and prepared first according to the appropriate instructions.

The separating gels were pipetted into the gap between the two glass sheets quickly after preparation, making sure that adequate space was left for the stacking gel. In order to prevent the diffusion of oxygen into the gel, which could inhibit the polymerization of the gel, the resolving gel was covered with 0.1% SDS w/v, isobutanol or water according to the acrylamide concentration (low, medium or high respectively), the gel was then placed for 5-15 minutes vertically at room temperature. The cover liquid was removed after the resolving gel polymerisation. Then the top of the gel was washed with water twice to remove the un-polymerised acrylamide. The liquid was removed completely from the top of the resolving gel. Then the stacking gel was prepared, pipetted on the resolving gel, and the comb was inserted immediately in order to avoid any air bubbles. The comb was removed after polymerisation to reveal the samples' wells. The prepared SDS gel had two separated layers: the upper stacking gel and the lower resolving gel (figure 3.1).

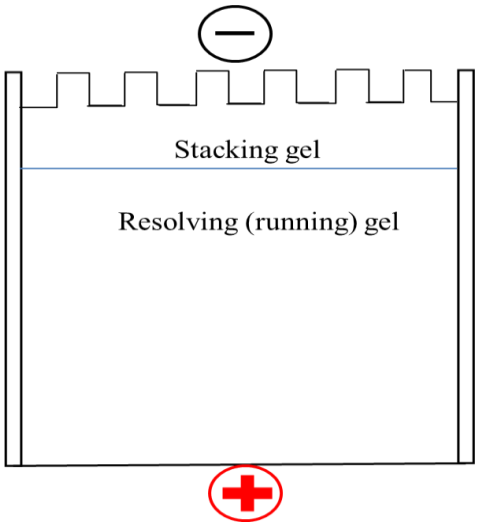

Figure 3.1 SDS-PAGE system gel consists of two components. The stacking and resolving (running) gels, the stacking gel has lower micro-pores sizes, pH and ionic strengths. The resolving gel has higher micro-pores sizes, pH and ionic strengths. The protein samples travel through the gel from the cathode (-) to the anode (+) after applying electric power to the running buffer.

The cell culture media or the cell lysate samples were prepared by mixing 25 µL 5x loading buffer (Appendix A.26) and 5 µL of β-mercaptoethanol was added to 95 µL of sample lysate or the cell culture media. Later this mixture was heated for 5 minutes at 90^{o}C. After processing the lysates with a loading buffer, samples were run through SDS-PAGE in order to separate proteins based on their molecular weight. The gel concentrations were selected to meet the size of the targeted proteins; 15 % v/v gels were used for small proteins with a molecular weight of up to 12-25 kiloDalton (kD). 10-12 % v/v were for proteins with a molecular weight from 10 – 70 kD, and less than 10% for those larger than that. Running buffer (Appendix A.27) was added to the running tank and samples were loaded in the stacking gel wells after being filled with the running buffer. An electrical current was applied to the running tank, using 10 to 15 V and 30 mA per cm of the gel. Visualisation of the targeted proteins was carried out by either the Coomassie Blue staining or blotting of the protein bands on a transfer membrane.

3.2.7.3 Staining Polyacrylamide SDS-PAGE Gels with Coomassie Blue

The SDS gel was washed with distilled water 3 times for 5 minutes each to remove the SDS because it interferes with the staining process. The water was removed and enough Coomassie Blue stain (Bio-safe™) was added to cover the gel. The gels were then gently shaken on a rocker for one hour. The proteins bands were usually visible within 20-30minutes. After the appearance of the bands, the gel was washed with distilled water for at least 30 minutes to reduce the background and the stained gels were stored in water at 4C.

3.2.7.4 Transferring the protein from the gel to the transfer membrane

The gel was removed from the running tank, the stacking gel and the no ladder corner of the separating gel were removed for orientation. The gel was transferred to transfer buffer (Appendix

A.28) for 20 minutes. The transfer membrane (0.45 μm pore size polyvinylidene difluoride (PVDF)) was submerged in methanol for 30 seconds and then washed in distilled water. Six filtered papers were submerged in the transfer buffer, three of them were put on the semi-dry transfer machine and all bubbles were removed. The transfer membrane was put on top of the filter papers. Then the gel was placed on the transfer membrane and the remaining three filter papers were put on top of the gel. An electrical current was applied for 1.5 hours to transfer protein bands from the gel to the transfer membrane (figure 3.2).

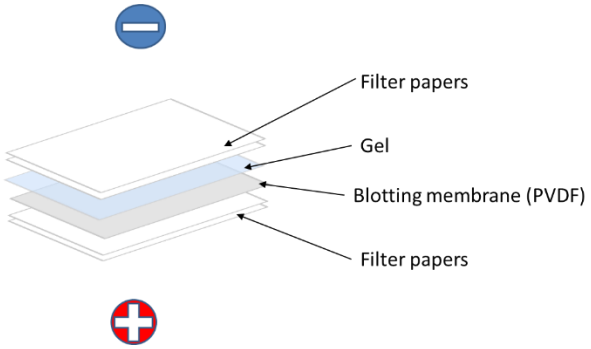

Figure 3.2 Sandwich semidry system of protein transfer after SDS page electrophoresis. The system was setup to transfer proteins from the SDS page gel to a solid blotting membrane for further analysis. The system consisted of 2-3 filter papers, the gel, the blotting membrane and finally 2-3 filter papers. The protein samples travel from the gel to the membrane (from the cathode (-) to the node (+)) after applying electric power.

The transferred membrane was moved into the tray, blocked with 5% dry skimmed milk, dissolved in Tris-Buffered Saline Tween (TBST) (Appendix A.29), for one hour at room temperature with agitation. The membrane was washed three times with TBST for 10 minutes each also with agitation. The primary antibody was added to the membrane after an appropriate dilution usually 1:1000 in 5% w/v BSA or low-fat milk (dissolved in TBST) and incubated overnight at 4^{o}C with agitation. The following day, the membrane was again washed in TBST three times, for 10 minutes each with agitation. A horseradish peroxidase (HRP) conjugated

secondary antibody, prepared and properly diluted (1:4000 in 1% w/v BSA or low-fat milk dissolved in TBST), was applied to the membrane for one hour at room temperature with agitation and finally the membrane was once again washed in TBST three times, 10 minutes each with agitation.

3.2.7.5 Imaging and data analysis

Amersham ECL Plus (substrate detection solution mix) was prepared and used to cover the membrane. Any protein bands were detected using Image Quant LAS 4000 mini - GE Healthcare machine.

3.2.8 Magnetic Activated Cell Sorting (MACS)

Magnetic activated cell sorting (MACS) is a common method used to isolate target cells. In MACS, magnetic microparticles are coated with antibodies to cell surface markers and cells expressing this marker then become associated with the beads. The cells are then transferred to a column and a magnetic field is then applied, then when the column is washed, unwanted cells are washed away, retaining the cells of interest. MACS was instrumental in our understanding behaviour of the isolated cells *in vitro.*

3.2.8.1 Labelling antibody with para magnetic beads

Pierce N-hydroxysuccinimide (NHS)-Activated Magnetic Beads were used for the immunoprecipitation of the Thy-1 target cells. This required binding a specific antibody with the magnetic beads.

The binding procedure was conducted using 300µL of magnetic beads (10mg/ml) in a 1.5ml microcentrifuge tube to bind 500µL of protein solution following the manufacture’s protocol.

The coupling and blocking procedure began by equilibrating the Thy-1 antibody solution and magnetic beads to room temperature and chilling the wash buffer (PBS) on ice.

The magnetic beads were mixed by gentle tapping and repeated inversion until no clumps were seen. Each 300µL of the magnetic beads were prepared individually and were then placed into a 1.5 microcentrifuge tube in a magnetic stand (Promega). The magnetic beads were attached to the side of the tube closest to magnet in a few seconds leaving a coluorless solution in the bottom of the tube, which was discarded while the tube was inside the magnetic stand. Then the tube was removed from the magnetic stand and the beads were washed with 1ml of ice-cold PBS and gently mixed by tapping for 15 seconds until the solution was homogeneous. The tube was returned into the magnetic stand, the beads again moved toward the side wall of the tube and quickly attached to the magnetic side, leaving a colourless solution which was discarded. The tube was taken out of the magnetic stand, the Thy-1 antibody solution (500µL containing 235µg of the Thy-1 antibody) was added immediately to the tube and mixed gently by tapping for 30 seconds.

It was then incubated overnight at 4°C on a rotator (the 1.5ml microcentrifuge tube was placed in a 20ml tube and put in a horizontal rotator). During the first 30 minutes of the incubation, the solution was mixed for 10 seconds every 5 minutes. Then the tube was mixed twice for 15 seconds every 15 minutes. Then left on the horizontal rotator until incubation was complete.

The bead-antibody complexes were collected with the magnetic stand and washed twice with PBS (1ml) each as previously described. One ml of ultrapure water was added and mixed for 15 seconds. The tube was placed into a magnetic stand where the bead-antibody complexes were collected and the supernatant was discarded. Then the beads were quenched by mixing with 1ml of quenching buffer for 30 seconds. The quenching buffer was 300µl of 3M ethanolamine in 5ml

of 1M HCl, pH 8.5. The pH was measured and drops of ethanolamine were added if it was acidic, but if it was alkaline HCl was added until the pH reached 8.5.

Then the tube was incubated for 2 hours at room temperature on a rotator. The beads-antibody complex was collected using the magnetic stand and the supernatant was discarded. Then 1 ml of ultrapure water was added to the bead-antibody complexes and mixed for 15 seconds. The tube was placed onto the magnetic stand, the bead-antibody complexes were again collected and the supernatant discarded. Finally, 1 ml of storage buffer [Coupling Buffer (50mM sodium bicarbonate) with 0.05% sodium azide] was added to the bead-antibody complexes and mixed for 15 seconds. The tube was placed onto the magnetic stand, the bead-antibody complexes were collected again and the supernatant was discarded. This wash was repeated two additional times and then the beads were stored in 300µL of storage buffer at 4°C until ready for use.

3.2.8.2 Binding the bead-antibody complexes to the target cells

MACS was applied to the primary adrenal cells after one day of culture in order to isolate the cells expressing Thy-1 protein in their cell membrane. The cultured cells were counted using a haemocytometer, then pelleted at 600g for 5 minutes at 4°C to remove the culture medium. Then 2 ml of sterile ice-cold PBS, containing 0.1% w/v bovine serum albumin (BSA) buffer, was used to re-suspend 2.5 million cells.

An appropriate volume (50µl) of Thy-1 antibody conjugated beads was prepared for each adrenal gland. Thy-1 antibody conjugated beads were pipetted into a 1.5 microcentrifuge tube. Then, 1 ml of PBS was added to the conjugated beads and mixed for 15 seconds. The tube was placed into a magnetic stand, the beads-antibody complexes were collected and the supernatant was discarded. This wash with PBS was repeated twice. The next step, pipetting, was conducted

slowly and gently to minimise harm to the cells. The cell suspension was added to the conjugated beads and incubated at 4°C on a rotator (Fisherbrand) with a slow rotation (20 RPM) for 30 minutes to bind the conjugated beads to the target cells. Again, the tube was placed onto the magnetic stand and the negative cells were collected. Then the tube was moved out of the magnetic stand and 1 mL of ice-cold PBS, containing 0.1% BSA, was added and gently mixed to remove any negative cells. The tube was placed onto the magnetic stand; the conjugated bead-cell complexes started to move toward the side wall of the tube and attached to the magnetic side in a few seconds leaving a clear solution, which was discarded. This wash step was repeated twice to remove negative cells.

The conjugated bead-cell complexes in each tube were re-suspended in a pre-warmed DMEM culture at 37°C and moved to one well of a 12 well plate. The plate was incubated at 37°C in a 5% CO2 humidified incubator for 10-14 days before changing the media.

3.2.9 Cells tracking and wound healing assays

The isolated cells were cultured in the DMEM media for over one year, cell tracking and wound healing assays were conducted to monitor cell proliferation and migration *in vitro*. Cells were prepared 1-7 days before the day of the assay, the cells seeded on a 12 and 24-well plate at 10-30% confluence for cell tracking assay and 70-90% confluence for wound healing assay. Cells were seeded in triplicated. Confluent cells underwent wound healing assay and were scratched by a 200µl pipette tip along the diameter of each well. Cells were rinsed twice with culture media to remove any floating cell debris. The cells were refreshed with fresh media before positioning under the microscope.

3.2.10 Immunocytofluorescence

Immunocytofluorescence assays were conducted to examine the expression of the protein of interest in the Thy-1 positive cells. Dual Immunocytofluorescence staining assays were conducted using primary mouse antibodies and rabbit antibodies. The cells were washed twice with PBS to remove the culture medium and then they were fixed with 4% paraformaldehyde in PBS (w/v) for 5 minutes, washed three times (3x) with PBS and blocked with 10% v/v goat serum in PBS for 30-60 minutes. After this, the cells were incubated with the primary antibodies (1:200 dilution in 1% v/v goat serum in PBS for each) overnight at 4°C. They were washed with PBS (3x), incubated with fluorescent Alexa-Fluor conjugated secondary antibody (anti-mouse and anti-rabbit) at a 1:200 dilution for 30 minutes before washing three times with PBS. The coverslips were mounted with DAPI (VECTASHIELD). In the dual immunocytofluorescence both primary and secondary antibodies (mouse and rabbit) were mixed together in the primary and secondary incubation steps, respectively. The slides were tested using a Zeiss-Axio Imager.

3.2.11 RNA isolation from cultured cells

The RNA was isolated from the cultured cells using an RNeasy mini kit after trypsinising the cells using TrypLE reagent (Gibco). The cells were washed with PBS and centrifuged at 800 x g for 5 minutes. The supernatant was completely aspirated.

The pelleted cells were loosened thoroughly by flicking the tube. They were then entered into the RNA isolation process. Several preparations were conducted before the use of the kit components following the provider's recommendations. The loose pelleted cells were disrupted by adding the appropriate volume of Buffer RLT (350-600µl).

The mix was pipetted and homogenised by passing slowly through a pipette tip and the bottom of the tube at least 10 times. Based on the volume of the RLT buffer that was added initially, one volume of 70% ethanol was added to the homogeneous lysate and mixed well by pipetting. The mixed sample (no more than 700µl) including any precipitate that may have formed was transferred to an RNeasy spin column and placed in a 2 ml collection tube. The lid was gently closed and the sample was centrifuged for 15 seconds at 8000 x g (10,000 rpm). The flow-through was discarded. If the sample volume exceeded 700 µl, it was divided and centrifuged in the same RNeasy spin column. The flow-through was discarded after each centrifugation. To eliminate genomic DNA contamination, an on-column DNase digestion was conducted.

To wash the spin column membrane, 350µl of buffer RW1 were added to the RNeasy spin column. The lid was gently closed and the column centrifuged for 15 seconds at 8,000 x g (10,000 rpm). The flow-through was discarded, and the collection tube was reused. Ten µl of DNase I stock solution was mixed gently with 70µl of buffer RDD. The mix (80µl) was added directly to the RNeasy spin column membrane and placed on the bench-top (20–30°C) for 15 minutes. The previous wash step was then repeated by adding 350µl of buffer RW1 to the spin column membrane. The lid was gently closed and the column centrifuged for 15 seconds at 8000 x g (10,000 rpm). The flow-through was discarded, and the collection tube was used again.

The spin column membrane was washed twice with buffer RPE to ensure that no ethanol was carried over during RNA elution because residual ethanol may interfere with downstream reactions. The first wash was conducted by adding 500µl of buffer RPE to the RNeasy spin column. The lid was closed carefully and the sample was centrifuged for 15 seconds at 8000 x g (10,000 rpm). The flow-through was discarded, and the collection tube was reused again. The second wash was conducted by adding 500µl of Buffer RPE to the RNeasy spin column. Again,

the lid was gently closed and the column centrifuged for 2 minutes at 8,000 x g (10,000 rpm). The flow-through was discarded. The RNeasy spin column was placed in a new 2 ml collection tube and the old collection tube was discarded with the flow-through. The lid was gently closed and the column centrifuged for 1 minute. The RNeasy spin column was placed in a new 1.5 ml collection tube and 30–50µl RNase-free water was added directly to the spin column membrane. The lid was gently closed and the column centrifuged for 1 minute to elute the RNA. The RNA concentration and purity were measured using a Nanodrop (2000).

The isolated RNA from rat adrenal tissue was usually obtained using the TRIzol Reagent method (section **2.2.1.1)** for the positive controls of the RT-PCR tests.

3.2.12 cDNA synthesis for RT-PCR

For synthesis of total cDNA, a cDNA synthesis kit was used as described in section (2.2.2).

Table 3.1 List of primers (invitrogen) used in the RT-PCR, their accession number, position in the mRNA sequence and their product size.

Gene symbol	Forward primer 5`-3` (position)	Reverse primer5`-3` (position)	Fragment Size(bp)	Accession number
GAPDH	CAAGGTCATCCATGACAACTTTG (540-562)	GTCCACCACCCTGTTGCTGTAG (1035-1014)	496	XM_017593963.1
Klf5	CACAGCGCCAGAGGTGAACAATATC (507-531)	ATGGATGCGTCGCTTCTCCAGATC (1020-997)	514	XM_006252403.3
Thy-1	CCTCCAAGCCACGGACTTCATTTC (865-888)	AAGGCTCAGCAGCGCTCTCCTATC (1377-1354)	513	XM_017595476.1
Tmem121	TTGGTAGGCGATGTGTGCTTCCTG (393-416)	ATCATCTTCTGCGGTGCGATGTGC (901-878)	509	XM_006240674.3
NR5a1	AGCCCGATAGCCACTGCCCTA (28-48)	GCCCCGCATTCGATCAGCAC (414-395)	387	NM_001191099.1
3BHSD	GCAGACCATCCTAGATGTCAATCTG (434-458)	CAAGTGGCACATAGCCCAGATCTC (1182-1159)	749	NM_001007719.3
steroidogenic acute regulatory protein (STAR)	GGAGAGTGGAACCCAAATGTCAAGG (549-573)	TGGTTGATGATGGTCTTTGGCAGCC (889-865)	341	NM_031558.3
CyP11B1	AAGAACACTTTGATTCCTGGGATA (761-784)	GTGTCAACACTTCCAGCAATAAGT (950-927)	190	NM_012537.3
Cyp21a1	ACTCACAGCTGTGTCCGGGACTTG (644-667)	CAGCAGCGTGAAGGTCTGGAGCAG (1423-1400)	780	XM_006255907.2
Aldo Synthase (Cyp11b2)	AAGAACATTTTGATGCCTGGGATG (805-828)	GTGTCAACGCTCCCAGCAGTGAGC (997-974)	193	XM_008765542.1
Scc (Cyp11a1)	GCACACAACTTGAAGGTACAGGAG (1018-1041)	CAGCCAAAGCCCAAGTACCGGAAG (1361-1338)	344	NM_017286.2
NPR	ATGGCGTGTGCTGACCTTCTCATC (472-495)	TTGACCGTCTTCACCTTGGTCCTG (980-957)	509	XM_017592662.1
CD29	ACTGAAGAGCGGCTGAGACCCG (1-22)	TGGCCGGAGCTTCTCTGCCAT (524-504)	524	XM_006255824.1
Etv5	GAAGTGGCCGCTCAGGAGGATCT (46-68)	GTGACAAAGGAGTGGCGGGC (565-546)	520	NM_001107082.1
Shh	ATCCAAAGCTCGCATCCACT (845-864)	GGTTGATGAGAATGGTGCCG (1344-1325)	500	NM_017221.1
Gli1	CCGACAGAGGTTGGGATGAAG (114-134)	ATGGAGAGATGGCCGTAGGA (590-571)	477	XM_008765375.1
Wt1	CCACACCAGGACTCATACAGG (1632-1652)	ACAACCGCTCTAATCCCAGC (2123-2104)	492	XM_006234622.2
Tert	TTCCTTCCACCAGGTGTCAT (207-226)	AGGCACGTTTGTACTGGTGA (726-707)	520	NM_053423.1
ID4	GAACGACTGCTACACTCGCC (204-223)	ACGGTGAATGCTTGTGAACG (723-704)	520	NM_175582.1

3.2.13 Generating amplicons of target genes by PCR

PCR was used to detect the expression of the genes of interest. The preparation of the PCR reactions and the PCR conditions followed by agarose gel electrophoresis were described in section (2.2.3).

3.2.14 Immunohistofluorescence

Adrenal cryosections were prepared and the Immunohistofluorescence assays were conducted as described in section (2.2.12).

3.2.15 Microscopy

The immunofluorescent imaging for immunocytofluorescent and Immunohistofluorescence experiments were examined using a Zeiss-Axio Imager A1 fluorescent microscope with four filters: Blue/cyan filter for (4',6-diamidino-2-phenylindole (DAPI)), Alexa Fluor (AF) 488 green AF 546 yellow and AF 660 red. The magnification powers of the objective lenses used in these experiments were 5x, 10x, 20x and 40x. The fluorescent microscope was fitted with a camera (Axio cam MRm) linked to a computer and controlled by AxioVison software (Rel.4.8). This software was used to adjust the coluors, and quality of the images.

The cell numbers and viability were measured using an inverted transmitted-light microscope (Leitz LABOVERT) fitted with a camera (WILD MPS 12). The magnification power of the 10x objective lens was usually used in the primary cell experiments.

Time-lapse images sequences were taken (every 10 or 15 min) for cell tracking and wound healing assays using a Nikon TiE Time Lapse System, which included a moveable stage and environmental chamber set at 37C with a continuous flow of CO_2 through the plate. The assays

were run using a 10X Nikon lens. The quality of the images was adjusted using the microscope fine adjustment.

3.2.16 Image analysis by Image J software

The time lapse videos of cell tracking and wound healing assays were analysed using image J (Fiji) software. Single cell tracking was conducted to measure the time required for each cell division (doubling time) and the ratio of cells undergoing division per day was also calculated.

The wound healing assays were carried out to measure and compare the differences of cell migration ability of Thy-1 positive cells. Image J (Fiji) software was used to measure the areas of the wounds after a certain amount of time.

3.2.17 Statistical analysis

The resulted data of ELISA after ACTH treatment to the adrenal primary cultured cells and cell migration assays for Thy-1 positive cells were analysed using "Dunnett's Multiple Comparison Test" and Tukey's multiple comparison test of one-way analysis of variance (ANOVA).

3.3 Results

The assays and the analysis of the results of the previous chapter suggested that the Thy-1 protein was a potential adrenocortical stem cell marker. The aims of this chapter were the isolation of Thy-1 positive cells and to study them *in vitro*. These aims required the primary culture of dispersed adrenal cortex cells and testing their viability and hormonal response *in vitro*.

3.3.1 Adrenal cell primary culture, ACTH treatment, and ELISA.

Primary cultures of adrenal gland cells were prepared successfully from freshly isolated rat adrenal glands after mechanical and enzymatic digestion. The isolated cells were cultured *in vitro* under controlled condition. The viability of the adrenal primary cells was examined using Trypan blue exclusion and showed 87±5% viable cells.

In addition to the viability test, a hormonal response induction test was conducted to evaluate the ability of these primary cells to release corticosterone hormone after treating them with ACTH.

The cells were subjected to treatment with ACTH and the corticosterone released from the cells was measured using ELISA. Cells were incubated for 24 hours before exposure to serial doses of ACTH (1nM, 100pM, 10pM, 1pM and control). The medium was collected after 4 hours of exposure to ACTH and the corticosterone released by the cells was measured in the medium. The ELISA results showed that the rat adrenal gland primary cells had responded to the ACTH treatment by releasing corticosterone hormone in the culture medium. The cells response to ACTH treatment was dose dependent, with corticosterone concentration increasing from the basal concentration (40ng/ml) in the control cells to (50- 80ng/ml) with cells that were treated

with (1-1000 picomole) of ACTH (figure 3.3). Generally, the results of ACTH treatment showed expected corticosterone releasing response of these primary cells. A statistical analysis of one-way ANOVA showed significant [** (P<0.01) and *** (P<0.001)] responses of ACTH treatments at the two highest concentrations (100pM and1000pM respectively).

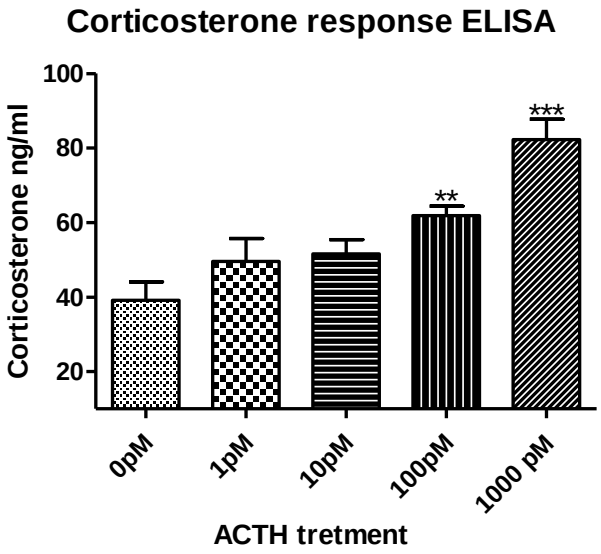

Figure 3.3 The effect of ACTH on corticosterone secretion from primary adrenal cultures. Cells were cultured at 100,000 cells/ml of DMEM media. The corticosterone response was measured by ELISA after 4 hours of ACTH treatments with (1nM, 100pM, 10pM, 1pM and control. Values are mean± standard error of mean (SEM) based on 3 independent cultures. summarized one-way ANOVA results revealed that significant [** (P<0.01) and *** (P<0.001)] responses of ACTH treatments at the two highest concentrations (100pM and1000pM respectively).

3.3.2 Production of anti-Thy-1 monoclonal antibody from hybridoma cells

The production of anti-Thy-1 monoclonal antibody on a large scale was necessary to accomplish a number of experiments in this project. This involved growing OX-7 hybridoma cells in RPMI medium which was successfully achieved in large scale. Samples of cultured media (RPMI) from several flasks were tested for the presence of the Thy-1 antibody using SDS-PAGE Coomassie

blue staining (figure 3.4), before proceeding with further production steps. The antibody was detected in all tested samples showing the presence of both heavy chain (~50KD) and light chains (~25KDa). The OX-7 hybridoma cells were transferred to the SFM medium to induce the cells to increase Thy-1 antibody production. The medium was collected and the anti-Thy-1 antibody was purified by utilising the binding affinity of the antibody to protein G (an immunoglobulin-binding protein). The Thy-1 antibody was subsequently recovered from the column. Acetonitrile was evaporated from the antibody solution (the evaporation of acetonitrile from the antibody solution reduced the volume of the anti-Thy-1 antibody solution from 10ml to 6ml) and the concentration of the protein was determined to be 0.781mg/ml. Thy-1 antibody solution was diluted to 500µg/ml with PBS. Samples from the media before and after the purification of the Thy-1 antibody and from the purified antibody solution were subjected to Western blotting to show the presence of the antibody light and heavy chains (figure 3.5). The bands of the purified antibody product were larger than the bands of the antibody before purification, which confirmed the successful purification. However, there was residual antibody that remained in the media after purification (figure 3.5), which might due to the limited binding capacity of the column. The intensity of the antibody band from the SFM culture before purification (figure 3.5) was more intense than one from the SFM culture after purification, which indicated the efficiency of the purification.

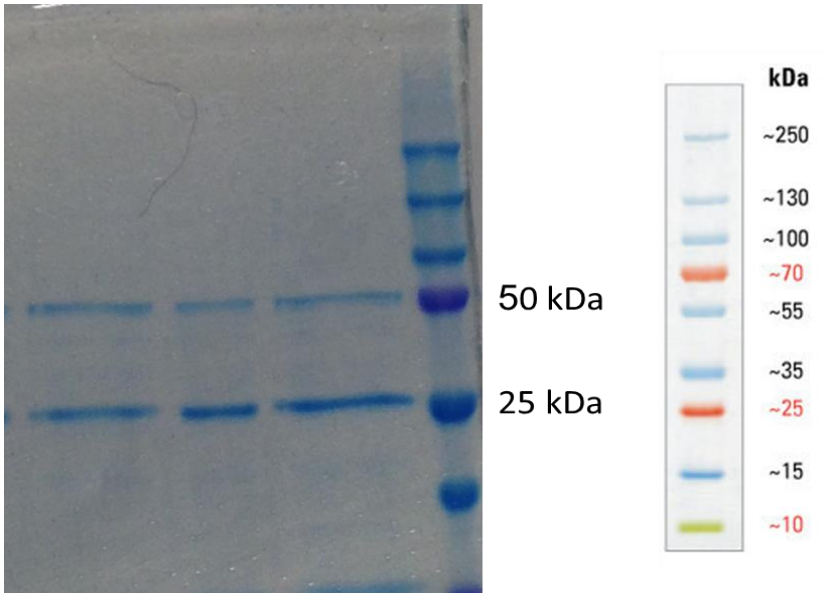

Figure 3.4 Three samples of the hybridoma culture media (RPMI) separated by SDS-page, showing the heavy chain (~50KDa) and light chains (~25KDa) of the reduced and SDS-denatured anti-Thy-1 antibody detected by Coomassie blue staining.

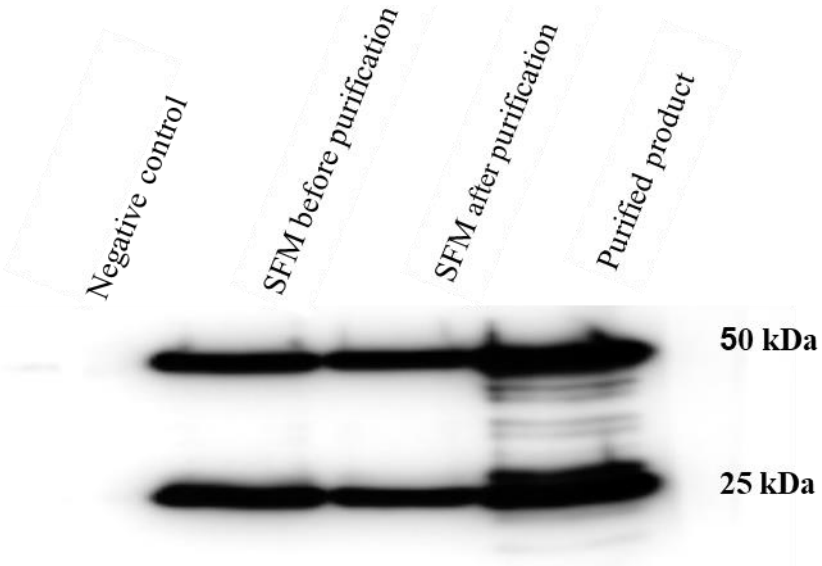

Figure 3.5 Detection of Thy-1 antibody resolved on a 10% SDS gel before Western blotting. The heavy chain (~50KDa) and light chains (~25KDa) of the denatured anti-Thy-1 antibody were detected by Western blots using HRP-goat anti-mouse IgG. (A) The lane loaded with fresh SFM medium as the negative control. (B)The lane loaded with SFM from the culture before purification. (C) The lane loaded with SFM from the culture after purification. (D)The lane loaded with the final purified product of the antibody solution.

3.3.4 MACS and the initial characterisation of the isolated cells

The para magnetic beads were used for the immunoprecipitation of the Thy-1 target cells. The process required labelling the magnetic beads with anti-Thy-1 antibody.

The labelling procedure was conducted usually by using 300μL of magnetic beads in a 1.5ml microcentrifuge tube to bind with anti-Thy-1 antibody from 500μL of anti-Thy-1 antibody solution. The final product was 300μL of Thy-1 conjugated beads. Fifty-microliter of Thy-1 conjugated beads was prepared for each adrenal gland. Primary culture of the freshly isolated adrenal gland was carried out after removing the adrenal medulla and most of the zF by adrenal gland enucleation. MACS was applied to the primary adrenal cells after one day of culture in order to isolate the cells expressing Thy-1 protein in their cell membrane.

The number of isolated cells was variable and was approximately $8\text{-}11x10^2$ from each adrenal gland. The isolated cells were then successfully cultured in the culture media. However, the Thy-1cells were slow growing cells and did not attach to the surface of the well until they spent approximately 10 days in culture.

3.3.5 Monitoring of Thy-1 cell proliferation and migration *in vitro*

The isolated cells were monitored from the first day of isolation until they had been in *in vitro* culture for 12 months. The cells were seeded at 1,000-5,000 cells/cm^2. Thy-1 positive cells spent 8-10 days floating or semi-attached to the plastic surface in culture before they fully attached. After then the attachment was relatively strong and consequently, 20-25min incubation with TrypLE was required to detach the cells from the wells. They were replenished with fresh DMEM every 2-3 weeks and passaged when they reached confluence every 5-6 weeks. The attached cells showed fibroblast cell like characteristics with cellular projections extending at certain times in column like projections. From the first month until one year in culture, the cells tended to form colonies during incubation (figure 3.6).

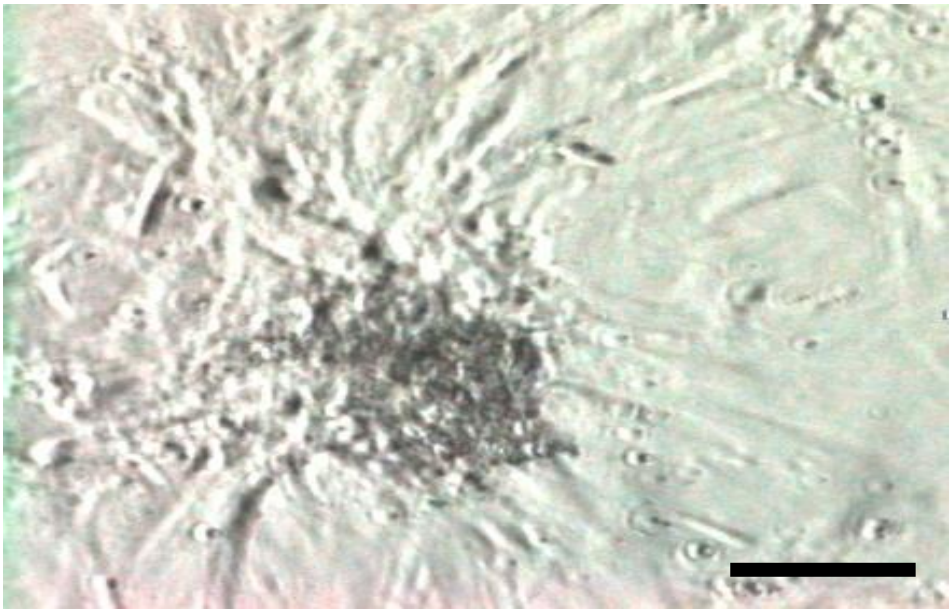

Figure 3.6 Thy-1 positive cells isolated from rat adrenal gland using MACS. The cells showed fibroblast cell like colony formation after 2months in the culture. The growing pattern of the confluent cells developed the whirlpool-like shape in culture. Scale bar 100um**.**

The morphology characteristics of the cells in culture remained relatively identical for the first 8-9 months but slight changes were recorded with time in culture, especially in the last two months *in vitro* (11-12 months). Cell size and body shape were the most changeable at that time and the vast majority of the cells became much smaller in comparison with cells of a younger age (figure 3.7). These morphological changes in Thy-1 positive cells over time might be associated with changing in these cells behavior *in vitro,* which required more investigation regarding cell proliferation and cell migration.

The cells division rates were calculated in terms of either the cell doubling time or number of days per cell cycle method. The cell division rates of the younger larger cells (2-7 months) in comparison with the older smaller cells (10-12months) were tracked in culture using time lapse. The division rate of the younger cells was slower than the older cells. In general, single cell tracking showed that cells in their 2nd month in culture, underwent division approximately every 3 days while the old cells (10-12 months) underwent division every 36-48 hours (figure 3.7). In order to study the difference in cell doubling times between cells in their 2nd month in culture and cells in their 12th month in culture, the younger cells required trypsinisation using a long incubation time (25 minutes) with TrypLE™, while the older cells required trypsinisation using a short incubation time (10 minutes) with TrypLE™.

The existence of a few large cells was recorded during the second month of cultivation (figure 3.7), these cells had the slowest proliferation and migration rate amongst the cells. Tracking these cells for over three days showed limited divisions amongst these cells at 2 months in culture and no divisions after 6 months of cultivation. However, at the age of 10 months, these cells had vanished.

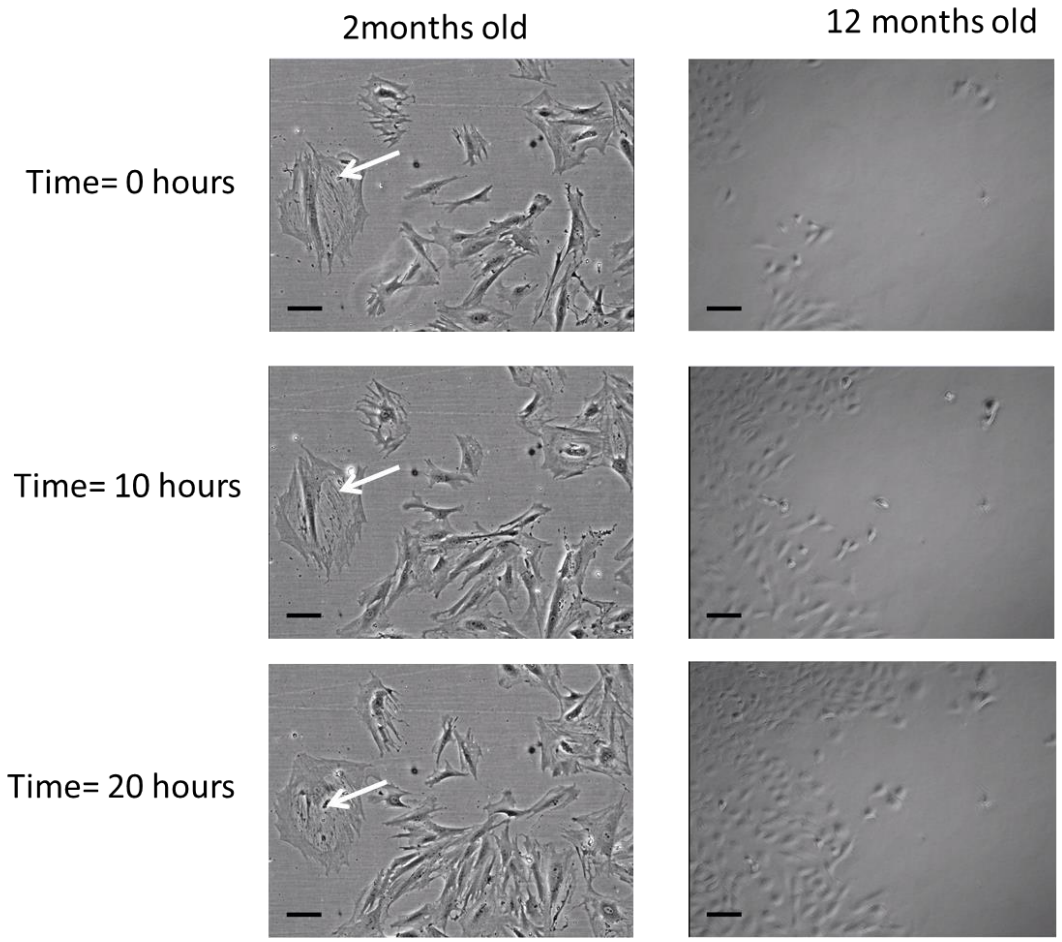

Figure 3.7 Comparison of Thy-1 positive cell proliferation between young cells (2 months in the culture) and older cells (12 months in the culture) using cell tracking assay. Cells were cultured to 30-40% confluent before cell tracking. Time lapse acquisition every 15 minutes was conducted. Proliferation of young cells was significantly less than the proliferation of the old cells. The arrow referred to the co-existence of large and slow proliferative cells with young cells. Scale bars: 50μm

The migration of the Thy-1 positive cells was tested using a wound-healing assay. A comparison between cells in their 2nd month in culture and cells in their 12th month in the culture were conducted after a long incubation time (25 minutes) with TrypLE™ for the younger cells and a short incubation time (10 minutes) with TrypLE™ for the older cells (figure 3.8). The old cells were found to migrate faster than the young cells. The wound of the old cells closed completely after 20 hours while only 53±7% of the wound closed after 20 hours for the young cells (figure 3.8). A statistic analysis of these results revealed significant ($P<0.01$) differences in wound closer between 10 and 20 hours of both groups and the older cells (12 month group) was significantly ($P<0.01$) migrating faster than the younger cells (2 month group).

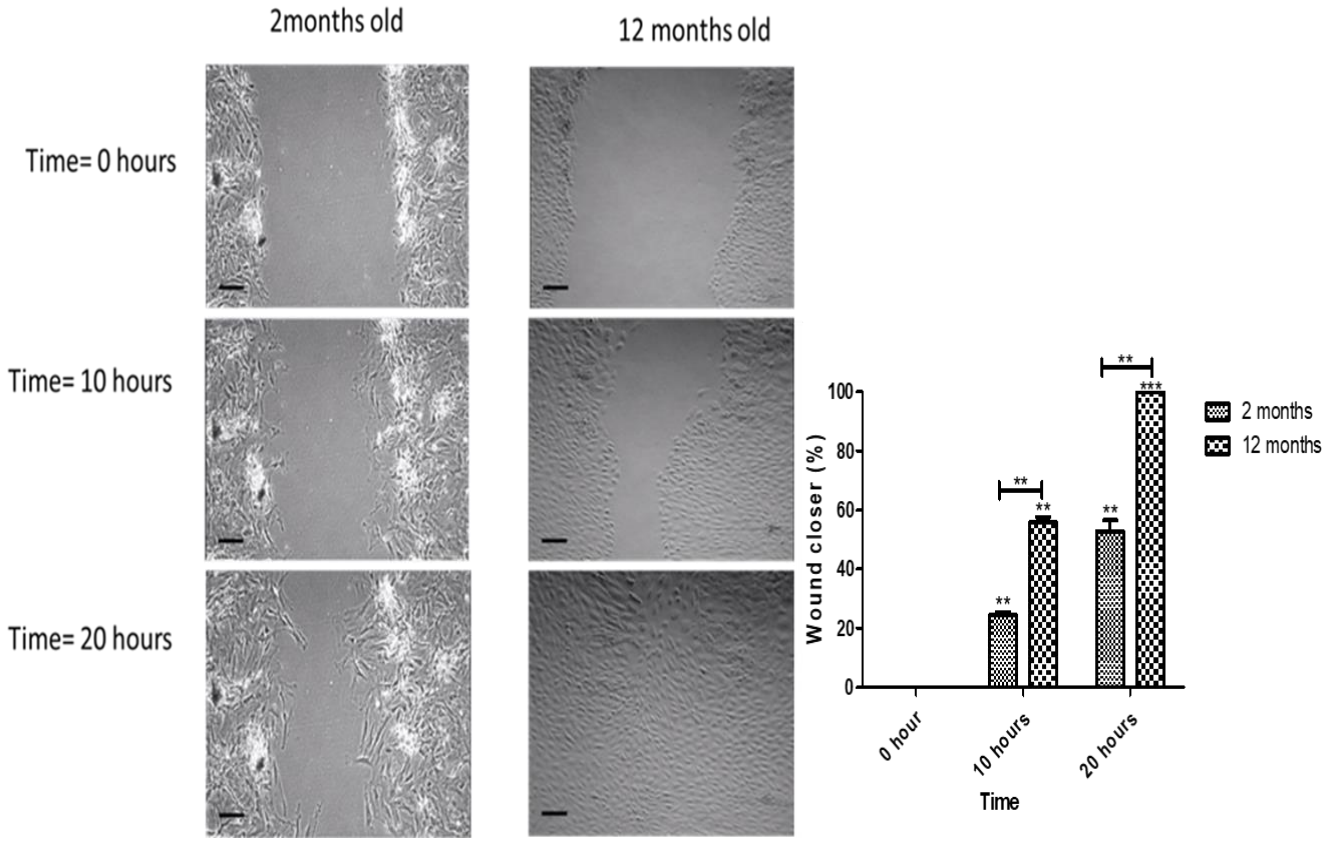

Figure 3.8 Comparison of Thy-1 positive cell migration between young cells (2 months in the culture) and old cells (12months in the culture) using wound healing assay. Cells were cultured to full confluency before scratching the wounds. Time lapse acquisition every 15 minutes was conducted. Migration of young cells was significantly less than the migration of the old cells. Independent experiments performed in triplicate. Scale bars: 50µm. Summarized one-way ANOVA results revealed significant ** ($P<0.01$) differences in wound closer between 10 and 20 hours of both groups and significant ** ($P<0.01$) differences of the 12 month group in comparison with 2 month group.

3.3.6 Characterisation of Thy-1 positive cells after two-weeks in culture

After two weeks, the putative Thy-1 positive cells were tested for Thy-1 expression using immunocytofluorescence (figure 3.9). Dual staining immunocytofluorescence assays were used to evaluate Thy-1 expression in the cells after two weeks in culture using anti-Thy-1 antibody and to test possible contamination with blood cells using anti-CD45 (blood cell marker). The results of the immunocytofluorescence showed that the vast majority of the cells were expressing Thy-1 but not CD45. This experiment therefore showed the isolated cells were not contaminated with blood cells and the majority of the cells (82±8%) were expressing Thy-1.

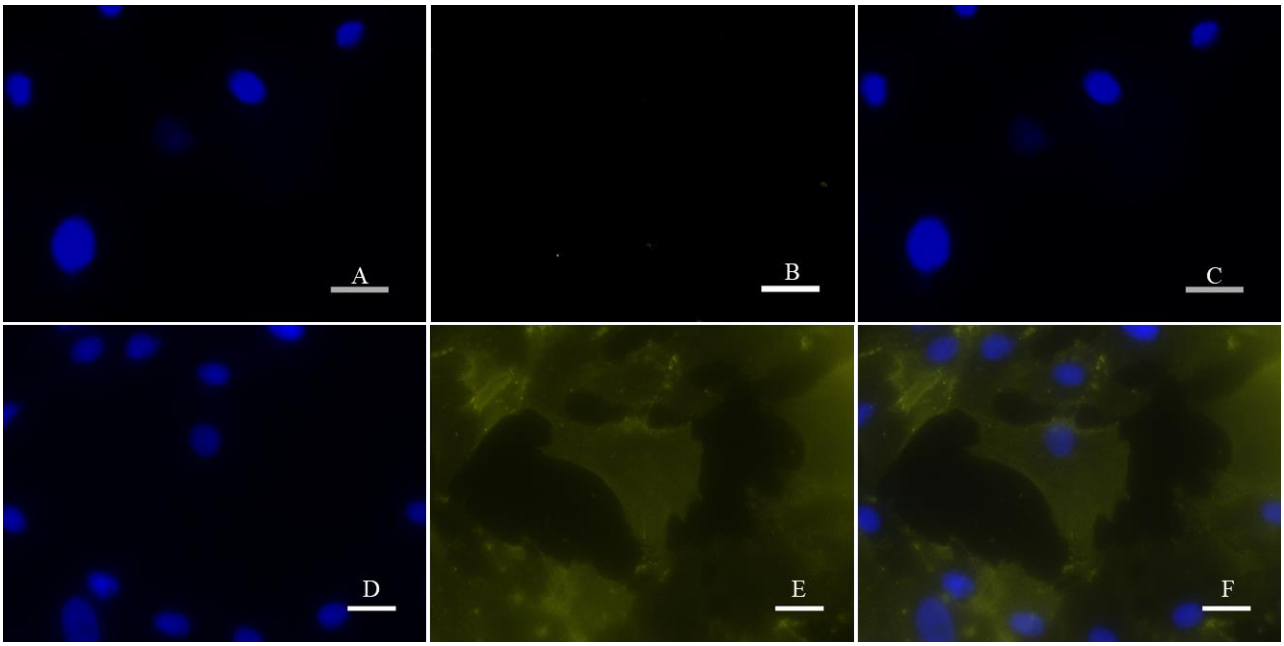

Figure 3.9 Immunocytofluorescence on 2 week old cultures of Thy-1 positive cells isolated using MACS. Cells were fixed, stained with DAPI (A, D) and incubated with either anti-CD45 antibody (Abcam) (B) or anti-Thy-1 antibody (E) before detection with anti-mouse Alexa 546 antibody. Merged images of (A) and (B) are shown in (C) and of (D) and (E) in (F). Scale bars: 20µm.

3.3.7 Characterisation of Thy-1 positive cells after eight weeks in culture

To determine if the cells retained their Thy-1 positive phenotype, eight weeks after isolation the cells were split into three groups. One group of cells was tested by immunocytofluorescence for Thy-1, to compare the expression of Thy-1 to the expression after two weeks of culture. The results (Figure 3.10) showed that after eight weeks post-MACS the Thy-1 positive cells had increased in number and had higher Thy-1 expression (detected by increased fluorescence). Whilst Thy-1 positive cells represented 82±8% of the isolated cells two weeks after MACS, at eight weeks they now represented 96±3% of the cells.

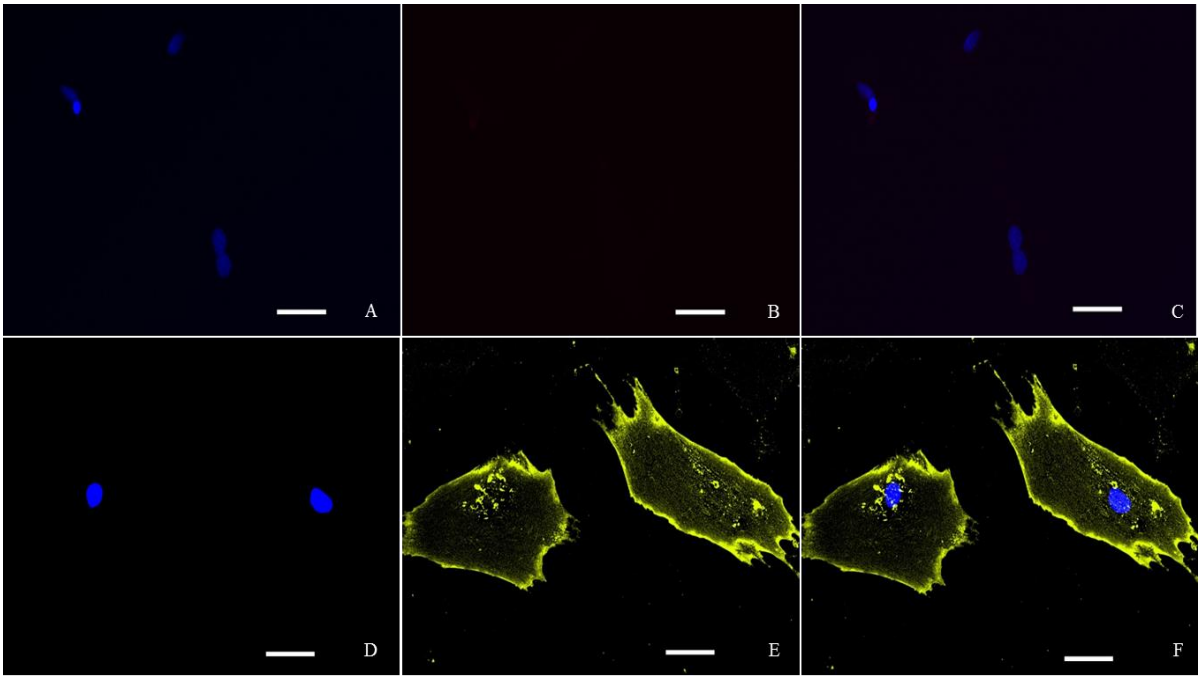

Figure 3.10 Immunocytofluorescence on 8 weeks old cultures of Thy-1 positive cells isolated using MACS. (B and E) Cells were incubated with either anti-CD45 antibody or with anti-Thy-1 antibody respectively before detection with anti-mouse Alexa 546 antibody. All samples were mounted and cell nuclei were stained with DAPI (A, D). Merged images of (A) and (B) are shown in (C) and of (D) and (E) in (F). Scale bars: 20µm.

After eight weeks post MACS, the expression of a number of different genes in the Thy-1 positive cells was evaluated (figure 3.8). This would determine if the Thy-1 positive cells were mainly differentiated cells or not, and also what other stem/progenitor cell markers they were expressing. RT-PCR was performed on RNA extracted from the Thy-1 positive cells to detect steroidogenic genes (SCC, Cyp11b2, Cyp11b1, Cyp21, 3BHSD, STAR1) and also SF1, WT1, Shh, Gli1 and TERT. The results of RT-PCR showed the expression of WT1 in addition to Thy-1 in the cDNA of the selected cells. No other steroidogenic genes or other markers in this experiment showed any product.

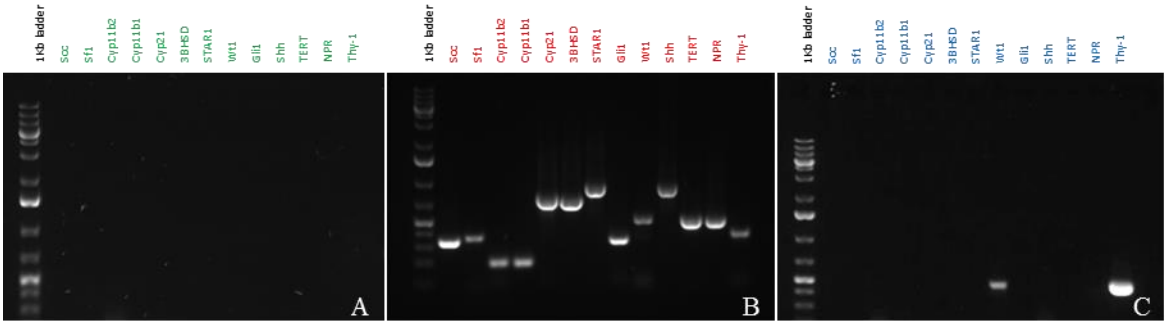

Figure 3.11 RT-PCR on RNA isolated from a 12 week culture of Thy-1 positive cells to determine the gene expression of SCC, SF1, Cyp11b2, Cyp11b1, Cyp21, 3BHSD, STAR1, WT1, Shh, Gli1, TERT, NPR, Thy-1. (A) Negative control (water template). (B) Positive control (whole adrenal cDNA). (C) Thy-1 positive cell cDNA.

3.3.8 Detection of Etv5 and ID4 stem cell markers after eight weeks in culture

Further investigations were conducted to identify the characteristics of these undifferentiated cells. The presence of Thy-1 on the cell membrane acts as a stem cell marker and as a cell surface antigen, which was a useful tool for the isolation of target cells and enabled culturing of them *in vitro* for further investigations. The expression of other stem cell markers was subsequently studied in the isolated cells. mRNA from both the stem cell markers Etv5 and ID4 was detected in the isolated cells (figure 3.12).

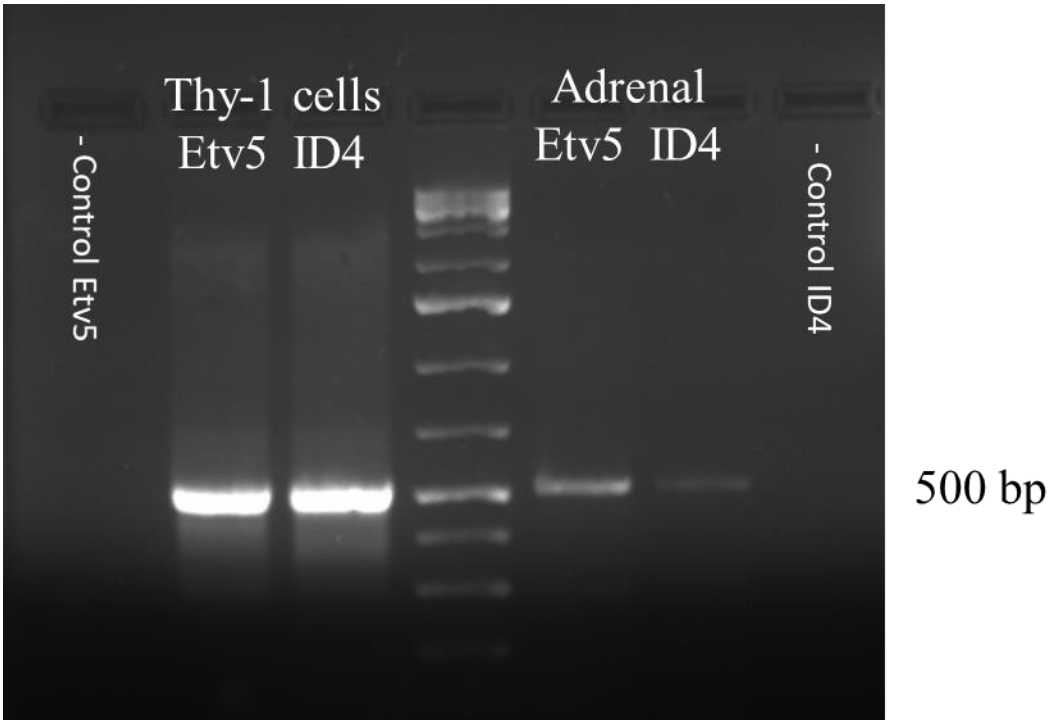

Figure 3.12 Agarose gel electrophoresis of RT-PCR products, which amplified approximatly 500bp of the stem cell markers Etv5 and ID4 in the Thy-1 positive cells using specific primers. The PCR products showed the mRNA expression of these two genes. The primers were used against a water template as negative control. The primers were used against whole adrenal cDNA as positive control.

The detection of Etv5 and ID4 mRNA expression was confirmed by immunocytofluorescence to detect their protein expression. The results showed their expression in the nucleus (figure 3.13). The majority of the cells were expressing ID4 (84 ±7%). While the expression of Etv5 was relatively lower than ID4 expression (81±6.3%). These findings were recorded when the cells were in their 8th week of *in vitro* culture.

Figure 3.13 Dual-immunocytofluorescence on 8 week old cultures of Thy-1 positive cells isolated using MACS. Cells were fixed with 4%PFA in PBS. Cells were incubated with mouse anti-CD45 antibody (Abcam) (B), mouse anti-Thy-1 antibody (F and J), control rabbit IgG (C), rabbit anti-Etv5 antibody (Abcam) (G) or with rabbit anti-ID4 antibody (Abcam) (K) before detection with anti-mouse Alexa 488 and anti-rabbit Alexa647. All samples were mounted and cell nuclei were stained with DAPI in (A, E and I). Merged images of (A), (B) and (C) are shown in (D) and of (E), (F) and (G) in (H), and (I), (J) and (K) in (L). The arrows in (G and J) refer to the location of Etv5 and ID4 expression in the nucleus, respectively. Scale bars: 20µm.

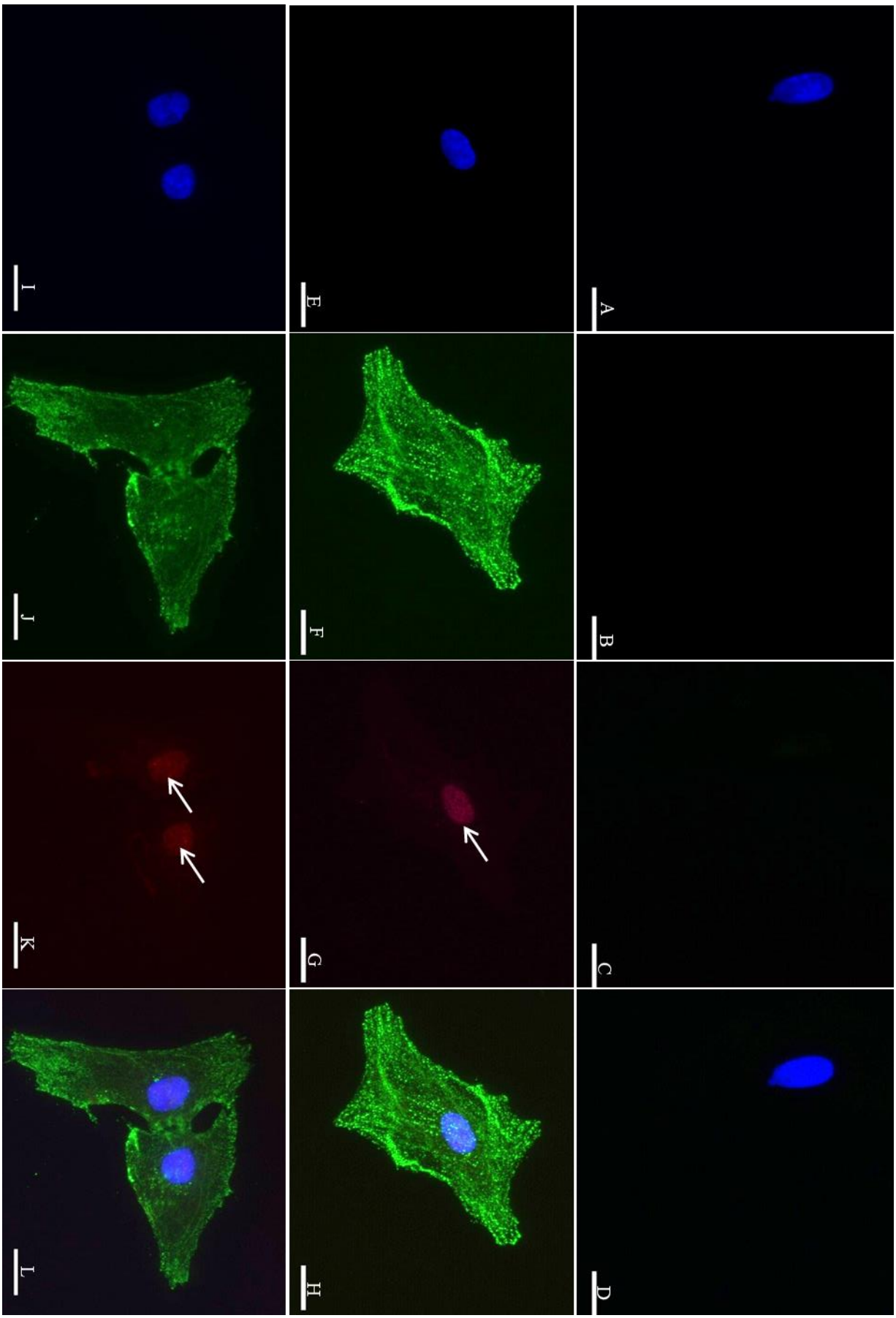
A
B
C
D
E
F
G
H
I
J
K
L

3.3.9 Characterisation of Thy-1 positive cells after twelve weeks in culture

Twelve weeks after isolation, immunocytofluorescence was used to confirm the expression of WT1 gene as it was shown in the RT-PCR results that were obtained from the Thy-1 positive cells after eight weeks in culture (figure 3.11).

The expression of WT1 was suggested as a stem cell maintenance factor of the undifferentiated adrenal-gonadal primordium. WT1 is a marker related to the mesenchymal origin of the adrenal capsule, which in turn represents the layer where adrenocortical stem cell niche would be, while Sf1 is a nuclear receptor and key regulator for steroidogenic enzymes (Val et al., 2007).

During development of adrenal gland, the WT1 positive cells give rise to cells which are WT1 negative but Sf1 positive that are characterised as progenitor/differentiated cells (Bandiera et al., 2013). Therefore, the co-expression of Thy-1 with the WT1 protein would potentially represent stem cells and the co-expression of Thy-1 with the Sf1 protein would potentially represent progenitor/differentiated cells. The differences of the co-expression ratios of each (Thy-1 with WT1 or Thy-1 with Sf1) would potentially suggest the ratio of stem cells (Thy-1 with WT1) against the ratio of progenitor/differentiated cells (Thy-1 with Sf1). These calculations would suggest Thy-1 positive cells were more likely to maintain the stemness state or they were more likely to be differentiating to progenitor/differentiated cells during cultivation *in vitro*.

Characterisation of Thy-1 positive cells after twelve weeks in culture included dual stain immunocytofluorescence, which was conducted to examine WT1 and Thy-1 protein expression and dual stain immunocytofluorescence was also used to examine Sf1 and Thy-1 protein expression. The results showed increased Thy-1 expression with 97± 1 % (in comparison with 82±8% during of the eight weeks immunocytofluorescence test) of the total cells now positive

for Thy-1, with Thy-1 mainly being observed in the cell membrane and in the endoplasmic reticulum (ER) (figure 3.14). The expression of WT1 was observed in 90± 2% of the Thy-1 positive cells, with expression localised in the nucleus and/or in the cytoplasm since the nature of WT1 protein is to shuttle between the two, however, the intensity of expression did vary between cells (figure 3.14). While only 1 ± 1% of the cells were expressing Sf1, which was mainly detected in the nucleus (figure 3.14).

Figure 3.14 Dual-staining immunocytofluorescence on three month old cultures of Thy-1 positive cells isolated using MACS. Cells were fixed with 4%PFA in PBS. (B) Cells were incubated with anti-CD45 antibody. (F and J) Cells were incubated with anti-Thy-1 antibody. (C, G or K) Cells were incubated with control rabbit IgG, anti-SF1 antibody or with anti-WT1 antibody (Abcam) before detection with anti-mouse Alexa 647 in (B, F and J) and with anti-rabbit Alexa546 in (C, G and K). All samples were mounted and cell nuclei were stained with DAPI in (A, E and I). Merged images of (A), (B) and (C) are shown in (D) and of (E), (F) and (G) in (H), and (I), (J) and (K) in (L). Arrows refer to Sf1 single cell expression. Scale bars: 20µm.

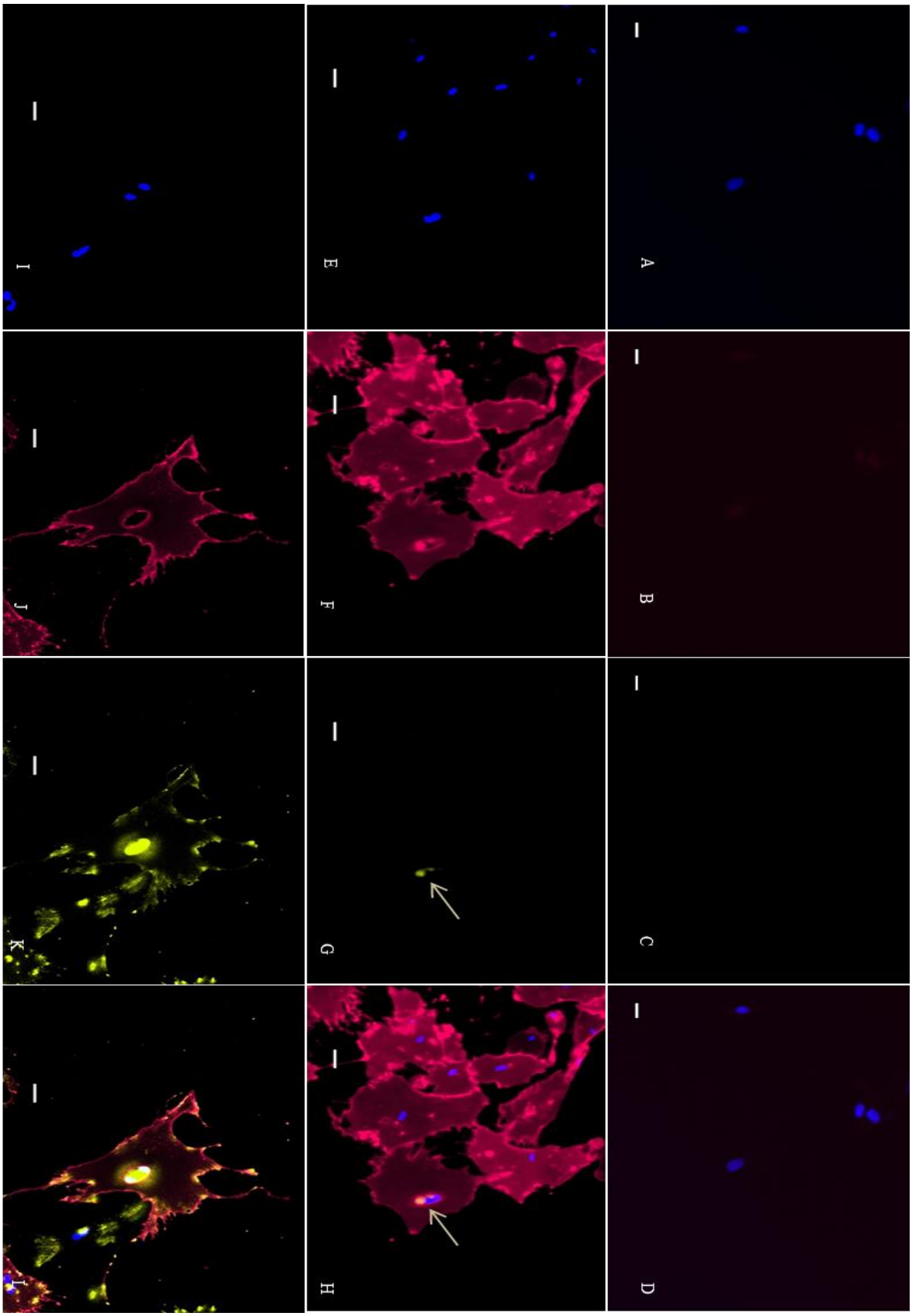
A
B
C
D
E
F
G
H
I
J
K
L

The high expression (90± 2%) of WT1 with Thy-1, led to an investigation of how the two proteins co-localised in the adrenal gland.

Immunohistotofluorescence assays were conducted to reveal the co-expression of both WT1 and Sf1 with Thy-1 in the capsule and sub-capsular areas of the adrenal gland (figure 3.15). The images were analysed by Spearman's rank correlation value using the Image J (Fiji) software. The co-expression of WT1 with Thy-1 in the capsule and sub-capsular areas was high (0.59±0.052), while the co-expression of Sf1 with Thy-1 was low (0.23±0.11).

Figure 3.15 Dual-staining immunohistofluorescence on rat adrenal gland cryosections. Adrenal gland sections were fixed with ice-cold acetone. (B) Adrenal sections were incubated with mouse IgG. (F and J) Adrenal sections were incubated with anti-Thy-1 antibody. (C, G or K) Adrenal sections were incubated with control rabbit IgG, anti-SF1 antibody or with anti-WT1 antibody (Abcam) before detection with secondary anti-mouse Alexa 647 in (B, F and J) and with anti-rabbit Alexa 546 in (C, G and K). All sections were mounted and cell nuclei were stained with DAPI in (A, E and I). Merged images of (A), (B) and (C) are shown in (D) and of (E), (F) and (G) in (H), and (I), (J) and (K) in (L). Scale bars: 50µm.

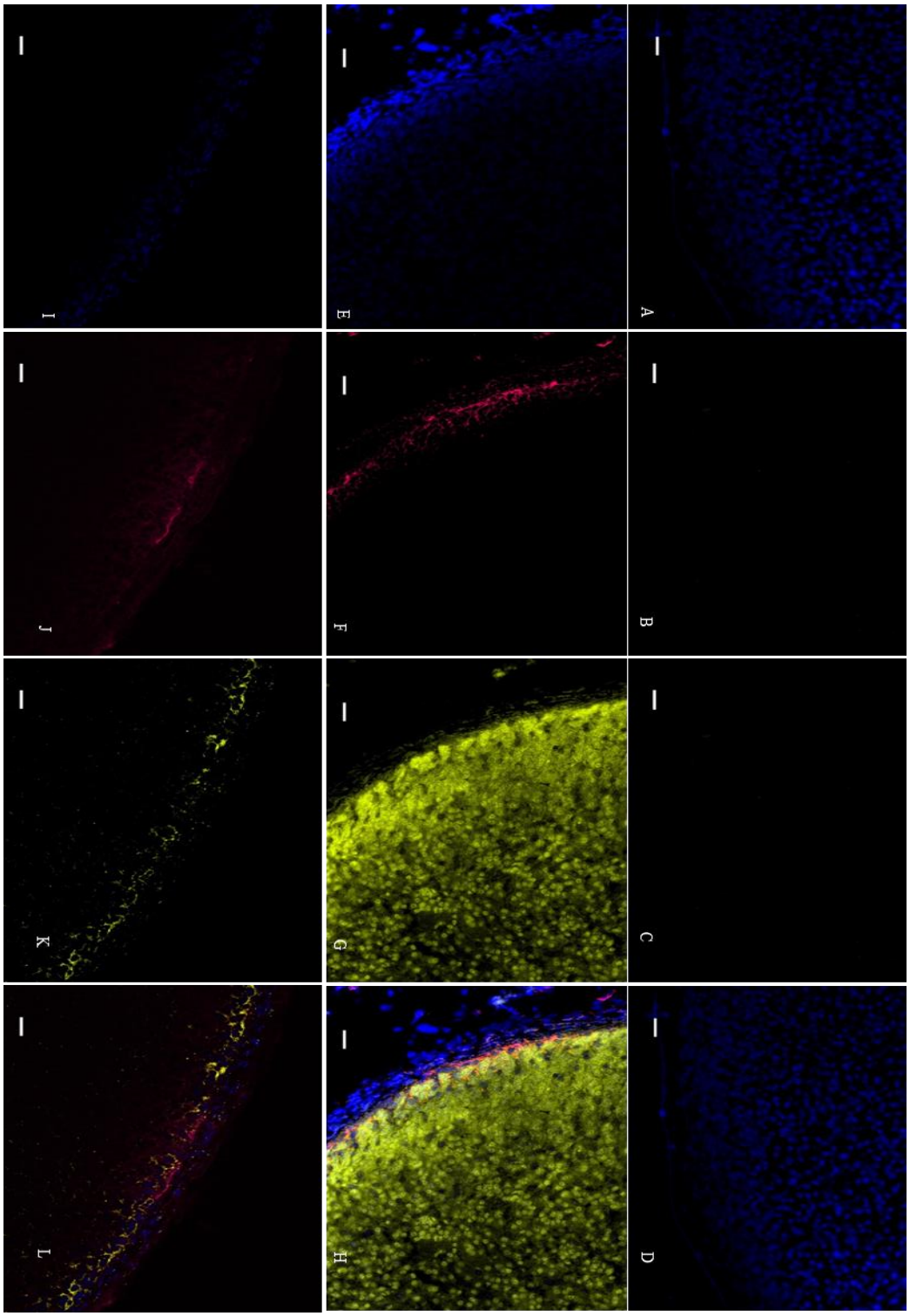
A
B
C
D
E
F
G
H
I
J
K
L

3.3.10 Immunocytofluorescence detection of Thy-1, WT1, Etv5 and ID4 after 10 months of culture.

The Thy-1cells were tested by immunocytofluorescence during the early periods of culture (2 weeks,8weeks and 12weeks) to investigate the expression patterns and specifically the changes in the expression of the proteins of interest because the cells were transferred to different microenvironment. These tests ran in parallel with RT-PCR experiment to continue monitoring the changes in the Thy-1 positive cells. The phenotype of the cells, proliferation rate and the expression pattern of the markers of interest was relatively unchanged from the early stages (after 8 weeks or 12 weeks of cultivation) as described earlier. Cell changes were noticed in the general cell shape and in the proliferation rate during their 9^{th} month in culture. These changes imply alteration in the expression of the stem cell markers such as the proteins of interest Thy-1, WT1, Etv5 and ID4.

The immunocytofluorescence test of the cells in their 10^{th} month in culture showed changes in the expression of the proteins of interest in comparison with young cells (2-3 months old in culture). Each dual staining included the test of Thy-1 expression co-localised with WT1, Etv5, ID4 or Sf1 protein expression. Random spots of different slides were used to calculate the ratios of the cells that expressed the protein of interest by counting the number of cells that expressed the protein of interest among the total number of cells, as calculated from the number of nuclei as visualised by DAPI stain.

In general, the expression level of all genes of interest decreased in the old cells. However, the expression of Thy-1 had the largest decrease of the others. WT1 expression decreased from

90±2% in the young cells to 68±15% in the old cells (figure 3.16). The expression of Etv5 underwent the smallest decrease amongst the other markers, with Etv5 expression being 71±16% in the young cells and was reduced to 62±18% (figure 3.17). ID4 protein expression decreased from 74 ±17 in the young cells to 46±23% in the old cells (figure 3.18). Sf1 expression was not detected in the old cells (figure 3.19).

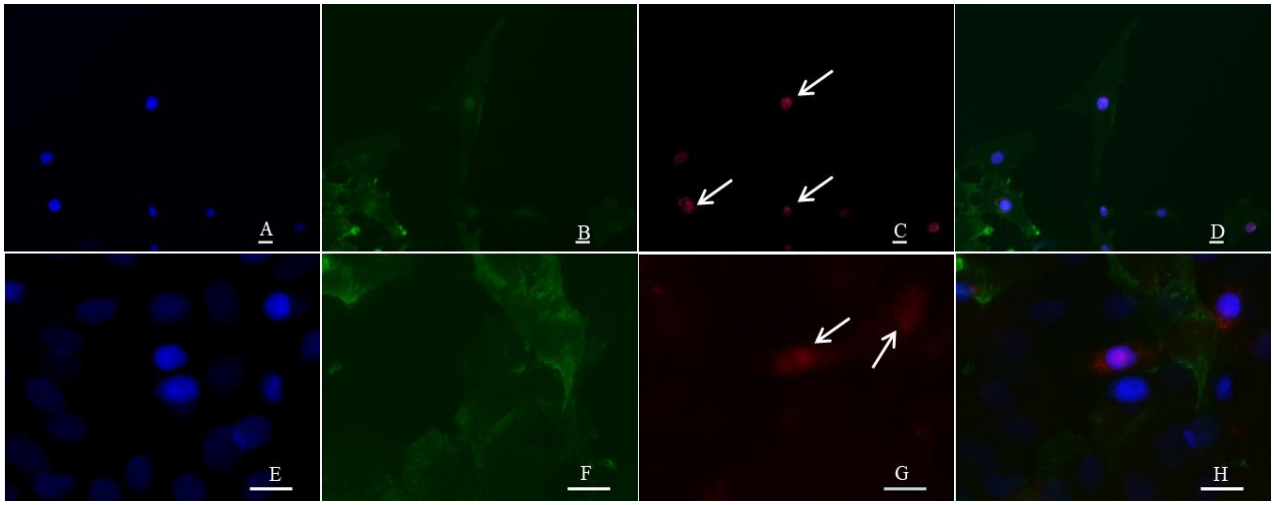

Figure 3.16 Dual-Immunocytofluorescence on 10 month old cultures of Thy-1 positive cells isolated using MACS. Cells were fixed with 4%PFA in PBS. Cells were incubated with mouse anti-Thy-1 antibody (B and F), or incubated Alexa 647. All samples were mounted and cell nuclei were stained with DAPI in (A and E). Merged images of (A), (B) and (C) are shown in (D) and of (E), (F) and (G) in (H). The upper row of photos are low magnification (A, B, C and D). The lower row of photos are high magnification (E, F, G and H). Arrows refer to the WT1 expression in the nucleus and in the cytoplasm of the cells. Scale bars: 20µm.

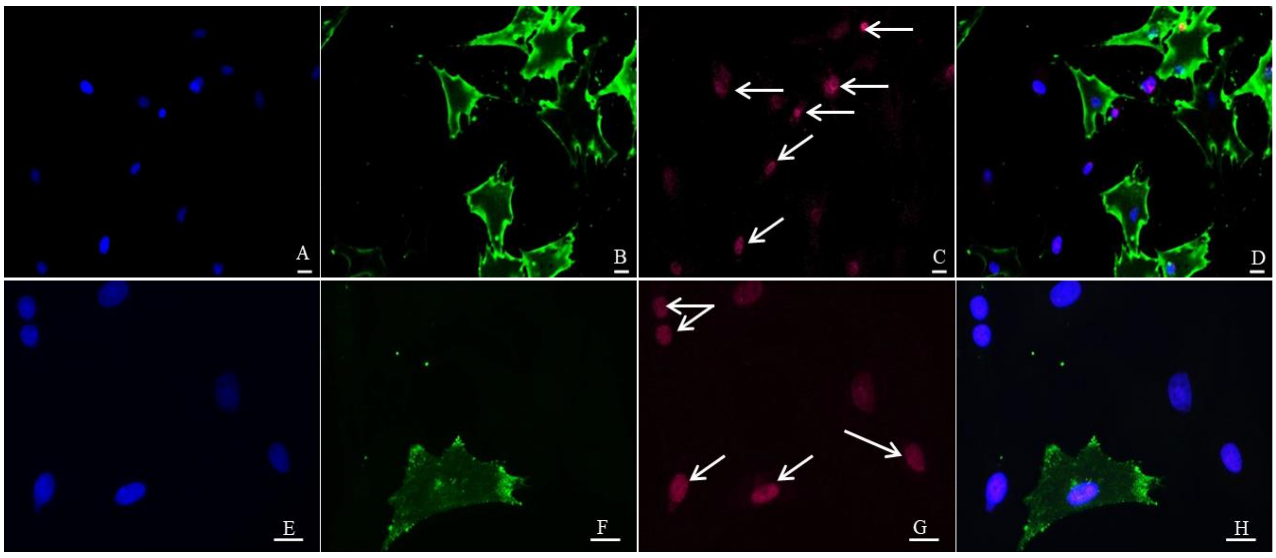

Figure 3.17 Dual-Immunocytofluorescence on 10 month old cultures of Thy-1 positive cells isolated using MACS. Cells were fixed with 4%PFA in PBS. Cells were incubated with mouse anti-Thy-1 antibody (B and F), or incubated with a rabbit anti-Etv5 antibody (Abcam) (C and G) before detection with anti-mouse Alexa 488 and anti-rabbit Alexa 647. All samples were mounted and cell nuclei were stained with DAPI in (A and E). Merged images of (A), (B) and (C) are shown in (D) and of (E), (F) and (G) in (H). The upper row of photos are low magnification (A, B, C and D). The lower row of photos are high magnification (E, F, G and H). Arrows refer to the Etv5 expression in the nucleus of the cells. Scale bars: 20µm.

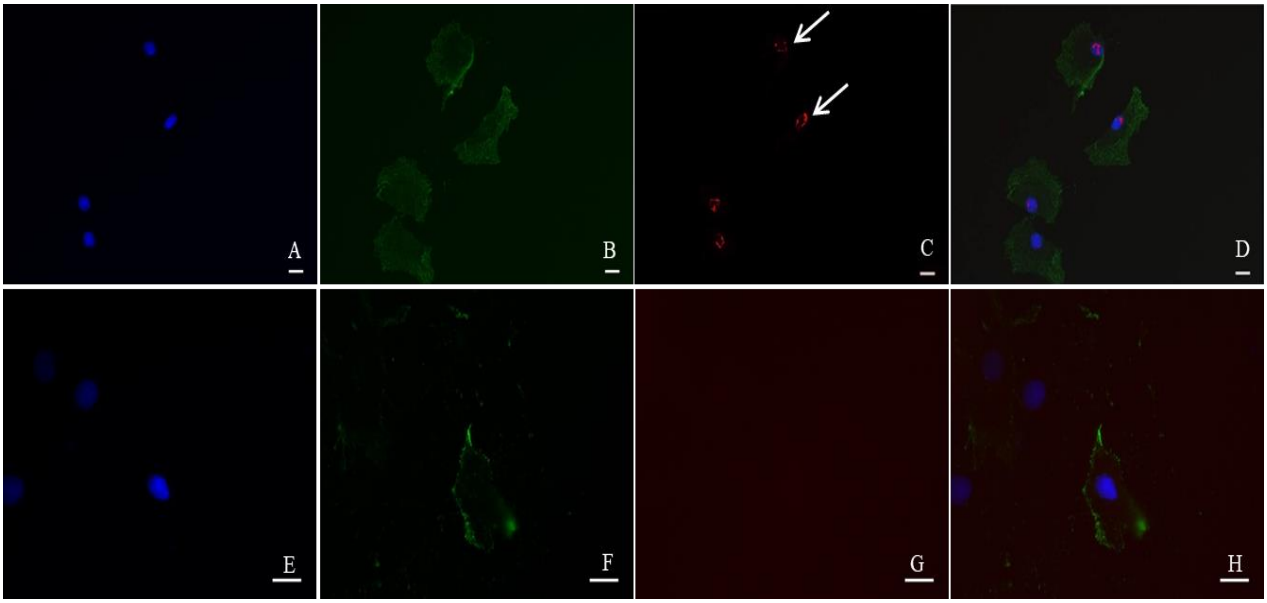

Figure 3.18 Dual-Immunocytofluorescence on 10 month old cultures of Thy-1 positive cells isolated using MACS. Cells were fixed with 4%PFA in PBS. Cells were incubated with mouse anti-Thy-1 antibody (B and F), or incubated with a rabbit anti-ID4 antibody (Abcam) (C and G) before detection with anti-mouse Alexa 488 and anti-rabbit Alexa 647. All samples were mounted and cell nuclei were stained with DAPI in (A and E). Merged images of (A), (B) and (C) are shown in (D) and of (E), (F) and (G) in (H). The upper row of photos are low magnification (A, B, C and D). The lower row of photos are high magnification (E, F, G and H). Arrows refer to the ID4 expression in the nucleus of the cells. Scale bars: 20µm.

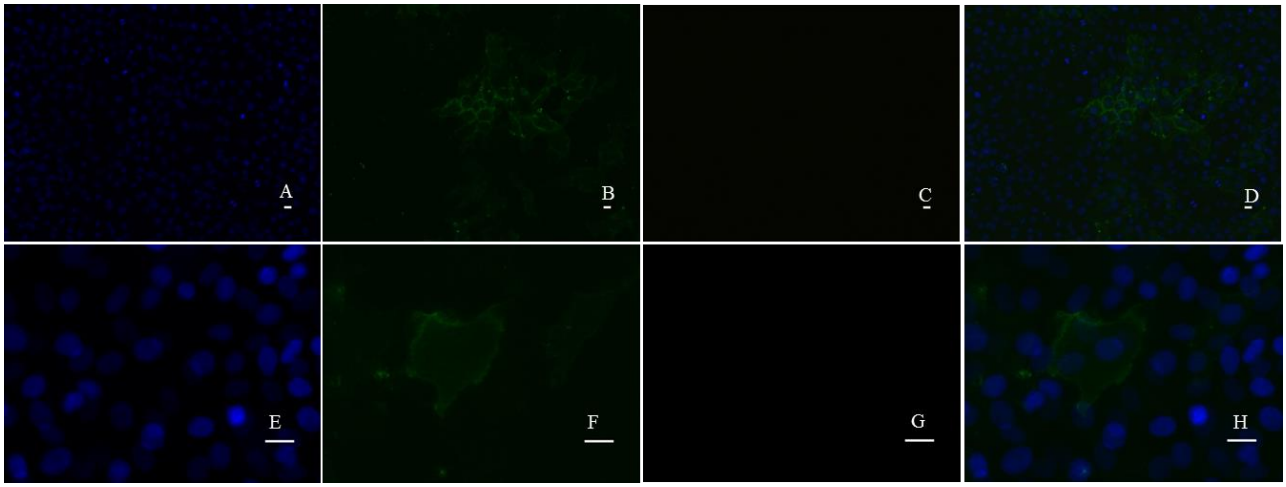

Figure 3.19 Dual-Immunocytofluorescence on 10 month old cultures of Thy-1 positive cells isolated using MACS. Cells were fixed with 4%PFA in PBS. Cells were incubated with mouse anti-Thy-1 antibody (B and F), or incubated with a rabbit anti-Sf1 antibody (Abcam) (C and G) before detection with anti-mouse Alexa 488 and anti-rabbit Alexa 647. All samples were mounted and cell nuclei were stained with DAPI in (A and E). Merged images of (A), (B) and (C) are shown in (D) and of (E), (F) and (G) in (H). The upper row of photos are low magnification (A, B, C and D). The lower row of photos are high magnification (E, F, G and H). The Sf1 expression was not detected in the cells. Scale bars: 20µm.

3.3.11 Characterisation of Thy-1 positive cells after one year in culture

Immunocytofluorescent assays were conducted to reveal the expression pattern of Thy-1 protein in and around the cell colony of old cells (1-year old). The results showed the fibroblast-like cells in and around the centre of the colony were expressing Thy-1, while cells far from the colony centre were lacking Thy-1 expression (figure 3.20).

The time lapse assays of the live cells showed that the smaller and far from the colony centre cells were propagating faster but they attached less to the plastic surface of the well. The reduction in cell attachment capacity in the old cells was associated with the reduction of Thy-1 expression in the cells of that age (figure 3.20). The general reduction of Thy-1 expression in old cells in comparison with younger cells was confirmed using Western blotting. Although Thy-1 expression increased in the cultured cells with time, its expression clearly reduced after 11 months in the culture (figure 3.21). These changes in Thy-1 expression over the time was statistically analysed and revealed that Thy-1 protein expression showed significant ($P<0.05$) increase from one month to six months in vitro. However the reduction in Thy-1 expression after 11 months was not significant ($P \geq 0.05$).

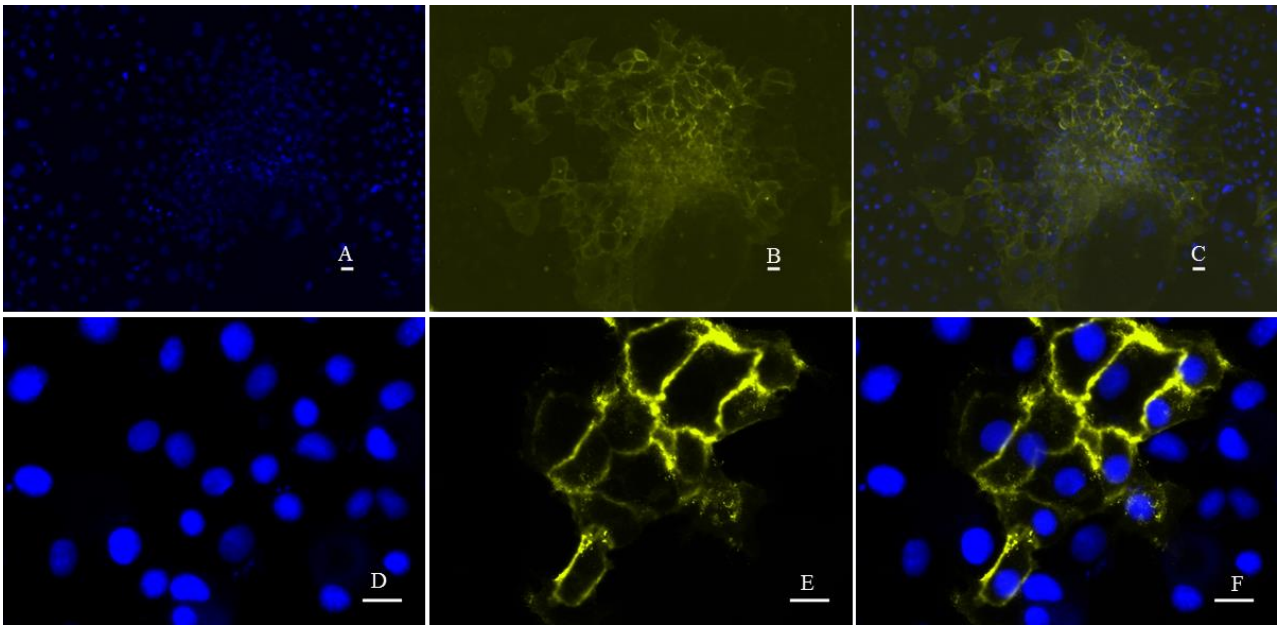

Figure 3.20 Immunocytofluorescence on 12 months old colony cultures of Thy-1 positive cells. Cells were fixed with 4%PFA in PBS. Cells were incubated with anti-Thy-1 antibody (B) before detection with anti-mouse Alexa 546. Merged images of (A) and (B) are shown in (C) and of (D) and (E) in (F). The expression of the Thy-1 protein was mainly located in the cells in and around the colony centre. While the cells growing far from the colony centre lost Thy-1 expression. The upper row of photos are low magnification (A, B and C). The lower row of photos are high magnification (D, E and F). All samples were mounted and cell nuclei were stained with DAPI (A). Merged images of (A) and (B) are shown in (C) and of (D) and (E) in (F). Scale bars: 20µm.

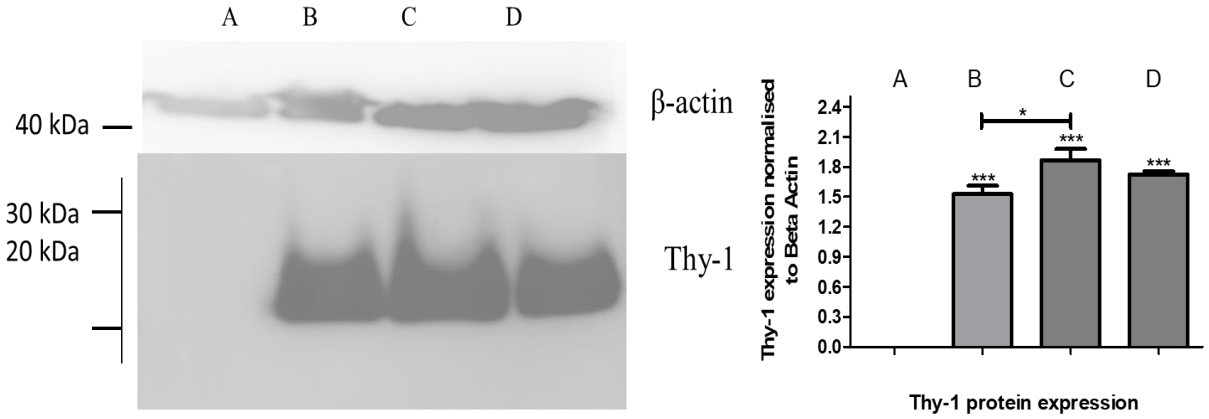

Figure 3.21. Detection of β actin and Thy-1 protein expression in Thy-1 positive cells using Western blotting after different periods of times *in vitro*. (A) Thy-1 negative cells collected directly after MACS. (B) Thy-1 positive cells collected after 1month *in vitro*. (C) Thy-1 positive cells collected after 6months *in vitro*. (D) Thy-1 positive cells collected after 11months *in vitro*. Cells were counted before lysis with RIPA buffer in the presence of Protease Inhibiter Cocktail (1:200). Proteins were resolved on a 10% SDS gel before Western blotting with mouse anti-Thy-1 antibody (1:1000). The graph shows the Western blotting analysis of Thy-1 expression levels normalised to the expression levels of the housekeeping protein (β Actin). Summarized one-way ANOVA results showed Thy-1 protein expression in Thy-1 positive cells was significant ($P<0.001$) in comparison with Thy-1 negative cells and a significant ($P<0.05$) differences in Thy-1 protein expression between the one month old Thy-1 positive cells and 6months old ones *in vitro*.

The results of this chapter described the isolation of potential adrenocortical stem cells using a specific marker. The characteristics of these cells (Thy-1 positive cells) in the early months in culture after MACS (younger cells) were different from Thy-1 positive cells in the later months in culture after MACS (older cells). However, these relative differences can be summarised in (table 3.2).

Table 3.2 Summary of the relative differences of the studied parameters in the young and old Thy-1 positive cells. Thy-1 expression was high in the young cells and it was increasing, but its expression deteriorated in the older cells. Young and old Thy-1 positive cells were negative to CD45 and steroidogenic genes. Stem cells markers such as WT1, Etv5 and ID4 were found to be expressed in the Thy-1 positive cells. However, their expressions were decreased in the old cells. Sf1 expression was already weak in the young cells and disappeared in the old cells. Cell proliferation and migration were slower in the young cells in comparison with the old cells. Senescent cells were detected among the young cells but not among the old cells.

Parameter	**Young Thy-1 positive cells (2-3 months)**	**Old Thy-1 positive cells (10-12 months)**
Thy-1	Highly expressed with increasing expression	Highly expressed with decreasing expression
CD45	No	No
WT1	Yes	Yes, but decreased
Etv5	Yes	Yes, but decreased
ID4	Yes	Yes, but decreased
Sf1	Weak 1%	No
Steroidogenic genes	No	No
Cell division Doubling time	Longer time for one division (3 days)	Shorter time for one division (36-48 hours)
Cell migration	Slower	Faster
Senescent cells	Few cells present	No

3.3 Discussion

The isolation and investigation of Thy-1 positive cells *in vitro* culture created an effective approach involving primary culture to investigate the cellular and molecular mechanisms controlling the cell behaviour, because it is difficult to explore specific cell behaviour *in vivo*. Adrenal gland primary culture was accomplished using mechanical and enzymatic digestion, this yielded viable primary cells. The hormonal response of the isolated cells to the ACTH treatment was another indicator of the cells interaction with their *in vitro* environment and it was generally in agreement with similar tests (Lefrancois-Martinez et al., 2011). Growing of the hybridoma cells, and inducing them to produce a monoclonal anti-Thy-1 antibody was also successful and confirmed using SDS-PAGE electrophoresis with Coomassie Blue staining (figure 3.4) and Western blotting (figure 3.5). The binding capacity and specificity of the anti-Thy-1 antibody was validated by immunocytofluorescence tests (figure 3.9), immunohistofluorescence tests (figure 3.15) and Western blotting (figure 3.21). The large-scale production of this antibody was important to produce the large quantities that were needed to conduct the later experiments. Further adrenal gland primary cultures were conducted after removing the medulla to eliminate the un-targeted part of adrenal gland because our findings suggested the isolation of the target cells after enucleating and discarding of the medulla and most of the zF, instead of using the whole adrenal would be more specific. This would eliminate most of the differentiated cells of the cortex as well as the medulla, which might contain their own stem cells. However, the zI was not the main target of this study since Thy-1 expression was confined only to the capsule and sub-capsular areas.

The binding of the anti-Thy-1 antibody to magnetic beads was successful and the antibody-magnetic beads complex was successfully applied to the primary cells and achieved isolation of

the targeted cells. The isolated cells were seeded at low densities as recommended for seeding mesenchymal stem cells (Mareschi et al., 2012) which allowed successful maintenance of the culture for over a year.

The phenotype of the isolated cells could be described as fibroblastic-like cells, which traditionally represent the capsular cells that are described as fibroblast-like capsular cells (Kim and Hammer, 2007a). The cells use to have long thin cytoplasmic extensions called telopods or projections, early histological studies proposed that these projections from the capsule cells might have a role in forming differentiated cells of the adrenal cortex (Baker, 1952). The cells attached to the plastic and they tended to form colonies and these general aspects are also what was originally used to characterise mesenchymal stem cells *in vitro* (Castro-Malaspina et al., 1980, Colter et al., 2001). The confluent cells developed a whirlpool-like shape growing patern in culture, which is in agreement with what has been described in the placental MSCs (Pelekanos et al., 2016).

During the long-term culture (up to one year), Thy-1 positive cells exhibited morphological and cellular behaviour changes. For example, the proliferation rate of the younger cells was slower than the older cells and the younger cells were more attached to the plastic surface and required trypsinisation for a long incubation time (25 minutes) with TrypLE™ to detach them in comparison with the older cells, which required a short incubation time (10 minutes) with TrypLE™ to be detached.

These changes were noticed during routine monitoring work such as changing the media and splitting after reaching confluency. These changes required more investigation to study the changes in cell cycle, cell migration and the expression of proteins of interest.

In order to determine the differences of cell division rates between the younger cells and the older cells, cells divisions rates were tracked in culture using time lapse and calculated in term of cell doubling time.

The single cell tracking assay showed that cells in their 2nd month in culture underwent division approximately every 3 days (younger Thy-1 positive cells showed 10-12% cell division every 24 hours). While the old cells (10-12 months) underwent division every 36-48 hours (older Thy-1 positive cells showed 30-46% cell division every 24 hours). The literature referred to a proliferation rate of rat adrenal gland primary cell culture of 10% after 21 days of cultivation. Then it was reduced to 1% after 100 days of cultivation (Arola et al., 1993). These results suggested Thy-1 positive cells were more constant and can survive longer *in vitro* in comparison to the whole adrenal primary culture which tends to lose its survival ability after 100 days *in vitro*.

Time lapse techinque was also used to test the cell migration changes of Thy-1 positive cells using a wound-healing assay (figure 3.8). The older cells (12^{th} months old in the culture) were significantly ($P<0.01$) migrating faster than younger cells (2^{nd} months old in culture).

Although the co-existence of large fibroblast-like cells was recorded in the primary culture of the rat adrenal gland (Guo and Liu, 2005), the co-existence of a few large slow/non-proliferative fibroblast-like cells within Thy-1 positive cells after the second month of cultivation (figure 3.7) might represent senescent cells. These cells died after few months of cultivation potentially due to reaching the Hayflick limit (Hayflick and Moorhead, 1961). Although, others suggested the decline in the senescent cell divisions might be observed after 8 doublings times in culture, it also might have randomly occurred (Rubin, 2002).

Investigating these few cells within the cells of interest revealed their common traits, which were the same as what had been recorded for senescent MSCs. These characteristics included morphological changes and reduction in both proliferation and differentiation potential (Zhu et al., 2015). This phenomenon is usually related to the age of the organism at the time of isolation (Yegorov and Zelenin, 2003). Although the presence of the senescent cells within the stem cells reduced the potential value of the stem cells, senescent cells have been recorded to accompany even the most potent stem cells such as human embryonic cells (Munoz-Espin et al., 2013) and mouse embryonic cells (Storer et al., 2013). Senescence has also been found to have a role contributing to the embryonic development, growth and cell patterning (Storer et al., 2013).

Thy-1 increased in expression after cultivation (figure 3.21), which increased in parallel with the ability of cells to attach to plastic and this ability decreased when Thy-1 expression decreased in the old cells, which was in agreement with the role of Thy-1 in cell adhesion (Rege and Hagood, 2006). As previously mentioned, the Thy-1 positive cells maintained a regular proliferation rate for more than six months in culture (10-12 % every 24 hours). However, the proliferation rate of the old cells increased in the last four months of cultivation. This rate increased to 20% in the old cells that lost their Thy-1 expression which was in agreement with the suggestion from (Mayani and Lansdorp, 1994) that Thy-1 acts as a proliferation inhibitor of the primitive cord blood stem/progenitor cells.

The survival capacity of the Thy-1cells *in vitro* for more than one year suggested a possible role of Thy-1 in self-renewal regulation that allows maintenance of these cells and other stem cells types for long periods *in vitro* in comparison with the differentiated cells (Ishigaki et al., 2009, Bernardo et al., 2007).

The expression of Thy-1 was confirmed by immunocytofluorescence using an anti-Thy-1 antibody and anti-CD45 antibody as a control after 2 weeks of culture. The results of the immunocytofluorescence against CD45 were negative, which meant that there was no contamination with blood cells, as this CD45 marker is well documented as a progenitor/adult blood cell marker (Shim et al., 2015). This was important because the presence of such blood cells might interfere with isolation of the target cells since they express Thy-1 as well. After eight weeks post-MACS, the immunocytofluorescence against Thy-1 revealed that it was still being expressed (figure 3.10). The immunocytofluorescence against Thy-1 also showed that the ratio of the number of cells that expressed Thy-1 was higher in comparison to the results of the first (two weeks post-MACS) immunocytofluorescence test, and the intensity of Thy-1 expression within the cells after eight weeks post-MACS was also higher than the first immunocytofluorescence test (two weeks post-MACS). This increase in the Thy-1 expression was confirmed by Western blotting (figure 3.21) and seemed to be maintained for a few months. This increase in Thy-1 expression after cultivation was in agreement with the results from RT-qPCR in human mesenchymal stem cells (Dudakovic et al., 2014).

The RT-PCR experiments showed the cells were mainly undifferentiated cells (figure 3.11), since none of the steroidogenic genes were detected. However the detection of a few cells expressing Sf1 that were conversely steroidogenically negative might represent the progenitors cells (Kim and Hammer, 2007b). However, These RT-PCR experiments showed the expression of other stem cell markers such as WT1, Etv5 and ID4 (figure 3.11 and figure 3.12).

The finding of WT1 expression in the isolated cells using RT-PCR was confirmed by immunocytofluorescent assay. The expression of WT1 in the adrenocortical stem cells was expected because it was described as an important protein in the embryonic

development of adrenal glands because WT1 knock-out mice die at embryonic day E13.5 due to deadly defects in their urogenital system (Moore et al., 1999). It was also proposed as a factor maintaining the undifferentiated adrenal-gonadal primordium state in the adrenal gland and also as an inhibitor of the differentiation process (Bandiera et al., 2013). The same study tracked the descendants of WT1 positive cells and found they gave rise to cells which were WT1 negative but Sf1 positive and expressed steroidogenic genes. On the other hand Shh and Gli1 were not detected in the assayed cells but both have been described as progenitor cell markers *in vivo* (Kim et al., 2009), suggesting the Thy-1 positive cells were more likely to be stem cells rather than progenitors cells.

As WT1 is a known stem cell marker with a specific role in the development of the adrenal cortex, this warranted further investigation into the native expression patterns of this protein in the capsule and sub-capsular areas of the adrenal gland. Furthermore, it was important to investigate the co-expression ratios of WT1 or Sf1 with Thy-1 in the isolated cells in comparison with their co-expression in adrenal gland cryosections. The finding of WT1 expression along the capsular line supports the hypothesis of the existence of capsular stem cells. The high co-expression ratio of WT1 with Thy-1 in the adrenal gland (0.59±0.052) and the low co-expression ratio of Sf1 with Thy-1 (0.23±0.11) supports the notion of Thy-1 as a stem cell marker. Furthermore, the co-expression of WT1 with Thy-1 increased to 90±2% in the isolated cells after 12 weeks of cultivation, which means these cells were maintaining a self-renewing capacity in culture and they can survive longer in comparison with the differentiated cells (Ishigaki et al., 2009). While the Thy-1 and Sf1 positive cells were the opposite of that. The co-expression of Thy-1 with Sf1 in the adrenal gland was low 0.23±0.11 and decreased to 1±1% in the isolated cells. These results suggested that WT1 expression is important in the maintenance

or activation of stem cells, which is in agreement with recent observations of nephrogenesis, which suggested a mechanism by which WT1 regulates stem cells (Akpa et al., 2016). So the expression of Sf1 in the isolated cells might represent the presence of progenitor cells rather than differentiated cells, especially as these cells were lacking other steroidogenic genes (figure 3.11) and they represented a low ratio (1±1%) in culture.

Detection of the stem cell markers Etv5 and ID4 in the isolated cells support the identity of these cells as stem cells. These transcriptional regulatory proteins are defined as stem cell markers because they contribute to stem cell properties such as self-renewal. Etv5 has been found to be a transcriptional regulator of the self-renewal process of the closest cell type to the adrenal cortex, which is the spermatogonial stem cell (Wu et al., 2011). The high level of expression of Etv5 in the isolated cells might have the same role in maintaining the self-renewal capacity of these cells since they survive for a long time in culture.

ID4 was also reported as a protein maintaining the stemness state of the spermatogonial stem cells (Oatley et al., 2011) and is essential for spermatogenesis (Sun et al., 2015). Recent findings also show the expression levels of ID4 are indicators of the regenerative capacity of spermatogonial stem cells (Helsel et al., 2017).

ID4 also called inhibitor of differentiation 4 (Patel et al., 2015), was identified as an inhibitor of other transcription factors known as basic helix-loop-helix (bHLH) transcription factors. These bHLH transcription factors have been described as the main controller of cellular differentiation of mesenchymal organs (Lu et al., 1998). So the expression of this protein in the cells of interest suggested that it maintained the undifferentiated state of the cells. The findings of two common

stem cell markers might reveal a developmental relationship between the two organs: the gonads and the adrenal cortex.

The transformation in the characteristics of the Thy-1 positive cells in their last few months *in vitro* is more likely to be what has been described as the immortal transformation of primary cells to cancer like cells. This phenomenon is not only recorded in the primary culture of adult differentiated cells but also recorded in the MSCs (Urraca et al., 2015). However, this transformation may not necessarily be an oncogenic transformation (Gordon et al., 2014). This transformation includes changes in cell morphology, the cells ability to attach to plastic, cell cycle, cells migration and alteration in the expression of the proteins of interest, especially Thy-1 that had reduced expression in older cells. However, the expression of Sf1 was already absent in these older cells (figure 3.19), which possibly suggests the cells remain undifferentiated.

Thy-1 expression reduced dramatically in the old cells. The changes in the old cells morphology and behaviour in comparison with the younger cells (especially the high proliferation and migration rate *in vitro*) can described as similar to the behaviour of cancer cells *in vitro*. These changes might have resulted from the reduction of Thy-1 expression in the old cells, because the Thy-1 protein was shown to have an inhibitory effect on ovarian cancer cells (Zeng et al., 2009). In agreement with these findings, the progenitor cells of leukemia that are able to maintain blood cancer both *in vivo* and *in vitro* were lacking in Thy-1 expression in comparison with normal hematopoietic progenitor cells (Blair et al., 1997). These results suggest that Thy-1 might has an inhibitory role in malignancy.

The old highly proliferative cells also showed a general decrease in the expression of the other markers of interest WT1, Etv5 and ID4.

WT1 expression declined in the old cells in comparison with its expression in the young cells. Although, WT1 expression is up-regulated in a number of cancer cells, it has an inhibitory effect in the developmentally close cancer cell types to the adrenal cortex such as breast cancer cells by targeting the beta-catenin signaling pathway (Zhang et al., 2003). WT1 transfection into ovarian cancer cells also reduces their proliferation rate (Huo et al., 2011).

This transformation of the old cells slightly lowered the expression of the Etv5 protein in comparison with its expression in the young cells. This slight change in Etv5 expression might result from the role of Etv5 as regulator not only of stem cells but also in cancer cells especially in ovarian cancer cells (Llaurado et al., 2012a, Llaurado et al., 2012b, Zhao et al., 2011).

On the contrary to Etv5, the old highly proliferative cells showed a clear decrease in ID4 expression. The reduction of ID4 would be expected from differentiated cells (Patel et al., 2015) and the senescent cells (Zhu et al., 2015). However, the old cells were essentially undifferentiated and they were propagating in a similar manner to cancer cells. ID4 reduction might be imputed to cancer like old cells because a number of primary cancers reported with low or no expression of the ID4 protein (Umetani et al., 2005, Wen et al., 2012, Baker et al., 2016).

In general, the results of monitoring these cells in the culture showed they exhibited characteristics of stem cells *in vitro.* In addition, the findings of a number of stem cell markers and the changes in the expression of these markers coupled with cell changes supported the stem cell state for most of the cells for at least eight months of cultivation. However, whether these cells could have the potential capacity to differentiate requires more investigation.

Chapter Four

In vitro differentiation of Thy-1 positive cells

4.1 Introduction

4.1.1 *In vitro* differentiation of stem cells

Stem cells differentiation is a process by which stem cells change from unspecialised cells into specialised cells like muscle, skin or neurons. The embryonic cells normally undergo differentiation due to several molecular chemical and physical factors that are eventually produced within the embryo. For example, differentiation factors released from adjacent cells or due to direct embryonic cell to cell or cell-matrix contacts. In addition, the mechanical or physical effect of embryonic movements during development might activate signaling pathways that contribute to the stem cells differentiation. Scientists basically attempt to mimic these differentiation factors to induce differentiation of stem cells *in vitro*. Numerous factors were used to differentiate different cell types including stem cells.

4.1.1.1 *In vitro* differentiation of ESCs and hiPSC

The differentiation of the pluripotent ESCs and hiPSC has it is advantagous because of their ability to generate a myriad of different cell types, it also has a disadvantage because it is difficult to direct their differentiation process to a specific cell type.

Scientists basically have developed several differentiation methods, such as using either extracellular matrix proteins or supportive stromal layers as a base to culture the ESCs on it or

promote the ESC to form embryoid bodies (three-dimensional suspension cultures of stem cell aggregates after treating the ESCs with Knockout re-placement media). However, each of these methods demonstrates broad spectrum of cell types after the differentiation of ESCs (Murry and Keller, 2008). More protocols were developed using approaches which improved the differentiation process to more specific cells types such as the differentiation of hESCs and hiPSCs into hepatocytes (Si-Tayeb et al., 2010, DeLaForest et al., 2011).

The differentiation of ESCs and hiPSC might be required to be directed into either ectoderm lineage, mesoderm lineage or endoderm lineage. The importance of differentiating ESCs into one of these lineages is based on the requirement of a specific cell type derived from one of these lineages.

For example, the endoderm gives rise to the internal organs such as the pancreas, liver, thyroid, and gallbladder (Lu et al., 2001). The differentiation of ESCs into these types of cells is important for treating diseases such as diabetes (type1) and chronic hepatitis. Several methods have been described to differentiate ESCs isolated from human and mouse into β cells (insulin-expressing cells). In the early attempts, scientists used a cell-trapping system to select cell clone that secreted insulin from the undifferentiated ESCs in culture (this system based on using transfection were the ESCs was transfected with a chimeric construct of antibiotic resistance and insulin so the survived cells after antibiotic treatment were also expressing insulin (Soria et al., 2000). While others reported that nestin positive progenitor cells isolated from mouse ES can produce insulin after *in vitro* differentiation using inhibitors of phosphoinositide 3-kinase which is a crucial regulator of intracellular signalling (Hori et al., 2002). Recent studies suggested small molecules that assist the differentiation of human iPSCs/ESCs into pancreatic cells such as

sodium cromoglycate which found to improve the derivation of β cells from hiPSC/hESC lines (Kondo et al., 2017).

The use of pancreatic progenitor cells derived from ESCs to cure patients with diabetes is undergoing clinical trials in countries like North America (Kieffer et al., 2017).

The differentiation of ESCs into mesenchymal lineages has been studied and conducted using different approaches such as raclure method which is based on the induction of spontaneous differentiation of ESCs or iPSCs when placed in appropriate growth conditions (Olivier and Bouhassira, 2011). For example, the ESCs were differentiated into adipogenic mesenchymal stem cells when exposed to retinoic acid (Ninagawa et al., 2011). Other factors such as Leukemia inhibitory factor (LIF) can promote germ cell differentiation from ESCs (Fukunaga et al., 2010).

The differentiation of ESCs into ectodermal lineages such as neurons or skin cells have also been studied and it was shown that several factors are important to direct differentiation. For example, small nuclear RNA called 7SK (Rn7SK) is crucial in the acquisition of a neural fate (Bazi et al., 2017) and the differentiation of the mouse ESCs into mature neurons can be accelerated by the nicotinamide (Griffin et al., 2017).

The differentiation of other stem cell types was studied using different approaches, such as the differentiation of the umbilical cord stem cells reported using 17β-estradiol and growth factors to differentiate these stem cells into the endometrial epithelial cell and endometrial stromal cell respectively (Shi et al., 2017). More details regarding the differentiation of the MSCs will be presented because they are well studied as they are present in almost all vascularised organs of the body (Crisan et al., 2008) in particular the adrenal cortex.

4.1.1.2 *In vitro* differentiation of MSCs

Although MSCs represent only a few cells within organs they are not immortal, but they are capable of propagating many-fold *in vitro* (Chamberlain et al., 2007). The replicative and differentiation capacity of MSCs give them the potential to have important applications in regenerative medicine.

The embryonic mesoderm gives rise to the kidneys, adrenal cortex, gonads and their genital ducts, the bone and its cartilage, muscles, connective tissue, heart, the vessels of the blood and lymph, the spleen and the serous membranes of the body cavity (Doss et al., 2012). These organs mostly contain MSCs that have the characteristics of their mesoderm origin and continuously replenish these organs. MSCs are defined as multipotent (Nuschke et al., 2016) and are capable of differentiating into several cell types such as adipocytes, osteoblasts and myoblasts (Augello and De Bari, 2010). The differentiation of several MSCs into their tissue of origin and other tissue types has been an area of intense study. For example, the murine MSC fibroblast cell line C3H10T 1/2 was differentiated into adipocytes (Chen et al., 2014) and also into chondrogenic and osteogenic cells (Ker et al., 2015). Bone marrow MSCs were also differentiated into hepatocyte-like cells (Khanjani et al., 2014). Although there are variously identified *in vitro* differentiation stimuli, they have their own limitations due to the different culture conditions and the source of MSCs. Furthermore, the phenotypic characteristics of cells can alter after their isolation and *in vitro* cultivation as the cells are exposed to a new environment, which can include eventual changes in the expression of certain markers (Jones et al., 2002). A number of pathways and molecules have been suggested as important regulators or factors in MSC differentiation such as the Wnt signaling pathway. The secreted proteins of the Wnt family are involved in spontaneous cell differentiation by directly influencing MSCs (Liu et al., 2009).

Others include the transforming growth factor beta (TGF- β) superfamily which is known to have a role in the differentiation of bone marrow derivative MSCs (Crane and Cao, 2014) and an enhancement of chondrogenic MSCs differentiation after up-regulation of TGF-β1(Kim et al., 2014). Fibroblast growth factor 2 (FGF-2) was also found to upregulate the kinetics of MSCs chondrogenesis and improve their differentiation (Cheng et al., 2012).

Recent studies targeted a number of microRNAs which might be related to pluripotency and induction of differentiation in pancreatic islet derived MSCs (Coskun et al., 2017). The use of inorganic matrices to enhance bone repair has been suggested to induce the *ex vivo* genesis of T-cells from progenitor cells (Poznansky et al., 2000), which then developed into artificial thymic organoids used to induce differentiation in hematopoietic stem cells (Seet et al., 2017). Several other factors and chemicals have been widely used to differentiate different types of cells other than what had been used in this project.

4.1.2 Cyclic AMP

The use of cyclic AMP analogs in the differentiation induction has been documented in variety of cells. Release of cyclic AMP as a differentiation factor normally occurs after activation of a receptor, such as FSH binding to its receptor, which stimulates cyclic AMP production (Bhattacharya et al., 2012). It has been used in vitro to differentiate mouse neural crest cells into dopamine neurons (Tremblay et al., 2010) and in the differentiation of mastocytoma cells (Goulding and Ralph, 1989), Cyclic AMP was also employed to obtain differentiated optic nerve-derived cells (Cohen et al., 1999), Schwann cells (Bacallao and Monje, 2015) and human placental cells (Yoshie et al., 2010). However, it has an inhibitory effect on the differentiation process of the stalk cells of Dictyostelium discoideum (Berks and Kay, 1988) and the

differentiation of megakaryocytes (Rubinstein et al., 2012). Others have also suggested that different cyclic AMP variants have different effects on the differentiation of human MSCs into osteocytes and adipocytes. For example, the expression of adipogenic genes in hMSCs were increased after treatment with 8-bromo-cAMP. While treatment with dibutyryl-cAMP induced the expression of the osteogenic marker (alkaline phosphatase) (Doorn et al., 2012). Both of these cAMP variants were also reported to induce the expression of STAR which is required for the differentiation of steroidogenic cells (Ruiz-Babot et al., 2018).

4.1.3 Forskolin

Similar to the cyclic AMP, forskolin analogs have also been used for the differentiation of a variety of cells. Different mechanisms have been suggested for the role of forskolin in stimulating differentiation. For instance, forskolin is used to stimulate cyclic AMP production, which in turn is used to differentiate spermatogonia (Bhattacharya et al., 2012). Forskolin has been used to differentiate placental cells (Wu et al., 2013), neurons (Cao et al., 2012), osteoblast (Li et al., 2014), spermatogonial (Bhattacharya et al., 2012) and many other cell types. Using forskolin to differentiate malignant cells such as gliomas gives the potential for a therapeutic method for cancer treatment (He et al., 2011). The use of forskolin in the differentiation of stem cells has been suggested by several studies, where it has been used to differentiate the iPSCs into brown adipocytes (Takeda et al., 2017), adipose-derived MSCs into neural cells(Blecker et al., 2017) and the differentiation of the embryonic stem cells and umbilical vein endothelial cells (Wang et al., 2017).

5.1.4 Steroidogenic factor one (Sf1)

Sf1 or also called Adrenal 4 binding protein (Ad4BP) is encoded by the nuclear receptor subfamily 5, group a, member 1gene (NR5A1). Sf1 is a nuclear receptor with the key role of steroidogenesis and is mainly expressed in the adrenal cortex, placenta and the gonads. In common with other nuclear receptors, Sf1 has an activation function domain at the amino-terminal 1 (AF-1), DNA-binding domain, hinge, ligand- binding domain and the second activation function domain at the carboxy-terminal (AF-2). Although the ligand- binding domain of Sf1 is highly conserved, there is no genuine identified ligand for Sf1 (Mlynarczuk et al., 2014, Desclozeaux et al., 2002) which make it an orphan receptor. This orphan receptor not only plays a regulatory role in the mature steroidogenic cells of adrenal cortex, placenta and gonad, it is also has a regulatory role in the development of steroidogenic cells (Wang et al., 2013). The importance of Sf1 expression in the gonads and adrenal cortex has been revealed by several studies. For example, adrenal tumours were induced after Sf1 overexpression (Doghman et al., 2007), while adrenal glands and gonads failed to develop in Sf1 knockout mice (Luo et al., 1994). In either case the irregular expression of Sf1 cause abnormal development of both gonads and adrenals (Shima et al., 2012). Although the placenta is considered as the key regulator and producer of steroids during pregnancy, Sf1 expression has been detected only slightly in the placenta (Ramayya et al., 1997). However, neither placental steroid production nor placental development was detected in Sf1 knockout mice (Sadovsky et al., 1995). These data suggested the importance of this nuclear receptor in the adrenal gland not only for the production of steroids but also it is essential for the development of the adrenal cortex.

The Thy-1 positive cells were identified as undifferentiated cells because they didn't show the expression of any of the steroidogenic enzymes and they showed the characteristics of MSCs. So

they probably have a potential capacity to differentiate into steroidogenic cells. The aim of this chapter was to promote the differentiation process in Thy-1 positive cells using external and internal inducers. The external inducers included the synthetic ACTH that had been tested earlier in chapter 3 on the rat adrenal primary cells and the cells showed a detectable response that was identified by detecting the production of corticosterone. Two other external factors were also used: forskolin as another synthetic differentiation factor and the naturally produced POMC from AtT20 cell line that contains the most effective peptides acting on the adrenal cortex cells.

The internal differentiation inducer was the Sf1. This experiment included transfecting Thy-1 positive cells with Sf1 gene. The transfection might start the steroidogenesis because this nuclear receptor represents the key role of steroidogenesis. The differentiation attempts were evaluated using immunostaining assays. Then the effect of Sf1 transfection was tested by measuring the mRNA expression of a number of steroidogenic enzymes in addition to its effects on the mRNA expression of other genes of interest.

4.2 Materials and methods

All materials were sourced from Thermo-Fisher Scientific unless stated otherwise.

4.2.1 Thy-1 positive cells differentiation

Differentiation is a normal process that usually occurs during development. The new (differentiated) cells rising from nonspecialised (undifferentiated) cells become more specialised and different from one another. Although all cells of a single organism have identical genomic information, the differentiated cells have specific gene expression activity that giving them different phenotype from other differentiated cells within the same organism.

The differentiation might be induced by activating different genes or pathways within the undifferentiated cell. The isolated Thy-1 positive cells were mainly undifferentiated. As a result, several treatments were carried out to achieve differentiation.

4.2.1.1 Differentiation by hormonal treatment

The isolated Thy-1 positive cells were treated with serial concentrations of steroidogenic differentiation factors to induce differentiation. The first treatment was with forskolin (Sigma) with 100nM, 1µM and 10µM, in 2ml of DMEM culture medium. The second was with ACTH 10nm, 100nm and 1 µM, in 2ml of DMEM culture medium and the third was with the AtT20 cell line media treatment. The AtT-20 is a POMC releasing cell line. This line was cloned from mouse pituitary tumor cells cultures, which was established after alternate passage of tumors in cell culture and in animals. This mouse pituitary tumor cell line was cultivated and the DMEM media of growing cells were collected before passaging to be used as a normal source of ACTH and all other POMC peptides that might induce differentiation. The collected media was filtered then mixed with fresh DMEM media 1:1 v/v and applied to Thy-1 positive cells.

The treatment lasted for 7 days, the cells were collected and the RNA was isolated. Then qPCR was conducted to compare the gene expression changes in comparison with un-treated cells.

4.2.1.2 Mammalian cells transfection

The mammalian cells transfection was used to study the effect of introducing the gene of interest and to achieve changes to the studied cells. This required transfection of the Thy-1 positive cells with the Sf1 gene is an attempt to induce differentiation.

4.2.1.2.1 Gene cloning

Mammalian cells transfection requires an appropriate vector with a detectable reporter. The cloning of the gene of interest into the mammalian cells was conducted using pIRES2 EGFP. pIRES2-EGFP vector (Appendix B.2) contains internal ribosomal entry site (IRES 1, 2) of encephalomyocarditis virus (EMCV), which is a small non-enveloped single-strand RNA virus between the multicloning site (MCS) and the enhanced green fluorescent protein (EGFP) coding region. This alignment permits both the EGFP gene and the gene of interest, which were cloned into the MCS to be translated. pIRES2-EGFP is designed for the efficient selection by fluorescent microscopy, flowcytometry or any other fluorescent methods of transiently transfected mammalian cells expressing the protein of interest and EGFP. The pIRES2 EGFP vector can also be used to express EGFP alone or to obtain stably transfected cell lines.

4.2.1.2.1.1 RNA isolation from rat adrenal tissue

Firstly, to prepare the coding sequence of the Sf1 gene, total RNA was isolated from freshly isolated adrenal tissues from adult Wistar-rats using TRIzol reagent (Ambion) as previously described in (2.2.1.1). The total RNA was analysed by spectrophotometry using a Nanodrop device to measure the concentration and the purity of isolated RNA.

4.2.1.2.1.2 cDNA synthesis

An aliquot of 1-5µg of total RNA was used for the synthesis of total cDNA using a cDNA synthesis kit as previously described in (2.2.2).

4.2.1.2.1.3 Electrophoresis

The isolated RNA, PCR products and DNA digestion products were analysed by agarose gel electrophoresis as previously described in (2.2.1.2).

4.2.1.2.1.4 Primers design for PCR

The full-length coding sequence of the gene of interest was identified using the NCBI website (https://www.ncbi.nlm.nih.gov/nucleotide/300797823). Primers were designed to target the coding sequences of the gene of interest. Primers sequences for the rat Sf1 gene were:
Forward primer 5' TCCTTCCGTTCAGCGGACGCC 3' and reverse primer 5' CAGTCCCCGCCCATCCTTGC 3'. The primers were used to amplify 1569bp of the target gene using PCR.

4.2.1.2.1.5 First cloning PCR

The PCR reaction volume was prepared in 25µl, by mixing 12.5µl pre-aliquot master mix (Promega) in 0.2 ml tubes, with 1µl of each primer (10µM), 2µl cDNA (20ng/µl) and 8.5µl of nuclease-free water.

The components of the reaction were mixed before cycling as follows: 94°C for 1 minute for the initial denaturation and activation of the Taq polymerase, followed by 39 cycles of 94°C for 20

seconds for denaturation, 58°C for 20 seconds for primer annealing, finally the extension at 72°C for 2 minutes which was carried out to ensure the completion of a full-length DNA product.

After cycling, PCR products were separated by electrophoresis on a 1.2% (w/v) agarose gel with 1kb plus ladder (generuler). The targeted band of the gene of interest was excised and the DNA purified as described in (2.2.4). The resulting DNA represents the full-length coding sequence which was used as the DNA template for the next PCR.

4.2.1.2.1.6 Second cloning PCR

The primers for this PCR were new and had the same sequences in addition to restriction site sequence and CGC or GCG platform sequence at the 5' of the primers. The two restriction sites of the two primers were chosen carefully to set the gene of interest correctly in the vector and not cut through the gene sequence. The EcoR1 restriction sequence (GAATTC) was added upstream the Sf1 forward primer and The BamH1restriction sequence (GGATCC) was added upstream the Sf1 reverse primer The primer sequences for cloning the rat Sf1 gene into pIRES2 EGFP vector were:

EcoR1-forward primer 5' GCGGAATTCTCCTTCCGTTCAGCGGACGCC 3'

and

BamH1-reverse primer 5' CGCGGATCCAGTCCCCGCCCATCCTTGC 3'.

The two restriction sites contained within the two primers were chosen by analysing the target sequence before adding them to the primers. The target sequence of Sf1 had to be tested against these restriction sequences using the website (**http://nc2.neb.com/NEBcutter2/**) and the result showed the sequence did not have any restriction sites for EcoR1 or BamH1 within that

sequence. This test was carried out before primer purchase for the cloning process to avoid digestion of the DNA segment in case it has the restriction sequence within them.

The components of the PCR reaction were mixed as described previously in (2.2.3). The targeted band of the Sf1 gene was excised and the DNA purified as described (2.3.2.2).

4.2.1.2.1.7 Digestion, ligation and transformation

Both the plasmid and insert were digested with restriction enzymes as described in (2.2.9), the digested DNA was mixed with 6 x loading buffer then profiled by agarose gel electrophoresis. The targeted bands of the digested vector and the digested gene of interest were excised and the DNA purified as described in (2.2.4). Ligation reactions were carried out using T4 ligase (Promega) to ligate the gene of interest to the pIRES2-EGFP vector as described in (2.2.5). The transformation of *E-coli* was conducted as described in (2.2.8). Three to six targeted colonies were picked; each colony was re-cultured in LB broth for purification of the plasmid.

4.2.1.2.1.8 Purification of plasmid

Plasmid DNA was isolated and purified from the transformed bacteria using either the Qiagen Miniprep as previously described in (2.2.7.1) where the purified plasmid was used for confirming cloning and detecting the targeted inserts. Or Plasmid DNA was purified using the Midiprep purification kit.

4.2.1.2.1.8.1 Midiprep

A single colony was picked from a freshly streaked selective plate and inoculated into a starter culture of 2–5 ml LB medium containing the appropriate selective antibiotic (kanamycin). The culture was then incubated for 3-4 hours at 37°C with vigorous shaking at 250 rpm. The culture

was used as a starter and diluted to 1/500 with LB medium containing the selective antibiotic. One hundred ml was inoculated and grew at 37°C for 8-12 hours with vigorous shaking at 300 rpm. The culture reached a cell density of approximately 3–4 x 10^9 cells per milliliter, which typically corresponds to a pellet wet weight of approximately 3g/liter.

The bacterial cells were centrifuged at 4000 g for 20 minutes at 4°C. The bacterial pellet was re-suspended in 6ml of Buffer P1 by vortexing. Then 6ml of Buffer P2 was added and mixed thoroughly by inverting the tube 6 times, and incubating at room temperature (15–25°C) for 5 minutes. The lysate appeared viscous. During the incubation, the QIAfilter Cartridge was prepared: the white cap was screwed onto the outlet nozzle of the QIAfilter Cartridge then placed into a convenient rack. Then 6 ml of chilled (4°C) Buffer P3 (Appendix A.12) was added to the lysate and mixed immediately by inverting vigorously 6 times. The lysate was then poured into the barrel of the QIAfilter Cartridge and incubated at room temperature for 10 minutes in a steady state without the plunger inside. After the 10 minute incubation, the HiSpeed Midi Tip was equilibrated by applying 4 ml of Buffer QBT (Appendix A.13) and the column was allowed to empty by gravity flow until it had drained completely.

After this, the cap was removed from the QIAfilter outlet nozzle. Then the plunger was gently inserted into the QIAfilter Cartridge and the cell lysate filtered into the previously equilibrated HiSpeed Tip. The filtration proceeded until approximately 15ml of the lysate had passed through the QIAfilter Cartridge, without applying extreme force. The cleared lysate passed in the resin by gravity flow. The HiSpeed Midi Tip was washed with 20 ml of Buffer QC (Appendix A.14). This was allowed to move through the HiSpeed Tip by gravity flow. The primary elution of the plasmid DNA was carried out with 5 ml of Buffer QF (Appendix A.15). The eluted DNA was collected in a 15 ml tube, mixed with 3.5 ml of room temperature isopropanol and then incubated

at room temperature for 5 minutes to precipitate the DNA. During the incubation, the plunger was removed from a 20 ml syringe and the QIAprecipitator attached to the outlet nozzle. The steps were carried out without excessive force and the QIAprecipitator was always removed from the syringe before pulling up the plunger. The QIAprecipitator was placed over a waste bottle, the eluate/isopropanol mixture was transferred into the 20 ml syringe, and the plunger inserted. The mixture was filtered through the QIAprecipitator using constant pressure. The QIAprecipitator was removed from the 20 ml syringe and the plunger pulled out. The QIAprecipitator was then re-attached and 2 ml of 70% ethanol was added to the syringe. The DNA was washed by inserting the plunger and pressing the ethanol through the QIAprecipitator using constant pressure.

The QIAprecipitator was again removed from the 20 ml syringe and the plunger pulled out. The QIAprecipitator was re-attached and the membrane was dried by pressing air through the QIAprecipitator quickly and forcefully. This drying process was repeated with the addition of an absorbent paper to dry the outlet nozzle of the QIAprecipitator to prevent ethanol carryover.

The QIAprecipitator was removed from the new 5ml syringe and the QIAprecipitator attached to the outlet nozzle. This was positioned over a 1.5ml collection tube, 1 ml of Buffer TE (Appendix A.16) was added to the 5 ml syringe. The plunger was inserted and the DNA was eluted into the collection tube using constant pressure.

The purified plasmids were digested with appropriate restriction enzymes and the resulting DNA was checked by agarose gel electrophoresis to ensure the presence of the insert in the plasmid.

4.2.1.2.1.9 Plasmids sequencing

The plasmids in this project were sequenced to verify the targeted nucleotides sequences within the vector as previously described in (2.2.8).

4.2.1.2.2 Transfection of the mammalian cells with gene of interest

The mammalian cells transfection with the target gene was carried out after the gene of interest was cloned into the pIRES2 EGFP vector. The vector was employed to carry the gene of interest to the target cells by binding it with a transfection reagent.

Transfection was usually conducted in a 6-well plate with each well being used. Cells were seeded on coverslips at least one day before transfection. The control wells were transfected with the empty vector only and the cells were 70-90% confluent at the day of transfection. The transfection reagent (TurboFect) was prepared immediately before transfection and briefly vortexed. Three micrograms of plasmid DNA (containing the gene of interest) was diluted in 300µL of serum-free DMEM. Three microliters of the transfection reagent was added to the diluted DNA and mixed by a brief vortex. This mix was incubated for about 20 minutes at room temperature; then 300µL of the mixture was dropped into each well of the six-well plate. It was then rocked gently to distribute the complexes. The plate was incubated at 37°C in a CO2 incubator for 5-6 hours before changing the media.

4.2.2 Examine the transfection

After 1-2 days of transfection, the transfected cells along with the control cells (those transfected with native plasmid and non-transfected cells) were examined using an inverted fluorescent microscope (Inverted Epifluorescent Microscope AXIO) to evaluate the rate of the transfected cells found amongst all the cells.

The transfected cells were tested by immunocytofluorescence to examine the expression of the genes of interest. After 2-3 days of transfection, dual staining assays were conducted using

primary mouse antibodies and rabbit antibodies as previously described in (3.2.10). The slides were examined using a Zeiss-Axio Imager.

4.2.3. RNA isolation from cultured cells

The RNA was isolated from the cultured cells before and after treatments using an RNeasy mini kit as previously described in (3.2.11).

4.2.4 Two-step quantitative RT- PCR (RT-qPCR)

The **RT-qPCR** was employed to investigate changes in the gene expression after a specific treatment. The two-step (RT-qPCR) started with the reverse transcription of the total RNA into the first-strand cDNA. Then the resulted cDNA was used as a template in real time PCR using specific primers. The concentrations of RNAs samples were measured and the concentration used in making each 40µl cDNA was 400ng as described in section (4.2.1.2.1.3) cDNA synthesis . The isolated RNAs from the biological replicates were mixed together before conducting the cDNA synthesis. The cDNAs were diluted 1:20 in RNase-DNase free water.

qPCR reactions were set up to analyse the gene expression of a number of steroidogenic genes and stem cell markers as fold changes using the ΔΔCt method in comparative quantification. This technique compares results from experimental samples with both a calibrator (untreated cells) and a normalizer which was β-Actin as a housekeeping gene. The choice of (β-Actin as the housekeeping gene) was made after running a qPCR stability test on GAPDH and β-Actin within the different treatments in the experiments. The stability test was conducted to reveal which of housekeeping genes are more stable after different treatments.

The Ct values for the gene of interest in the untreated cells and treated cells are adjusted in relation to β-Actin Ct from the same untreated cells and treated cells. The resulted ΔΔCt value was integrated to determine the fold difference in expression which was equal to $2^{-\Delta\Delta Ct}$.

qPCR primers were designed to meet specific criteria of the target gene. All primers were designed using the NCBI website tool called Primer-Blast, after detection of the gene mRNA sequence, using the gene accession number which can be found online from the option Nucleotide in the NCBI website (https://www.ncbi.nlm.nih.gov/nucleotide) Each primer was designed to be 18-22bp in long, with melting temperature (Tm) around 60°C and to amplify a single DNA segment located within the coding sequence of the target gene. The amplicon length ranged between 80-250bp. Primer efficiencies were tested prior to the actual experiments on cDNA of RNA isolated from the whole adrenal gland to validate the amplicons signal curve (ct), the threshold cycle and their melting curve. The tested samples were run on agarose gel electrophoresis after adding the loading buffer to verify the size and singularity of the amplified segments. The details of qPCR primers are in (Table 4.1).

All qPCR experiments were conducted in 96 well plates and the reaction of each well was set up as follows: 0.3µL primers mix (5µM) each, 7µl of 2x quantiTect SYBER Green PCR master mix (Qiagen) and 6.7 µl of the diluted cDNA.

The qPCR program for initial denaturation at 95°C for 15 minutes was used and then 40 cycles of 95°C for 15 seconds followed by 59°C for 1 minute were carried out. The final step was to show the melting curve of the products by raising the temperature slowly to 95°C for 15 seconds. The qPCR was performed using an AB Applied Biosystem device connected to a computer with StepOne software specifically for monitoring and analyzing qPCR experiments.

Table 4.1 List of primers (Invitrogen) used in the RT-qPCR, their accession number, position in the mRNA sequence and their product size.

Gene	**Forward primer 5`-3` (position)**	**Reverse primer5`-3` (position)**	Fragment Size(bp)	Accession number
Sf1	TCCAGTGTGTGGTGACAAGG (183-202)	TTTGCAGCTCTGACTCTCGG (312-293)	130	NM_001191099.1
Gapdh	CCCAGCAAGGATACTGAGAGC (1097-1117)	TCCTGTTGTTATGGGGTCTGG (1218-1198)	122	NM_017008.4
Itgb2	AGAGCCTGCAGATTGTTCCG (2741-2760)	GCCACCTTTACTGAGACCCC (2827-2808)	87	NM_001037780.2
β-Actin	CACCCGCGAGTACAACCTTC (15-34)	CCCATACCCACCATCACACC (221-202)	207	NM_031144.3
Cyp11a1	TCAGCGATGACCTATTCCGC (612-631)	AGTCTGGAGGCATGTTGAGC (779-760)	168	NM_017286.3
Thy-1	CAAAACGCGGGGAGAAATGG (680-699)	ACTAATCAGAAGCAGCCCCG (831-812)	152	NM_012673.2
3βHSD	TGTCATGATACTTGCGGCCC (749-768)	AGCCAGAATATGTGCCCAGG (860-641)	112	NM_001007719.3
Cyp21	CAAGCAGGACAGCACTTTGC (542-561)	TTGGACGGACCAGTGATTCC (623-604)	82	NM_057101.2
Wt1	CCACACCAGGACTCATACAGG (1632-1652)	CTGGTGCATGTTGTGATGGC (1740-1721)	109	XM_006234622.2
Gli1	ATGAAGAGGCAGTTGGGACG (129-148)	ACATGGTGTCTCAGCGAAGG (217-198)	89	XM_008765375.1
Etv5	AAGTCACTTTTCAGTGCAAGAGG (55-77)	GTCCTCTGACCGAGATTTCCC (214-194)	160	XM_008768798.1
Tert	TCCTTCCACCAGGTGTCATCC (208-228)	TGGGCAAGTAGCTATGCACG (373-354)	166	NM_053423.1
ID4	GCAGGTCCAGGATGTAGTCG (192-211)	CCTGCAGTGCGATATGAACG (316-297)	125	NM_175582.1

4.2.5 Microscopy

Immunocytofluorescence assays were used to examine the expression of the gene of interest after the transfection using a Zeiss-Axio Imager A1 fluorescent microscope with four filters: Blue/cyan filter for (4',6-diamidino-2-phenylindole (DAPI)), Alexa Fluor (AF) 488 green, AF 546 yellow, and AF 660 red as previously described in (2.2.13).

4.2.6 Statistical analysis

RT-qPCR data were analysed using ΔΔCt which normalised with the expression of housekeeping gene (β-Actin) before conversion to relative fold difference values. Results were examined using Dunnett's Multiple Comparison Test of one-way analysis of variance (ANOVA).

4.3 Results

The differentiation experiments of Thy-1 positive cells were conducted using two approaches.First, experiments designed to use external differentiation factors (specific such as ACTH and generally such as forskolin), which supposed to induce differentiation in the cells after binding to their cell membrane receptors which in turn activating pathways that cause differentiation.

Second, experiments designed to induce differentiation by imitating the development process of adrenal cortex using transfection with Sf1 gene to change the gene regulatory pathway of Thy-1 positive cells that may start the differentiation.

4.3.1 RT-qPCR assays to determine the appropriate housekeeping gene and the appropriate RNA concentration

Before starting the qPCR assays to detect changes in the genes of interest after the differentiation attempts, there were two tests required: first, a stability test, which was conducted to select an appropriate normaliser between the two housekeeping genes (GAPDH and β actin) in the tested samples.

The stability test revealed both of the housekeeping genes were stable in the control and treated cells (Figure 4.1). However, β actin was more stable against both hormonal treatments and Sf1 transfection.

Second, a relative standard curve was employed to determine the appropriate RNA concentration for this test. The RNA was isolated from the cells and then 400ng of RNA (as measured by Nanodrop) was used to make 40µl cDNA. Then series of 10 dilutions of cDNA were prepared based on the RNA concentration (1 - 00.2ng/µl of RNA into qPCR reaction mix) to create a

trendline between the Ct value and the RNA concentration for β actin as normaliser in the control and treated cells. The trendline results showed similar Ct values of β actin between control and treated cells (Figure 4.2) and the coefficient of determination values (R^2) showed high correlation between the Ct value and the RNA concentration. Further trendlines for the genes of interest were also used such as Thy-1 and WT1, which showed similar correlation values. These data also showed that RNA concentration from 1 - 0.25ng/µl was appropriate for threshold of Ct values of β actin, which was approximately 20 cycles.

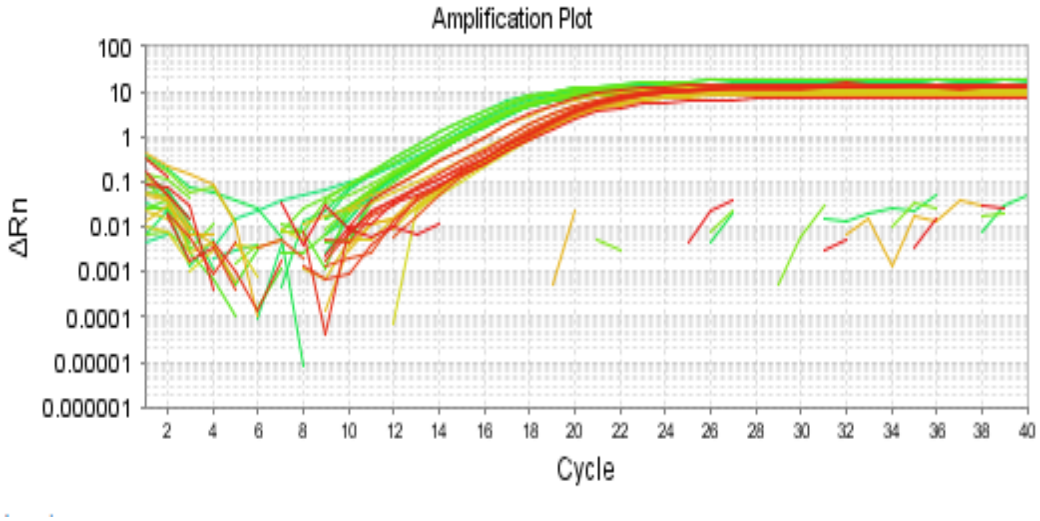

Figure 4.1 Amplification plots of the stability test for two housekeeping genes GAPDH and β actin using RT-qPCR on RNA isolated from 3 month old Thy-1 positive cells in culture including (untreated cells, cells after 2 days of transfection with Sf1 and cells after 2 days of transfection with native-plasmid). The red curves represent GAPDH and the green curves represent β actin. The picture was acquired from this test using StepOne software connected to qPCR machine (Applied Biosystems).

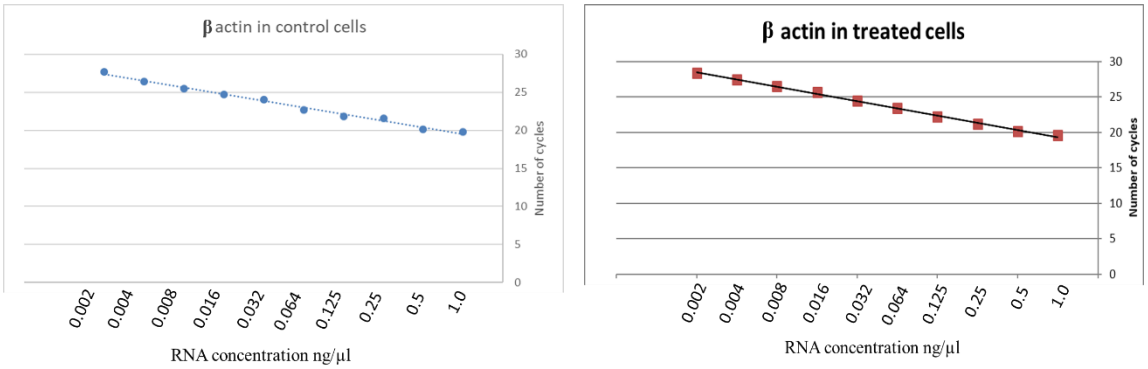

Figure 4.2 Trendline plots of β actin expression against serial dilutions of RNA in the cDNA solution used for RT-qPCR (1ng/µl – 0.002 ng/µl) in both treated and control Thy-1 positive cells after 2 days of transfection with Sf1.

4.3. 2 Thy-1 positive cells differentiation by hormonal treatment

The use of hormones to induce differentiation was conducted to investigate the response in the Sf1 gene expression and the expression of steroidogenic main genes Cyp11A1 and 3βHSD because both are usually expressed in the beginning of the steroidogenesis in the zG and zF of the adrenal cortex. The relative quantification RQ values were used to represent the number of the fold changes in the expression of the genes of interest after the differentiation treatments. RQ value analyses the difference in the mRNA expression of the genes of interest in the treated sample relative to the reference sample (as represented by the untreated control cells).

The isolated Thy-1 positive cells were treated with serial concentrations of the differentiation factors forskolin, ACTH and AtT20 cell line media to induce differentiation of Thy-1 positive cells during their 3rd month of *in vitro* culture. The treatment lasted for 7 days then the cells were collected and the RNA was isolated using an RNeasy mini kit. Then RT-qPCR was conducted to measure the changes in the gene expression of Sf1, Cyp11A1 and 3βHSD in comparison with untreated cells. The Ct values were normalised to β actin. The relative fold differences of the genes of interest were determined using the ΔΔCt value and presented in logarithm 10 of relative quantitation as fold changes. The results of the RT-qPCR (Figure 4.3) were showed no significant ($p \geq 0.05$) response to all of these treatments.

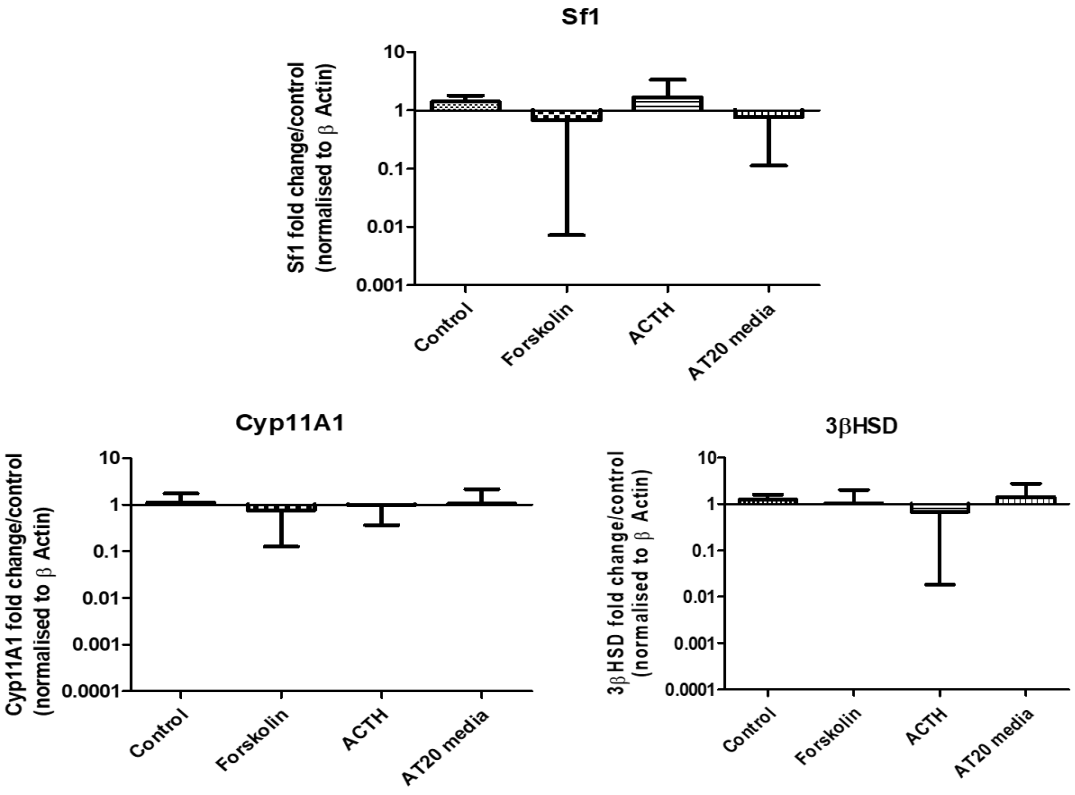

Figure 4.3 RT-qPCR relative quantification represented in fold changes of the mRNA expression of Sf1, CYP11A1, and 3βHSD in the Thy-1 positive cells after one week of treatment with ACTH, AT20 cell line media and forskolin. The cells were treated in their 3rd month of *in vitro* cultivation. The mRNA expression of all three genes showed no significant ($p \geq 0.05$) response to all of these treatments. Three biological replicates were used in this experiment.

4.3.3 The differentiation of Thy-1 positive cells by transfection with Sf1

This differentiation of Thy-1 positive cells using Sf1 required designing a vector-Sf1 complex that can be used to induce temporary expression of Sf1 gene in the Thy-1 positive cells using mammalian cell transfection procedure. A number of experiments were conducted to prepare an appropriate vector-Sf1 complex before transfecting the cells.

4.3.3.1 Gene cloning

The transfection of Thy-1 positive cells with Sf1 gene was conducted to induce differentiation. This experiment required cloning the Sf1 coding sequence in an appropriate vector that has a reporter gene (pIRES2 EGFP vector). Therefore, appropriate primers were designed to target the coding sequence of Sf1 mRNA in the whole adrenal cDNA using RT-PCR which was successfully achieved (Figure 4.4).

The Sf1 band was excised and the DNA was purified. This purified DNA was then used as a DNA template for the next PCR. The primers for this PCR had the same sequences in addition to restriction site sequences and CGC or GCG platform sequence at the 5` of the primers. The addition of each restriction sequence to each primer was designed to be similar in annealing temperature and to orient the gene of interest into pIRES2 EGFP vector. The second PCR product was analysed using agarose gel electrophoresis and the result showed the desired band (Figure 4.4).

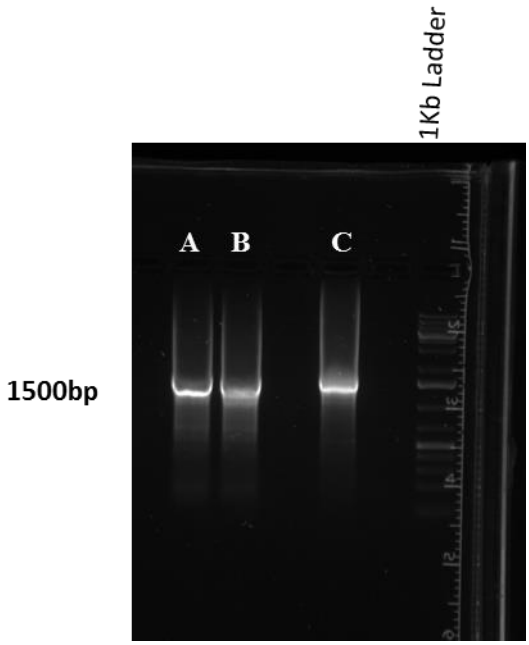

Figure 4.4 Agarose gel electrophoresis of Sf1 RT-PCR products. A&B are the bands of RT-PCR products using appropriate pair of primers against whole adrenal gland cDNA to amplify the full coding sequence of the rat SF1. (C) is the single band represents the product of second PCR after using the first product as template DNA with primers designed to add EcoR1 restriction sequences to the 5' of the SF1 sequence and to add BamH1 restriction sequences to the 3' end of the SF1 sequence.

The Sf1 band from the second PCR was excised and purified successfully in order to digest it with EcoR1 and BamH1 enzymes. The Sf1 DNA was successfully digested with the two restriction enzymes. The digested DNA was then separated using agarose gel electrophoresis (Figure 4.5).

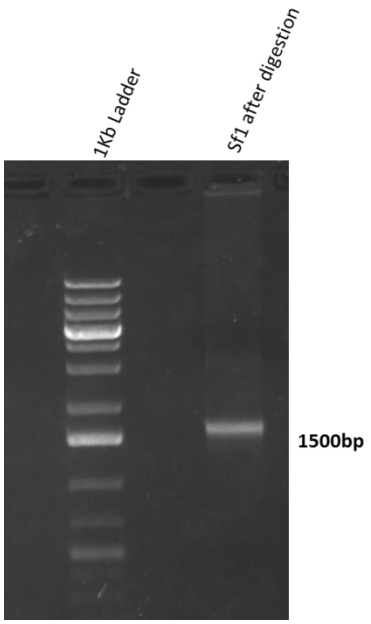

Figure 4.5 Agarose gel electrophoresis of the Sf1 DNA coding sequence after PCR and subsequent restriction digest. The targeted band was amplified using specific primers in a PCR reaction with primers containing EcoR1 and BamH1 restriction sites to amplify the full coding sequence of the rat SF1. The Sf1 DNA product was then flanked with restriction sites that were then digested with EcoR1 and BamH1 enzymes.

The digestion of the pIRES2 EGFP vector was successfully conducted with the same restriction enzymes (EcoR1 and BamH1) and the digested vector was also purified in order to undergo ligation with Sf1. The ligation mixture was used in the transformation of *E coli* in parallel with a native-plasmid as a control. The transformation was successfully achieved and several colonies of each (transformed with Sf1 and control) were picked and used to inoculate 5ml of LB broth, then the plasmids were successfully extracted from 3ml of the culture using mini-prep. The extracted plasmid with the potential Sf1 insert was analysed using PCR which showed the presence of single band representing Sf1 (Figure 4.6). Then the plasmid was digested with EcoR1 and BamH1 enzymes to confirm the presence of a vector with the Sf1 insert (Figure 4.7).

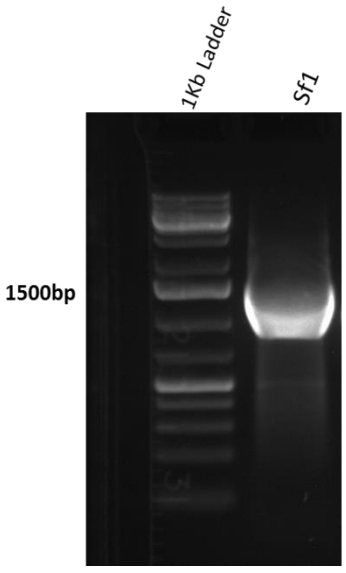

Figure 4.6 Agarose gel electrophoresis of PCR products to amplify the full coding sequence of the rat SF1 using the extracted plasmid as the DNA template with appropriate pair of primers. The single DNA band represents the full coding sequence of the rat SF1 at approximately 1500bp.

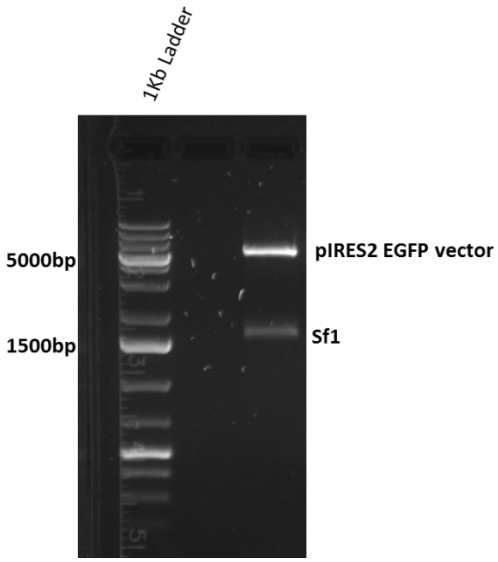

Figure 4.7 Agarose gel electrophoresis of the extracted plasmid after digestion with EcoR1 and BamH1, showing the presence of the Sf1 at approximately 1500bp and the pIRES2 EGFP vector at approximately 5000bp.

The plasmids were extracted using Midi prep kit to gain the appropriate quantity and the concentration of the vector required for mammalian cells transfection. The process was successfully achieved and the concentration of the vector with insert was 360ng/µl and the native vector was 500ng/µl. An aliquot of the plasmid with Sf1 was sent for sequencing and data successfully matched the Sf1 sequence.

4.3.1.2 Transfection of the Thy-1 positive cells with Sf1

Transfection of Sf1 into Thy-1 positive cells was conducted to study the gene product and function of this gene in the initiation steroidogenesis in Thy-1 positive cells. The cells were transfected with Sf1 at two-time points during cultivation: after 3 months and 8 months of culture. These experiments were conducted in triplicates, 1-2 days after of transfection, the transfection efficiency was examined by visualising the expressing of GFP under the fluorescence microscope. The cells showed a transfection rate of approximately 30-45% both with native-plasmid and Sf1 plasmid. The effect of Sf1 transfection was tested using RT-qPCR and immunocytofluorescence. Specifically, changes in the expression of the genes of interest were tracked using RT-qPCR after Sf1 transfection. The gene's expression in transfected cells was tested after 2, 4 and 7 days of transfection.

4.3.1.3 mRNA isolation after transfection of the Thy-1 positive cells with Sf1

mRNA isolation from Thy-1 positive cells transfected with Sf1 were conducted at different intervals 2, 4 and 7 days along with the control cells (those transfected with native-plasmid and non-transfected cells). Two-step reverse transcription-quantitative polymerase chain reaction (RT-qPCR) was used to analyse the changes in the gene expression of the genes of interests.

4.3.1.4 Relative quantification of genes of interest after Sf1 transfection using qPCR

After the Sf1 transfection as a differentiation experiment, qPCR assays were carried out to investigate changes in the mRNA expression of genes of interest and also to verify the Sf1 expression after transfecting Thy-1 positive cells with Sf1. The RT-qPCR assays were conducted after transfection of the Thy-1 positive cells with Sf1 in two main periods of the cells life in vitro (after 3months and after 8months in vitro).

4.3.1.4.1 RT-qPCR of the Sf1 transfection into the Thy-1 positive cells after 3months

The RT-qPCR results of the Sf1 transfection into the Thy-1 positive cells after 3months of culture were showed changes in the genes of interests.

Sf1 mRNA expression showed a significant increase ($P < 0.001$) after Sf1 transfection in the all test periods after Sf1 transfection (2, 4 and 7days) in comparison with untreated cells and the cells that were transfected with native-plasmid (Figure 4.8).

Thy-1 mRNA expression showed slight non significant ($P \geq 0.05$) changes after Sf1 transfection in the all tested periods (2, 4 and 7 days) in comparison with control cells (Figure 4.8).

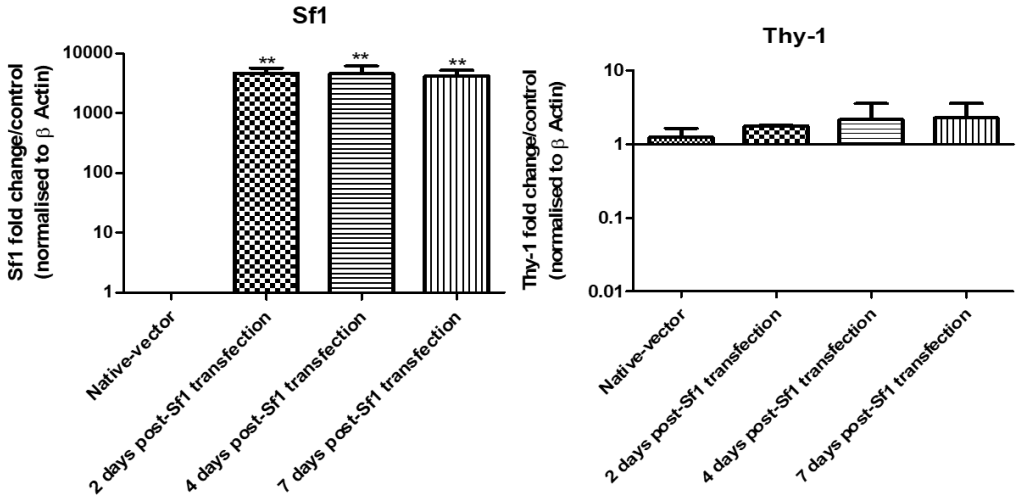

Figure 4.8 RT-qPCR relative quantification represented fold changes of mRNA expression of Sf1 and Thy-1 in the Thy-1 positive cells after Sf1 transfection. The cells were transfected in their 3rd month of *in vitro* cultivation and the mRNA expression was then tested at three interval periods 2, 4 and 7 days after transfection. Three biological replicates were used in this experiment. Summarized one-way ANOVA results showed significant ** ($P<0.01$) increase in Sf1 expression.

Changes in the key steroidogenic pathway genes were detected in response to Sf1 transfection (Figure 4.9, Figure 4.10). In comparison with untreated cells and the cells that transfected with native-plasmid, the expression of steroidogenic gene Cyp11A1 increased in response to the Sf1 transfection and this increase was elevated with time after transfection, which reached a significant increase ($P< 0.05$) after 7 days of Sf1 transfection (Figure 4.9). This elevated increase of Cyp11A1 might indicate that Sf1 transfection triggers the differentiation of Thy-1 positive cells.

In comparison with untreated cells mean 3βHSD mRNA expression was also increased in response to the Sf1 transfection but this increase was not significant ($P \geq 0.05$) at either 2,4 or 7 days (Figure 4.9).

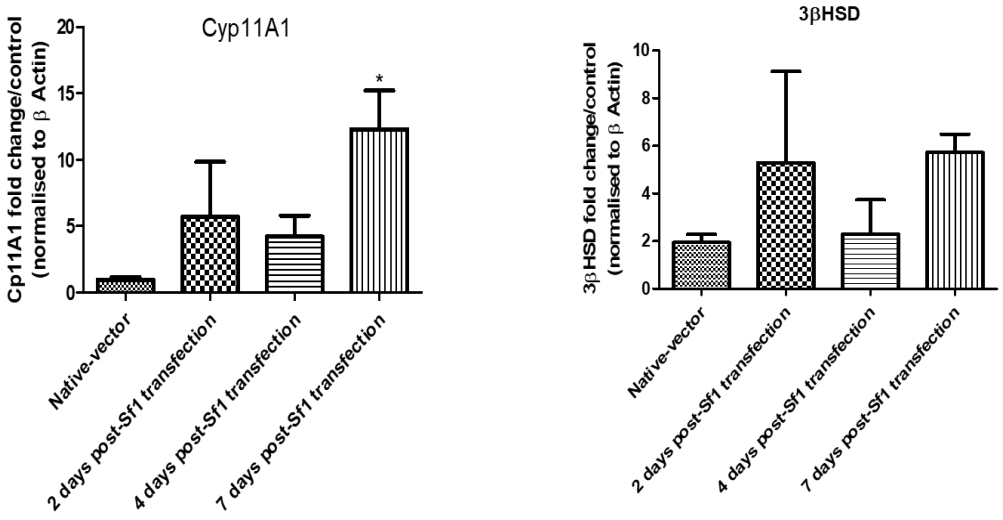

Figure 4.9 RT-qPCR relative quantification represented fold changes of mRNA expression of 3βHSD and CYP11A1 in the Thy-1 positive cells after Sf1 transfection. The cells were transfected in their 3rd month of *in vitro* cultivation and the mRNA expression was tested at three interval periods 2, 4 and 7 days after transfection. Three biological replicates were used in this experiment. Summarized one-way ANOVA results showed significant * ($P<0.05$) increase in Cyp11A1 expression.

Cyp21mRNA expression showed a minimal not significant ($P \geq 0.05$) response to Sf1 transfection (Figure 4.10) in all testing periods. In comparison with untreated cells and the cells that transfected with native-plasmid. Gli1 mRNA expression showed a gradual increase after Sf1 transfection (Figure 4.10), and this response increased to reache a significant increase ($P< 0.05$) after 7 days of Sf1 transfection.

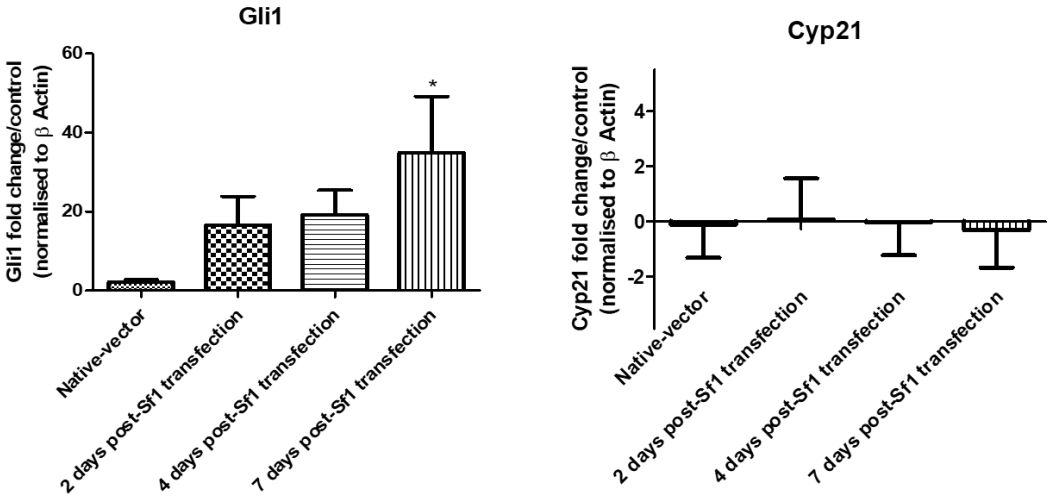

Figure 4.10 RT-qPCR relative quantification represented fold changes of mRNA expression of Gli1 and Cyp21in the Thy-1 positive cells after Sf1 transfection. The cells were transfected in their 3rd month of *in vitro* cultivation and the mRNA expression was tested at three interval periods 2, 4 and 7 days after transfection. Three biological replicates were used in this experiment. Summarized one-way ANOVA results showed significant * ($P<0.05$) increase in Gli1 expression.

ID4 and Tert mRNA expression both decreased dramatically after Sf1 transfection in all the test periods (2, 4 and 7 days), in comparison with untreated cells. ID4 showed a significant decrease ($P < 0.05$) after 7 days of Sf1 transfection. This decline in ID4 expression confirm the differentiation effect of Sf1 transfection. However, ID4 expression also showed non-significant ($P \geq 0.05$) decreased in the cells that were transfected with native-plasmid (Figure 4.11).

Tert was decreased to 0.1 fold, 2 days after Sf1 transfection. This decrease continued to reach the 4th day after Sf1 transfection then the cells lost Tert mRNA expression after 7 days after Sf1 transfection. However, Tert also decreased slightly in the cells that were transfected with native-plasmid (Figure 4.11).

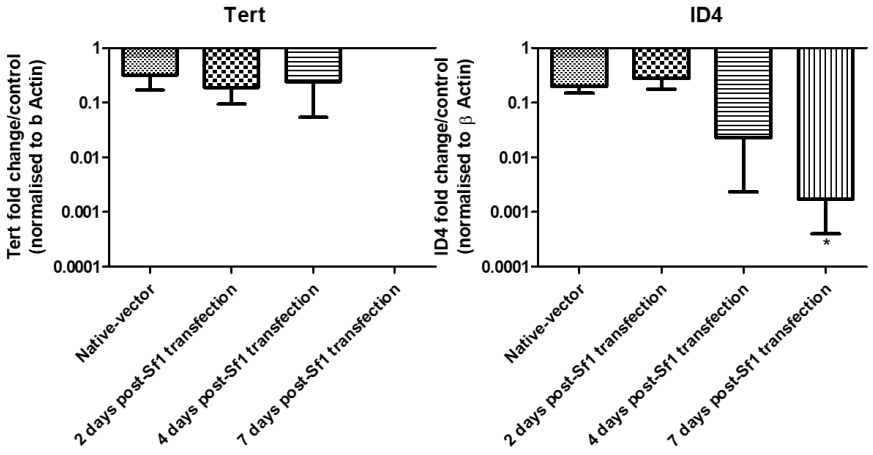

Figure 4.11 RT-qPCR relative quantification represented fold changes of mRNA expression of ID4 and Tert in the Thy-1 positive cells after Sf1 transfection. The cells were transfected in their 3rd month of *in vitro* cultivation and the mRNA expression was tested at three interval periods 2, 4 and 7 days after transfection. Three biological replicates were used in this experiment. Summarized one-way ANOVA results showed significant * ($P<0.05$) decrease in ID4 expression.

4.3.1.4.2 RT-qPCR of the Sf1 transfection into the Thy-1 positive cells after 8months

The RT-qPCR results of the Sf1 transfection into the Thy-1 positive cells after 8months of cultivation are demonstrated in (Figure 4.12 - Figure 4.16)

Sf1 mRNA expression showed a high significant increase ($P< 0.01$) after Sf1 transfection in the all test periods after Sf1 transfection (2, 4 and 7 days) in comparison with the untreated cells and the cells that were transfected with native-plasmid (Figure 4.12).

In comparison with untreated cells, Thy-1 mRNA expression slightly decreased in the all test periods (2, 4 and 7 days) after Sf1 transfection which showed non-significant ($P \geq 0.05$) decrease in Thy-1 mRNA expression in comparison with the cells transfected with native-plasmid (Figure 4.12).

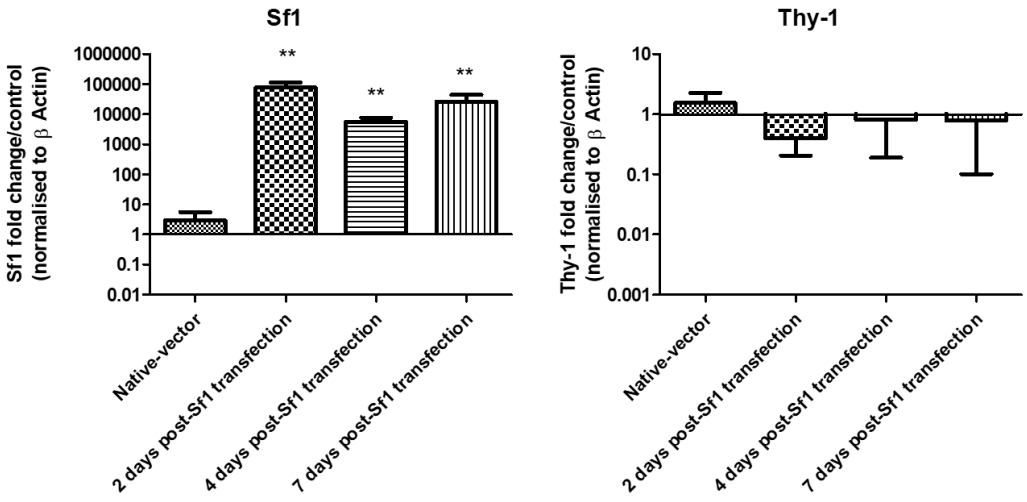

Figure 4.12 RT-qPCR relative quantification represented fold changes of mRNA expression of Sf1 and Thy-1 in the Thy-1 positive cells after Sf1 transfection. The cells were transfected in their 8th month of *in vitro* cultivation and the mRNA expression was tested at three interval periods 2, 4 and 7 days after transfection. Three biological replicates were used in this experiment. Summarized one-way ANOVA results showed significant ** ($P<0.01$) increase in Sf1 expression.

Changes in key steroidogenic pathway genes were detected in response to Sf1 transfection (Figure 4.12). The first steroidogenic gene Cyp11A1 has a slight increase in expression in response to the Sf1 transfection at 2 and 4 days after transfection. Furthermore, a significant increase ($P< 0.05$) in Cyp11A1mRNA expression was recorded after 7 days of Sf1 transfection, in comparison with untreated cells and the cells that were transfected with native-plasmid (Figure 4.13). In comparison with untreated cells and the cells that transfected with native-plasmid, 3βHSD mRNA expression was also increased in response to the Sf1 transfection and this increase elevated with time after Sf1 transfection, which reached a significant increase ($P< 0.05$) after 7 days of Sf1 transfection (Figure 4.13).

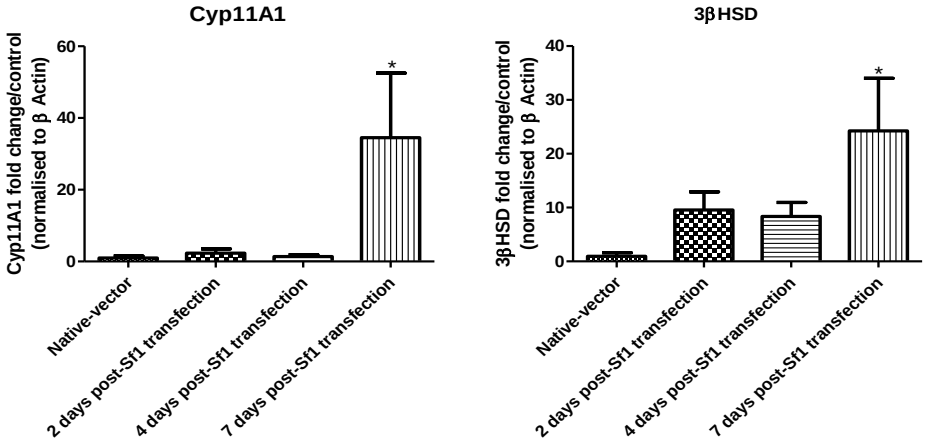

Figure 4.13 RT-qPCR relative quantification represented fold changes of mRNA expression of Cyp11A1 and 3βHSD in the Thy-1 positive cells after Sf1 transfection. The cells were transfected in their 8th month of *in vitro* cultivation and the mRNA expression was tested at three interval periods 2, 4 and 7 days after transfection. Three biological replicates were used in this experiment. Summarized one-way ANOVA results showed significant * ($P<0.05$) increase in Cyp11A1 and 3βHSD expression.

ID4 mRNA expression as in the previous experiment decreased after Sf1 transfection in all test periods (2, 4 and 7 days) in comparison with untreated cells. However, this reduction in ID4 expression was not significant ($P \geq 0.05$) in comparison with untreated cells and cells transfected with native-plasmid (Figure 4.14). While Gli1 mRNA expression recorded gradual non-significant ($P \geq 0.05$) increase after Sf1 transfection in comparison with untreated cells and cells that transfected with native-plasmid (Figure 4.14).

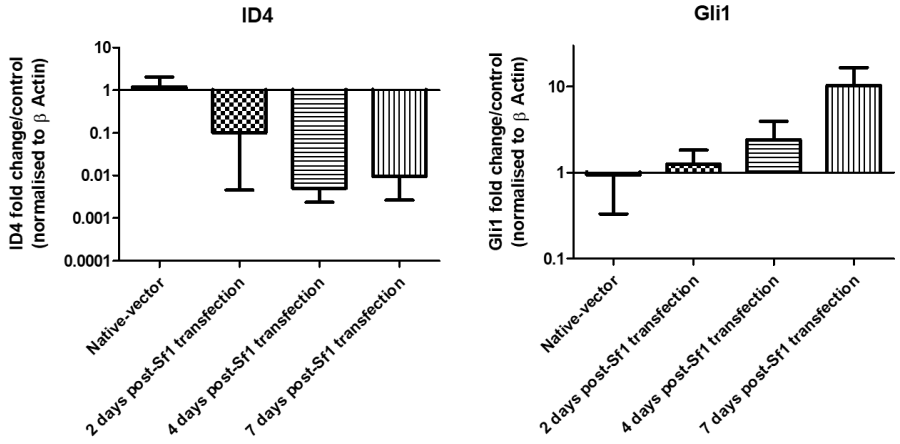

Figure 4.14 RT-qPCR relative quantification represented fold changes of mRNA expression of Gli1 and ID4 in the Thy-1 positive cells after Sf1 transfection. The cells were transfected in their 8th month of *in vitro* cultivation and the mRNA expression was tested at three interval periods 2, 4 and 7 days after transfection. Three biological replicates were used in this experiment.

Tert expression showed a slight but not significant ($P \geq 0.05$) decrease after Sf1 transfection in all test periods (2, 4 and 7 days after Sf1 transfection) in comparison with untreated cells and in the cells that were transfected with native-plasmid (Figure 4.15). While Cyp21mRNA expression showed a weak, non-significant ($P \geq 0.05$) and irregular response to Sf1 transfection (Figure 4.15) in all test periods (2, 4 and 7 days) in comparison with untreated cells and the cells that were transfected with native-plasmid.

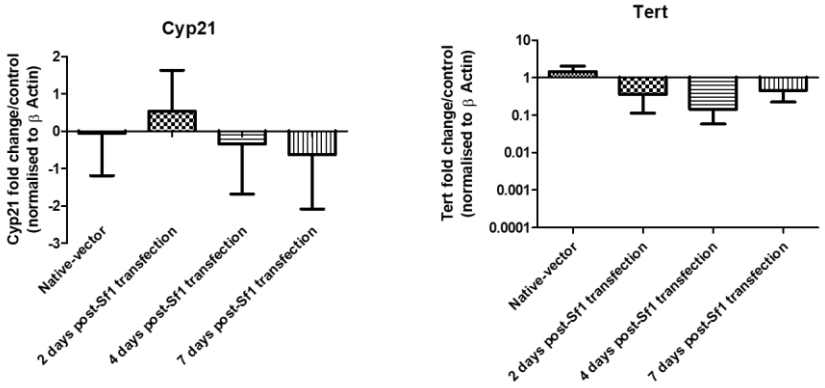

Figure 4.15 RT-qPCR relative quantification represented fold changes of mRNA expression of Cyp21 and Tert in the Thy-1 positive cells after Sf1 transfection. The cells were transfected in their 8th month of *in vitro* cultivation and the mRNA expression was tested at three interval periods 2, 4 and 7 days after transfection. Three biological replicates were used in this experiment.

4.3.1.5 Immunocytofluorescence detection of Thy-1, GFP and Sf1 after transfection Thy-1 positive cells with Sf1

The RT-qPCR results of the transfected Thy-1 positive cells of both periods (3rd month and 8th month) showed a high significant (P< 0.01) increase in Sf1 mRNA expression which in turn influenced changes in the expression of the other genes of interest. This increase in Sf1 after transfection and its effects especially on the expression of Cyp11A1, Gli1, ID4 and 3βHSD might be relevant to the activity of Sf1 protein as a nuclear receptor and differentiation factor.

Therefore, in order to confirm the high significant increase (P< 0.01) in Sf1 expression, this experiment was conducted to detect the Sf1 protein expression and the co-expression of Sf1 with the GFP from the vector in Thy-1 positive cells.

Dual-staining immunocytofluorescent assays were conducted to investigate the Sf1 protein expression in the Thy-1 positive cells after Sf1 transfection.

The transfected cells were subjected to test using a dual-staining immunocytofluorescent assay two days after transfection. The results of the transfection experiments (Figure 4.16) in the Thy-1 positive cells at three months showed the co-expression of SF1 protein expression in the nucleus (detected by anti-Sf1 antibody) with gene fluorescent protein (GFP) expression in the cytoplasm (from the GFP in the pIRES2 EGFP vector). The results of the transfection experiments in the Thy-1 positive cells at eight months also showed the co-expression of SF1 protein expression in the nucleus (detected by anti-Sf1 antibody) with GFP expression in the cytoplasm (from the GFP in the pIRES2 EGFP vector). Also, few cells with low Thy-1 expression showed the co-expressionof Sf1 in the nucleus with GFP expression in the cytoplasm (Figure 4.17), which might be related the negative effect of differentiation on the expression of Thy-1.

Figure 4.16 Dual-Immunocytofluorescence staining on 3 months old cultures of Thy-1 positive cells isolated using MACS and transfected with the rat Sf1 gene cloned into the pIRES2 EGFP vector. Cells were fixed 2 days after transfection and incubated with mouse anti-Thy-1 antibody (B), incubated with a rabbit anti-Sf1 antibody (Abcam) (C) before detection with anti-mouse Alexa 546 and anti-rabbit Alexa 647. The GFP expression from pIRES2 EGFP vector is shown in (D). All samples were mounted and cell nuclei were stained with DAPI in (A). Merged images of (A), (B), (C) and (D) are shown in (E). Arrow in (C) refers to the Sf1 expression in the nucleus of the cells. Circles in (D) refer to the GFP expression from the pIRES2 EGFP vector in the cytoplasm of the cells. Scale bars: 20µm.

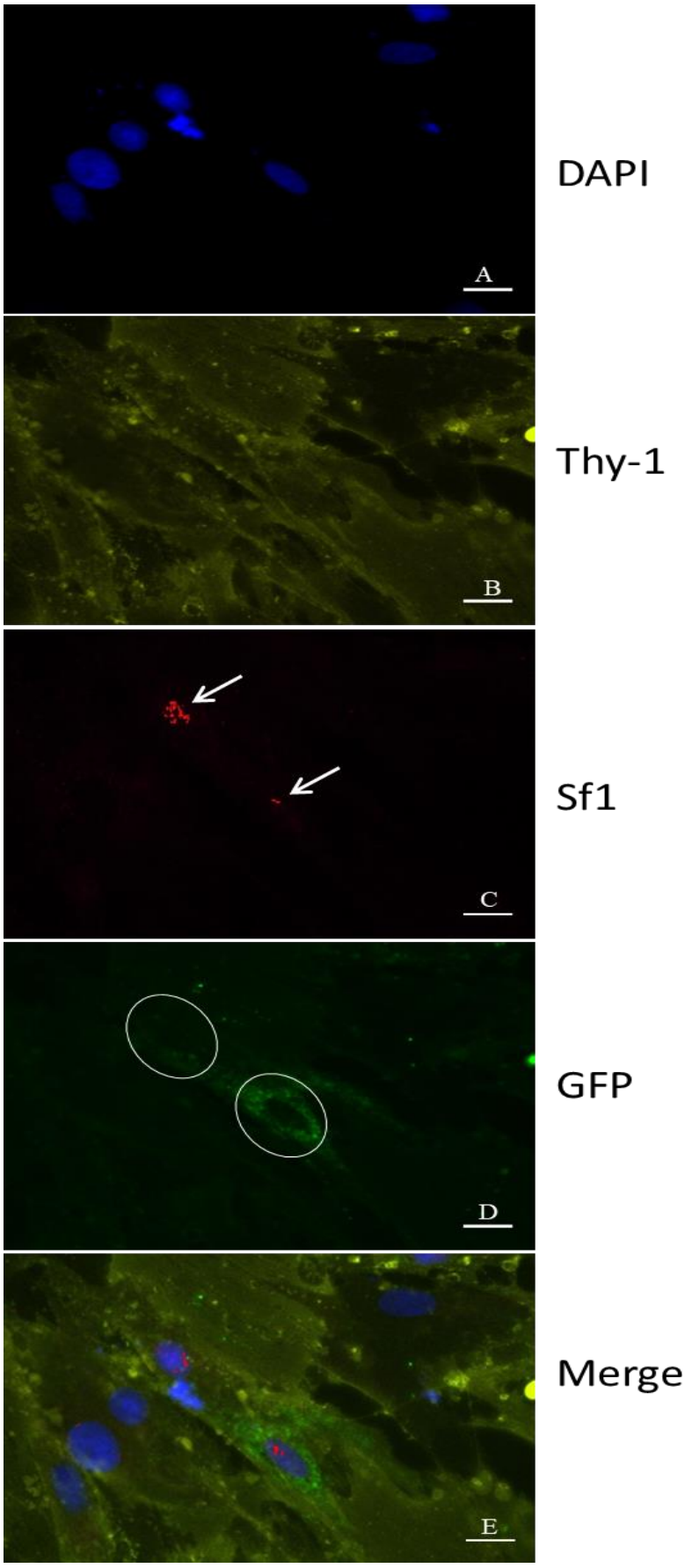
DAPI
A
Thy-1
B
Sf1
C
GFP
D
Merge
E

Figure 4.17 Dual-Immunocytofluorescence staining on 8 months old cultures of Thy-1 positive cells isolated using MACS and transfected with the rat Sf1 gene cloned into the pIRES2 EGFP vector. Cells were fixed 2 days after transfection and incubated with mouse anti-Thy-1 antibody (B), incubated with a rabbit anti-Sf1 antibody (Abcam) (C) before detection with anti-mouse Alexa 546 and anti-rabbit Alexa 647. The GFP expression of the pIRES2 EGFP vector is shown in (D). All samples were mounted and cell nuclei were stained with DAPI in (A). Merged images of (A), (B), (C) and (D) are shown in (E). Arrows in (C) refer to the Sf1 expression in the nucleus of the cells. Circles in (D) refer to the GFP expression from the pIRES2 EGFP vector in the cytoplasm of the cells. Scale bars: 20µm.

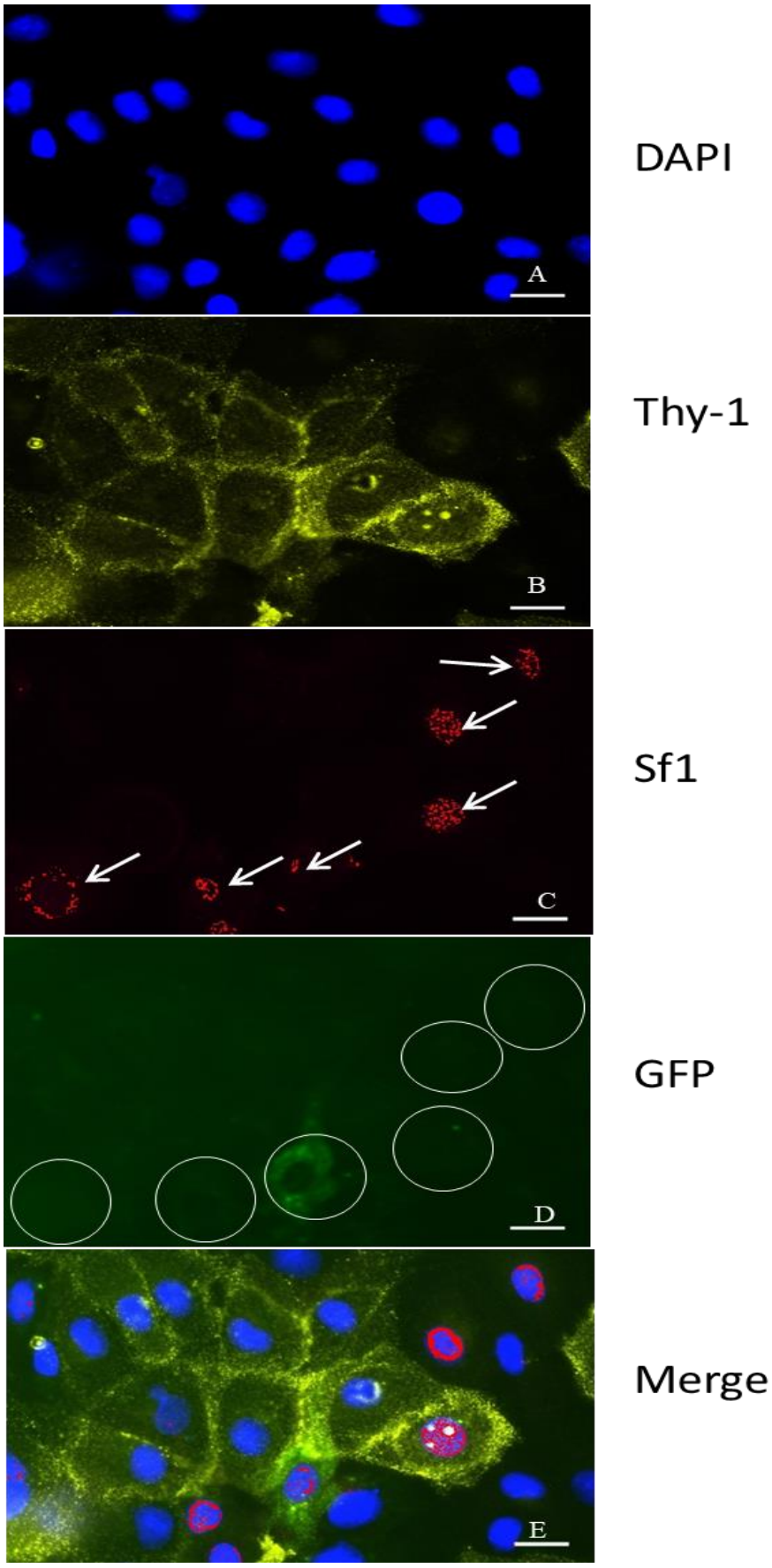
DAPI
A
Thy-1
B
Sf1
C
GFP
D
Merge
E

The results of this chapter described attempts conducted to promote the differentiation process in Thy-1 positive cells using external factors (ACTH, forskolin and the naturally produced POMC from AtT20 cell line), which all failed to induce differentiation. However, the transfection of Thy-1 positive cells with Sf1 gene up-regulated mRNA expression of a number of steroidogenic enzymes and Gli1 (progenitor cells marker) in addition to decrease expression of ID4 (differentiation inhibition marker). All these findings support that Sf1 transfection initiates the differentiation process. All these results of Sf1 transfection can be summarised in (table 4.2).

Table 4.2 Summary of the effects of Sf1 transfection to the Thy-1 positive cells on the expression of the genes of interest that related to the differentiation response.

Parameter	**Young Thy-1 positive cells (3 months)**	**Old Thy-1 positive cells (8 months)**
Sf1	Highly increased	Highly increased
Cyp11A1	Increased	Increased
3βHSD	Increased	increased
Cyp21	NO	NO
ID4	Decreased	Decreased
Thy-1	No	Decreased
Gli1	Increased	Increased
Tert	Decreased	Decreased

5.3 Discussion

Differentiation process normally occrues during development and proceeds to adulthood, in which cells divide to change from the non-specialised cell into the more specialised daughter cell. Differentiation is important for the normal cell turnover that maintains organs and to repair damaged tissues after injuries. During the embryonic development and adult cell differentiation, the gene expression patterns of the primary cell determine its fate as differentiated cells with a specific phenotype. During the development and the formation of the adrenal cortex, the minority of AGP cells that migrate dorsomedially and distant to form adrenal foetal zone start expressing higher levels of SF1 as the first characteristics of their differentiation (Xing et al., 2015). Therefore, the *in vitro* differentiation attempts basically seek for imitate the differentiation process that accrues *in vivo*.

Thy-1 positive cells previously isolated using MACS were generally undifferentiated cells and they have several characteristics of mesenchymal stem cells. One of the main aspects of stem cells is their potential capacity to differentiate into their original somatic cell types. So, investigations of the Thy-1 positive cells were carried out to test their differentiation capacity. The choice of differentiation factors in this study was initially based on the expected effect of these factors on the target cells.

The first attempt to differentiate Thy-1 positive cells was conducted using different concentrations of the differentiation factors forskolin, ACTH and AT20 cell line media. forskolin induces differentiation by stimulating intracellular cyclic AMP production, which in turn induces differentiation (Bhattacharya et al., 2012, Gilissen et al., 2015). The release of cyclic AMP as a differentiation factor normally occurs after activation of a steroidogenic receptor, such as when ACTH or FSH bind to its receptor, which stimulates cyclic AMP production (Bhattacharya et al.,

2012, Beall and Sayers, 1972). However, Thy-1 positive cells showed no significant ($P \geq 0.05$) increase in the expression of steroidogenic genes (CYP11A1 and 3βHSD), and SF1 after 7 days of treatment with forskolin.

There are several reasons that might be behind the un-successful differentiation attempt using forskolin: several differentiation attempts carried out using forskolin to differentiate MScs into neurons suggested that cAMP pathway that induces differentiation by Forskolin was proposed to be involved in changing the morphology of the cells but not the expression of the growth associated protein that changed MSCs into neurons (Wislet-Gendebien et al., 2012). Other researcher concluded that cAMP could not complete the differentiation of bone marrow derived MSCs and most of differentiation effect result from modifying the culture conditions rather than the forskolin treatment (Rooney et al., 2009, Zhang et al., 2011).

ACTH and AT20 cell line media (as a source of normal POMC peptides) also failed to induce differentiation in the Thy-1 positive cells. The differentiation effects of ACTH required the presence of its receptor in the cell membrane. Thy-1 positive cells lacked the expression of the melanocortin receptor type 2 (MC2R), which is specific for ACTH. In general, Thy-1 positive cells showed no significant ($P \geq 0.05$) increase in the expression of steroidogenic genes (CYP11A1 and 3βHSD), and SF1 after 7 days of any of the three external treatments.

The second attempt to differentiate Thy-1 positive cells was conducted by transfecting these cells with Sf1 gene. Sf1 has been used in several differentiation experiments on a variety of stem cell types, for example with the mesenchymal non-steroidogenic stem cells (Yazawa et al., 2015) and murine embryonic stem cells (Jadhav and Jameson, 2011). Three steroidogenic genes were

basically proven to be under the regulation of Sf1: Cyp11A1 that encodes Scc (Hu et al., 2001b), *3*β*HSD* (Leers-Sucheta et al., 1997) and Cyp 21 (Lee et al., 1996).

In order to attempt to differentiate the Thy-1 positive cells, Sf1 gene expression was induced using gene cloning and mammalian cells transfection. The full coding sequence of the rat Sf1 was amplified successfully using specific primers during a PCR experiment, this was followed by another PCR experiment using specific primers which have the same sequence as the first primers but with a restriction site added to the 5` of each primer using the previous PCR product as a template in order to flank the Sf1 amplicon with these two restriction sites (EcoR1 and BamHI). Flanking the amplicon with restriction sites was achieved successfully and was followed by successful digestion of the amplicon and the vector at both restriction sites (EcoR1 and BamHI). The following steps of ligation the Sf1 amplicon into the vector and transformation of competent *E.coli* with the construct (Sf1-vector) was achieved successfully. Targeted colonies were picked and tested for possession of the vector and the Sf1 amplicon using PCR and sequencing, and the digestion showed the expected size of both Sf1 amplicon and the vector. Since all test were positive for the presence of the Sf1 insert, the construct was purified using midiprep kit in order to transfect Thy-1 positive cells because the transfection required relatively high volumes and quality above what the miniprep kit can provide. Plasmid transfection into Thy-1 positive cells was conducted at two-time points during their one year of *in vitro* cultivation: at three months and eight months after initial isolation. Three months after isolation the cells were tested and they were mainly found to be undifferentiated. While eight months after isolation the cells remained undifferentiated but they were transforming to immortal *in vitro* as previously discussed in chapter three. This cloning process of the Sf1 coding sequence into the pIRES2 EGFP vector followed by transfection into Thy-1 positive cells was conducted to induce

temporary expression of the Sf1 gene in the cells to attempt differentiation. The successful transfection was achieved after several optimisation experiments which were analysed one day after transfection with both plasmids (with the Sf1 gene and the native-plasmid). The changes in Sf1 gene expression and other genes of interest in the transfected cells were tracked using RT-qPCR and immunocytofluorescence assays.

The RQ analysis of RT-qPCR assays showed a significant ($P< 0.01$) increase in Sf1 expression which up-regulated Sf1 to over 4000 fold in the treated cells in comparison with untreated cells and the cells that were transfected with native-plasmid. This high Sf1 mRNA expression was expected because of the cytomegalovirus (CMV) promoter up-stream the Sf1 gene in the pIRES2 EGFP vector. This significant expression of Sf1 mRNA was maintained for at least 7 days after transfection in both experiments which were conducted during the third month and the eight month after isolation which might be maintained because of the low proliferation rate of the Thy-1 positive cells in their 3rd month *in vitro*. However, the old Thy-1 positive cells in their 8th month *in vitro* showed also high significant increase ($P< 0.01$) in Sf1 expression that continued for 7 days after Sf1 transfection in spite of their high proliferation rate.

Tert associated with telomere maintenance is one of the cellular reprogramming factors that are related to pluripotency of embryonic stem cells (Orkin and Hochedlinger, 2011) and is highly expressed in spermatogonial stem cells (Bai et al., 2016). However, in this study, the Ct values of this epigenetic factor were around 30 cycles in the untreated cells after three months and eight months of isolation which represents very low mRNA expression. However, the transfection with Sf1 lowered the Tert expression in both Sf1 treated groups and this reduction in Tert expression continued with time after transfection to reach its lowest expression 7 days after Sf1 transfection for the 3 months group (Figure 4.11). The reduction in Tert expression due to Sf1

transfection in the 8 months group was also in similar pattern of the 3 months group (Figure 4.15). Although the adult normal adrenal cortex cells do not have telomerase activity (Yang et al., 2001), long-term *in vitro* cultivation might induce a number of epigenetic key factors such as Tert due to distribution of *in vitro* environment (Gabory et al., 2011).

ID4 mRNA expression was recorded to have a gradual decrease in both Sf1 transfection groups with continues reduction 2, 4 and 7 days after Sf1 transfection respectively. This reduction in ID4 mRNA expression after Sf1 transfection reached a significant ($P< 0.05$) decrease after Sf1 transfection in the 3rd month group. This reduction in ID4 mRNA expression was in agreement with the role of ID4 as an inhibitor of differentiation (Patel et al., 2015) which confirm the differentiation effect of Sf1 transfection.

Gli1 mRNA expression showed a gradual non-significant ($P \geq 0.05$) increase after 2 and 4 days of Sf1 transfection in both groups (3rd month and 8th moth groups). However, Gli1 mRNA expression reached a significant increase ($P< 0.05$) after 7 days of Sf1 expression in the 3rd month group. This up-regulation of Gli1 expression due to Sf1 transfection might be related to the proposed role of Gli1 in the progenitor transition between stem cell and differentiated cells (Kim et al., 2009).

The main target of Sf1 transfection is to enhance the expression of the steroidogenic genes that represent in the differentiated adrenocortical cells (Cyp11A1, 3βHSD and Cyp21) because several studies refer to Sf1 as a regulator of steroidogenic genes (Val et al., 2003). Others suggested Sf1 initiates differentiation of MSCs to steroidogenic lineage (Mizutani et al., 2015). Both Cyp11A1 and 3βHSD were significantly ($P \geq 0.05$) up-regulated after Sf1 transfection in the 8th month group and Cyp11A1 showed significant ($P \geq 0.05$) increase after

Sf1 transfection in the 3rd month group, which suggested that Sf1 might start steroidogenesis in the Thy-1 undifferentiated cells which was in agreement with Mizutani et al., (2015). This up-regulating effect of Sf1 to Cyp11A1 might due to the two binding sites that Sf1 has at −40 and −1,600 upstream the CYP11A1 gene which triggers CYP11A1 cAMP-dependent gene expression *in vitro* (Guo et al., 1994, Watanabe et al., 1994, Hu et al., 2001a). Sf1 also regulates the 3βHSD gene (Baba et al., 2014). However, Cyp21 did not show any significant ($P \geq 0.05$) response to Sf1 transfection.

Immunocytofluorescence assays were conducted to reveal the presence of Sf1 protein expression in the nucleus after transfection and if it co-expressed with GFP protein. The up-regulation of Sf1 mRNA expression after transfection might not result in the functional translation of Sf1 protein which localised in the nuclei of the transfected cells. Therefore, immunocytofluorescence assays were required to confirm the protein expression of Sf1 in the nucleus, which was expected to initiate the differentiation by up-regulating the expression of Cyp11A1 and 3βHSD. The immunocytofluorescence results confirmed that and showed the Sf1 protein expression in the transfected cells in both groups. The green fluorescent protein in the cytoplasm co-expressed with the Sf1 protein expression in the nucleus, which indicated that the transfection of Thy-1 positive cells with Sf1 gene successfully increased functional protein expression of Sf1.

In general, the differentiation response of Thy-1 positive cells after force expression of Sf1 was in agreement with a number of attempts used Sf1 to differentiate stem cells. The capacity of Sf1 protein to differentiate several stem cell types into steroidogenic lineage has been reported in mesenchymal stem cell types such as bone marrow stem cells (Gondo et al., 2004) and adipose tissue-derived stem cells (Gondo et al., 2008) and even embryonic stem cells (Jadhav and Jameson, 2011).

Chapter five

General discussion and future work

5.1 Detection of potential adrenocortical stem cell marker mRNAs and proteins

The aims of this study were primarily to isolate and study the adrenocortical stem cell *in vitro* because it had been described before as a difficult goal "It has proven difficult to isolate and characterise adrenocortical stem cell populations" (Pihlajoki et al., 2015).

This project started with bioinformatics analysis of a whole rat adrenal transcriptome microarray data set. The data showed the expression of potential stem or progenitor cell markers based on their high expression in the capsule, or capsule and zI, in comparison with zF, because most of the research referred to these two zones (capsule and zI) as potential stem cell niches. The potential stem cell markers expressed in the capsule or capsule and zI when compared with zF displayed a 50-800 fold increase in expression. Over 60 potential stem/progenitor cell markers of the rat whole transcriptome were observed. Criteria for selection of these 60 potential stem cell markers were constructed based on a combination of the bioinformatics analysis results of the array data and the information in the literature. The literature criteria implied potential roles in stem/progenitor cell characteristics, cell proliferation, and cell migration. In addition, we included the rarely studied proteins that showed high expression in the capsule of the adrenal cortex. Three potential markers were selected to be tested: Transmembrane protein121 (Tmem121), Thy-1 cell surface antigen (Thy-1) and Krüppel-like factor 5 (KLF5).

Several molecular experiments were conducted in order to examine the existence of these markers followed by cloning into the p-GEM®-T Easy vector. This was followed by *in vitro*

transcription to produce probes to detect the mRNA expression patterns of these markers in the rat adrenal cortex by FISH. Immunohistofluorescence experiments also followed to detect the localisation of the proteins of interest in adrenal sections.

In situ hybridisation experiments faced a number of difficulties and took a long time to be successful. Several *In situ* methods were conducted to achieve *in situ* hybridisation, these included the whole mount *in situ* hybridisation procedure described by (Nieto et al., 1996), as well as wax and cryosection *in situ* hybridisation protocols. Although the best working protocol with the adrenal sections was found to be the one described by (Lomthaisong, 2001), several modifications were required to reduce RNA degradation and increase the stringency such as increasing the hybridisation temperature and only using RNase free material.

The *in situ* hybridisation results confirmed the microarray data and showed mRNA expression of the genes of interest in the capsular and the sub-capsular areas of the adrenal cortex (Figure 2.9).

Klf5 mRNA had a high narrow and intense expression in the capsule with weak and expanded expression in the zG and zF (Figure 2.9). The Klf5 protein expression pattern was in agreement with *in situ* hybridisation with a low-level expansion in the zG and Zf, meaning that not all the mRNA was transcribed to protein. Although the Klf5 protein is considered to be one of the pluripotency markers in certain embryonic stages (Hou et al., 2016), the expansion of Klf5 protein expression in the two main differentiated zones (zG and zF) might not be related to the pluripotent stem cells within the adult adrenal cortex. This result suggested that Klf5 is not a stem cell marker in the adrenal cortex.

Tmem121 mRNA expression was high in the capsule, but it showed a minor expansion in the zG, this pattern of expression represents most of the capsular area and a small fraction of the zG. The Tmem121 protein expression agreed with the *in situ* hybridisation results. The long

expanded line of Tmem121 protein expression along with capsule and sub-capsular areas reduced the probability of considering the Tmem121 from being a stem cell marker. This possible exclusion of Tmem121 can be explained by the presence of stem cell populations within the adult tissue, which have a limited existence, as seen in adipose tissue (Zaman et al., 2014), heart (Navarro-Betancourt and Hernandez, 2015) and bone-marrow (Guerin et al., 2015), which represent less than 0.1% of the main cell populations. However, this interesting expression pattern of Tmem121 might suggest a role for Tmem121 in adrenal cortex cell proliferation and migration, because the adrenal cortex undergoes centripetal migration that starts from the subcapsular area towards the adrenal cortex medulla border where the cell proliferation rate was high. The detection of Tmem121 protein expression co-expressing with the Ki67 proliferation marker (Figure 2.13), primarily revealed a high co-expression between the two proteins (0.74 according to Spearman's rank correlation value). This value may refer to the existence of Tmem121 protein during cell proliferation (based on the Ki67) and that it might participate or have a role in cell proliferation, but it might not be essential to this process since not all the proliferative cells were expressing it. The interesting finding regarding the Tmem121 protein that related to the proliferation activity of the adrenal cortex cells suggests more investigation of the role of Tmem121 in the induction of cell proliferation is needed.

Thy-1 protein had the most potential as a marker amongst the nominated markers. Several characteristics nominated Thy-1 as a marker for isolating the potential stem cells from adrenal gland primary cells:

Firstly, the expression pattern of Thy-1 in the capsule that was distributed in a pattern of small pockets typically signifies the distribution pattern of stem cells in the adult tissues.

Secondly, the molecular structure of the Thy-1 protein in the cells as a cell surface antigen facilitated the use of a specific antibody to isolate the target cells.

Furthermore, Thy-1 has the lowest expression level in the zG and zF, these zones represent the most differentiated part of the adrenal cortex.

The results of *in situ* hybridisation and immunohistofluorescence experiments aimed to establish expression in the capsule and sub-capsular area as the stem cells niche. In this study we excluded the adrenal cortex zI, in spite of Mitani et al.,(2003) suggestion, which refers to the zI as stem/progenitor cell niche. This suggestion might be down to strain differences in the rats used in the experiments as we used the Wistar-rats strain, while Mitani and co-workers used Sprague-Dawley strain. It has also been suggested that the adrenal cortical stem cells are Sf1 negative but the progenitor cells are Sf1 positive as they start to express Sf1 before differentiation and commencing steroidogenesis (Kim et al., 2009). In our study, the mRNA expression of Sf1 (Figure 2.9) and protein expression of SF1 (figure 3.15) was detected in most of the adrenal cortex including the area where zI expected to be.

Generally, our results showed that a few cells within the capsule express a high level of the Thy-1 protein, which represents a specific cell type within the capsule, that might be stem cells according to the most identified adrenal cortex stem cells hypothesis (Walczak and Hammer, 2015).

5.2 Isolation and characterisation of Thy-1 positive cells

Chapter 3 demonstrated the isolation of Thy-1 positive cells and the study of them *in vitro* because it is difficult to investigate cell behaviour *in vivo*. Isolation and investigation of Thy-1 positive cells *in vitro* created an effective approach involving primary culture to investigate the cellular and molecular mechanisms controlling the cell behaviour. Once the FISH and immunostaining assays analysis suggested the Thy-1 protein as robust potential stem cell

marker, the isolation of Thy-1 positive cells from the primary culture of rat adrenal gland was determined. Before starting the isolation process using MACS, two main preparations were required:

First, an adequate amount of monoclonal anti-Thy-1 antibody was required for the isolation process and later *in vitro* assays. This was accomplished in-house by maintaing of the OX-7 hybridoma cells in specific media to produce an adequate amount of the monoclonal anti-Thy-1 antibody. The production of monoclonal anti-Thy-1 antibody was successful and confirmed using SDS-PAGE electrophoresis with Coomassie Blue staining (figure 3.4) and Western blotting (figure 3.5). The binding capacity and specificity of the anti-Thy-1 antibody were validated by immunocytofluorescence tests (figure 3.9) and Western blotting (figure 3.21). The large-scale production of this antibody was also important to conduct the later experiments.

Second, primary culture of rat adrenal gland was accomplished using mechanical and enzymatic digestion, yielding viable primary cells from the whole adrenal gland. The isolated primary cells showed expected hormonal response towards ACTH treatment, which was another indicator of cell interaction with it's *in vitro* environment. Further adrenal gland primary cultures were conducted after removing the medulla and the un-targeted part of adrenal gland. Our findings suggested the isolation of the target cells after enucleating and discarding of the medulla and most of the zF, instead of using the whole adrenal would eliminate most of the differentiated cells of the cortex as well as the medulla. However, the zI was not the main target of this study since Thy-1 expression was confined to the capsule and sub-capsular areas.

MACS was carried out using the anti-Thy-1 antibody to enrich the Thy-1 positive cells of the adrenocortical primary cultures. MACS is a well-documented method used for isolating target cells such as stem cells (Amiri et al., 2015, Zhong et al., 2015).

The primary diagnosis of Thy-1 positive cells using a light microscope under the 10x power showed fibroblastic-like cells. These cells traditionally represented the capsular cells that were described as fibroblast-like capsular cells (Kim and Hammer, 2007a). The cells use to have long thin cytoplasmic extensions called telopods or projections, which might have a role in forming differentiated cells of the adrenal cortex (Baker, 1952). The cells showed MSC characteristics *in vitro* such as attaching to plastic and they tended to form colonies (Castro-Malaspina et al., 1980, Colter et al., 2001). The confluent cells also developed a whirlpool-like shape growing pattern in culture, which is in agreement with what has been described in MSCs (Pelekanos et al., 2016).

Thy-1 positive cells exhibited morphological and cellular behavioural changes during *in vitro* cultivation. For example, the division rate of the younger cells was slower than the older cells. The younger cells were more attached to the plastic surface and required trypsinisation for a long incubation time (25 minutes with TrypLE™) to detach them in comparison with the older cells, which required a shorter incubation time (10 minutes with TrypLE™) to be detached.

These changes were noticed during routine monitoring work such as changing the media and passaging before reaching confluency. These observations required more investigation to study the changes in the cell cycle, cell migration and the expression of proteins of interest. Therefore, the cell division rates were tracked in culture using time lapse microscopy. The cell tracking assay showed that young cells (2-6 months) especially in their 2nd month in

culture, underwent division approximately every 3 days. The old cells (10-12 months) underwent division every 36-48 hours.

While proliferation studies of rat adrenal gland primary cell culture showed the cells underwent division approximately every 2 days (after 21 days of cultivation). Then it was reduced to one division every 5 days (after 100 days of cultivation) (Arola et al., 1993), which was probably because these cells became senescent cells after 100 days of cultivation. Our results suggested Thy-1 positive cells were more stable and can survive longer *in vitro* in comparison to the whole adrenal primary culture which tends to lose its survival ability after 100 days *in vitro*. Time lapse techinque was also used to test the cell migration changes of Thy-1 positive cells using a wound-healing assay (figure 3.8). The older cells (12th months old in the culture) were significantly ($P<0.01$) migrating faster than younger cells (2nd months old in culture). These fast migrating cells were most likely immortalised cells because it is one of the characteristics of cancer cells *in vitro* because the cancer cells deform and reduce the nucleus size to minimum because it the most hardest cellular component in order to be efficiently able to pass through narrow spaces (Paul et al., 2017).

The co-existence of senescent cells among the Thy-1 positive cells (figure 3.7) was not abnormal phenomenon because it was observed in the primary culture of the rat adrenal gland (Guo and Liu, 2005). These senescent cells died after few months of cultivation potentially due to reaching the Hayflick limit (Hayflick and Moorhead, 1961). Investigating these few cells within the cells of interest revealed their common traits, which were the same as what had been recorded for senescent MSCs. These characteristics included morphological changes and reduction in both proliferation and differentiation potential (Zhu et al., 2015). This phenomenon is usually related to the age of the organism at the time of isolation (Yegorov and Zelenin, 2003). However, the senescent cells have been recorded to accompany

even the most potent stem cells such as human embryonic cells (Munoz-Espin et al., 2013) and mouse embryonic cells (Storer et al., 2013). Senescence has also been found to have a role contributing to embryonic development, growth and cell patterning (Storer et al., 2013).

Investigating Thy-1 positive cells also showed an increase in Thy-1 expression after cultivation (figure 3.21). This increase was in parallel with the ability of the cells to attach to plastic and this ability decreased when Thy-1 expression decreased in the old Thy-1 positive cells, which was in agreement with the role of Thy-1 in cell adhesion (Rege and Hagood, 2006). The cell division rate of the old cells increased in the last four months of cultivation. This increase in cell division rate in the old cells was synchronised with the decrease of Thy-1 expression. This synchronisation was in agreement with what was Thy-1 suggested mode action as a proliferation inhibitor of the primitive cord blood stem/progenitor cells (Mayani and Lansdorp, 1994).

Thy-1 positive cells survived *in vitro* for more than one year, which suggested a possible role of Thy-1 in self-renewal regulation that allows maintenance of these cells and other stem cells types for long periods *in vitro* in comparison with the differentiated cells (Ishigaki et al., 2009, Bernardo et al., 2007).

The protein expression of Thy-1 in Thy-1 positive cells was confirmed by immunocytofluorescence using an anti-Thy-1 antibody and anti-CD45 antibody as a control after 2 weeks of culture.

After eight weeks post-MACS, the immunocytofluorescence against Thy-1 revealed that it was still being expressed (figure 3.10). The immunocytofluorescence against Thy-1 also showed that the ratio of the number of cells that expressed Thy-1 was higher in comparison to the results of the first (two weeks post-MACS) immunocytofluorescence test, and the

intensity of Thy-1 expression within the cells eight weeks post-MACS was also higher than the first immunocytofluorescence test (two weeks post-MACS). This increase in the Thy-1 expression was confirmed by Western blotting (figure 3.21) and seemed to be maintained for a few months. This increase in Thy-1 expression after cultivation was in agreement with the results from RT-qPCR in human mesenchymal stem cells (Dudakovic et al., 2014).

The adrenocortical differentiated cells usually express steroidogenic genes. Therefore, Thy-1 positive cells were tested against the expression of steroidogenic genes to identify if Thy-1 positive cells were differentiated or undifferentiated cells. The RT-PCR experiments showed the cells were mainly undifferentiated cells (figure 3.11). However, these RT-PCR experiments showed the expression of other stem cell markers such as WT1, Etv5 and ID4 (figure 3.11 and figure 3.12).

The finding of WT1 expression in the isolated cells using RT-PCR was confirmed by immunocytofluorescent assay. The expression of WT1 in the adrenocortical stem cells was expected because it was described as an important protein in the embryonic development of adrenal glands because WT1 knock-out mice die at embryonic day E13.5 due to deadly defects in their urogenital system (Moore et al., 1999). It was also proposed as a factor maintaining the undifferentiated adrenal-gonadal primordium state in the adrenal gland and also as an inhibitor of the differentiation process (Bandiera et al., 2013). The same study tracked the descendants of WT1 positive cells and found they gave rise to cells which were WT1 negative but Sf1 positive and expressed steroidogenic genes. On the other hand, Shh and Gli1 were not detected in the assayed cells but both have been described as progenitor cell markers *in vivo* (Kim et al., 2009), suggesting the Thy-1 positive cells were more likely to be stem cells rather than progenitor cells.

It was important to investigate the co-expression ratios of WT1 or Sf1 with Thy-1 in Thy-1 positive cells in comparison with their co-expression in adrenal gland cryosections to reveal which factors increased after cultivation that might be related to maintaining Thy-1 positive cells for a long time *in vitro*. The observation of WT1 expression along the capsular line supports the hypothesis of the existence of capsular stem cells. The high co-localisation ratio of WT1 with Thy-1 in the adrenal gland (0.59±0.052) and the low co-expression ratio of Sf1 with Thy-1 (0.23±0.11) supported the notion of Thy-1 as a stem cell marker. Furthermore, the co-localisation of WT1 with Thy-1 increased to 90±2% in the Thy-1 positive cells after 12 weeks of cultivation. This suggested these cells were maintaining a self-renewal capacity (as one of the characteristics of stem cells) in culture and that they can survive longer in comparison with the differentiated cells (Ishigaki et al., 2009). While the Thy-1 and Sf1 positive cells were the opposite of that. The co-expression of Thy-1 with Sf1 in the adrenal gland was low (0.23±0.11) and decreased to 1±1% in the isolated cells. These results suggested that WT1 expression is important in the maintenance or activation of stem cells, which is in agreement with recent observations of nephrogenesis, which suggested a mechanism by which WT1 regulates stem cells (Akpa et al., 2016). So, the expression of Sf1 in the isolated cells might represent the presence of progenitor cells rather than differentiated cells, especially as these cells were lacking other steroidogenic genes (figure 3.11) and they represented a low ratio (1±1%) in culture.

Thy-1 positive cells also expressed transcriptional regulatory proteins (Etv5 and ID4), which are defined as stem cell markers because they contribute to stem cell properties such as the self-renewal of the spermatogonial stem cells (Wu et al., 2011, Oatley et al., 2011, Helsel et al., 2017). The high level of expression of Etv5 in the isolated cells might have the same role

in maintaining the self-renewal capacity of these cells since they survive for a long time in culture.

In addition to the role of ID4 in the self-renewal state of stem cells, it has also an important role as a differentiation inhibitor (Patel et al., 2015). Therefore, the expression of this protein in the cells of interest suggested that it maintained the undifferentiated state of the cells. The findings of two common spermatogonial stem cell markers (Etv5 and ID4) might be related to the developmental relationship between the gonads and the adrenal cortex.

The immortal transformation of the Thy-1 positive cells in the last few months *in vitro* was not only recorded in the primary culture of adult differentiated cells but also recorded in MSCs (Urraca et al., 2015). However, this transformation may not necessarily be an oncogenic transformation (Gordon et al., 2014). This transformation includes changes in cell morphology, the ability of cells to attach to plastic, cell cycle, cell migration and alteration in the expression of the proteins of interest, especially Thy-1. However, these cells remain undifferentiated because they did not show the expression of the steroidogenic genes.

One of the other aspects of the old Thy-1 positive cells was the reduction in the expression of Thy-1 protein. The changes in the morphology of old cells and their behaviour in comparison with the younger cells (especially the high division and migration rate *in vitro*) can be described as similar to the behaviour of cancer cells *in vitro*. These changes might have resulted from the reduction of Thy-1 expression in the old cells because the Thy-1 protein was shown to have an inhibitory effect on ovarian cancer cells (Zeng et al., 2009). In agreement with these findings, the progenitor cells of leukemia that are able to maintain blood cancer both *in vivo* and *in vitro* were lacking in Thy-1 expression in comparison with normal hematopoietic progenitor cells (Blair et al., 1997). These results suggest that Thy-1

might have an inhibitory role in tumourgenesis. The old Thy-1 positive cells also showed a general decrease in the expression of WT1, Etv5 and ID4.

Although, WT1 expression declined in the (cancer-like) older Thy-1 cells in comparison with its expression in the younger cells, WT1 expression in cancer cells showed slight controversial results. For example, WT1 expression has been found to be up-regulated in a number of cancer cells. However, WT1 transfection into ovarian cancer cells caused a reduction in their proliferation rate (Huo et al., 2011).

The expression of the Etv5 protein in the older Thy-1 positive cells slightly decreased in comparison with its expression in the younger cells. This slight change in Etv5 expression might result from the role of Etv5 as regulator not only of stem cells but also in cancer cells especially in ovarian cancer cells (Llaurado et al., 2012a, Llaurado et al., 2012b, Zhao et al., 2011).

The older Thy-1 positive cells showed a clear decrease in ID4 expression. The reduction of ID4 would be expected from differentiated cells (Patel et al., 2015) and the senescent cells (Zhu et al., 2015). However, the old cells were essentially undifferentiated and they were propagating in a similar manner to cancer cells. The ID4 reduction in the (cancer like) Thy-1 cells might be imputed to the number of primary cancers that showed low or no expression of the ID4 protein (Umetani et al., 2005, Wen et al., 2012, Baker et al., 2016). Although the findings of this chapter did not completely confirm the Thy-1 positive cells as stem cells, the Thy-1 positive cells exhibited the characteristics of stem cells *in vitro*.

5.3 *In vitro* differentiation of Thy-1 positive cells

Work in chapter four demonstrated the differentiation of Thy-1 positive cells. Since Thy-1 positive cells were generally undifferentiated cells and they have several characteristics of

mesenchymal stem cells. One of the main aspects of the adult stem cells is that they are multipotent.

The differentiation of different cell types including stem cells has been conducted by the scientists using several differentiation factors. During embryonic development and adult cell differentiation, the gene expression patterns of the primary cell change to determine its fate as differentiated cells with a specific phenotype. Scientists have used approaches and materials that were similar to these factors, which are normally involved inducing differentiation.

The choice of differentiation factors in this study was initially based on the expected effect of these factors on the target cells. For example, external factors such as forskolin and ACTH were used successfully to induce differentiation in several types of cells such as placental cells (Wu et al., 2013), neurones (Cao et al., 2012) and osteoblast (Li et al., 2014). The other method which was expected to induce differentiation was originally based on the development and event in the formation of adrenal cortex. These events usually start when a few AGP cells migrate dorsomedially and are destined to form an adrenal foetal zone. At that time these cells start expressing high levels of SF1 as the first characteristic of their differentiation (Xing et al., 2015). Therefore, we tried to imitate that event by transfecting Thy-1 positive cells with the Sf1 gene.

Attempts to differentiate Thy-1 positive cells were first conducted using different concentrations of forskolin, ACTH (as a synthetic form of ACTH) and AT20 cell line media (as a mouse cell product form of all POMC peptides). The differentiation pathway of both Forskolin and ACTH are quite similar, which usually starts by stimulating intracellular cyclic AMP production, which in turn induces differentiation (Bhattacharya et al., 2012, Gilissen et al., 2015). The release of cyclic AMP as a differentiation factor normally occurs after

activation of a steroidogenic receptor, such as FSH to its receptor, which stimulates cyclic AMP production (Bhattacharya et al., 2012).

However, Thy-1 positive cells showed no significant ($P \geq 0.05$) response in the expression of steroidogenic genes (CYP11A1 and 3BHSD) and SF1 after 7 days of treatment with forskolin.

The literature might explain the un-successful differentiation attempt using Forskolin. For example, the differentiation attempts that were carried out using forskolin to differentiate MScs into neurons suggested that cAMP pathway that induced by forskolin involved in changing the morphology of the cells but not the expression of the growth associated proteins that differentiate MSCs into neurons (Wislet-Gendebien et al., 2012). Other researchers concluded that cAMP could not complete the differentiation of bone marrow derived MSCs and most of the differentiation effect resulted from modifying the culture conditions rather than the forskolin treatment (Rooney et al., 2009, Zhang et al., 2011). However, Thy-1 positive cells might lack forskolin receptor or a factor of the cAMP regulatory pathway required for forskolin effect.

ACTH and AT20 cell line media also failed to induce differentiation in the Thy-1 positive cells. The differentiation effects of ACTH required the presence of its receptor in the cell membrane. Thy-1 positive cells lacked the expression of the melanocortin receptor type 2 (MC2R), which is specific for ACTH. In general, Thy-1 positive cells showed no significant ($P \geq 0.05$) response in the expression of steroidogenic genes (CYP11A1 and 3βHSD), and SF1 after 7 days of any of the three treatments (forskolin, ACTH and AT20 cell line media).

The transfection of Thy-1 positive cells with the Sf1 gene showed significant responses. Sf1 has been used in several differentiation experiments on a variety of stem cell types. For

example, Sf1 has been used to differentiate the mesenchymal non-steroidogenic stem cells (Yazawa et al., 2015) and murine embryonic stem cells (Jadhav and Jameson, 2011). Even after this study a recent literature revealed the potentials of Sf1 as a differentiation factor toward steroidogenesis which used to transform a fully differentiated cells such as urine-derived cells, fibroblasts and blood cells into human induced steroidogenic cells (Ruiz-Babot et al., 2018).

Three steroidogenic genes were proven to be under the regulation of Sf1: Cyp11A1 that encodes Scc (Hu et al., 2001b), 3βHSD (Leers-Sucheta et al., 1997) and Cyp 21 (Lee et al., 1996).

Thy-1 positive cells were transfected with the pIRES2 EGFP vector, which contained Sf1 coding sequence at two-time points during their one year of *in vitro* cultivation: at three months and at eight months after initial isolation. The cells at both of these ages were undifferentiated. However, Thy-1 positive cells in their eighth month *in vitro* were transforming into immortal cells as previously discussed. Sf1 transfection into Thy-1 positive cells was conducted to induce temporary expression of the Sf1 gene in the cells to attempt differentiation. The successful transfection was achieved after several optimisation experiments, which were analysed one day after transfection with both plasmids (with the Sf1 gene and the native-plasmid). The changes in Sf1 gene expression and other genes of interest in the transfected cells were tracked using RT-qPCR and immunocytofluorescence assays.

The RQ analysis of RT-qPCR assays showed a significant ($P< 0.01$) increase in Sf1 expression, which up-regulated Sf1 to over 4000 fold in the treated cells in comparison with untreated cells and the cells that were transfected with native-plasmid. However, the old Thy-1 positive cells in their 8th month *in vitro* showed also high significant increase ($P< 0.01$) in

Sf1 expression that continued for 7 days after Sf1 transfection, in spite of their high proliferation rate. The high relative increase in Sf1 expression came from the very weak to no expression of Sf1 in the Thy-1 cells in addition to the successful transfection.

The expression changes of several genes in Thy-1 positive cells were studied after transfection with Sf1.

The main target of Sf1 transfection is to enhance the expression of the steroidogenic genes that are represented in differentiated adrenocortical cells (Cyp11A1, 3βHSD and Cyp 21), because several studies refer to Sf1 as a regulator of steroidogenic genes (Val et al., 2003). Others have suggested Sf1 initiates differentiation of MSCs to steroidogenic lineage (Mizutani et al., 2015).

Both Cyp11A1 and 3βHSD were successfully up-regulated significantly ($P \geq 0.05$) after Sf1 transfection in the 8th month group and Cyp11A1 showed significant ($P \geq 0.05$) increase after Sf1 transfection in the 3rd month group, which suggested that Sf1 might start steroidogenesis in the Thy-1 undifferentiated cells, which is in agreement with Mizutani et al., (2015). This up-regulating effect of Sf1 to Cyp11A1 might due to the two binding sites that Sf1 has at −40 and −1,600 upstream of the CYP11A1 gene, which triggers CYP11A1 cAMP-dependent gene expression *in vitro* (Guo et al., 1994, Watanabe et al., 1994, Hu et al., 2001a). Sf1 also regulates the 3BHSD gene (Baba et al., 2014). However, Cyp21 did not show a significant ($P \geq 0.05$) response to the Sf1 transfection, which might be due to the sequence of differentiation events that required more than 7 days to show a detectable response of Cyp21, or that it required the interference of other factors.

Sf1 transfection caused a reduction in ID4 mRNA expression in both groups with continued reduction 1, 4 and 7 days after Sf1 transfection respectively. Sf1 transfection significantly ($P< 0.05$) decrease ID4 mRNA expression in the 3rd month group

This reduction in ID4 mRNA expression after Sf1 transfection was in agreement with the role of ID4 as an inhibitor of differentiation (Patel et al., 2015). Gli1 also showed a gradual but non-significant ($P \geq 0.05$) increase after 2 and 4 days of Sf1 transfection in both groups (3rd month and 8th moth groups). However, Gli1 mRNA expression reached a significant increase ($P< 0.05$) after 7 days of Sf1 expression in the 3rd month group. These changes might be related to the proposed role of Gli1 in the progenitor transition between stem cells and differentiated cells (Kim et al., 2009). From these results, we can propose that the Sf1 transfection caused the transition of Thy-1 positive cells into progenitor/differentiated cells.

Immunocytofluorescence assays also confirmed Sf1 protein expression in the transfected cells in both groups. The green fluorescent protein in the cytoplasm co-expressed with the Sf1 protein expression in the nucleus, which indicated that the transfection of Thy-1 positive cells with Sf1 gene successfully increased protein expression of Sf1. Although the expression of the genes of interest was traced only till 7 days after transfection, the characteristics of Thy-1 positive cells after transfection with Sf1 were changed toward differentiation.

The amount of time and the appropriate *in vitro* microenvironment required to reach a fully differentiated state still unknown. Therefore, we recommend further investigations to induce specific differentiation of Thy-1 positive cells, which may start with Sf1 transfection and incubation for longer than 7 days and involve other differentiation factors *in vitro*. Or re-inoculate Thy-1 positive cells into rat adrenal glands and trace their changes *in vivo*.

Other possible future work regarding differentiation may include using the properties of the adrenal cortex extracellular matrix, which is have been described as quite complex (Ruiz-Babot et al., 2015). The reasons after this complexity are related to the different extracellular matrix components (collagen IV, fibronectin, and laminin (Chamoux et al., 2001), and each of them influences adrenal cortex cells differently. For example, collagen IV or laminin were found to enhance proliferation of human fetal adrenal cells, but fibronectin was found as an inducer of cell apoptosis. Furthermore, fibronectin and laminin decreased cell sensitivity to ACTH, whereas collagen increased cell sensitivity to ACTH (Chamoux et al., 2002). These characteristics of the adrenal cortex extracellular matrix may be harness-able to the purposes of Thy-1 positive cells differentiation.

In terms of steroid identification and quantification after differentiation attempts, the future study might include the use of the multicomponent mass spectrometric detection technique. This technique can be combined to the detection of mRNA expression of the steroidogenic enzyme using RT-qPCR.

Summary

The investigation of adrenocortical stem cells in this study presented suggestion, detection and evaluation of three potential stem cells markers Klf5, Thy-1 and Tmem121. These markers showed interesting expression patterns in the adrenal cortex. However, the most representative stem cell marker (Thy-1) was used to isolate Thy-1 positive cells. The isolated cells were cultured *in vitro* and monitored for over one year. These cells demonstrated characteristics similar to those of MSCs *in vitro.* Furthermore, other stem cell markers were detected in these cells (WT1, Etv5 and ID4). These cells were tested for their potential differentiation capacity using differentiation factors such as forskolin, ACTH, AT20 cell line media and transfection with the Sf1 gene. The differentiation responses were only observed after Sf1 transfection, which significantly ($P<0.05$) elevated the expression of Gli1, Cyp11A1 and 3BHSD. This study provides seminal findings for more investigation of adrenocortical stem cells *in vitro and in vivo.*

Appendix

Appendix A: Stock solutions

A.1. 10x DNase I reaction buffer

100 mM Tris-HCl (pH 7.5)

25 mM $MgCl_2$

1 mM $CaCl_2$

A.2. cDNA synthesis 5X reaction buffer

250 mM Tris HCl (pH 8.3)

250 mM KCl

20 mM $MgCl_2$

50 mM DTT)

A.3. Buffer QC (wash buffer)

1.0M NaCl

50 mM MOPS pH 7.0

15% isopropanol

A.4. Buffer PE

10 mM Tris-HCl pH 7.5

80% ethanol

A.5. 10x ligation buffer

300mMTris-HCl (pH 7.8)
100mM MgCl2
100mM DTT and 10mM ATP

A.6.A.Luria-Bertani (LB) broth

10 g of Tryptone, 5g yeast extract and 10 g NaCl dissolved in 1 Litre of sterile distilled water and autoclaved.

A.6.B. LB agar plate

For LB agar plate: as above togather with 15g of agar. Then autoclaved and allowed to cool to 55C before addition of 2ml of 50mg/ml ampicillin in sterile distilled water. The mixture was poured into 10cm petri dishes and once set used directly or stored at 4C.

A.7. Inoue transformation buffer

Preparation of Inoue transformation buffer for Competent Cells

Inoue transformation buffer was prepared (chilled on ice bath before use). 0.5 M PIPES (pH 6.7) (piperazine-1,2-bis[2-ethanesulfonic acid]) was Prepared by dissolving 15.1 g of PIPES in 80 ml of pure H2O, the pH of the solution was adjusted to 6.7 with 5 M KOH, and then pure H2O was added to bring the final volume to 100 ml. The solution Sterilized by filtration and divided into aliquots and stored frozen at -20ºC. Inoue transformation buffer was prepared by dissolving all of the solutes listed below in 800 ml of pure H2O and then 20 ml of 0.5 M PIPES (pH 6.7) was added and the volume of the Inoue transformation buffer adjusted to 1 litter with pure H2O.

Reagent	Amount per litre	Final concentration
$MnCl_2.4H_2O$	10.88g	55mM
$CaCl_2.2H_2O$	2.20g	15mM
KCl	18.65g	250mM
PIPES(0.5 M, pH 6.7)	20 ml	10mM
H_2O	To 1 litre	

A.8.Buffer P1

- 50 mM Tris-HCl pH 8.0
- 10 mM EDTA
- 100 μg/ml RNaseA

A.9. Buffer P2

- 200 mM NaOH
- 1% SDS
- 3.0 M potassium acetate pH 5.5

A.10.Buffer N3

- 4.2 M Gu-HCl
- 0.9 M potassium acetate
- pH 4.8

A.11.Buffer PE

- 10 mM Tris-HCl pH 7.5
- 80% ethanol

A.12.Buffer P3 :

3.0 M potassium acetate, pH 5.5

A.13. Buffer QBT (equilibration buffer)

- 750 mM NaCl
- 50 mM MOPS pH 7.0
- 15% isopropanol
- 0.15% triton X-100

A.14. Buffer QC (wash buffer)

- 1.0M NaCl
- 50 mM MOPS pH 7.0
- 15% isopropanol

A.15 Buffer QF (elution buffer)

- 1.25M NaCl
- 50 mM Tris-HCl pH 8.5
- 15% isopropanol

A.16 Buffer TE

- 10 mM Tris·Cl, pH 8.0
- 1 mM EDTA

A.17.10X MULTI-CORE™ Buffer

- 250mM Tris-acetate (pH 7.5 at 37°C)
- 1000mM potassium acetate
- 100mM magnesium acetate
- 10mM DTT

A.18. 5x Transcription buffer

- 250 mM Tris-HCl (pH 8.3 at 25°C)
- 375 mM KCl
- 15 mM MgCl2

▪ 50 mM DTT

A.19. 4%PFA in PBS

For 1 L of 4% Formaldehyde, 800 mL of 1X PBS was added to a glass beaker on a stir plate in at 60 °C. 40 g of paraformaldehyde powder was added to the heated PBS solution. Once the paraformaldehyde is dissolved, the solution should be cooled and filtered. The pH, rechecked and adjusted to approximately 6.9. The volume of the solution was completed to 1 L with 1X PBS. The solution aliquoted and frozen at -20°C for up to one month.

A.20. Hybridisation buffer

50 ml of
50%Formamide
SSC (5X)
100ug/ml Fish sperm DNA (Sigma)

A.21. 20x SSC (1 litre) stock solution

1.	NaCL	175.3g
2.	Tri-Sodium citrate	88.2g
3.	Dissolve in water	800ml
4.	Adjust pH to 7.0 with 10N NaOH/HCL	
5.	DEPC	1ml

Stand at RT overnight in fume hood. Sterilise by Autoclave. 5x,2x and 0.2x SSC dilute of 20x in DEPC H2O.

A.22. RNA wash buffer

400mM NaCl

10mM TrisHCl, pH 7,5

5mM EDTA

A.23. Post-fixation solution

Prepare a solution of 2% formaldehyde in PBS, containing 20 mg/mL bovine serum albumin. This solution can be used immediately or stored at 4°C for up to six months.

A.24 PBT (500ml)

Water	500ml
PBS tablet	5

Shake properly and stand at RT overnight in fume hood, loose lid. Sterilise by Autoclave. Pre-warm the triton. Then add 500ul Triton X-100.

A.25. TMB

50mM sodium acetate anhydrous,3.6g citric acid, dissolve in 600ml water then add:

270mg TMB (from sigma) dissolved in 400ml methanol, store in dark at 4^{o}C.

Western Blotting Solution and Reagents

A.26.Loading buffer (5X):

5mL 0.3M Tris•HCl, pH6.8, 5% SDS, 50% glycerol, lane marker tracking dye

A.27. 5X Tris –Glycin electrophoresis (Running Buffer)

1 Litter:

1. 15.1g Tris base
2. 94g Glycine (in 900ml ddH_2O)
3. Then add 50ml of 10%SDS
4. Complete to 1 litter by ddH_2O

1X Tris –Glycin electrophoresis (Running Buffer)
1 Litter:

1. 200ml of 5X Tris –Glycin electrophoresis (Running Buffer)
2. Add 800ml of ddH_2O

Check the pH and adjust to pH 8.3

A.28. Transfer Buffer

1 Litter:

1. 2.9g Glycine
2. 2.8g Trise base
3. 200ml Methanol
4. Complete to 1 litter by ddH_2O

Check the pH and adjust to pH 8.3 **if necessary**

A.29. 10X Tris Buffer Saline (TBS)

1 Litter:

1. 80g of NaCl
2. 2g KCl
3. 30g Tris base
4. Add 800ml of ddH_2O

5. Adjust to the pH to <u>7.4</u> using concentrated HCl

6. Complete to 1 litter by ddH_2O

1X Tris Buffer Saline Tween (TBST)

1 Litter:

1. 100ml of 10X TBS
2. 900ml of ddH_2O
3. 1ml of Tween 20

Check the pH and adjust to pH 8.3 **if necessary**

Running Buffer 10X.

35 mM SDS	(10.08 g)
250 mM Tris	(30.3 g)
1,92 M glycine	(144g)

In one liter volume. Dilute to 1X before use

Appendix B: Vectors structure

B.1 pGEM®-T Easy Vector

showing the two EcoRI sites in the flank where the A/T cloning site

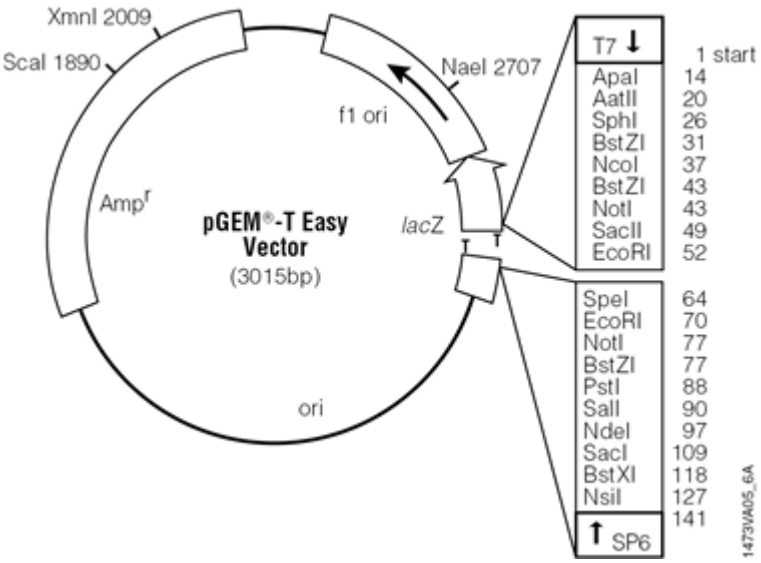

B.2. pIRES2 EGFP

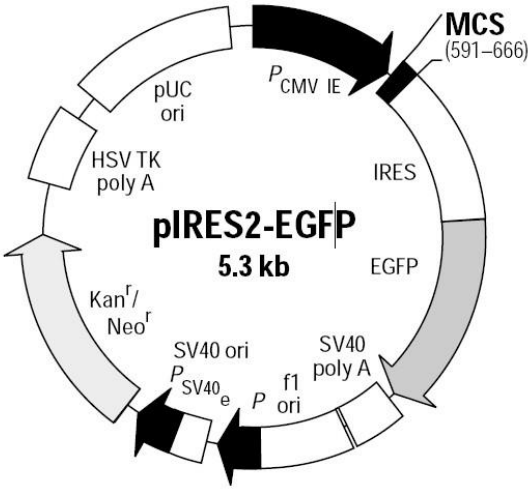

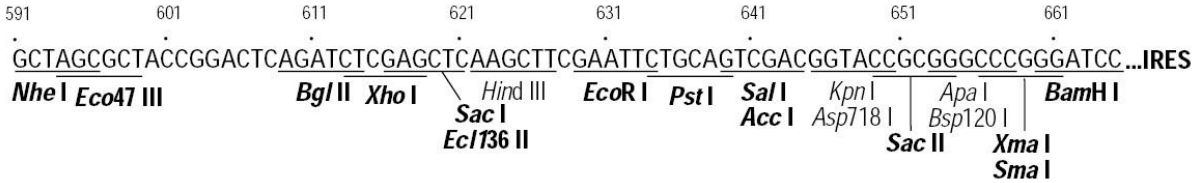

Restriction Map and Multiple Cloning Site (MCS) of pIRES2-EGFP Vector. Unique restriction sites are in bold. Note that the *Eco*47 III site has not been confirmed in the final construct.

References

AKAGI, T., KUURE, S., URANISHI, K., KOIDE, H., COSTANTINI, F. & YOKOTA, T. 2015. ETS-related transcription factors ETV4 and ETV5 are involved in proliferation and induction of differentiation-associated genes in embryonic stem (ES) cells. J Biol Chem, 290, 22460-73.

AKPA, M. M., IGLESIAS, D., CHU, L., THIEBAUT, A., JENTOFT, I., HAMMOND, L., TORBAN, E. & GOODYER, P. R. 2016. Wilms Tumor Suppressor, WT1, Cooperates with MicroRNA-26a and MicroRNA-101 to Suppress Translation of the Polycomb Protein, EZH2, in Mesenchymal Stem Cells. J Biol Chem, 291, 3785-95.

ALANKARAGE, D., LAVERY, R., SVINGEN, T., KELLY, S., LUDBROOK, L., BAGHERI-FAM, S., KOOPMAN, P. & HARLEY, V. 2016. SOX9 regulates expression of the male fertility gene Ets variant factor 5 (ETV5) during mammalian sex development. Int J Biochem Cell Biol, 79, 41-51.

AL-DUJAILI, E. A., WILLIAMS, B. C., EDWARDS, C. R. W., SALACINSKI, P. & LOWRY, P. J. 1982. Human γ-melanotropin precursor potentiates corticotropin-induced adrenal steroidogenesis by stimulating mRNA synthesis. Biochemical Journal, 204, 301.

AMIRI, F., HALABIAN, R., DEHGAN HARATI, M., BAHADORI, M., MEHDIPOUR, A., MOHAMMADI ROUSHANDEH, A. & HABIBI ROUDKENAR, M. 2015. Positive selection of Wharton's jelly-derived CD105(+) cells by MACS technique and their subsequent cultivation under suspension culture condition: A simple, versatile culturing method to enhance the multipotentiality of mesenchymal stem cells. Hematology, 20, 208-16.

ARAI, F. & SUDA, T. 2008. Quiescent stem cells in the niche. StemBook. Cambridge (MA): Harvard Stem Cell Institute. Copyright: (c) 2008 Fumio Arai and Toshio Suda.

AROLA, J., HEIKKILA, P. & KAHRI, A. I. 1993. Biphasic effect of ACTH on growth of rat adrenocortical cells in primary culture. Cell Tissue Res, 271, 169-76.

AUGELLO, A. & DE BARI, C. 2010. The regulation of differentiation in mesenchymal stem cells. Hum Gene Ther, 21, 1226-38.

BABA, T., OTAKE, H., SATO, T., MIYABAYASHI, K., SHISHIDO, Y., WANG, C. Y., SHIMA, Y., KIMURA, H., YAGI, M., ISHIHARA, Y., HINO, S., OGAWA, H., NAKAO, M., YAMAZAKI, T., KANG, D., OHKAWA, Y., SUYAMA, M., CHUNG, B. C. & MOROHASHI, K. 2014. Glycolytic genes are targets of the nuclear receptor Ad4BP/SF-1. Nat Commun, 5, 3634.

BACALLAO, K. & MONJE, P. V. 2015. Requirement of cAMP signalling for Schwann cell differentiation restricts the onset of myelination. PLoS One, 10, e0116948.

BAI, Y., FENG, M., LIU, S., WEI, H., LI, L., ZHANG, X., SHEN, C., ZHANG, S. & MA, N. 2016. Differential gene expression in mouse spermatogonial stem cells and embryonic stem cells. Int J Mol Med, 38, 423-32.

BAKER, B. L. 1952. A comparison of the histological changes induced by experimental hyperadrenocorticalism and inanition. Recent Prog. Hormone Res., 7, 331.

BAKER, L. A., HOLLIDAY, H. & SWARBRICK, A. 2016. ID4 controls luminal lineage commitment in normal mammary epithelium and inhibits BRCA1 function in basal-like breast cancer. Endocr Relat Cancer, 23, R381-92.

BALKWILL, F. 2004. Cancer and the chemokine network. Nat Rev Cancer, 4, 540-50.

BALL, S. G., SHUTTLEWORTH, C. A. & KIELTY, C. M. 2007. Vascular endothelial growth factor can signal through platelet-derived growth factor receptors. J Cell Biol, 177, 489-500.

BANDIERA, R., VIDAL, V. P. I., RANC, F., CLARKSON, M., SAHUT-BARNOLA, I., VON GISE, A., PU, W. T., HOHENSTEIN, P., MARTINEZ, A. & SCHEDL, A. 2013. WT1 maintains adrenal-gonadal-primordium (AGP) identity and marks a novel population of AGP-like progenitors within the adult adrenal gland. Developmental cell, 27, 5-18.

BARCLAY, A. N., LETARTE-MUIRHEAD, M., WILLIAMS, A. F. & FAULKES, R. A. 1976. Chemical characterisation of the Thy-1 glycoproteins from the membranes of rat thymocytes and brain. Nature, 263, 563-7.

BATOULI, S., MIURA, M., BRAHIM, J., TSUTSUI, T. W., FISHER, L. W., GRONTHOS, S., ROBEY, P. G. & SHI, S. 2003. Comparison of stem-cell-mediated osteogenesis and dentinogenesis. J Dent Res, 82, 976-81.

BAYLIN, S. B. & JONES, P. A. 2011. A decade of exploring the cancer epigenome - biological and translational implications. Nat Rev Cancer, 11, 726-34.

BAZI, Z., BERTACCHI, M., ABASI, M., MOHAMMADI-YEGANEH, S., SOLEIMANI, M., WAGNER, N. & GHANBARIAN, H. 2017. Rn7SK small nuclear RNA is involved in Neuronal Differentiation. J Cell Biochem.

BEALL, R. J. & SAYERS, G. 1972. Isolated adrenal cells: Steroidogenesis and cyclic AMP accumulation in response to ACTH. Archives of Biochemistry and Biophysics, 148, 70-76.

BEERAVOLU, N., MCKEE, C., ALAMRI, A., MIKHAEL, S., BROWN, C., PEREZ-CRUET, M. & CHAUDHRY, G. R. 2017. Isolation and Characterization of Mesenchymal Stromal Cells from Human Umbilical Cord and Fetal Placenta. J Vis Exp.

BELL, P. H. 1954. PURIFICATION AND STRUCTURE OF β-CORTICOTROPIN. Journal of the American Chemical Society, 76, 5565-5567.

BENNETT, H. P. J. 1984. Isolation and characterization of the 1 to 49 amino-terminal sequence of pro-opiomelanocortin from bovine posterior pituitaries. Biochemical and Biophysical Research Communications, 125, 229-236.

BERKS, M. & KAY, R. R. 1988. Cyclic AMP is an inhibitor of stalk cell differentiation in Dictyostelium discoideum. Developmental Biology, 126, 108-114.

BERNARD, P. & HARLEY, V. R. 2007. Wnt4 action in gonadal development and sex determination. Int J Biochem Cell Biol, 39, 31-43.

BERNARDO, M. E., ZAFFARONI, N., NOVARA, F., COMETA, A. M., AVANZINI, M. A., MORETTA, A., MONTAGNA, D., MACCARIO, R., VILLA, R., DAIDONE, M. G., ZUFFARDI, O. & LOCATELLI, F. 2007. Human bone marrow derived mesenchymal stem cells do not undergo transformation after long-term in vitro culture and do not exhibit telomere maintenance mechanisms. Cancer Res, 67, 9142-9.

BERRY, R. L., OZDEMIR, D. D., ARONOW, B., LINDSTROM, N. O., DUDNAKOVA, T., THORNBURN, A., PERRY, P., BALDOCK, R., ARMIT, C., JOSHI, A., JEANPIERRE, C., SHAN, J., VAINIO, S., BAILY, J., BROWNSTEIN, D., DAVIES, J., HASTIE, N. D. & HOHENSTEIN, P. 2015. Deducing the stage of origin of Wilms' tumours from a developmental series of Wt1-mutant mice. Dis Model Mech, 8, 903-17.

BERTHON, A., FAUCZ, F. R., ESPIARD, S., DROUGAT, L., BERTHERAT, J. & STRATAKIS, C. A. 2017. Age-dependent effects of Armc5 haploinsufficiency on adrenocortical function. Hum Mol Genet, 26, 3495-3507.

BESTERVELT, L. L., PITT, J. A., NOLAN, C. J. & PIPER, W. N. 1993. TCDD alters pituitary-adrenal function. II: Evidence for decreased bioactivity of ACTH. Neurotoxicol Teratol, 15, 371-6.

BHATTACHARYA, I., PRADHAN, B. S., SARDA, K., GAUTAM, M., BASU, S. & MAJUMDAR, S. S. 2012. A switch in Sertoli cell responsiveness to FSH may be responsible for robust onset of germ cell differentiation during prepubartal testicular maturation in rats. Am J Physiol Endocrinol Metab, 303, E886-98.

BICKNELL, A. B. 1997. Molecular biology of the stress axis. PhD, University of Reading.

BICKNELL, A. B. 2016. 60 YEARS OF POMC: N-terminal POMC peptides and adrenal growth. J Mol Endocrinol, 56, T39-48.

BICKNELL, A. B., LOMTHAISONG, K., WOODS, R. J., HUTCHINSON, E. G., BENNETT, H. P., GLADWELL, R. T. & LOWRY, P. J. 2001. Characterization of a serine protease that cleaves pro-gamma-melanotropin at the adrenal to stimulate growth. Cell, 105, 903-12.

BITGOOD, M. J. & MCMAHON, A. P. 1995. Hedgehog and Bmp genes are coexpressed at many diverse sites of cell-cell interaction in the mouse embryo. Dev Biol, 172, 126-38.

BLAIR, A., HOGGE, D. E., AILLES, L. E., LANSDORP, P. M. & SUTHERLAND, H. J. 1997. Lack of Expression of Thy-1 (CD90) on Acute Myeloid Leukemia Cells With Long-Term Proliferative Ability In Vitro and In Vivo. Blood, 89, 3104-3112.

BLAND, M. L., DESCLOZEAUX, M. & INGRAHAM, H. A. 2003. Tissue growth and remodeling of the embryonic and adult adrenal gland. Ann N Y Acad Sci, 995, 59-72.

BLANK, U., KARLSSON, G. & KARLSSON, S. 2008. Signaling pathways governing stem-cell fate. Blood, 111, 492-503.

BLECKER, D., ELASHRY, M. I., HEIMANN, M., WENISCH, S. & ARNHOLD, S. 2017. New Insights into the Neural Differentiation Potential of Canine Adipose Tissue-Derived Mesenchymal Stem Cells. Anat Histol Embryol, 46, 304-315.

BORAKATI, A., MAFI, R., MAFI, P. & KHAN, W. 2017. A systematic review and meta-analysis of clinical trials of mesenchymal stem cell therapy for cartilage repair. Curr Stem Cell Res Ther.

BRANN, J. H., ELLIS, D. P., KU, B. S., SPINAZZI, E. F. & FIRESTEIN, S. 2015. Injury in aged animals robustly activates quiescent olfactory neural stem cells. Front Neurosci, 9, 367.

BRONNEKE, S., BRUCKNER, B., SOHLE, J., SIEGNER, R., SMUDA, C., STAB, F., WENCK, H., KOLBE, L., GRONNIGER, E. & WINNEFELD, M. 2015. Genome-wide expression analysis of wounded skin reveals novel genes involved in angiogenesis. Angiogenesis, 18, 361-71.

BRUGGER, P. C. & PRAYER, D. 2006. Fetal abdominal magnetic resonance imaging. Eur J Radiol, 57, 278-93.

BRZOSKA, T., LUGER, T. A., MAASER, C., ABELS, C. & BOHM, M. 2008. Alpha-melanocyte-stimulating hormone and related tripeptides: biochemistry, antiinflammatory and protective effects in vitro and in vivo, and future perspectives for the treatment of immune-mediated inflammatory diseases. Endocr Rev, 29, 581-602.

BUHRING, H. J., BATTULA, V. L., TREML, S., SCHEWE, B., KANZ, L. & VOGEL, W. 2007. Novel markers for the prospective isolation of human MSC. Ann N Y Acad Sci, 1106, 262-71.

BURKE, R., NELLEN, D., BELLOTTO, M., HAFEN, E., SENTI, K. A., DICKSON, B. J. & BASLER, K. 1999. Dispatched, a novel sterol-sensing domain protein dedicated to the release of cholesterol-modified hedgehog from signaling cells. Cell, 99, 803-15.

CAO, W., RAZANAU, A., FENG, D., LOBO, V. G. & XIE, J. 2012. Control of alternative splicing by forskolin through hnRNP K during neuronal differentiation. Nucleic Acids Res, 40, 8059-71.

CAROCCIA, B., FASSINA, A., SECCIA, T. M., RECARTI, C., PETRELLI, L., BELLONI, A. S., PELIZZO, M. R. & ROSSI, G. P. 2010. Isolation of human adrenocortical aldosterone-producing cells by a novel immunomagnetic beads method. Endocrinology, 151, 1375-80.

CARUSO, V., LAGERSTROM, M. C., OLSZEWSKI, P. K., FREDRIKSSON, R. & SCHIOTH, H. B. 2014. Synaptic changes induced by melanocortin signalling. Nat Rev Neurosci, 15, 98-110.

CASTRO, R., ZOU, J., SECOMBES, C. J. & MARTIN, S. A. M. 2011. Cortisol modulates the induction of inflammatory gene expression in a rainbow trout macrophage cell line. Fish & Shellfish Immunology, 30, 215-223.

CASTRO-MALASPINA, H., GAY, R. E., RESNICK, G., KAPOOR, N., MEYERS, P., CHIARIERI, D., MCKENZIE, S., BROXMEYER, H. E. & MOORE, M. A. 1980. Characterization of human bone marrow fibroblast colony-forming cells (CFU-F) and their progeny. Blood, 56, 289-301.

CHAMBERLAIN, G., FOX, J., ASHTON, B. & MIDDLETON, J. 2007. Concise Review: Mesenchymal Stem Cells: Their Phenotype, Differentiation Capacity, Immunological Features, and Potential for Homing. STEM CELLS, 25, 2739-2749.

CHAMOUX, E., BOLDUC, L., LEHOUX, J. G. & GALLO-PAYET, N. 2001. Identification of extracellular matrix components and their integrin receptors in the human fetal adrenal gland. J Clin Endocrinol Metab, 86, 2090-8.

CHANG, S. P., MORRISON, H. D., NILSSON, F., KENYON, C. J., WEST, J. D. & MORLEY, S. D. 2013. Cell proliferation, movement and differentiation during maintenance of the adult mouse adrenal cortex. PLoS One, 8, e81865.

CHARMANDARI, E., TSIGOS, C. & CHROUSOS, G. 2005. ENDOCRINOLOGY OF THE STRESS RESPONSE. Annual Review of Physiology, 67, 259-284.

CHEN, J. D., XU, F. F., ZHU, H., LI, X. M., TANG, B., LIU, Y. L. & ZHANG, Y. 2014. [ICAM-1 regulates differentiation of MSC to adipocytes via activating MAPK pathway]. Zhongguo Shi Yan Xue Ye Xue Za Zhi, 22, 160-5.

CHENG, T., YANG, C., WEBER, N., KIM, H. T. & KUO, A. C. 2012. Fibroblast growth factor 2 enhances the kinetics of mesenchymal stem cell chondrogenesis. Biochem Biophys Res Commun, 426, 544-50.

CHICHAGOVA, V., SANCHEZ-VERA, I., ARMSTRONG, L., STEEL, D. & LAKO, M. 2015. Generation of Human Induced Pluripotent Stem Cells Using RNA-Based Sendai Virus System and Pluripotency Validation of the Resulting Cell Population. Methods Mol Biol.

CHING, S. & VILAIN, E. 2009. Targeted disruption of Sonic Hedgehog in the mouse adrenal leads to adrenocortical hypoplasia. genesis, 47, 628-637.

CHU, J., TU, Y., CHEN, J., TAN, D., LIU, X. & PI, R. 2015. Effects of melatonin and its analogues on neural stem cells. Mol Cell Endocrinol.

COHEN, R. I., MCKAY, R. & ALMAZAN, G. 1999. Cyclic AMP regulates PDGF-stimulated signal transduction and differentiation of an immortalized optic-nerve-derived cell line. The Journal of Experimental Biology, 202, 461.

COLL, A. P., FASSNACHT, M., KLAMMER, S., HAHNER, S., SCHULTE, D. M., PIPER, S., TUNG, Y. C. L., CHALLIS, B. G., WEINSTEIN, Y., ALLOLIO, B., O'RAHILLY, S. & BEUSCHLEIN, F. 2006. Peripheral administration of the N-terminal pro-opiomelanocortin fragment 1–28 to Pomc−/− mice reduces food intake and weight but does not affect adrenal growth or corticosterone production. Journal of Endocrinology, 190, 515-525.

COLTER, D. C., SEKIYA, I. & PROCKOP, D. J. 2001. Identification of a subpopulation of rapidly self-renewing and multipotential adult stem cells in colonies of human marrow stromal cells. Proceedings of the National Academy of Sciences, 98, 7841-7845.

CONE, R. D. 2006. Studies on the physiological functions of the melanocortin system. Endocr Rev, 27, 736-49.

CONLEY, A. J. & BIRD, I. M. 1997. The role of cytochrome P450 17 alpha-hydroxylase and 3 beta-hydroxysteroid dehydrogenase in the integration of gonadal and adrenal steroidogenesis via the delta 5 and delta 4 pathways of steroidogenesis in mammals. Biol Reprod, 56, 789-99.

COSKUN, E., ERCIN, M. & GEZGINCI-OKTAYOGLU, S. 2017. The Role of Epigenetic Regulation and Pluripotency-Related MicroRNAs in Differentiation of Pancreatic Stem Cells to Beta Cells.

CRANE, J. L. & CAO, X. 2014. Bone marrow mesenchymal stem cells and TGF-beta signaling in bone remodeling. J Clin Invest, 124, 466-72.

CRISAN, M., YAP, S., CASTEILLA, L., CHEN, C. W., CORSELLI, M., PARK, T. S., ANDRIOLO, G., SUN, B., ZHENG, B., ZHANG, L., NOROTTE, C., TENG, P. N., TRAAS, J., SCHUGAR, R., DEASY, B. M., BADYLAK, S., BUHRING, H. J., GIACOBINO, J. P., LAZZARI, L., HUARD, J. & PEAULT, B. 2008. A perivascular origin for mesenchymal stem cells in multiple human organs. Cell Stem Cell, 3, 301-13.

CUI, L. L., NITZSCHE, F., PRYAZHNIKOV, E., TIBEYKINA, M., TOLPPANEN, L., RYTKONEN, J., HUHTALA, T., MU, J. W., KHIROUG, L., BOLTZE, J. & JOLKKONEN, J. 2017. Integrin alpha4 Overexpression on Rat Mesenchymal Stem Cells Enhances Transmigration and Reduces Cerebral Embolism After Intracarotid Injection. Stroke.

DE MENDONCA, P. O., COSTA, I. C. & LOTFI, C. F. 2014. The involvement of Nek2 and Notch in the proliferation of rat adrenal cortex triggered by POMC-derived peptides. PLoS One, 9, e108657.

DE MENDONCA, P. O., LIRIA, C. W., MACHINI, M. T. & LOTFI, C. F. 2013. N-POMC1-28 increases cyclin D expression and inhibits P27(kip1) in the adrenal cortex. Mol Cell Endocrinol, 371, 166-73.

DE WERT, G. & MUMMERY, C. 2003. Human embryonic stem cells: research, ethics and policy. Hum Reprod, 18, 672-82.

DELAFOREST, A., NAGAOKA, M., SI-TAYEB, K., NOTO, F. K., KONOPKA, G., BATTLE, M. A. & DUNCAN, S. A. 2011. HNF4A is essential for specification of hepatic progenitors from human pluripotent stem cells. Development, 138, 4143-53.

DENNIS, J. E., ESTERLY, K., AWADALLAH, A., PARRISH, C. R., POYNTER, G. M. & GOLTRY, K. L. 2007. Clinical-scale expansion of a mixed population of bone-marrow-derived stem and progenitor cells for potential use in bone-tissue regeneration. Stem Cells, 25, 2575-82.

DESCLOZEAUX, M., KRYLOVA, I. N., HORN, F., FLETTERICK, R. J. & INGRAHAM, H. A. 2002. Phosphorylation and intramolecular stabilization of the ligand binding domain in the nuclear receptor steroidogenic factor 1. Mol Cell Biol, 22, 7193-203.

DIDERHOLM, H. & HELLMAN, B. 1960. The cell migration in the adrenal cortex of rats studied with tritiated thymidine. Acta Physiol Scand, 50, 197-202.

DOGHMAN, M., KARPOVA, T., RODRIGUES, G. A., ARHATTE, M., DE MOURA, J., CAVALLI, L. R., VIROLLE, V., BARBRY, P., ZAMBETTI, G. P., FIGUEIREDO, B. C., HECKERT, L. L. & LALLI, E. 2007. Increased steroidogenic factor-1 dosage triggers adrenocortical cell proliferation and cancer. Mol Endocrinol, 21, 2968-87.

DOMINICI, M., LE BLANC, K., MUELLER, I., SLAPER-CORTENBACH, I., MARINI, F. C., KRAUSE, D. S., DEANS, R. J., KEATING, A., PROCKOP, D. J. & HORWITZ, E. M. 2006b. Minimal criteria for defining multipotent mesenchymal stromal cells. The International Society for Cellular Therapy position statement. Cytotherapy, 8, 315-317.

DOORN, J., LEUSINK, M., GROEN, N., VAN DE PEPPEL, J., VAN LEEUWEN, J. P., VAN BLITTERSWIJK, C. A. & DE BOER, J. 2012. Diverse effects of cyclic AMP variants on osteogenic and adipogenic differentiation of human mesenchymal stromal cells. Tissue Eng Part A, 18, 1431-42.

DORES, R. M., LONDRAVILLE, R. L., PROKOP, J., DAVIS, P., DEWEY, N. & LESINSKI, N. 2014. Molecular evolution of GPCRs: Melanocortin/melanocortin receptors. J Mol Endocrinol, 52, T29-42.

DOSS, M. X., GASPAR, J. A., WINKLER, J., HESCHELER, J., SCHULZ, H. & SACHINIDIS, A. 2012. Specific gene signatures and pathways in mesodermal cells and their derivatives derived from embryonic stem cells. Stem Cell Rev, 8, 43-54.

DRELON, C., BERTHON, A., SAHUT-BARNOLA, I., MATHIEU, M., DUMONTET, T., RODRIGUEZ, S., BATISSE-LIGNIER, M., TABBAL, H., TAUVERON, I.,

LEFRANCOIS-MARTINEZ, A. M., POINTUD, J. C., GOMEZ-SANCHEZ, C. E., VAINIO, S., SHAN, J., SACCO, S., SCHEDL, A., STRATAKIS, C. A., MARTINEZ, A. & VAL, P. 2016. PKA inhibits WNT signalling in adrenal cortex zonation and prevents malignant tumour development. Nat Commun, 7, 12751.

DUDAKOVIC, A., CAMILLERI, E., RIESTER, S. M., LEWALLEN, E. A., KVASHA, S., CHEN, X., RADEL, D. J., ANDERSON, J. M., NAIR, A. A., EVANS, J. M., KRYCH, A. J., SMITH, J., DEYLE, D. R., STEIN, J. L., STEIN, G. S., IM, H. J., COOL, S. M., WESTENDORF, J. J., KAKAR, S., DIETZ, A. B. & VAN WIJNEN, A. J. 2014. High-resolution molecular validation of self-renewal and spontaneous differentiation in clinical-grade adipose-tissue derived human mesenchymal stem cells. J Cell Biochem, 115, 1816-28.

DUNN, J. C. Y., CHU, Y., LAM, M. M., WU, B. M., ATKINSON, J. B. & MCCABE, E. R. 2004. Adrenal cortical cell transplantation. Journal of Pediatric Surgery, 39, 1856-1858.

DWYER, R. M., POTTER-BEIRNE, S. M., HARRINGTON, K. A., LOWERY, A. J., HENNESSY, E., MURPHY, J. M., BARRY, F. P., O'BRIEN, T. & KERIN, M. J. 2007. Monocyte chemotactic protein-1 secreted by primary breast tumors stimulates migration of mesenchymal stem cells. Clin Cancer Res, 13, 5020-7.

EHRLICH, M. 2009. DNA hypomethylation in cancer cells. Epigenomics, 1, 239-59.

EISELLEOVA, L., PETERKOVA, I., NERADIL, J., SLANINOVA, I., HAMPL, A. & DVORAK, P. 2008. Comparative study of mouse and human feeder cells for human embryonic stem cells. Int J Dev Biol, 52, 353-63.

EL-KHAIRI, R., MARTINEZ-AGUAYO, A., FERRAZ-DE-SOUZA, B., LIN, L. & ACHERMANN, J. C. 2011. Role of DAX-1 (NR0B1) and steroidogenic factor-1 (NR5A1) in human adrenal function. Endocr Dev, 20, 38-46.

ESTIVARIZ, F. E., CARINO, M., LOWRY, P. J. & JACKSON, S. 1988a. Further evidence that N-terminal pro-opiomelanocortin peptides are involved in adrenal mitogenesis. J Endocrinol, 116, 201-6.

ESTIVARIZ, F. E., HOPE, J., MCLEAN, C. & LOWRY, P. J. 1980. Purification and characterization of a γ-melanotropin precursor from frozen human pituitary glands. Biochemical Journal, 191, 125.

ESTIVARIZ, F. E., ITURRIZA, F., MCLEAN, C., HOPE, J. & LOWRY, P. J. 1982. Stimulation of adrenal mitogenesis by N-terminal proopiocortin peptides. Nature, 297, 419.

ESTIVARIZ, F. E., MORANO, M. I., CARINO, M., JACKSON, S. & LOWRY, P. J. 1988b. Adrenal regeneration in the rat is mediated by mitogenic N-terminal pro-opiomelanocortin peptides generated by changes in precursor processing in the anterior pituitary. Journal of Endocrinology, 116, 207-216.

FAUZA, D. O. 2017. Transamniotic stem cell therapy (TRASCET): A novel strategy for the prenatal management of congenital anomalies. Pediatr Res.

FIEDLER, J., RODERER, G., GUNTHER, K. P. & BRENNER, R. E. 2002. BMP-2, BMP-4, and PDGF-bb stimulate chemotactic migration of primary human mesenchymal progenitor cells. J Cell Biochem, 87, 305-12.

FINAN, A. & RICHARD, S. 2015. Stimulating endogenous cardiac repair. Front Cell Dev Biol, 3, 57.

FINCO, I., LERARIO, A. M. & HAMMER, G. D. 2018. Sonic Hedgehog and WNT Signaling Promote Adrenal Gland Regeneration in Male Mice. Endocrinology.

FISCHBACH, G. D. & FISCHBACH, R. L. 2004. Stem cells: science, policy, and ethics. Journal of Clinical Investigation, 114, 1364-1370.

FLORES-TORALES, E., OROZCO-BAROCIO, A., GONZALEZ-RAMELLA, O. R., CARRASCO-YALAN, A., GAZARIAN, K. & CUNEO-PARETO, S. 2010. The CD271 expression could be alone for establisher phenotypic marker in Bone Marrow derived mesenchymal stem cells. Folia Histochem Cytobiol, 48, 682-6.

FORTE, G., MINIERI, M., COSSA, P., ANTENUCCI, D., SALA, M., GNOCCHI, V., FIACCAVENTO, R., CAROTENUTO, F., DE VITO, P., BALDINI, P. M., PRAT, M. & DI NARDO, P. 2006. Hepatocyte growth factor effects on mesenchymal stem cells: proliferation, migration, and differentiation. Stem Cells, 24, 23-33.

FRANCESCHETTI, T. & DE BARI, C. 2017. The potential role of adult stem cells in the management of the rheumatic diseases. Ther Adv Musculoskelet Dis, 9, 165-179.

FUKUNAGA, N., TERAMURA, T., ONODERA, Y., TAKEHARA, T., FUKUDA, K. & HOSOI, Y. 2010. Leukemia inhibitory factor (LIF) enhances germ cell differentiation from primate embryonic stem cells. Cell Reprogram, 12, 369-76.

FUSAKI, N., BAN, H., NISHIYAMA, A., SAEKI, K. & HASEGAWA, M. 2009. Efficient induction of transgene-free human pluripotent stem cells using a vector based on Sendai virus, an RNA virus that does not integrate into the host genome. Proc Jpn Acad Ser B Phys Biol Sci, 85, 348-62.

GABORY, A., ATTIG, L. & JUNIEN, C. 2011. Epigenetic mechanisms involved in developmental nutritional programming. World Journal of Diabetes, 2, 164-175.

GAO, D., HAO, G., MENG, Z., NING, N., YANG, G., LIU, Z., DONG, X. & NIU, X. 2015. Rosiglitzone Suppresses Angiotensin II-Induced Production of KLF5 and Cell Proliferation in Rat Vascular Smooth Muscle Cells. PLoS ONE, 10, e0123724.

GAO, L., WANG, Y. X., JIANG, W. X., HE, Z. Y., ZHU, C. L. & MA, R. 2015. [Immortalization of human dental pulp stem cells caused by transferring hTERT gene]. Shanghai Kou Qiang Yi Xue, 24, 135-40.

GILISSEN, J., GEUBELLE, P., DUPUIS, N., LASCHET, C., PIROTTE, B. & HANSON, J. 2015. Forskolin-free cAMP assay for Gi-coupled receptors. Biochem Pharmacol, 98, 381-91.

GONCHAROVA, N. D. 2013. Stress Responsiveness of the Hypothalamic–Pituitary–Adrenal Axis: Age-Related Features of the Vasopressinergic Regulation. Frontiers in Endocrinology, 4, 26.

GONDO, S., OKABE, T., TANAKA, T., MORINAGA, H., NOMURA, M., TAKAYANAGI, R., NAWATA, H. & YANASE, T. 2008. Adipose tissue-derived and bone marrow-derived mesenchymal cells develop into different lineage of steroidogenic cells by forced expression of steroidogenic factor 1. Endocrinology, 149, 4717-25.

GONDO, S., YANASE, T., OKABE, T., TANAKA, T., MORINAGA, H., NOMURA, M., GOTO, K. & NAWATA, H. 2004. SF-1/Ad4BP transforms primary long-term cultured bone marrow cells into ACTH-responsive steroidogenic cells. Genes Cells, 9, 1239-47.

GORDON, K., CLOUAIRE, T., BAO, X. X., KEMP, S. E., XENOPHONTOS, M., DE LAS HERAS, J. I. & STANCHEVA, I. 2014. Immortality, but not oncogenic transformation, of primary human cells leads to epigenetic reprogramming of DNA methylation and gene expression. Nucleic Acids Research, 42, 3529-3541.

GOTO, M., PIPER HANLEY, K., MARCOS, J., WOOD, P. J., WRIGHT, S., POSTLE, A. D., CAMERON, I. T., MASON, J. I., WILSON, D. I. & HANLEY, N. A. 2006. In humans, early cortisol biosynthesis provides a mechanism to safeguard female sexual development. J Clin Invest, 116, 953-60.

GOULDING, M. D. & RALPH, R. K. 1989. Cyclic-AMP-induced c-fos expression and its relevance to differentiation of a transformed mast cell line. Biochim Biophys Acta, 1007, 99-108.

GRIFFIN, S. M., PICKARD, M. R., ORME, R. P., HAWKINS, C. P., WILLIAMS, A. C. & FRICKER, R. A. 2017. Nicotinamide alone accelerates the conversion of mouse embryonic stem cells into mature neuronal populations. 12, e0183358.

GUASTI, L., PAUL, A., LAUFER, E. & KING, P. 2011. Localization of Sonic hedgehog secreting and receiving cells in the developing and adult rat adrenal cortex. Mol Cell Endocrinol, 336, 117-22.

GUERIN, C. L., LOYER, X., VILAR, J., CRAS, A., MIRAULT, T., GAUSSEM, P., SILVESTRE, J. S. & SMADJA, D. M. 2015. Bone-marrow-derived very small embryonic-like stem cells in patients with critical leg ischaemia: evidence of vasculogenic potential. Thromb Haemost, 113, 1084-94.

GUERIN, C. L., LOYER, X., VILAR, J., CRAS, A., MIRAULT, T., GAUSSEM, P., SILVESTRE, J. S. & SMADJA, D. M. 2015. Bone-marrow-derived very small embryonic-like stem cells in patients with critical leg ischaemia: evidence of vasculogenic potential. Thromb Haemost, 113, 1084-94.

GUO, H. & LIU, H. T. 2005. [Primary monolayer culture of rat adrenal cortical cells]. Zhongguo Ying Yong Sheng Li Xue Za Zhi, 21, 117-9.

GUO, I. C., TSAI, H. M. & CHUNG, B. C. 1994. Actions of two different cAMP-responsive sequences and an enhancer of the human CYP11A1 (P450scc) gene in adrenal Y1 and placental JEG-3 cells. J Biol Chem, 269, 6362-9.

HAN, T. S., WALKER, B. R., ARLT, W. & ROSS, R. J. 2014. Treatment and health outcomes in adults with congenital adrenal hyperplasia. Nat Rev Endocrinol, 10, 115-124.

HANLEY, N. A., BALL, S. G., CLEMENT-JONES, M., HAGAN, D. M., STRACHAN, T., LINDSAY, S., ROBSON, S., OSTRER, H., PARKER, K. L. & WILSON, D. I. 1999. Expression of steroidogenic factor 1 and Wilms' tumour 1 during early human gonadal development and sex determination. Mech Dev, 87, 175-80.

HANLEY, N. A., RAINEY, W. E., WILSON, D. I., BALL, S. G. & PARKER, K. L. 2001. Expression profiles of SF-1, DAX1, and CYP17 in the human fetal adrenal gland: potential interactions in gene regulation. Mol Endocrinol, 15, 57-68.

HARICHANDAN, A., SIVASUBRAMANIYAN, K. & BUHRING, H. J. 2013. Prospective isolation and characterization of human bone marrow-derived MSCs. Adv Biochem Eng Biotechnol, 129, 1-17.

HATANO, O., TAKAKUSU, A., NOMURA, M. & MOROHASHI, K. 1996. Identical origin of adrenal cortex and gonad revealed by expression profiles of Ad4BP/SF-1. Genes Cells, 1, 663-71.

HAUSBURG, F., JUNG, J. J., HOCH, M., WOLFIEN, M., YAVARI, A., RIMMBACH, C. & DAVID, R. 2017. (Re-)programming of subtype specific cardiomyocytes. Adv Drug Deliv Rev.

HAYASHI, S., MANABE, I., SUZUKI, Y., RELAIX, F. & OISHI, Y. 2016. Klf5 regulates muscle differentiation by directly targeting muscle-specific genes in cooperation with MyoD in mice. Elife, 5.

HAYASHI, Y., CABONI, L., DAS, D., YUMOTO, F., CLAYTON, T., DELLER, M. C., NGUYEN, P., FARR, C. L., CHIU, H. J., MILLER, M. D., ELSLIGER, M. A., DEACON, A. M., GODZIK, A., LESLEY, S. A., TOMODA, K., CONKLIN, B. R., WILSON, I. A., YAMANAKA, S. & FLETTERICK, R. J. 2015. Structure-based discovery of NANOG variant with enhanced properties to promote self-renewal and reprogramming of pluripotent stem cells. Proc Natl Acad Sci U S A, 112, 4666-71.

HAYFLICK, L. & MOORHEAD, P. S. 1961. The serial cultivation of human diploid cell strains. Exp Cell Res, 25, 585-621.

HE, H. T., NAQUET, P., CAILLOL, D. & PIERRES, M. 1991. Thy-1 supports adhesion of mouse thymocytes to thymic epithelial cells through a Ca2(+)-independent mechanism. J Exp Med, 173, 515-8.

HE, S., ZHU, W., ZHOU, Y., HUANG, Y., OU, Y., LI, Y. & YAN, G. 2011. Transcriptional and post-transcriptional down-regulation of cyclin D1 contributes to C6 glioma cell differentiation induced by forskolin. J Cell Biochem, 112, 2241-9.

HEIKKILA, M., PELTOKETO, H., LEPPALUOTO, J., ILVES, M., VUOLTEENAHO, O. & VAINIO, S. 2002. Wnt-4 deficiency alters mouse adrenal cortex function, reducing aldosterone production. Endocrinology, 143, 4358-65.

HELSEL, A. R., YANG, Q. E. & OATLEY, M. J. 2017. ID4 levels dictate the stem cell state in mouse spermatogonia. 144, 624-634.

HENDERSON, K., SLIGAR, A. D., LE, V. P., LEE, J. & BAKER, A. B. 2017. Biomechanical Regulation of Mesenchymal Stem Cells for Cardiovascular Tissue Engineering. Adv Healthc Mater.

HENRIQUEZ, M., HERRERA-MOLINA, R., VALDIVIA, A., ALVAREZ, A., KONG, M., MUNOZ, N., EISNER, V., JAIMOVICH, E., SCHNEIDER, P., QUEST, A. F. & LEYTON, L. 2011. ATP release due to Thy-1-integrin binding induces P2X7-mediated calcium entry required for focal adhesion formation. J Cell Sci, 124, 1581-8.

HERBERMAN, R. B., NUNN, M. E. & HOLDEN, H. T. 1978. Low Density of Thy 1 Antigen on Mouse Effector Cells Mediating Natural Cytotoxicity Against Tumor Cells. The Journal of Immunology, 121, 304.

HERRERA, M. B., BRUNO, S., BUTTIGLIERI, S., TETTA, C., GATTI, S., DEREGIBUS, M. C., BUSSOLATI, B. & CAMUSSI, G. 2006. Isolation and characterization of a stem cell population from adult human liver. Stem Cells, 24, 2840-50.

HIGUITA-CASTRO, N., NELSON, M. T., SHUKLA, V., AGUDELO-GARCIA, P. A., ZHANG, W., DUARTE-SANMIGUEL, S. M., ENGLERT, J. A., LANNUTTI, J. J., HANSFORD, D. J. & GHADIALI, S. N. 2017. Using a Novel Microfabricated Model of the Alveolar-Capillary Barrier to Investigate the Effect of Matrix Structure on Atelectrauma. 7, 11623.

HOLLWECK, T., HAGL, C. & EISSNER, G. 2012. Mesenchymal stem cells from umbilical cord tissue as potential therapeutics for cardiomyodegenerative diseases - a review. Int J Mol Cell Med, 1, 119-32.

HORI, Y., RULIFSON, I. C., TSAI, B. C., HEIT, J. J., CAHOY, J. D. & KIM, S. K. 2002. Growth inhibitors promote differentiation of insulin-producing tissue from embryonic stem cells. Proc Natl Acad Sci U S A, 99, 16105-10.

HORIGUCHI, K., NAKAKURA, T., YOSHIDA, S., TSUKADA, T., KANNO, N., HASEGAWA, R., TAKIGAMI, S., OHSAKO, S., KATO, T. & KATO, Y. 2016. Identification of THY1 as a novel thyrotrope marker and THY1 antibody-mediated thyrotrope isolation in the rat anterior pituitary gland. Biochem Biophys Res Commun, 480, 273-279.

HOU, D. R., JIN, Y., NIE, X. W., ZHANG, M. L., TA, N., ZHAO, L. H., YANG, N., CHEN, Y., WU, Z. Q., JIANG, H. B., LI, Y. R., SUN, Q. Y., DAI, Y. F. & LI, R. F. 2016. Derivation of Porcine Embryonic Stem-Like Cells from In Vitro-Produced Blastocyst-Stage Embryos. Sci Rep, 6, 25838.

HOWARD, K. S., SHEPHERD, R. G., EIGNER, E. A., DAVIES, D. S. & BELL, P. H. 1955. STRUCTURE OF β-CORTICOTROPIN: FINAL SEQUENCE STUDIES. Journal of the American Chemical Society, 77, 3419-3420.

HU, M.-C., HSU, N.-C., PAI, C.-I., WANG, C.-K. L. & CHUNG, B.-C. 2001a. Functions of the Upstream and Proximal Steroidogenic Factor 1 (SF-1)-Binding Sites in the CYP11A1 Promoter in Basal Transcription and Hormonal Response. Molecular Endocrinology, 15, 812-818.

HUO, X., REN, L., SHANG, L., WANG, X. & WANG, J. 2011. Effect of WT1 antisense mRNA on the induction of apoptosis in ovarian carcinoma SKOV3 cells. Eur J Gynaecol Oncol, 32, 651-6.

INGHAM, P. W. & MCMAHON, A. P. 2001. Hedgehog signaling in animal development: paradigms and principles. Genes Dev, 15, 3059-87.

INGLE, D. J. & HIGGINS, G. M. 1938. AUTOTRANSPLANTATION AND REGENERATION OF THE ADRENAL GLAND. Endocrinology, 22, 458-464.

IP, J. E., WU, Y., HUANG, J., ZHANG, L., PRATT, R. E. & DZAU, V. J. 2007. Mesenchymal stem cells use integrin beta1 not CXC chemokine receptor 4 for myocardial migration and engraftment. Mol Biol Cell, 18, 2873-82.

ISHIGAKI, T., SUDO, K., HIROYAMA, T., MIHARADA, K., NINOMIYA, H., CHIBA, S., NAGASAWA, T. & NAKAMURA, Y. 2009. Human hematopoietic stem cells can survive in vitro for several months. Adv Hematol, 2009, 936761.

ISHII, K., KANATSU-SHINOHARA, M., TOYOKUNI, S. & SHINOHARA, T. 2012. FGF2 mediates mouse spermatogonial stem cell self-renewal via upregulation of Etv5 and Bcl6b through MAP2K1 activation. Development, 139, 1734-43.

ISHIMOTO, H. & JAFFE, R. B. 2011. Development and Function of the Human Fetal Adrenal Cortex: A Key Component in the Feto-Placental Unit. Endocrine Reviews, 32, 317-355.

IWASAKU, M., SHINZAWA, M., TANAKA, S., KIMACHI, K. & KAWAKAMI, K. 2017. Clinical characteristics of adrenal crisis in adult population with and without predisposing chronic adrenal insufficiency: a retrospective cohort study. BMC Endocr Disord, 17, 58.

JADHAV, U. & JAMESON, J. L. 2011. Steroidogenic Factor-1 (SF-1)-Driven Differentiation of Murine Embryonic Stem (ES) Cells into a Gonadal Lineage. Endocrinology, 152, 2870-2882.

JEAYS-WARD, K., HOYLE, C., BRENNAN, J., DANDONNEAU, M., ALLDUS, G., CAPEL, B. & SWAIN, A. 2003. Endothelial and steroidogenic cell migration are regulated by WNT4 in the developing mammalian gonad. Development, 130, 3663-70.

JEFCOATE, C. R., MCNAMARA, B. C., ARTEMENKO, I. & YAMAZAKI, T. 1992. Regulation of cholesterol movement to mitochondrial cytochrome P450scc in steroid hormone synthesis. J Steroid Biochem Mol Biol, 43, 751-67.

JENSEN, T. J., SHUI, J. E. & FINCK, C. M. 2017. The effect of meconium exposure on the expression and differentiation of amniotic fluid mesenchymal stem cells. J Neonatal Perinatal Med.

JIANG, S. & ZHANG, S. 2017. Differentiation of cardiomyocytes from amniotic fluidderived mesenchymal stem cells by combined induction with transforming growth factor beta1 and 5azacytidine. Mol Med Rep.

JONES, E. A., KINSEY, S. E., ENGLISH, A., JONES, R. A., STRASZYNSKI, L., MEREDITH, D. M., MARKHAM, A. F., JACK, A., EMERY, P. & MCGONAGLE, D. 2002. Isolation and characterization of bone marrow multipotential mesenchymal progenitor cells. Arthritis Rheum, 46, 3349-60.

JONES, P. A. & BAYLIN, S. B. 2002. The fundamental role of epigenetic events in cancer. Nat Rev Genet, 3, 415-28.

JOO, S. Y., CHO, K. A., JUNG, Y. J., KIM, H. S., PARK, S. Y., CHOI, Y. B., HONG, K. M., WOO, S. Y., SEOH, J. Y., CHO, S. J. & RYU, K. H. 2010. Mesenchymal stromal cells inhibit graft-versus-host disease of mice in a dose-dependent manner. Cytotherapy, 12, 361-70.

JU, S. H., CHO, G. B. & SOHN, J. W. 2018. Understanding Melanocortin-4 Receptor Control of Neuronal Circuits: Toward Novel Therapeutics for Obesity Syndrome. Pharmacol Res.

JUNANKAR, S., BAKER, L. A., RODEN, D. L., NAIR, R., ELSWORTH, B., GALLEGO-ORTEGA, D., LACAZE, P., CAZET, A., NIKOLIC, I., TEO, W. S., YANG, J., MCFARLAND, A., HARVEY, K., NAYLOR, M. J., LAKHANI, S. R., SIMPSON, P. T., RAGHAVENDRA, A., SAUNUS, J., MADORE, J., KAPLAN, W., ORMANDY, C., MILLAR, E. K., O'TOOLE, S., YUN, K. & SWARBRICK, A. 2015. ID4 controls mammary stem cells and marks breast cancers with a stem cell-like phenotype. Nat Commun, 6, 6548.

KER, D. F. E., SHARMA, R., WANG, E. T. H. & YANG, Y. P. 2015. Development of mRuby2-Transfected C3H10T1/2 Fibroblasts for Musculoskeletal Tissue Engineering. PLoS ONE, 10, e0139054.

KHANJANI, S., KHANMOHAMMADI, M., ZARNANI, A. H., AKHONDI, M. M., AHANI, A., GHAEMPANAH, Z., NADERI, M. M., EGHTESAD, S. & KAZEMNEJAD, S. 2014. Comparative evaluation of differentiation potential of menstrual blood- versus bone marrow-derived stem cells into hepatocyte-like cells. PLoS One, 9, e86075.

KIEFFER, T. J., WOLTJEN, K., OSAFUNE, K., YABE, D. & INAGAKI, N. 2017. Beta cell replacement strategies for diabetes. J Diabetes Investig.

KILLINGTON, K., MAFI, R., MAFI, P. & KHAN, W. 2017. A Systematic Review Of Clinical Studies Investigating Mesenchymal Stem Cells For Fracture Non-Union And Bone Defects. Curr Stem Cell Res Ther.

KIM, A. & HAMMER, G. D. 2007a. Adrenocortical Cells with Stem/Progenitor Cell Properties: Recent Advances. Molecular and cellular endocrinology, 265-266, 10-16.

KIM, A. C. & HAMMER, G. D. 2007b. Adrenocortical cells with stem/progenitor cell properties: recent advances. Mol Cell Endocrinol, 265-266, 10-6.

KIM, A. C., BARLASKAR, F. M., HEATON, J. H., ELSE, T., KELLY, V. R., KRILL, K. T., SCHEYS, J. O., SIMON, D. P., TROVATO, A., YANG, W. H. & HAMMER, G. D. 2009. In search of adrenocortical stem and progenitor cells. Endocr Rev, 30, 241-63.

KIM, N. & CHO, S.-G. 2013. Clinical applications of mesenchymal stem cells. The Korean Journal of Internal Medicine, 28, 387-402.

KIM, Y. I., RYU, J. S., YEO, J. E., CHOI, Y. J., KIM, Y. S., KO, K. & KOH, Y. G. 2014. Overexpression of TGF-beta1 enhances chondrogenic differentiation and proliferation of human synovium-derived stem cells. Biochem Biophys Res Commun, 450, 1593-9.

KING, P., PAUL, A. & LAUFER, E. 2009. Shh signaling regulates adrenocortical development and identifies progenitors of steroidogenic lineages. Proceedings of the National Academy of Sciences of the United States of America, 106, 21185-21190.

KOMIYA, Y. & HABAS, R. 2008. Wnt signal transduction pathways. Organogenesis, 4, 68-75.

KONDO, Y., TOYODA, T., ITO, R., FUNATO, M., HOSOKAWA, Y., MATSUI, S., SUDO, T., NAKAMURA, M., OKADA, C., ZHUANG, X., WATANABE, A., OHTA, A., INAGAKI, N. & OSAFUNE, K. 2017. Identification of a small molecule that facilitates the differentiation of human iPSCs/ESCs and mouse embryonic pancreatic explants into pancreatic endocrine cells. Diabetologia, 60, 1454-1466.

KURODA, Y., KITADA, M., WAKAO, S., NISHIKAWA, K., TANIMURA, Y., MAKINOSHIMA, H., GODA, M., AKASHI, H., INUTSUKA, A., NIWA, A., SHIGEMOTO, T., NABESHIMA, Y., NAKAHATA, T., NABESHIMA, Y., FUJIYOSHI, Y. & DEZAWA, M. 2010. Unique multipotent cells in adult human mesenchymal cell populations. Proc Natl Acad Sci U S A, 107, 8639-43.

KURUVILLA, J. G., GHALEB, A. M., BIALKOWSKA, A. B., NANDAN, M. O. & YANG, V. W. 2015. Role of Kruppel-like factor 5 in the maintenance of the stem cell niche in the intestinal crypt. Stem Cell Transl Investig, 2.

LACINA, L., PLZAK, J., KODET, O., SZABO, P., CHOVANEC, M., DVORANKOVA, B. & SMETANA, K., JR. 2015. Cancer Microenvironment: What Can We Learn from the Stem Cell Niche. Int J Mol Sci, 16, 24094-110.

LAGER, I. 1991. The insulin-antagonistic effect of the counterregulatory hormones. J Intern Med Suppl, 735, 41-7.

LEBOUVIER, A., POIGNARD, A., COQUELIN-SALSAC, L., LEOTOT, J., HOMMA, Y., JULLIEN, N., BIERLING, P., GALACTEROS, F., HERNIGOU, P., CHEVALLIER, N. & ROUARD, H. 2015. Autologous bone marrow stromal cells are promising candidates for cell therapy approaches to treat bone degeneration in sickle cell disease. Stem Cell Res, 15, 584-594.

LEE, S. L., SADOVSKY, Y., SWIRNOFF, A. H., POLISH, J. A., GODA, P., GAVRILINA, G. & MILBRANDT, J. 1996. Luteinizing hormone deficiency and female infertility in mice lacking the transcription factor NGFI-A (Egr-1). Science, 273, 1219-21.

LEE, S., YU, K. R., RYU, Y. S., OH, Y. S., HONG, I. S., KIM, H. S., LEE, J. Y., KIM, S., SEO, K. W. & KANG, K. S. 2014. miR-543 and miR-590-3p regulate human mesenchymal stem cell aging via direct targeting of AIMP3/p18. Age (Dordr), 36, 9724.

LEE, W. C., SHI, H., POON, Z., NYAN, L. M., KAUSHIK, T., SHIVASHANKAR, G. V., CHAN, J. K., LIM, C. T., HAN, J. & VAN VLIET, K. J. 2014. Multivariate biophysical markers predictive of mesenchymal stromal cell multipotency. Proc Natl Acad Sci U S A, 111, E4409-18.

LEERS-SUCHETA, S., MOROHASHI, K., MASON, J. I. & MELNER, M. H. 1997. Synergistic activation of the human type II 3beta-hydroxysteroid dehydrogenase/delta5-delta4 isomerase promoter by the transcription factor steroidogenic factor-1/adrenal 4-binding protein and phorbol ester. J Biol Chem, 272, 7960-7.

LEFRANCOIS-MARTINEZ, A. M., BLONDET-TRICHARD, A., BINART, N., VAL, P., CHAMBON, C., SAHUT-BARNOLA, I., POINTUD, J. C. & MARTINEZ, A. 2011. Transcriptional control of adrenal steroidogenesis: novel connection between Janus kinase (JAK) 2 protein and protein kinase A (PKA) through stabilization of cAMP response element-binding protein (CREB) transcription factor. J Biol Chem, 286, 32976-85.

LESAGE, F., ZIA, S., JIMENEZ, J., DEPREST, J. & TOELEN, J. 2017. The amniotic fluid as a source of mesenchymal stem cells with lung-specific characteristics. Prenat Diagn.

LI, H., JEONG, H. M., CHOI, Y. H., KIM, J. H., CHOI, J. K., YEO, C. Y., JEONG, H. G., JEONG, T. C., CHUN, C. & LEE, K. Y. 2014. Protein kinase a phosphorylates Dlx3 and regulates the function of Dlx3 during osteoblast differentiation. J Cell Biochem, 115, 2004-11.

LI, L. & CLEVERS, H. 2010. Coexistence of quiescent and active adult stem cells in mammals. Science, 327, 542-5.

LIEBAU, S., STOCKMANN, M., ILLING, A., SEUFFERLEIN, T. & KLEGER, A. 2014. [Induced pluripotent stem cells. A new resource in modern medicine]. Internist (Berl), 55, 460-9.

LIM, C., SHINKAWA, H., HASEGAWA, K., BHANGUI, P., SALLOUM, C., GOMEZ GAVARA, C., LAHAT, E., OMICHI, K., ARITA, J., SAKAMOTO, Y., COMPAGNON, P., FERAY, C., KOKUDO, N. & AZOULAY, D. 2017. Salvage Liver Transplantation or Repeat Hepatectomy for Recurrent Hepatocellular Carcinoma: An Intent-to-treat Analysis. Liver Transpl.

LIN, S.-C. J., WANI, M. A., WHITSETT, J. A. & WELLS, J. M. 2010. Klf5 regulates lineage formation in the pre-implantation mouse embryo. Development (Cambridge, England), 137, 3953-3963.

LISAK, R. P. & BENJAMINS, J. A. 2017. Melanocortins, Melanocortin Receptors and Multiple Sclerosis. Brain Sci, 7.

LIU, G., VIJAYAKUMAR, S., GRUMOLATO, L., ARROYAVE, R., QIAO, H., AKIRI, G. & AARONSON, S. A. 2009. Canonical Wnts function as potent regulators of osteogenesis by human mesenchymal stem cells. J Cell Biol, 185, 67-75.

LIU, T. M., NG, W. M., TAN, H. S., VINITHA, D., YANG, Z., FAN, J. B., ZOU, Y., HUI, J. H., LEE, E. H. & LIM, B. 2013. Molecular basis of immortalization of human mesenchymal stem cells by combination of p53 knockdown and human telomerase reverse transcriptase overexpression. Stem Cells Dev, 22, 268-78.

LIU, X., NEFZGER, C. M. & ROSSELLO, F. J. 2017. Comprehensive characterization of distinct states of human naive pluripotency generated by reprogramming.

LLAURADO, M., ABAL, M., CASTELLVI, J., CABRERA, S., GIL-MORENO, A., PEREZ-BENAVENTE, A., COLAS, E., DOLL, A., DOLCET, X., MATIAS-GUIU, X., VAZQUEZ-LEVIN, M., REVENTOS, J. & RUIZ, A. 2012a. ETV5 transcription factor is overexpressed in ovarian cancer and regulates cell adhesion in ovarian cancer cells. Int J Cancer, 130, 1532-43.

LLAURADO, M., MAJEM, B., CASTELLVI, J., CABRERA, S., GIL-MORENO, A., REVENTOS, J. & RUIZ, A. 2012b. Analysis of gene expression regulated by the ETV5 transcription factor in OV90 ovarian cancer cells identifies FOXM1 overexpression in ovarian cancer. Mol Cancer Res, 10, 914-24.

LOH, Y. H., WU, Q., CHEW, J. L., VEGA, V. B., ZHANG, W., CHEN, X., BOURQUE, G., GEORGE, J., LEONG, B., LIU, J., WONG, K. Y., SUNG, K. W., LEE, C. W., ZHAO, X. D., CHIU, K. P., LIPOVICH, L., KUZNETSOV, V. A., ROBSON, P., STANTON, L. W., WEI, C. L., RUAN, Y., LIM, B. & NG, H. H. 2006. The Oct4 and Nanog transcription network regulates pluripotency in mouse embryonic stem cells. Nat Genet, 38, 431-40.

LOMTHAISONG, K. 2001. investigation of a novel secretory protease expressed in the rat adrenal gland. PhD, University of Reading.

LOW, M. G. & KINCADE, P. W. 1985. Phosphatidylinositol is the membrane-anchoring domain of the Thy-1 glycoprotein. Nature, 318, 62-4.

LOWRY, P. J. 1984. Pro-opiocortin: the multiple adrenal hormone precursor. Review. Biosci Rep, 4, 467-82.

LOWRY, P. J., SILAS, L., MCLEAN, C., LINTON, E. A. & ESTIVARIZ, F. E. 1983. Pro-γ-melanocyte-stimulating hormone cleavage in adrenal gland undergoing compensatory growth. Nature, 306, 70.

LU, C. C., BRENNAN, J. & ROBERTSON, E. J. 2001. From fertilization to gastrulation: axis formation in the mouse embryo. Curr Opin Genet Dev, 11, 384-92.

LU, F. & ZHANG, Y. 2015. Cell totipotency: molecular features, induction, and maintenance. Natl Sci Rev, 2, 217-225.

LU, J., RICHARDSON, J. A. & OLSON, E. N. 1998. Capsulin: a novel bHLH transcription factor expressed in epicardial progenitors and mesenchyme of visceral organs. Mech Dev, 73, 23-32.

LUBECKA-PIETRUSZEWSKA, K., KAUFMAN-SZYMCZYK, A., STEFANSKA, B., CEBULA-OBRZUT, B., SMOLEWSKI, P. & FABIANOWSKA-MAJEWSKA, K. 2015. Sulforaphane Alone and in Combination with Clofarabine Epigenetically Regulates the Expression of DNA Methylation-Silenced Tumour Suppressor Genes in Human Breast Cancer Cells. J Nutrigenet Nutrigenomics, 8, 91-101.

LUCACIU, O., SORITAU, O., GHEBAN, D., CIUCA, D. R., VIRTIC, O., VULPOI, A., DIRZU, N., CAMPIAN, R., BACIUT, G., POPA, C., SIMON, S., BERCE, P., BACIUT, M. & CRISAN, B. 2015. Dental follicle stem cells in bone regeneration on titanium implants. BMC Biotechnol, 15, 114.

LUCARELLI, G., GALLEGGIANTE, V., RUTIGLIANO, M., VAVALLO, A., DITONNO, P. & BATTAGLIA, M. 2015. Isolation and characterization of cancer stem cells in renal cell carcinoma. Urologia, 82, 46-53.

LUGER, T. A., SCHOLZEN, T. E., BRZOSKA, T. & BOHM, M. 2003. New insights into the functions of alpha-MSH and related peptides in the immune system. Ann N Y Acad Sci, 994, 133-40.

LUO, X., IKEDA, Y. & PARKER, K. L. 1994. A cell-specific nuclear receptor is essential for adrenal and gonadal development and sexual differentiation. Cell, 77, 481-90.

MACFARLANE, D. P., FORBES, S. & WALKER, B. R. 2008. Glucocorticoids and fatty acid metabolism in humans: fuelling fat redistribution in the metabolic syndrome. J Endocrinol, 197, 189-204.

MAINS, R. E., EIPPER, B. A. & LING, N. 1977. Common precursor to corticotropins and endorphins. Proc Natl Acad Sci U S A, 74, 3014-8.

MAKHOUL, G., CHIU, R. C. & CECERE, R. 2013. Placental mesenchymal stem cells: a unique source for cellular cardiomyoplasty. Ann Thorac Surg, 95, 1827-33.

MALENDOWICZ, L. K. 2010. 100th anniversary of the discovery of the human adrenal fetal zone by Stella Starkel and Leslaw Wegrzynowski: how far have we come? Folia Histochem Cytobiol, 48, 491-506.

MARESCHI, K., RUSTICHELLI, D., CALABRESE, R., GUNETTI, M., SANAVIO, F., CASTIGLIA, S., RISSO, A., FERRERO, I., TARELLA, C. & FAGIOLI, F. 2012. Multipotent mesenchymal stromal stem cell expansion by plating whole bone marrow at a low cellular density: a more advantageous method for clinical use. Stem Cells Int, 2012, 920581.

MASSON, N. M., CURRIE, I. S., TERRACE, J. D., GARDEN, O. J., PARKS, R. W. & ROSS, J. A. 2006. Hepatic progenitor cells in human fetal liver express the oval cell marker Thy-1. Am J Physiol Gastrointest Liver Physiol, 291, G45-54.

MAYANI, H. & LANSDORP, P. M. 1994. Thy-1 expression is linked to functional properties of primitive hematopoietic progenitor cells from human umbilical cord blood. Blood, 83, 2410-7.

MAZZEI, L., GARCIA, M., CALVO, J. P., CASAROTTO, M., FORNES, M., ABUD, M. A., CUELLO-CARRION, D., FERDER, L. & MANUCHA, W. 2016. Changes in renal WT-1 expression preceding hypertension development. BMC Nephrol, 17, 34.

MCDONALD, C. A., FAHEY, M. C., JENKIN, G. & MILLER, S. L. 2017. Umbilical cord blood cells for treatment of cerebral palsy; timing and treatment options. Pediatr Res.

MCNUTT, N. S. & JONES, A. L. 1970. Observations on the ultrastructure of cytodifferentiation in the human fetal adrenal cortex. Lab Invest, 22, 513-27.

MERSMANN, H. J. & SEGAL, H. L. 1969. Glucocorticoid control of the liver glycogen synthetase-activating system. J Biol Chem, 244, 1701-4.

MESIANO, S., COULTER, C. L. & JAFFE, R. B. 1993. Localization of cytochrome P450 cholesterol side-chain cleavage, cytochrome P450 17 alpha-hydroxylase/17, 20-lyase, and 3 beta-hydroxysteroid dehydrogenase isomerase steroidogenic enzymes in human and rhesus monkey fetal adrenal glands: reappraisal of functional zonation. J Clin Endocrinol Metab, 77, 1184-9.

MILLINGTON, G. W. 2007. The role of proopiomelanocortin (POMC) neurones in feeding behaviour. Nutr Metab (Lond), 4, 18.

MITALIPOV, S. & WOLF, D. 2009. Totipotency, Pluripotency and Nuclear Reprogramming. In: MARTIN, U. (ed.) Engineering of Stem Cells. Springer Berlin Heidelberg.

MITANI, F. 2014. Functional zonation of the rat adrenal cortex: the development and maintenance. Proc Jpn Acad Ser B Phys Biol Sci, 90, 163-83.

MITANI, F., SUZUKI, H., HATA, J., OGISHIMA, T., SHIMADA, H. & ISHIMURA, Y. 1994. A novel cell layer without corticosteroid-synthesizing enzymes in rat adrenal cortex: histochemical detection and possible physiological role. Endocrinology, 135, 431-8.

MIZUTANI, T., KAWABE, S., ISHIKANE, S., IMAMICHI, Y., UMEZAWA, A. & MIYAMOTO, K. 2015. Identification of novel steroidogenic factor 1 (SF-1)-target genes and components of the SF-1 nuclear complex. Mol Cell Endocrinol, 408, 133-7.

MLYNARCZUK, J., WROBEL, M. H. & KOTWICA, J. 2014. The orphan nuclear receptor SF-1 is involved in the effect of PCBs, DDT, and DDE on the secretion of steroid hormones and oxytocin from bovine luteal cells during the estrous cycle in vitro. Theriogenology, 81, 877-86.

MOISEENKO, A., KHEIROLLAHI, V., CHAO, C. M., AHMADVAND, N., QUANTIUS, J., WILHELM, J., HEROLD, S., AHLBRECHT, K., MORTY, R. E., RIZVANOV, A. A., MINOO, P., EL AGHA, E. & BELLUSCI, S. 2017. Origin and characterization of alpha smooth muscle actin-positive cells during murine lung development.

MOORE, A. W., MCINNES, L., KREIDBERG, J., HASTIE, N. D. & SCHEDL, A. 1999. YAC complementation shows a requirement for Wt1 in the development of epicardium, adrenal gland and throughout nephrogenesis. Development, 126, 1845-57.

MORGANI, S. M., CANHAM, M. A., NICHOLS, J., SHAROV, A. A., MIGUELES, R. P., KO, M. S. & BRICKMAN, J. M. 2013. Totipotent embryonic stem cells arise in ground-state culture conditions. Cell Rep, 3, 1945-57.

MORRISON, S. J. & KIMBLE, J. 2006. Asymmetric and symmetric stem-cell divisions in development and cancer. Nature, 441, 1068-1074.

MOUNTJOY, K. G. 2010. Functions for pro-opiomelanocortin-derived peptides in obesity and diabetes. Biochem J, 428, 305-24.

MOUNTJOY, K. G. 2015. Pro-Opiomelanocortin (POMC) Neurones, POMC-Derived Peptides, Melanocortin Receptors and Obesity: How Understanding of this System has Changed Over the Last Decade. J Neuroendocrinol, 27, 406-18.

MOUNTJOY, K. G., ROBBINS, L. S., MORTRUD, M. T. & CONE, R. D. 1992. The cloning of a family of genes that encode the melanocortin receptors. Science, 257, 1248-51.

MULROW, P. J. 1972. The adrenal cortex. Annu Rev Physiol, 34, 409-24.

MUNOZ-ESPIN, D., CANAMERO, M., MARAVER, A., GOMEZ-LOPEZ, G., CONTRERAS, J., MURILLO-CUESTA, S., RODRIGUEZ-BAEZA, A., VARELA-NIETO, I., RUBERTE, J., COLLADO, M. & SERRANO, M. 2013. Programmed cell senescence during mammalian embryonic development. Cell, 155, 1104-18.

MURAGLIA, A., CANCEDDA, R. & QUARTO, R. 2000. Clonal mesenchymal progenitors from human bone marrow differentiate in vitro according to a hierarchical model. J Cell Sci, 113 (Pt 7), 1161-6.

MURRY, C. E. & KELLER, G. 2008. Differentiation of Embryonic Stem Cells to Clinically Relevant Populations: Lessons from Embryonic Development. Cell, 132, 661-680.

NAKAMIZO, A., MARINI, F., AMANO, T., KHAN, A., STUDENY, M., GUMIN, J., CHEN, J., HENTSCHEL, S., VECIL, G., DEMBINSKI, J., ANDREEFF, M. & LANG, F. F. 2005. Human bone marrow-derived mesenchymal stem cells in the treatment of gliomas. Cancer Res, 65, 3307-18.

NAKANISHI, M. & OTSU, M. 2012. Development of Sendai virus vectors and their potential applications in gene therapy and regenerative medicine. Curr Gene Ther, 12, 410-6.

NAVARRO-BETANCOURT, J. R. & HERNANDEZ, S. 2015. On the existence of cardiomesenchymal stem cells. Med Hypotheses, 84, 511-5.

NICOLAIDES, N. C., KYRATZI, E., LAMPROKOSTOPOULOU, A., CHROUSOS, G. P. & CHARMANDARI, E. 2015. Stress, the stress system and the role of glucocorticoids. Neuroimmunomodulation, 22, 6-19.

NIETO, M. A., PATEL, K. & WILKINSON, D. G. 1996. In situ hybridization analysis of chick embryos in whole mount and tissue sections. Methods Cell Biol, 51, 219-35.

NINAGAWA, N., MURAKAMI, R., ISOBE, E., TANAKA, Y., NAKAGAWA, H. & TORIHASHI, S. 2011. Mesenchymal stem cells originating from ES cells show high telomerase activity and therapeutic benefits. Differentiation, 82, 153-164.

NISHIMOTO, K., NAKAGAWA, K., LI, D., KOSAKA, T., OYA, M., MIKAMI, S., SHIBATA, H., ITOH, H., MITANI, F., YAMAZAKI, T., OGISHIMA, T., SUEMATSU, M. & MUKAI, K. 2010. Adrenocortical zonation in humans under normal and pathological conditions. J Clin Endocrinol Metab, 95, 2296-305.

NORRIS, D. O. & CARR, J. A. 2013. Chapter 8 - The Mammalian Adrenal Glands: Cortical and Chromaffin Cells. Vertebrate Endocrinology (Fifth Edition). San Diego: Academic Press.

NUSCHKE, A., RODRIGUES, M., WELLS, A. W., SYLAKOWSKI, K. & WELLS, A. 2016. Mesenchymal stem cells/multipotent stromal cells (MSCs) are glycolytic and thus glucose is a limiting factor of in vitro models of MSC starvation. Stem Cell Res Ther, 7, 179.

NUSSLEIN-VOLHARD, C. & WIESCHAUS, E. 1980. Mutations affecting segment number and polarity in Drosophila. Nature, 287, 795-801.

OATLEY, M. J., KAUCHER, A. V., RACICOT, K. E. & OATLEY, J. M. 2011. Inhibitor of DNA binding 4 is expressed selectively by single spermatogonia in the male germline and regulates the self-renewal of spermatogonial stem cells in mice. Biol Reprod, 85, 347-56.

O'HARE, M. J. & NEVILLE, A. M. 1973. Effects of Adrenocorticotrophin on Steroidogenesis and Proliferation by Adult Adrenal Cells in Monolayer Culture. Biochemical Society Transactions, 1, 1088-1091.

OLIVIER, E. N. & BOUHASSIRA, E. E. 2011. Differentiation of human embryonic stem cells into mesenchymal stem cells by the "raclure" method. Methods Mol Biol, 690, 183-93.

OLTULU, F., AKTUG, H., UYSAL, A., TURGAN, N., OKTEM, G., ERBAS, O., YAVASOGLU, N. K. & YAVASOGLU, A. 2015. Immunoexpressions of embryonic and nonembryonic stem cell markers (Nanog, Thy-1, c-kit) and cellular connections (connexin 43 and occludin) on testicular tissue in thyrotoxicosis rat model. Hum Exp Toxicol, 34, 601-11.

ORKIN, S. H. & HOCHEDLINGER, K. 2011. Chromatin connections to pluripotency and cellular reprogramming. Cell, 145, 835-50.

PALUMBO, R. & BIANCHI, M. E. 2004. High mobility group box 1 protein, a cue for stem cell recruitment. Biochem Pharmacol, 68, 1165-70.

PALUMBO, R., GALVEZ, B. G., PUSTERLA, T., DE MARCHIS, F., COSSU, G., MARCU, K. B. & BIANCHI, M. E. 2007. Cells migrating to sites of tissue damage in response to the danger signal HMGB1 require NF-kappaB activation. J Cell Biol, 179, 33-40.

PARSONS, M. T., BUCHANAN, D. D., THOMPSON, B., YOUNG, J. P. & SPURDLE, A. B. 2012. Correlation of tumour BRAF mutations and MLH1 methylation with germline mismatch repair (MMR) gene mutation status: a literature review assessing utility of tumour features for MMR variant classification. J Med Genet, 49, 151-7.

PARTIDA, G. J., STRADLEIGH, T. W., OGATA, G., GODZDANKER, I. & ISHIDA, A. T. 2012. Thy1 associates with the cation channel subunit HCN4 in adult rat retina. Invest Ophthalmol Vis Sci, 53, 1696-703.

PATEL, D., MORTON, D. J., CAREY, J., HAVRDA, M. C. & CHAUDHARY, J. 2015. Inhibitor of differentiation 4 (ID4): From development to cancer. Biochim Biophys Acta, 1855, 92-103.

PAUL, C. D., MISTRIOTIS, P. & KONSTANTOPOULOS, K. 2017. Cancer cell motility: lessons from migration in confined spaces. Nature reviews. Cancer, 17, 131-140.

PELEKANOS, R. A., SARDESAI, V. S., FUTREGA, K., LOTT, W. B., KUHN, M. & DORAN, M. R. 2016. Isolation and Expansion of Mesenchymal Stem/Stromal Cells Derived from Human Placenta Tissue. Journal of Visualized Experiments : JoVE, 54204.

PETERSEN, B. E., GOFF, J. P., GREENBERGER, J. S. & MICHALOPOULOS, G. K. 1998. Hepatic oval cells express the hematopoietic stem cell marker thy-1 in the rat. Hepatology, 27, 433-445.

PIHLAJOKI, M., DORNER, J., COCHRAN, R. S., HEIKINHEIMO, M. & WILSON, D. B. 2015. Adrenocortical zonation, renewal, and remodeling. Front Endocrinol (Lausanne), 6, 27.

PITTENGER, M. F., MACKAY, A. M., BECK, S. C., JAISWAL, R. K., DOUGLAS, R., MOSCA, J. D., MOORMAN, M. A., SIMONETTI, D. W., CRAIG, S. & MARSHAK, D. R. 1999. Multilineage potential of adult human mesenchymal stem cells. Science, 284, 143-7.

PLONES, T., FISCHER, M., HOHNE, K., SATO, H., MULLER-QUERNHEIM, J. & ZISSEL, G. 2017. Turning back the Wheel: Inducing Mesenchymal to Epithelial Transition via Wilms Tumor 1 Knockdown in Human Mesothelioma Cell Lines to Influence Proliferation, Invasiveness, and Chemotaxis. Pathol Oncol Res.

POLO, J. M., ANDERSSEN, E., WALSH, R. M., SCHWARZ, B. A., NEFZGER, C. M., LIM, S. M., BORKENT, M., APOSTOLOU, E., ALAEI, S., CLOUTIER, J., BAR-NUR, O., CHELOUFI, S., STADTFELD, M., FIGUEROA, M. E., ROBINTON, D., NATESAN, S., MELNICK, A., ZHU, J., RAMASWAMY, S. & HOCHEDLINGER, K. 2012. A molecular roadmap of reprogramming somatic cells into iPS cells. Cell, 151, 1617-32.

PONT, S. 1987. Thy-1: a lymphoid cell subset marker capable of delivering an activation signal to mouse T lymphocytes. Biochimie, 69, 315-320.

PONTIKOGLOU, C., LANGONNE, A., BA, M. A., VARIN, A., ROSSET, P., CHARBORD, P., SENSEBE, L. & DESCHASEAUX, F. 2016. CD200 expression in human cultured bone marrow mesenchymal stem cells is induced by pro-osteogenic and pro-inflammatory cues. J Cell Mol Med, 20, 655-65.

POOLMAN, R. A. & BROOKS, G. 1998. Expressions and activities of cell cycle regulatory molecules during the transition from myocyte hyperplasia to hypertrophy. J Mol Cell Cardiol, 30, 2121-35.

POP, D. M., SORITAU, O., SUSMAN, S., RUS-CIUCA, D., GROZA, I. S., CIORTEA, R., MIHU, D. & MIHU, C. M. 2015. Potential of placental-derived human mesenchymal stem cells for osteogenesis and neurogenesis. Rom J Morphol Embryol, 56, 989-96.

POZNANSKY, M. C., EVANS, R. H., FOXALL, R. B., OLSZAK, I. T., PIASCIK, A. H., HARTMAN, K. E., BRANDER, C., MEYER, T. H., PYKETT, M. J., CHABNER, K. T., KALAMS, S. A., ROSENZWEIG, M. & SCADDEN, D. T. 2000. Efficient generation of human T cells from a tissue-engineered thymic organoid. Nat Biotechnol, 18, 729-34.

PRITCHARD, L. E., TURNBULL, A. V. & WHITE, A. 2002. Pro-opiomelanocortin processing in the hypothalamus: impact on melanocortin signalling and obesity. J Endocrinol, 172, 411-21.

RAMAYYA, M. S., ZHOU, J., KINO, T., SEGARS, J. H., BONDY, C. A. & CHROUSOS, G. P. 1997. Steroidogenic factor 1 messenger ribonucleic acid expression in steroidogenic and nonsteroidogenic human tissues: Northern blot and in situ hybridization studies. J Clin Endocrinol Metab, 82, 1799-806.

RAO, A. J., LONG, J. A. & RAMACHANDRAN, J. 1978. Effects of Antiserum to Adrenocorticotropin on Adrenal Growth and Function*. Endocrinology, 102, 371-378.

REGE, T. A. & HAGOOD, J. S. 2006. Thy-1 as a regulator of cell-cell and cell-matrix interactions in axon regeneration, apoptosis, adhesion, migration, cancer, and fibrosis. FASEB J, 20, 1045-54.

REINDERS, J. & SICKMANN, A. 2007. Modificomics: Posttranslational modifications beyond protein phosphorylation and glycosylation. Biomolecular Engineering, 24, 169-177.

ROBERTS, J. L. & HERBERT, E. 1977. Characterization of a common precursor to corticotropin and beta-lipotropin: identification of beta-lipotropin peptides and their arrangement relative to corticotropin in the precursor synthesized in a cell-free system. Proc Natl Acad Sci U S A, 74, 5300-4.

ROONEY, G. E., HOWARD, L., O'BRIEN, T., WINDEBANK, A. J. & BARRY, F. P. 2009. Elevation of cAMP in mesenchymal stem cells transiently upregulates neural markers rather than inducing neural differentiation. Stem Cells Dev, 18, 387-98.

RUBIN, H. 2002. The disparity between human cell senescence in vitro and lifelong replication in vivo. Nat Biotechnol, 20, 675-81.

RUBINSTEIN, J. D., ELAGIB, K. E. & GOLDFARB, A. N. 2012. Cyclic AMP signaling inhibits megakaryocytic differentiation by targeting transcription factor 3 (E2A) cyclin-dependent kinase inhibitor 1A (CDKN1A) transcriptional axis. J Biol Chem, 287, 19207-15.

RUIZ-BABOT, G., BALYURA, M., HADJIDEMETRIOU, I., AJODHA, S. J., TAYLOR, D. R., GHATAORE, L., TAYLOR, N. F., SCHUBERT, U., ZIEGLER, C. G., STORR, H. L., DRUCE, M. R., GEVERS, E. F., DRAKE, W. M., SRIRANGALINGAM, U., CONWAY, G. S., KING, P. J., METHERELL, L. A., BORNSTEIN, S. R. & GUASTI, L. 2018. Modeling Congenital Adrenal Hyperplasia and Testing Interventions for Adrenal Insufficiency Using Donor-Specific Reprogrammed Cells. Cell Reports, 22, 1236-1249.

RUIZ-BABOT, G., HADJIDEMETRIOU, I., KING, P. J. & GUASTI, L. 2015. New directions for the treatment of adrenal insufficiency. Front Endocrinol (Lausanne), 6, 70.

RUSSELL, K. C., PHINNEY, D. G., LACEY, M. R., BARRILLEAUX, B. L., MEYERTHOLEN, K. E. & O'CONNOR, K. C. 2010. In vitro high-capacity assay to quantify the clonal heterogeneity in trilineage potential of mesenchymal stem cells reveals a complex hierarchy of lineage commitment. Stem Cells, 28, 788-98.

SADOVSKY, Y., CRAWFORD, P. A., WOODSON, K. G., POLISH, J. A., CLEMENTS, M. A., TOURTELLOTTE, L. M., SIMBURGER, K. & MILBRANDT, J. 1995. Mice deficient in the orphan receptor steroidogenic factor 1 lack adrenal glands and gonads but express P450 side-chain-cleavage enzyme in the placenta and have normal embryonic serum levels of corticosteroids. Proc Natl Acad Sci U S A, 92, 10939-43.

SALMON, T. N. & ZWEMER, R. L. 1941. A study of the life history of cortico-adrenal gland cells of the rat by means of trypan blue injections. The Anatomical Record, 80, 421-429.

SAMPSON, V. B., DAVID, J. M., PUIG, I., PATIL, P. U., DE HERREROS, A. G., THOMAS, G. V. & RAJASEKARAN, A. K. 2014. Wilms' tumor protein induces an epithelial-mesenchymal hybrid differentiation state in clear cell renal cell carcinoma. PLoS One, 9, e102041.

SAMSONRAJ, R. M., RAI, B., SATHIYANATHAN, P., PUAN, K. J., ROTZSCHKE, O., HUI, J. H., RAGHUNATH, M., STANTON, L. W., NURCOMBE, V. & COOL, S. M. 2015. Establishing criteria for human mesenchymal stem cell potency. Stem Cells, 33, 1878-91.

SCHIMMER, B. P. & WHITE, P. C. 2010. Minireview: steroidogenic factor 1: its roles in differentiation, development, and disease. Mol Endocrinol, 24, 1322-37.

SCHNABEL, C. A., SELLERI, L. & CLEARY, M. L. 2003. Pbx1 is essential for adrenal development and urogenital differentiation. Genesis, 37, 123-30.

SEET, C. S., HE, C., BETHUNE, M. T., LI, S., CHICK, B., GSCHWENG, E. H., ZHU, Y., KIM, K., KOHN, D. B., BALTIMORE, D., CROOKS, G. M. & MONTEL-HAGEN, A. 2017. Generation of mature T cells from human hematopoietic stem and progenitor cells in artificial thymic organoids. Nat Methods, 14, 521-530.

SHANG, J., YAO, Y., FAN, X., SHANGGUAN, L., LI, J., LIU, H. & ZHOU, Y. 2016. miR-29c-3p promotes senescence of human mesenchymal stem cells by targeting CNOT6 through p53-p21 and p16-pRB pathways. Biochim Biophys Acta, 1863, 520-32.

SHARMA, N., KAUR, M., AGARWAL, T., SANGWAN, V. S. & VAJPAYEE, R. B. 2017. Treatment of Acute Ocular Chemical Burns. Surv Ophthalmol.

SHARMA, P. M., BOWMAN, M., MADDEN, S. L., RAUSCHER, F. J., 3RD & SUKUMAR, S. 1994. RNA editing in the Wilms' tumor susceptibility gene, WT1. Genes Dev, 8, 720-31.

SHARROCKS, A. D. 2001. The ETS-domain transcription factor family. Nat Rev Mol Cell Biol, 2, 827-37.

SHI, Q., GAO, J., JIANG, Y., SUN, B., LU, W., SU, M., XU, Y., YANG, X. & ZHANG, Y. 2017. Differentiation of human umbilical cord Wharton's jelly-derived mesenchymal stem cells into endometrial cells. Stem Cell Res Ther, 8, 246.

SHIBATA, M., CHIBA, T., MATSUOKA, T., MIHARA, N., KAWASHIRI, S. & IMAI, K. 2015. Kruppel-like factors 4 and 5 expression and their involvement in differentiation of oral carcinomas. Int J Clin Exp Pathol, 8, 3701-9.

SHIM, Y., NAM, M. H., HYUK, S. W., YOON, S. Y. & SONG, J. M. 2015. Concurrent hypermulticolor monitoring of CD31, CD34, CD45 and CD146 endothelial progenitor cell markers for acute myocardial infarction. Anal Chim Acta, 853, 501-7.

SHIMA, Y., MIYABAYASHI, K., BABA, T., OTAKE, H., OKA, S., ZUBAIR, M. & MOROHASHI, K.-I. 2012. Identification of an Enhancer in the Ad4BP/SF-1 Gene Specific for Fetal Leydig Cells. Endocrinology, 153, 417-425.

SI-TAYEB, K., LEMAIGRE, F. P. & DUNCAN, S. A. 2010. Organogenesis and development of the liver. Dev Cell, 18, 175-89.

SMITH, P. E. 1930. Hypophysectomy and a replacement therapy in the rat. American Journal of Anatomy, 45, 205-273.

SON, B. R., MARQUEZ-CURTIS, L. A., KUCIA, M., WYSOCZYNSKI, M., TURNER, A. R., RATAJCZAK, J., RATAJCZAK, M. Z. & JANOWSKA-WIECZOREK, A. 2006. Migration of bone marrow and cord blood mesenchymal stem cells in vitro is regulated by stromal-derived factor-1-CXCR4 and hepatocyte growth factor-c-met axes and involves matrix metalloproteinases. Stem Cells, 24, 1254-64.

SORIA, B., ROCHE, E., BERNA, G., LEON-QUINTO, T., REIG, J. A. & MARTIN, F. 2000. Insulin-secreting cells derived from embryonic stem cells normalize glycemia in streptozotocin-induced diabetic mice. Diabetes, 49, 157-62.

SRINIVASAN, P. P., PATEL, V. N., LIU, S., HARRINGTON, D. A., HOFFMAN, M. P., JIA, X., WITT, R. L., FARACH-CARSON, M. C. & PRADHAN-BHATT, S. 2017. Primary Salivary Human Stem/Progenitor Cells Undergo Microenvironment-Driven Acinar-Like Differentiation in Hyaluronate Hydrogel Culture. Stem Cells Transl Med, 6, 110-120.

STACHENKO, J. & GIROUD, C. J. 1964. Further observations on the functional zonation of the adrenal cortex. Can J Biochem, 42, 1777-86.

STADTFELD, M. & HOCHEDLINGER, K. 2010. Induced pluripotency: history, mechanisms, and applications. Genes & Development, 24, 2239-2263.

STORER, M., MAS, A., ROBERT-MORENO, A., PECORARO, M., ORTELLS, M. C., DI GIACOMO, V., YOSEF, R., PILPEL, N., KRIZHANOVSKY, V., SHARPE, J. & KEYES, W. M. 2013. Senescence is a developmental mechanism that contributes to embryonic growth and patterning. Cell, 155, 1119-30.

SUCHESTON, M. E. & CANNON, M. S. 1968. Development of zonular patterns in the human adrenal gland. J Morphol, 126, 477-91.

SUN, F., XU, Q., ZHAO, D. & DEGUI CHEN, C. 2015. Id4 Marks Spermatogonial Stem Cells in the Mouse Testis. Sci Rep, 5, 17594.

TAKEDA, Y., HARADA, Y., YOSHIKAWA, T. & DAI, P. 2017. Direct conversion of human fibroblasts to brown adipocytes by small chemical compounds. Sci Rep, 7, 4304.

TANG, Y., LIU, L., WANG, P., CHEN, D., WU, Z. & TANG, C. 2017. Periostin promotes migration and osteogenic differentiation of human periodontal ligament mesenchymal stem cells via the Jun amino-terminal kinases (JNK) pathway under inflammatory conditions. Cell Prolif.

TENG, Z., YOSHIDA, T., OKABE, M., TODA, A., HIGUCHI, O., NOGAMI, M., YONEDA, N., ZHOU, K., KYO, S., KIYONO, T. & NIKAIDO, T. 2013. Establishment of immortalized human amniotic mesenchymal stem cells. Cell Transplant, 22, 267-78.

THOMAS, T., NOWKA, K., LAN, L. & DERWAHL, M. 2006. Expression of endoderm stem cell markers: evidence for the presence of adult stem cells in human thyroid glands. Thyroid, 16, 537-44.

TORRES, T. E. P., DE MENDONÇA, P. O. R. & LOTFI, C. F. P. 2010. Synthetic modified N-POMC1–28 controls in vivo proliferation and blocks apoptosis in rat adrenal cortex. Cell and Tissue Research, 341, 239-250.

TREMBLAY, R. G., SIKORSKA, M., SANDHU, J. K., LANTHIER, P., RIBECCO-LUTKIEWICZ, M. & BANI-YAGHOUB, M. 2010. Differentiation of mouse Neuro 2A cells into dopamine neurons. J Neurosci Methods, 186, 60-7.

TSUJI, Y., YOSHIMURA, N., AOKI, H., SHAROV, A. A., KO, M. S. H., MOTOHASHI, T. & KUNISADA, T. 2008. Maintenance of undifferentiated mouse embryonic stem cells in suspension by the serum- and feeder-free defined culture condition. Developmental dynamics : an official publication of the American Association of Anatomists, 237, 2129-2138.

TURINETTO, V. & GIACHINO, C. 2015. Histone variants as emerging regulators of embryonic stem cell identity. Epigenetics, 10, 563-73.

UMETANI, N., MORI, T., KOYANAGI, K., SHINOZAKI, M., KIM, J., GIULIANO, A. E. & HOON, D. S. 2005. Aberrant hypermethylation of ID4 gene promoter region increases risk of lymph node metastasis in T1 breast cancer. Oncogene, 24, 4721-7.

URRACA, N., MEMON, R., EL-IYACHI, I., GOORHA, S., VALDEZ, C., TRAN, Q. T., SCROGGS, R., MIRANDA-CARBONI, G. A., DONALDSON, M., BRIDGES, D. & REITER, L. T. 2015. Characterization of neurons from immortalized dental pulp stem cells for the study of neurogenetic disorders. Stem Cell Res, 15, 722-30.

VAL, P., LEFRANÇOIS-MARTINEZ, A.-M., VEYSSIÈRE, G. & MARTINEZ, A. 2003. SF-1 a key player in the development and differentiation of steroidogenic tissues. Nuclear Receptor, 1, 8.

VAL, P., MARTINEZ-BARBERA, J. P. & SWAIN, A. 2007. Adrenal development is initiated by Cited2 and Wt1 through modulation of Sf-1 dosage. Development, 134, 2349-58.

VAN WEERDEN, W. M., BIERINGS, H. G., VAN STEENBRUGGE, G. J., DE JONG, F. H. & SCHRODER, F. H. 1992. Adrenal glands of mouse and rat do not synthesize androgens. Life Sci, 50, 857-61.

VERMILYEA, S. C., GUTHRIE, S., MEYER, M., SMUGA-OTTO, K., BRAUN, K., HOWDEN, S., THOMSON, J. A., ZHANG, S. C., EMBORG, M. E. & GOLOS, T. G. 2017. Induced Pluripotent Stem Cell-Derived Dopaminergic Neurons from Adult Common Marmoset Fibroblasts. Stem Cells Dev, 26, 1225-1235.

VISVADER, J. E. & LINDEMAN, G. J. 2008. Cancer stem cells in solid tumours: accumulating evidence and unresolved questions. Nat Rev Cancer, 8, 755-68.

WALCZAK, E. M. & HAMMER, G. D. 2015. Regulation of the adrenocortical stem cell niche: implications for disease. Nat Rev Endocrinol, 11, 14-28.

WANG, C. Y., CHEN, W. Y., LAI, P. Y. & CHUNG, B. C. 2013. Distinct functions of steroidogenic factor-1 (NR5A1) in the nucleus and the centrosome. Mol Cell Endocrinol, 371, 148-53.

WANG, S., MO, M., WANG, J., SADIA, S., SHI, B., FU, X., YU, L., TREDGET, E. E. & WU, Y. 2017. Platelet-derived growth factor receptor beta identifies mesenchymal stem cells with enhanced engraftment to tissue injury and pro-angiogenic property. Cell Mol Life Sci.

WANG, T. & RAINEY, W. E. 2012. Human adrenocortical carcinoma cell lines. Mol Cell Endocrinol, 351, 58-65.

WANG, Y., MAO, X. & YANG, T. 2017. [Comparison of differentiated endothelial cells from the embryonic stem cells with human umbilical vein endothelial cells]. Zhong Nan Da Xue Xue Bao Yi Xue Ban, 42, 374-379.

WATANABE, N., INOUE, H. & FUJII-KURIYAMA, Y. 1994. Regulatory mechanisms of cAMP-dependent and cell-specific expression of human steroidogenic cytochrome P450scc (CYP11A1) gene. Eur J Biochem, 222, 825-34.

WEN, Q., WANG, Y., TANG, J., CHENG, C. Y. & LIU, Y. X. 2016. Sertoli Cell Wt1 Regulates Peritubular Myoid Cell and Fetal Leydig Cell Differentiation during Fetal Testis Development. PLoS One, 11, e0167920.

WEN, Y. H., HO, A., PATIL, S., AKRAM, M., CATALANO, J., EATON, A., NORTON, L., BENEZRA, R. & BROGI, E. 2012. Id4 protein is highly expressed in triple-negative breast carcinomas: possible implications for BRCA1 downregulation. Breast Cancer Res Treat, 135, 93-102.

WILHELM, D. & ENGLERT, C. 2002. The Wilms tumor suppressor WT1 regulates early gonad development by activation of Sf1. Genes Dev, 16, 1839-51.

WILKINSON, A. C. & GOTTGENS, B. 2013. Transcriptional regulation of haematopoietic stem cells. Adv Exp Med Biol, 786, 187-212.

WILLENBERG, H. S. & BORNSTEIN, S. R. 2000. Adrenal Cortex; Development, Anatomy, Physiology. In: DE GROOT, L. J., CHROUSOS, G., DUNGAN, K., FEINGOLD, K. R., GROSSMAN, A., HERSHMAN, J. M., KOCH, C., KORBONITS, M., MCLACHLAN, R., NEW, M., PURNELL, J., REBAR, R., SINGER, F. & VINIK, A. (eds.) Endotext. South Dartmouth (MA): MDText.com, Inc.

WINNER, M., KOONG, A. C., RENDON, B. E., ZUNDEL, W. & MITCHELL, R. A. 2007. Amplification of tumor hypoxic responses by macrophage migration inhibitory factor-dependent hypoxia-inducible factor stabilization. Cancer Res, 67, 186-93.

WISLET-GENDEBIEN, S., LAUDET, E., NEIRINCKX, V., ALIX, P., LEPRINCE, P., GLEJZER, A., POULET, C., HENNUY, B., SOMMER, L., SHAKHOVA, O. & ROGISTER, B. 2012. Mesenchymal stem cells and neural crest stem cells from adult bone marrow: characterization of their surprising similarities and differences. Cell Mol Life Sci, 69, 2593-608.

WU, X., GOODYEAR, S. M., TOBIAS, J. W., AVARBOCK, M. R. & BRINSTER, R. L. 2011. Spermatogonial stem cell self-renewal requires ETV5-mediated downstream activation of Brachyury in mice. Biol Reprod, 85, 1114-23.

WU, Y. H., LO, H. F., CHEN, S. H. & CHEN, H. 2013. Caspase-14 suppresses GCM1 acetylation and inhibits placental cell differentiation. Faseb j, 27, 2818-28.

XIE, K. & ABBRUZZESE, J. L. 2003. Developmental biology informs cancer: the emerging role of the hedgehog signaling pathway in upper gastrointestinal cancers. Cancer Cell, 4, 245-7.

XIE, L., ZHOU, B., HE, Y., LIN, T., ZHU, L. & LYU, J. 2014. [Isolation and identification of cancer stem cells from human LACC cell line]. Zhonghua Yan Ke Za Zhi, 50, 753-7.

XING, C., CI, X., SUN, X., FU, X., ZHANG, Z., DONG, E. N., HAO, Z.-Z. & DONG, J.-T. 2014. Klf5 Deletion Promotes Pten Deletion–Initiated Luminal-Type Mouse Prostate Tumors through Multiple Oncogenic Signaling Pathways. Neoplasia (New York, N.Y.), 16, 883-899.

XING, Y., LERARIO, A. M., RAINEY, W. & HAMMER, G. D. 2015. Development of adrenal cortex zonation. Endocrinol Metab Clin North Am, 44, 243-74.

XING, Y., LERARIO, A., RAINEY, W. & HAMMER, G. D. 2015. Development of Adrenal Cortex Zonation. Endocrinology and metabolism clinics of North America, 44, 243-274.

XING, Y., MOROHASHI, K. I., INGRAHAM, H. A. & HAMMER, G. D. 2017. Timing of adrenal regression controlled by synergistic interaction between Sf1 SUMOylation and Dax1.

XU, F., YI, J., WANG, Z., HU, Y., HAN, C., XUE, Q., ZHANG, X. & LUAN, X. 2017. IL-27 regulates the adherence, proliferation, and migration of MSCs and enhances their regulatory effects on Th1 and Th2 subset generations. Immunol Res, 65, 903-912.

XU, J., HUANG, Z., LIN, L., FU, M., SONG, Y., SHEN, Y., REN, D., GAO, Y., SU, Y., ZOU, Y., CHEN, Y., ZHANG, D., HU, W., QIAN, J. & GE, J. 2015. miRNA-130b is required for the ERK/FOXM1 pathway activation-mediated protective effects of isosorbide dinitrate against mesenchymal stem cell senescence induced by high glucose. Int J Mol Med, 35, 59-71.

YANG, L. & LAI, D. 2013. Ovarian cancer stem cells enrichment. Methods Mol Biol, 1049, 337-45.

YANG, L., SUWA, T., WRIGHT, W. E., SHAY, J. W. & HORNSBY, P. J. 2001. Telomere shortening and decline in replicative potential as a function of donor age in human adrenocortical cells. Mech Ageing Dev, 122, 1685-94.

YASUI, T., MABUCHI, Y., TORIUMI, H., EBINE, T., NIIBE, K., HOULIHAN, D. D., MORIKAWA, S., ONIZAWA, K., KAWANA, H., AKAZAWA, C., SUZUKI, N., NAKAGAWA, T., OKANO, H. & MATSUZAKI, Y. 2015. Purified Human Dental Pulp Stem Cells Promote Osteogenic Regeneration. J Dent Res.

YATES, R., KATUGAMPOLA, H., CAVLAN, D., COGGER, K., MEIMARIDOU, E., HUGHES, C., METHERELL, L., GUASTI, L. & KING, P. 2013. Adrenocortical development, maintenance, and disease. Curr Top Dev Biol, 106, 239-312.

YAZAWA, T., IMAMICHI, Y., MIYAMOTO, K., KHAN, M. R., UWADA, J., UMEZAWA, A. & TANIGUCHI, T. 2015. Regulation of Steroidogenesis, Development, and Cell Differentiation by Steroidogenic Factor-1 and Liver Receptor Homolog-1. Zoolog Sci, 32, 323-30.

YE, Z., WANG, Y., XIE, H. Y. & ZHENG, S. S. 2008. Immunosuppressive effects of rat mesenchymal stem cells: involvement of CD4+CD25+ regulatory T cells. Hepatobiliary Pancreat Dis Int, 7, 608-14.

YEGOROV, Y. E. & ZELENIN, A. V. 2003. Duration of senescent cell survival in vitro as a characteristic of organism longevity, an additional to the proliferative potential of fibroblasts. FEBS Letters, 541, 6-10.

YIN, X., MAYR, M., XIAO, Q., WANG, W. & XU, Q. 2006. Proteomic analysis reveals higher demand for antioxidant protection in embryonic stem cell-derived smooth muscle cells. Proteomics, 6, 6437-46.

YOO, J. K., KIM, C. H., JUNG, H. Y., LEE, D. R. & KIM, J. K. 2014. Discovery and characterization of miRNA during cellular senescence in bone marrow-derived human mesenchymal stem cells. Exp Gerontol, 58, 139-45.

YOSHIE, M., KANEYAMA, K., KUSAMA, K., HIGUMA, C., NISHI, H., ISAKA, K. & TAMURA, K. 2010. Possible role of the exchange protein directly activated by cyclic AMP (Epac) in the cyclic AMP-dependent functional differentiation and syncytialization of human placental BeWo cells. Hum Reprod, 25, 2229-38.

YUN, K., MANTANI, A., GAREL, S., RUBENSTEIN, J. & ISRAEL, M. A. 2004. Id4 regulates neural progenitor proliferation and differentiation in vivo. Development, 131, 5441-8.

ZAJICEK, G., ARIEL, I. & ARBER, N. 1986. The streaming adrenal cortex: direct evidence of centripetal migration of adrenocytes by estimation of cell turnover rate. J Endocrinol, 111, 477-82.

ZAMAN, W. S., MAKPOL, S., SATHAPAN, S. & CHUA, K. H. 2014. Long-term in vitro expansion of human adipose-derived stem cells showed low risk of tumourigenicity. J Tissue Eng Regen Med, 8, 67-76.

ZENG, L., PENG, Z. & ZHANG, M. 2009. [Construction of THY1 eukaryotic expression plasmid and its effects on growth of ovarian cancer SKOV3 cells]. Sheng Wu Yi Xue Gong Cheng Xue Za Zhi, 26, 620-4.

ZHANG, L., SEITZ, L. C., ABRAMCZYK, A. M., LIU, L. & CHAN, C. 2011. cAMP initiates early phase neuron-like morphology changes and late phase neural differentiation in mesenchymal stem cells. Cell Mol Life Sci, 68, 863-76.

ZHANG, T. F., YU, S. Q., GUAN, L. S. & WANG, Z. Y. 2003. Inhibition of breast cancer cell growth by the Wilms' tumor suppressor WT1 is associated with a destabilization of beta-catenin. Anticancer Res, 23, 3575-84.

ZHAO, G., CHEN, J., DENG, Y., GAO, F., ZHU, J., FENG, Z., LV, X. & ZHAO, Z. 2011. Identification of NDRG1-regulated genes associated with invasive potential in cervical and ovarian cancer cells. Biochem Biophys Res Commun, 408, 154-9.

ZHAO, W., JI, X., ZHANG, F., LI, L. & MA, L. 2012. Embryonic stem cell markers. Molecules, 17, 6196-236.

ZHONG, X. Y., YU, T., ZHONG, W., LI, J. Y., XIA, Z. S., YUAN, Y. H., YU, Z. & CHEN, Q. K. 2015. Lgr5 positive stem cells sorted from small intestines of diabetic mice differentiate into higher proportion of absorptive cells and Paneth cells in vitro. Dev Growth Differ, 57, 453-65.

ZHOU, J., LI, Y., LIANG, P., YUAN, W., YE, X., ZHU, C., CHENG, Y., WANG, Y., LI, G., WU, X. & LIU, M. 2005. A novel six-transmembrane protein hhole functions as a suppressor in MAPK signaling pathways. Biochem Biophys Res Commun, 333, 344-52.

ZHU, H., WANG, F. & WANG, Y. 2015. [DEVELOPMENT PROGRESS OF MESENCHYMAL STEM CELLS SENESCENCE]. Zhongguo Xiu Fu Chong Jian Wai Ke Za Zhi, 29, 899-904.

ZHU, Y., YANG, Y., ZHANG, Y., HAO, G., LIU, T., WANG, L., YANG, T., WANG, Q., ZHANG, G., WEI, J. & LI, Y. 2014. Placental mesenchymal stem cells of fetal and maternal origins demonstrate different therapeutic potentials. Stem Cell Res Ther, 5, 48.

ZUBAIR, M., PARKER, K. L. & MOROHASHI, K. 2008. Developmental links between the fetal and adult zones of the adrenal cortex revealed by lineage tracing. Mol Cell Biol, 28, 7030-40.